Exhibit A

Review of the nervous system and cardiovascular effects of methylmercury exposure

Deborah C. Rice, Ph.D.
Environmental and Occupational Health Program
Maine Center for Disease Control and Prevention
Augusta, ME
March 2006
Report to the Illinois EPA

Introduction

The tragic outbreak of neurological disease in Minamata, Japan, in the late 1950s focused attention on the potential for devastation by neurotoxic agents released into the environment. The source of the exposure was a plant that used methylmercury as a catalyzer to produce acetaldehyde. Methylmercury was dumped directly into surface water, which was then accumulated by marine biota, passed up the food chain to fish, and eventually ingested by the human population of the area. Thousands of people were exposed and hundreds of people became clinically ill during the years before and shortly after the hazard was recognized (WHO, 1990). In 1963-1965, another outbreak of methylmercury poisoning was identified in Niigata Prefecture involving hundreds of people; the source was a fertilizer factory that released methylmercury into a river that flowed into a bay from which fish were caught. The signs and symptoms of adult Minamata disease have been well characterized (e.g. WHO, 1990; Tsubaki and Irukayama, 1977; Igata, 1993). Early in the exploration of effects of methylmercury poisoning, attention was largely focused on constrictions of visual fields and other visual abnormalities. However, peripheral neuropathy is also a cardinal feature of methylmercury intoxication in humans. Sensory impairment is of the glove-and-stocking type, sometimes with perioral dysesthesia. Other manifestations of methylmercury intoxication included hearing deficits, ataxia, muscle weakness, tremor, and mental deterioration. It became clear that the fetus is more sensitive to methylmercury-induced neurotoxicity than is the adult, and the effects may be different. Effects included cerebral palsy, blindness, deafness, and severe mental retardation. Lower doses produced deficits in vision and hearing, as well as motor and speech impairment (WHO, 1990; Harada, 1978).

Our understanding of the devastating damage that methylmercury can produce in the nervous system is due to description of the neuropathology produced by the episodes of human poisoning in Minamata (reviewed by Reuhl and Chang, 1979). Neuropathological lesions were relatively localized to the cerebellum, motor and somatosensory cortices, and visual cortex, with substantial cell loss in highly exposed individuals. Consistent with this pattern of more global and severe deficits as a consequence of fetal versus adult exposure, neuropathology was also more widespread and severe. Brains were often small and malformed, without the normal

gyration pattern. Cellular architecture was disrupted, as a result of failure of cells to migrate to the appropriate area or layer of the brain. This effect was permanent, and would disrupt formation of normal circuitry of the cerebrum. Similar effects were observed in brain of infants in the poisoning episode in Iraq.

A second episode of human poisoning occurred in Iraq in the 1970s, when methylmercury-treated seed grain intended for planting was ground into flour and consumed. Exposures were of shorter duration than those in Japan, and may have been higher (NRC, 2000). The constellation of effects was consistent with that in Minamata. The most highly affected children exposed prenatally had severe sensory impairment (including blindness and deafness), cerebral palsy, hypersensitive reflexes, and impaired mental development (Amin-Zaki *et al.*, 1974). In a follow-up study, Marsh *et al.* (1987) studied the development of 81 infants exposed prenatally. Assessment consisted of a clinical neurological examination and a maternal interview regarding the age at which developmental milestones such as walking and talking were reached. There was an apparent dose-response relationship between methylmercury exposure and neurological signs, including increased deep tendon reflexes, hypotonicity, ataxia, and athetoid movements. Seizures were also observed in the most highly exposed children. Maternal hair mercury ranged from 1 to 674 ppm. There was also an exposure-related increase in delayed walking and talking as reported retrospectively by the mothers. Modeling of the dose-effect relationship identified a threshold for delayed walking and neurological signs of about 10 ppm in maternal hair (Cox *et al.*, 1989). Assessment of affected individuals in this nomadic culture presented significant challenges, as discussed by the NRC (2000).

Longitudinal prospective epidemiological studies

As a result of the episodes of mass human poisoning from methylmercury, three longitudinal prospective studies were mounted in the late 1970s and 1980s. Since it was clear from the poisoning episodes that the fetus was more sensitive than the adult, these studies assessed the effects of environmental mercury exposure on the developing organism, particularly as a consequence of prenatal exposure.

New Zealand study

The study in New Zealand was designed as a case-control study. On the initial assessment, seventy-three women who consumed fish more than three times a week, with hair levels above 6 ppm, were chosen from 935 women (Kjellström *et al.*, 1986). The 74 children of those women were designated as the high-mercury group. This study included children from several ethnic groups, including white, Maori, and Pacific Islander. The most commonly consumed fish was snapper, and snapper consumption was the greatest predictor of hair mercury compared to other fish. Each high-mercury child was matched with a child based on age, mother's age, ethnicity, and hospital of birth. When the children were four years old, they were tested on the Denver Developmental Screening Test (DDST). Fifty-two percent of the high-mercury children had abnormal results, compared to 17% of the children in the control group. The high-mercury group was tested again at 6 years of age (Kjellström *et al.*, 1989). Each child was matched with three children on the basis of age, ethnic group, maternal age and smoking, area of residence, and duration of maternal residence in New Zealand. The mean maternal hair mercury concentration in the high-exposure group was 8.3 ppm (range 6-86 ppm). The three control groups were chosen with respect to maternal hair mercury levels and fish consumption. The control groups had maternal hair levels of 0-3 or 3-6 ppm. A battery of 26 psychological and

scholastic tests were administered. Multiple regression analyses were performed for five main variables: the Test of Language Development_spoken language quotient (TOLD_SL), the Wechsler Intelligence Scale for Children Revised (WISC-R) full scale and performance IQ, and the McCarthy Scales perceptual performance and motor scale. Results were controlled for a number of covariates. Maternal hair mercury was associated with 4 endpoints. In additional analyses using maternal hair as a continuous variable, none of the five primary endpoints were associated with mercury (Crump *et al.*, 1998). However, the negative results were a consequence of one child whose mother had a hair level of 86 ppm (more than 4 times the nearest concentration) but the child's scores were not outliers. When data from this child were excluded, two endpoints from the initial analysis were significant. When all 26 endpoints were analyzed, impairment on 6 was associated with maternal hair mercury concentrations at $p < 0.10$ when the most highly exposed child was excluded.

Seychelles Islands study

A longitudinal prospective study was carried out in about 750 children in the Seychelles Islands in the Indian Ocean. This is a black population. Median maternal hair mercury levels were 5.9 ppm (interquartile range 6.0 ppm). Exposure was through frequent (daily) consumption of fish. Offspring were evaluated longitudinally, including a neurological assessment, the DDST-Revised, and the Fagan Test of Infant Intelligence during infancy and age at achievement of milestones. The Bayley Scales of Infant Development (BSID) were administered at 19 and 29 months. No mercury-related effects were identified (see NRC, 2000 for review). Seven hundred and eleven children from this cohort were evaluated at 66 months on the McCarthy Scales of Children's Abilities, Preschool Language Scale, letter-word recognition subtest of the Woodcock-Johnson Tests of Achievement, the Bender Gestalt Test, and the Child Behavior Checklist (Davidson *et al.*, 1998). Mean maternal hair level of children tested at 66 months was 6.5 ppm (range 0.9-25.8 ppm). The investigators reported no adverse effects associated with prenatal exposure to methylmercury in their standard analyses; in fact, increased mercury exposure was associated with better performance on some measures. In a subsequent analysis using nonlinear models, adverse associations were identified for the Preschool Language Scale (prenatal exposure) and the McCarthy GCI (postnatal exposure) above 10 ppm (Axtell *et al.*, 2000). The results for various endpoints was complex, and the authors concluded that there was no overall evidence for adverse effects.

Children were assessed again at 9 years on a number of endpoints including WISC III full-scale IQ, California Verbal Learning short and long delayed recall, Boston Naming Test, and Woodcock-Johnson recognition and applied problems, continuous performance task, grooved pegboard, finger tapping, haptic discrimination, Trailmaking, and a test of visual-motor integration (Myers *et al.*, 2003). Some of these endpoints had also been assessed in the Faroe Islands study (see below). An adverse association was found between postnatal exposure and performance on the grooved pegboard using the non-preferred hand, with no other adverse effects. Better outcome on the hyperactivity index of the Connor's teachers rating scale was associated with maternal hair mercury. A subsequent exploration of potential non-linear associations suggested adverse effects above 12 ppm in maternal hair on several measures, including full-scale IQ (Huang *et al.*, 2005).

A pilot study was carried out in the Seychelles Islands, prior to the longitudinal study, by the same team of investigators (Myers *et al.*, 1995). Maternal hair mercury mean concentration was 6.1 ppm (range 0.6 to 36.4). A variety of endpoints was assessed between 5 and 109 weeks

of age by a pediatric neurologist blinded to the mercury status of the mother. Children were also tested on the DDST-R during that time period. No mercury-related effects were found. A total of 317 children from the pilot study were assessed at 66 months of age on the same instruments as in the main study. Mean maternal hair mercury was 7.1 ppm (range 1.0 to 36.4). Increased maternal hair mercury levels were associated with significantly lower scores on the General Cognitive Index and perceptual-performance scales of the McCarthy, and auditory comprehension on the Preschool Language Scale. These results are in contrast to those in the main Seychelles Island study. In the pilot study, important covariates that are frequently associated with neuropsychological function were not measured, including socioeconomic status, maternal IQ, and quality of the home environment. Eighty-seven children from this cohort were evaluated at 9 years on the same endpoints as the main cohort (Davidson *et al.*, 2000). Decreased performance on the grooved pegboard in females was associated with maternal hair mercury, whereas better performance in males was associated with maternal hair mercury on three endpoints. The negative association on grooved pegboard was observed in both sexes in the main cohort.

Faroe Islands study

The Faroe Islands study is a longitudinal prospective study of over 900 children in a homogeneous white population in the North Atlantic. Women were recruited during pregnancy and their offspring were tested at 7 years of age. This population consumed fish frequently, with 48% of the cohort consuming fish dinners three or more times per week (Grandjean *et al.*, 1992). However, the fish species consumed generally have low concentrations of mercury. A main source of methylmercury exposure in this cohort was meat from pilot whales, which were landed on average less than once per month (NIEHS, 1998), although women consumed dried whale meat "snacks" on a regular basis. Pilot whale meat averaged 1.9 ppm mercury (NIEHS, 1998). About half this was inorganic mercury, which would not cross the placenta. Consumption of whale blubber in the Faroese population resulted in significant exposure to PCBs in those women consuming blubber. In a separate study, milk PCB concentrations in Faroese women were found to exceed those of most other countries (Grandjean *et al.*, 1995). In the developmental study, cord blood mercury concentrations were used as the main independent variable, although maternal hair mercury levels at birth were also used as a measure of mercury exposure (Grandjean *et al.*, 1997). Average maternal hair mercury level was 4.27 ppm (geometric mean).

At 7 years of age, 917 children were tested on a series of psychological assessments (Grandjean *et al.*, 1997). A statistically significant ($p < 0.10$) association was observed between cord blood mercury levels and poorer performance after control for confounders for the following measures: NES2 finger tapping, preferred hand; NES2 continuous performance test, reaction time and number of missed responses; WISC-R digit spans; Bender Gestalt reproduction ($p = 0.10$); Boston Naming, with and without cues; California Verbal Learning, short- and long-term recall. The following tests were found not to be significantly associated with cord blood mercury levels: NES2 finger tapping, nonpreferred or both hands; NES2 hand-eye coordination, error score; tactile performance test, preferred hand; WISC-R, similarities and block design; Bender-Gestalt, errors or copying; California Verbal Learning, learning and recognition.

Visual and auditory brainstem evoked potentials were measured in the Faroe Island study at 7 years of age (Murata *et al.*, 1999a). Delays in peak I-III of the auditory evoked potentials were observed. There were no effects on visual evoked potentials. (However, visual evoked potentials are a less sensitive measure of visual function than assessment of vision *per se*.)

Auditory evoked potentials were assessed again at 14 years (Murata *et al.*, 2004; Grandjean *et al.*, 2004). As was the case at 7 years, cord blood mercury levels were associated with a prolonged I-III interpeak intervals. In addition, the child's hair mercury concentration at 14 years was associated with a prolonged III-V interpeak interval. Geometric mean hair mercury concentration was 0.96 ppm (interquartile range 0.45-2.29) at 14 years.

Other prospective studies

A prospective study in the Philippines assessed the relationship between cord blood mercury (prenatal exposure) and hair or blood mercury in about 120 children at 2 years of age on language development and a visuospatial-problem solving task (Ramirez *et al.*, 2003). Subjects were recruited from two towns with the same ethnic background and language, one a gold mining community. Mercury was detected in 17% of cord blood samples, and of those, the mean was 53 ug/L. Higher cord blood mercury was associated with poorer expressive language development and poorer performance on the visuospatial task, with no effect on receptive language. These results are consistent with those from the Faroe Islands study with respect to domains affected (visuospatial and expressive language).

A recent prospective study in Massachusetts assessed the relationship between maternal hair mercury levels and fish intake with performance on a test of short-term visual memory in 135 infants at six months of age (Oken *et al.*, 2005). Geometric mean maternal hair levels were 0.45 ppm, with 10% of women having hair mercury levels greater than 1.2 ppm (the hair level associated with the U.S. EPA reference dose of 0.1 ug/kg/day) (discussed below). Women consumed an average of 1.2 meals per week of fish, including tuna, dark meat, white meat, and shellfish. Increased hair mercury was significantly associated with poorer performance after covariate adjustment, and increased fish intake was associated with improved performance. For each additional fish meal, infant score improved by 4.0 points. However, each 1 ppm increase in hair mercury was associated with a decrement of 7.5 points. Scores were highest in infants of mothers who ate > two fish meals per week but had mercury hair levels <= 1.2 ppm. These results are consistent with those from the Faroe Islands with respect to effects on memory.

A study in Poland assessed performance of 233 on the Bayley Scale of Infant development in one-year-old infants as a function of mercury concentrations in cord blood and maternal blood at delivery (Jedrychowski *et al.*, 2006). Children were dichotomized according to normal (score > 84) or delayed (score < 85). The maternal blood mercury level was significantly lower in the normal group (geometric mean = 0.52 ug/L, CI, 0.45-0.58 ug/L) than in the delayed group (GM = 0.75 ug/L, CI, 0.59-0.94). A similar pattern was observed for cord blood mercury levels (0.85 ug/L versus 1.05 ug/L), which was marginally significantly different (p = 0.07). Risk for delayed performance was significantly elevated at cord blood levels greater than 0.80 ug/L (RR = 3.58, CI, 1.40-9.14) on maternal blood mercury levels greater than 0.50 ug/L (RR = 2.82, CI, 1.17-6.79).

Comparison of prospective studies

At least two expert panels have addressed the issue of what factors might account for the differing findings in the Faroe and Seychelles Islands studies (NIEHS, 1999; NRC, 2000). Both studies are relatively large, well-controlled studies deemed to be of high quality. An initial suggestion was that the domain-specific tests used in the Faroe Islands were more sensitive than the global clinical instruments used in the Seychelles study; however, some of the endpoints (e.g.

IQ) assessed in the Seychelles Islands were impaired in the New Zealand study. In addition, assessment of the Seychelles cohort at 9 years, using many of the same tests used in the Faroe Islands at 7 years, found little evidence of adverse effects.

Another suggestion was that the age of assessment in the Seychelles study, 5.5 years, was problematic because children are undergoing rapid cognitive development at that age, resulting in increased variability (and therefore less power to detect an effect). In contrast, children in the Faroe Islands study were tested at 7 years, a more optimal age for testing. However, the Seychelles Islands study reports little evidence for adverse effects even at older ages.

A third possibility is co-exposure to relatively high levels of PCBs in the Faroe Islands study, which may have interacted with methylmercury, resulting in deficits that would not be present otherwise. Of the nine endpoints identified as significantly correlated ($p < 0.10$) with methylmercury exposure in the Faroe Islands study, four were also associated with PCB exposure ($p < 0.10$) (Grandjean *et al.*, 2001). These were reaction time on the continuous performance task, Boston Naming with and without cues, and California Verbal learning long-term recall. It is important to explore the possibility that effects observed on these four variables are the result of PCB exposure rather than methylmercury exposure, or are the results of an interaction between PCBs and methylmercury. When both PCBs and methylmercury were included in the multiple regression analysis, only CPT reaction time was independently related to mercury exposure (Grandjean *et al.*, 2001). For the other three outcomes, the association with either mercury or PCBs was not statistically significant. Analyses relevant to this issue of a potential mercury-PCB interaction were performed by Budtz-Jørgensen *et al.* (1999). They divided the Faroese subjects into tertiles with respect to cord tissue PCB levels, and performed regression analyses for the effect of mercury separately for each of the four endpoints previously reported to be associated with PCB exposure, listed above, as well as finger tapping. (The authors did not state why this measure was included in the analysis.) There were not statistical differences in the regression coefficients for the three tertiles, thereby failing to provide evidence for a PCB-methylmercury interaction. In addition, these authors failed to find evidence of a mercury x PCB interaction for any of these five endpoints when the mercury and PCB exposure variables and their interaction terms were included in regression analyses (Budtz-Jørgensen *et al.*, 1999). In addition, effects were found in the New Zealand study as well as in a number of cross-sectional studies (discussed below) at comparable body burdens, in which PCB exposure was assumed not to occur because of the source and species of fish consumed. The NRC (2000) also examined this issue in detail (see section on NRC analysis) and concluded that the effects of methylmercury and PCB were independent.

A fourth suggestion was that methylmercury exposure in the Faroe Islands may have included episodes of meals high in mercury as a result of ingestion of whale meat, and that such bolus doses might have produced effects different from effects resulting from continuous lower-dose exposure. An analysis of the effect of variability in hair mercury levels during pregnancy revealed that exclusion of children whose mothers had the most variable hair mercury concentrations had no impact on the conclusions of the study (Grandjean *et al.*, 2003). In fact, some associations were stronger after elimination of the 10% of women with the most variable hair mercury level. These results suggest that variable exposure was not the explanation for the discrepancy between the Faroe Islands and Seychelles Islands studies.

Cross-Sectional Studies

Developmental studies

A study was performed in 149 first graders, in the Madeira Islands, a Portuguese island in the mid-Atlantic (Murata *et al.*, 1999b), by the Faroe Islands investigators. This is a fish-eating population; fish mercury levels were 0.7-1.8 ppm. Concurrent hair mercury concentrations in the mothers of these children averaged 9.64 ppm (geometric mean), with the highest hair mercury level at 54.4 ppm. 52.4% of the mothers had hair mercury levels greater than 10 ppm, and 80% of mothers reported that they had not changed their diet since they were pregnant with the child who was a subject in the study. An association was found between both auditory and visual evoked potentials and maternal hair mercury. As in the Faroe Island study, delays in the I-III peak were observed for auditory evoked potentials. There were no associations for any of the other tests, which included finger tapping, hand-eye coordination, continuous performance, digit spans, block design, and Stanford-Binet bead memory.

The Faröe Islands team also investigated the effects of methylmercury exposure in children in the Brazilian Amazon (Grandjean *et al.*, 1999). In the Amazon, elemental mercury used in gold mining is vaporized by heating, as well as being discharged directly into waterways. It is converted to methylmercury and bioaccumulates and bioconcentrates in fish. In a cross-sectional study, 351 children between the ages of 7 and 12 from a total of four villages were studied, although for any one endpoint, only two or three villages were assessed. Average hair mercury level was 11.0 ppm (geometric mean) for the children, and 11.6 ppm for the mothers. More than 80% of the children had hair mercury levels greater than 10 ppm. One village had a distribution of mercury levels lower than the other three villages (Village A), with most of the children having hair mercury levels below 10 ppm. When data were analyzed from that village alone, mercury-related effects were found on Santa Ana pegboard and Stanford-Binet copying, but not on finger tapping, digit spans, or Stanford-Binet bead memory. (Data were not presented separately for the villages other than Village A.) When the villages were analyzed together correcting for community, these measures plus Stanford-Binet recall were significantly associated with mercury hair concentrations. However, when the villages were analyzed together without correcting for community, all measures were significant. This may be the result of added statistical power and the fact that a wider range of mercury hair levels was represented, particularly between Village A compared to the other three villages. However, there were differences between villages that may have confounded the results.

A study in French Guiana (a gold mining area) assessed a variety of endpoints in about 370 children from infancy to 12 years of age in three communities with different levels of exposure (Cordier *et al.*, 2002). Geometric mean mercury hair levels in the children were 10.2, 6.5, and 1.4 ppm for the three communities. Increased neurological signs were observed in boys only as a function of methylmercury exposure. Deficits in Stanford-Binet Copying and McCarthy digit span forward and backward were observed as a function of increased hair mercury concentrations after appropriate covariate control (e.g. age, sex, examiner, mother's Rauen score, parity as required). No effect was observed on fine motor (finger tap) or gross motor (leg coordination) function.

In another study in a gold-mining area, auditory function was assessed in children and adults in Ecuador (Counter *et al.*, 1998). Median blood mercury levels were 15 ug/L in the study area (range 4-67 ug/L) and 2.0 ug/L in the reference area, documenting increased exposure in the

gold-mining area. Auditory brain stem response was assessed in the study area, and there was a relationship between increased blood mercury and a I-III interpeak latency on the left side. There was one statistically-significant effect on pure tone auditory thresholds between 2-8 kHz: at 3 kHz in the right ear in children. The effects on auditory evoked responses is consistent with effects observed in other studies (Grandjean *et al.*, 2004; Murata *et al.*, 2004, 1999b). High-frequency auditory thresholds may be affected before lower ones (Rice and Gilbert, 1992, 1990). Eight kHz is about an octave lower than the upper range of human hearing; perhaps testing at higher frequencies would have revealed deficits.

The relationship between blood lead and urine mercury and visual function, as measured by visual evoked potentials and contrast sensitivity, was assessed in a study in Germany (Altmann *et al.*, 1998). This cross-sectional study included 384 6-year-old children who had no known elevated exposure to mercury. Urinary mercury level were associated with decreased contrast sensitivity at some frequencies between 1.5 and 18 cycle/degrees. The highest frequency tested is in the middle range of frequencies detectable by humans; high frequencies were not tested. Average mercury excretion was 0.157 ug/24 hour period. Median urinary mercury levels in women in the NHANES survey was about 0.6 ug/L, with a 95th percentile of about 4.0 ug/L for 1999-2002. Although results are not directly comparable, the data suggest that the German children were not highly exposed. The number of amalgam fillings averaged less than 2, but there was a relationship between fillings and urinary mercury levels. It is not possible to determine whether the observed effects were the result of exposure to inorganic or organic mercury; however, effects on visual contrast sensitivity are known to be associated with methylmercury but not inorganic mercury exposure.

In a study in Cree in northern Quebec, psychomotor function was assessed in 234 12-30-month-old children (McKeown-Eyssen *et al.*, 1983). Mean hair mercury concentration was 6.0 ppm. There was little evidence of a deleterious effect on language, fine or gross motor status, or social scales. Abnormal muscle tone was associated with prenatal mercury exposure in boys but not in girls.

Adult studies

In a study in frequent tuna consumers versus non-consumers in Italy, tests of cognitive function and fine and gross motor function were assessed (Carta *et al.*, 2004). Average age of the men was 51 years. The median of total mercury in blood of the fish eaters was 44 ug/L, and in the non-fish eaters it was 3.9 ug/L. Forty-one percent of fish eaters ate fish more than three times per week, and 65% of all fish meals in the exposed group was fresh tuna. Color word reaction time and digit symbol reaction time (both tests of speed of information processing and cognitive flexibility) were associated with total urinary mercury and organic mercury in blood (available for only a subset of the population), whereas simple reaction time, finger tapping, digit span, and the Luria-Nebraska battery of motor performance were not. The Branches Alternation Movement Test of gross motor integration was affected. Serum prolactin was also higher in the exposed versus control group.

In a study in the Brazilian Amazon, 68 individuals between 15 and 79 underwent assessment of motor performance (Dolbec *et al.*, 2000). Median hair mercury level was 9 ppm. Hair mercury levels were associated with deficits on the Santa Ana dexterity test, grooved pegboard test of dexterity and fine motor movement, and fingertapping speed. In another study of 91 adults between 15-81 years (Lebel *et al.*, 1997,1998), median hair mercury levels were

about 12 ppm, with a peak of about 17 ppm. Deficits in coordination on the Branch Alternating Movement were found, as in the Carta *et al.* (2003) study. Constriction of visual field was associated with peak hair mercury levels, and decreased contrast sensitivity at all but low frequencies was associated with peak mercury hair levels in younger but not older individuals. The latter effect was also observed in developmentally-exposed monkeys (see below) and probably reflects developmental exposure in this study. Gold mining began about 25 years before the study was performed, so that older individuals were presumably exposed to less mercury during development. Constriction of visual fields and deficits in gross motor movement could be the result of adult and/or developmental exposure. Cytotoxicity has also been documented in this study population (Amorim *et al.*, 2000).

In a study in the United States, a cross-sectional assessment was performed on 474 participants, 50-70 years old, in the Baltimore Memory Study (Weil *et al.*, 2005). Average blood mercury concentration was 2.76 ug/L (SD = 2.35 ug/L). Twenty endpoints assessing cognitive and motor function were analyzed. A negative association was found between blood mercury levels and delayed recall on a visual memory task (Rey complex figure delayed recall), with a marginal effect on a verbal memory task (Rey auditory delayed recall). In contrast, increased mercury levels predicted better performance on a finger tapping task of fine motor function. The authors concluded that there was no strong evidence that blood mercury levels were associated with worse neurobehavioral performance. However, recall memory was affected in the Faroe Islands and other studies, so the negative association with memory may not be spurious.

A study of neuropsychological function was conducted in 129 men from six fishing villages in Brazil (Yokoo *et al.*, 2003). Mean hair mercury was 4.2 ppm, and the median was 3.7 ppm. Analyses were performed for 21 endpoints of cognitive and motor function, as well as a questionnaire of mood. Six of the comparisons were statistically significant with respect to the relationship between hair mercury levels and performance, all in the direction of poorer performance. It is unlikely that these results were solely due to chance. Deficits were observed, after covariate adjustment, on fine motor speed, logical memory, digit span forward and backward (tests of working memory), and easy learning from the Portuguese version of the Wechsler Adult Intelligence Scale. Increased hair mercury levels also predicted increased errors of commission on the Concentrated Attention Test of the Toulouse Pierrin Factorial Battery. This finding suggests a deficit in impulse control.

The relationship between motor effects and methylmercury exposure was assessed in a total of 66 Cree over 40 years old in Quebec (Beuter and Edwards, 1998; Beuter *et al.*, 1999). Active, static, and postural tremor were measured objectively, and there were differences between exposed (hair mercury range 2.3-31.1 ppm) and unexposed groups for several measures of all three tremor types. In addition, differences were identified between high hair mercury (27 ppm) and low-mercury (8 ppm) groups. Rotational movement of the hands was also objectively assessed in these same subjects. There was some evidence that the higher exposure group had impaired motor control relative to the controls.

Review of the Health Effects of Methylmercury by the National Research Council

The U.S. Environmental Protection Agency (EPA) derived a reference dose (RfD) for methylmercury, based on the Iraqi study in 1995. An RfD is defined as "an estimation of a daily exposure to the human population (including sensitive subgroups) that is likely to be without appreciable risk of deleterious effects during the lifetime." The reference dose was 0.1

ug/kg/day. In 1997, Congress mandated that EPA fund an expert panel under the auspices of the National Research Council (NRC) to determine whether the RfD was scientifically justifiable. The NRC panel concluded that an RfD of 0.1 ug/kg/day was scientifically justifiable based on its review and analysis (NRC, 2000). Information from studies not available in 1995 was thoroughly reviewed by the expert panel: specifically, the longitudinal prospective studies in New Zealand, the Faroe Islands, and the Seychelles Islands. The latter two studies had been previously reviewed by an expert panel (NIEHS, 1999) and deemed to be of high quality. The conclusion of the NRC panel was that all three studies were high-quality, well-designed studies. The NRC panel performed extensive analysis of all three studies, including exposure (body burden)-response modeling and a bench-mark dose (BMD) analysis of a number of endpoints. A BMD analysis identifies a point on the exposure-effect curve that is associated with a defined risk.

The first step in BMD analysis is determining the shape of the relationship between exposure and effect. The NRC modeled the relationship between maternal body burden and the child's performance on five endpoints from the Faroe Islands study from a total of nine that had been reported as significantly affected by methylmercury exposure (Grandjean et al., 1997) (Table I). Similarly, five endpoints negatively associated with methylmercury exposure in the New Zealand study (Kjellstrom et al., 1989) were used in the BMD analysis by the NRC. All of the endpoints assessed in the Seychelles study were also modeled, even though the Seychelles study was reported as negative. For the Faroe Islands study, maternal blood mercury concentration was used as the exposure metric; for the other two studies, only hair mercury levels were available.

In BMD analysis, the first step is to model the relationship between the endpoint (neuropsychological performance) and exposure (body burden). The NRC used the K power model, and determined the K value that best fit the data. The model was constrained to K >= 1. This allowed a sublinear relationship: i.e., a lower slope at lower body burdens and a comparatively greater slope at higher body burdens. The NRC reasoned that a supralinear model was biologically implausible. Under these conditions, the best fit to the data was K=1, or a linear dose-effect relationship, which was the model used for all endpoints from all three studies. In fact, for the Faroe Islands endpoints, supralinear models such as the square root or logarithmic transformations were a better fit than the linear model (Budtz-Jørgensen et al., 2000). In other words, there was evidence that the slope was actually steeper at lower body burdens compared to higher ones. This was also the case for the endpoints from the New Zealand study (Louise Ryan, statistician on the NRC panel, personal communication). This means that there was no evidence of a threshold within the body burdens of these studies (range of 0.17-39.1 ppm in hair in the Faroe Islands study [Grandjean *et al.*, 2005]).

Benchmark dose analysis requires two additional decisions once an appropriate model has been chosen. When continuous data are used, a point on the curve below which responses are considered "abnormal" must be chosen, termed P_0. A value of $P_0 = 0.05$ was used in the NRC assessment: that is, the cutoff for abnormal response was set at the lowest 5% (5th percentile) of children. This is roughly comparable to an IQ of 75 in terms of population distribution. The second decision that must be made is the choice of the increase in the proportion of individuals that will be expected to perform in the "abnormal" category in an exposed versus an unexposed population. This is defined as the benchmark response (BMR). A BMR of 0.05 was chosen for this assessment, which would result in a doubling of the number of

children with a response at or below the 5th percentile in an unexposed population. The lower 95% confidence limit on the BMD (BMDL) was determined for each endpoint.

The BMDLs were highest for the Seychelles Islands study and lowest for the New Zealand study (Table II). The NRC also performed a combined BMD analysis, using hair methylmercury data from all three studies. The BMDLs from the Faroe Islands study were 12-15 ppm total mercury in maternal hair, whereas those in the New Zealand study were 4-6 ppm. BMDLs from the Seychelles Islands study were 17-25, about 50% higher than those in the Faroe Islands and 250-300% higher than those from the New Zealand study. It is important to recognize that the BMDL represents a defined risk level: in this case, a doubling of the number of children performing in the abnormal range. It is therefore not equivalent to the NOAEL (no observed adverse effect level), which be definition is a level at which no adverse effects are identified.

The NRC examined the issue of potential confounding by PCBs in the Faroe Islands study in some detail. PCB body burden data were available for half the cohort (about 450 children). Analyses were performed controlling or not controlling for PCBs, with no systematic effects on BMDLs (Table III). Additional analyses were performed dividing the cohort into tertiles with respect to PCB levels; again there was no evidence that higher PCB body burden was related to a greater effect of methylmercury.

The NRC believed that the negative Seychelles Islands study should not be used as the basis for risk assessment, given the evidence of adverse effects found in the Faroe Islands and New Zealand studies. The NRC recommended the Faroe Islands study as the study upon which to base a hazard analysis for several reasons. First, the Faroe Island study is considerably larger than the New Zealand study. In addition, this study has been "... extensively analyzed and re-analyzed to explore the possibility of confounding, outliers, differential sensitivity, and other factors" (NRC, 2000, p. 299). The NRC recommended the cord blood concentration of 58 ug/L associated with the BMDL from the Boston Naming Test as a suitable basis for derivation of the RfD.

Conversion of Cord Blood Concentration to Maternal Methylmercury Intake

Cord blood was a better predictor of performance than hair in the only study that used both biomarkers (Faroe study), although maternal hair mercury was also associated with decrements in performance in both the Faroe and New Zealand studies. Hair mercury represents an integration of exposure throughout gestation if a sufficient length of hair is analyzed. Cord blood mercury represents exposure more proximal to delivery. Hair represents an excretion compartment more removed for the fetus than cord blood. The NRC stated that there was no compelling evidence to consider one biomarker more appropriate than the other. The committee recommended the use of cord blood because it explained "... more of the variability in more of the outcomes" (NRC, 2000, p. 286). In addition, modeling the association between cord blood and maternal mercury intake is more straightforward than inclusion of a hair excretion compartment.

The U.S. EPA (2001) used a one-compartment pharmacokinetic (PK) model to estimate the intake associated with BMDLs from a number of endpoints from both the Faroe Islands and New Zealand studies, as well as the integrated analysis of all three studies. The EPA used

central tendencies for the parameters rather than estimating distributions. The EPA also assumed that the ratio of cord:maternal blood mercury concentration was 1.0, even though EPA acknowledged that it was probably greater than one. The EPA applied a total uncertainty factor (UF) of 10 below the BMDLs from the various endpoints modeled by the NAS (EPA, 2005; Rice *et al.*, 2003) (Table II). It is unclear whether this UF provides sufficient protection against adverse effects, given that there was no evidence of a threshold in the modeling performed by the NRC, as well as new analyses regarding the pharmacokinetics of methylmercury.

Since the EPA assessment, two important analyses have been published. A distributional analysis of the cord:maternal blood ratio identified a central tendency of 1.7, and a 90th percentile of 3.3 (Stern and Smith, 2003). Using the central tendency of 1.7, 58 ug/L in cord blood would be associated with 34 ug/L in maternal blood. For mother-fetal pairs at the 90th percentile, a cord blood level of 58 ug/L would be associated with a maternal blood level of about 18 ug/L. These are maternal blood levels associated with a doubling in the number of children performing in the abnormal range on the Boston Naming Test of the Faroe Islands study.

Stern subsequently performed a probabilistic (Monte Carlo) full distribution analysis of the one-compartment PK model (Stern, 2005). The one-compartment model is preferable to a physiologically based (PB) PK model because it requires fewer assumptions. In addition, the one-compartment model provides a good predictor of the relationship between intake and blood mercury levels under steady-state (chronic intake) conditions. Stern expanded the model used by EPA (2001) to include the cord blood:maternal blood ratio:

$$D = \frac{C \times (1/R) \times b \times V}{W \times A \times F}$$

where D = maternal intake of meHg (ug/kg)
C = mercury concentration in cord blood (58 ug/L)
R = ratio of cord:maternal blood (unitless)
b = rate constant of elimination from blood (day^{-1})
V = maternal blood volume (L)
W = maternal body weight (kg)
A = fraction of ingested dose that is absorbed (unitless)
F = fraction of absorbed dose in blood (unitless)

The BMDL value of 58 ug/L recommended by the NRC was used in the analysis. Distributions for each variable were chosen from the published literature, with preference given to third-trimester data. Studies were chosen for which distributions were provided in the publication under consideration or could be derived from the data provided in the paper. Results were based on the average of five separate simulations of 5000 iterations each. Sensitivity analyses of variability revealed that R made the biggest contribution to output variability, followed by b, F, and W. V and A made no significant contribution to the variability. Sensitivity analysis of central tendency suggested that uncertainty in the most uncertain input parameters would likely influence the estimate of maternal dose by <= 20%.

The analysis identified a mean intake of 0.99 ug/kg/day and a median (50th percentile) of 0.81 ug/kg/day associated with a cord blood concentration of 58 ug/L. The 5th percentile was

0.30 ug/kg/day, and the 1st percentile was 0.20 ug/kg/day. In other words, for 1% of U.S. women, an intake of 0.20 ug/kg/day would result in a cord blood mercury concentration of 58 ug/L. This is only a factor of two greater than the RfD, and may provide no safety factor against risk for these mother-infant pairs.

Behavioral effects in animals

Neuropathological effects of developmental exposure to methylmercury have been characterized in humans, monkeys, and rodents (see reviews by Reuhl and Chang, 1979; Burbacher *et al.*, 1990a). There are both similarities and differences, with the pattern of damage in the monkey being more like that of the human than is the pattern in the rodent. Nonetheless, in all species, methylmercury exposure at high doses produces decreased brain size; damage to cortex, basal ganglia, and other brain areas; loss of cells; disorganized cell layers; ectopic cells; and loss of myelin. Therefore animal models may provide important information regarding mechanism of action of methylmercury toxicity, as well as characterization of functional deficits.

Effects in monkeys

There is a substantial database documenting adverse effects produced by methylmercury exposure in animals, particularly following developmental exposure (NAS, 2000; Newland and Paletz, 2000; Rice, 1996a; Gilbert and Grant-Webster, 1995). A significant body of research has been performed in monkeys, for several reasons. The structure of the monkey brain is more similar to that of the human than is the rodent brain. The rodent brain has a smooth (lyssencephalic) cerebral cortex, whereas the cortex of the primate (including human) brain has a highly convoluted surface (gyrencephalic brain). This difference is particularly important with respect to the damage produced by methylmercury, which preferentially damages structures within sulci. The kinetics of methylmercury in rodents is quite different from that in the primate. Methylmercury is bound to sulfur in red blood cells, and the ratio of red blood cells to plasma is much higher in the rat than the primate. The ratio of methylmercury in the brain compared to the blood is about 1:10 in rodents, but between 2:1 and 5:1 in primates (see Rice, 1996a). The monkey is capable of more complex behavior than the rodent. The visual system of the monkey is virtually identical to that of the human, whereas the rodent system is quite different. This is particularly important since visual deficits are a hallmark of methylmercury exposure. Finally, episodes of human poisoning and the resulting recognition of the potentially devastating effects of methylmercury encouraged research in the most appropriate species.

Research on macaque monkeys was performed in two laboratories (University of Washington and Health Canada), in which cohorts of monkeys were exposed *in utero* only, *in utero* plus postnatally through adolescence, or beginning at birth through young adulthood (7 years). In all these studies, infants were separated from their mothers at birth and reared in a primate nursery. In the studies in which monkeys were exposed prenatally, the mothers were dosed until blood mercury levels were stable, before initiation of breeding, to mimic environmental exposure in humans.

Visual function was assessed in all cohorts using a behavioral procedure in which the stimuli and experimental task were controlled by computer. Deficits in spatial visual function were observed in all three cohorts (Burbacher *et al.*, 2005; Rice, 1996a; Rice and Gilbert, 1982). High frequency and low luminance vision were most affected. Assessment of temporal visual function indicated remodeling of the visual system during development, with preferential

damage to small cells. Auditory function was assessed in monkeys exposed pre- plus postnatal or postnatally only (Rice, 1998; Rice and Gilbert, 1992). Individuals in the former cohort were impaired in their ability to detect pure tones across a range of frequencies. The monkeys exposed beginning at birth were impaired only at high or high and middle frequencies, with low frequencies spared. The ability of the monkeys in these cohorts to detect a vibrating needle in contact with the tip of the finger was also determined (Rice and Gilbert, 1995). As in the other assessments of sensory system function, the stimulus presentation was controlled by computer. The monkey's hand was held in position over the blunt needle, and the frequency and amplitude of the vibration were precisely controlled. Monkeys in both cohorts exhibited impairment in their ability to detect vibration over a range of frequencies, which probably resulted from central rather than peripheral damage. Monkeys in both cohorts were also impaired on a fine motor task during middle age (Rice, 1996b), presumably as a consequence of somatosensory impairment (see section on delayed neurotoxicity).

Experiments in monkeys also provide evidence for cognitive impairment. Monkeys exposed to methylmercury only during gestation were impaired on an object permanence task during infancy (Burbacher *et al.*, 1988). This task tested the infants' ability to realize that a desired object placed behind a screen was still present, as measured by their reaching behind the screen to retrieve it. Methylmercury-exposed infants took longer to learn the task, and were retarded in the development of the skill of simple reaching for the object when it was in view. These same monkeys were also deficient on a series of visual recognition tasks (Gunderson *et al.*, 1986, 1988). In this task, the subject is shown a stimulus (usually a picture), and after a delay the subject is shown the original stimulus and a novel one. A normal animal or human infant will gaze longer at the novel stimulus, which is considered to be indicative of recognition memory and is a reasonable predictor of later IQ. Methylmercury-exposed monkeys were impaired, exhibiting a decreased percentage of time looking at the novel stimulus compared to controls. The results of this study could also be due to deficits in higher-order visual processing, however, as discussed by Newland and Palentz (2000). Deficits were also reported on this task in U.S. infants at low maternal body burdens (Oken *et al.*, 2005). This cohort also behaved differently than controls in a social situation, exhibiting increased nonsocial and passive behavior, and decreased rough-and-tumble play but not quiet social interaction (Burbacher *et al.*, 1990b).

The effects of methylmercury have been assessed on performance on a fixed interval (FI) schedule of reinforcement. On this schedule, a response after a certain period of time has elapsed is reinforced with food. Even though only one response is required, the FI engenders a response pattern characterized by a gradually accelerating rate of response terminating in reinforcement. One aspect of performance assessed by this schedule is the temporal control of behavior, which may be considered a higher-order cognitive ("executive") function. Monkeys exposed prenatally only (Gilbert *et al.*, 1996) or pre- plus postnatally (Rice, 1992) exhibited a different temporal pattern of performance compared to controls.

In a study in squirrel monkeys exposed prenatally (Newland *et al.*, 1994), the effects of methylmercury were determined on a complex learning task that required adaptive response to changing environmental contingencies. In the concurrent random interval-random interval schedule, responses were reinforced on each of two levers, with one delivering a reinforcement for a response at a shorter interval than the other. A normal subject will apportion responses accordingly (e.g. if one lever pays off four times as frequently as the other, the subject will respond on it about four times as often). After the monkey learned the task, the relative

frequencies of reinforcement opportunity between levers was changed. Control monkeys followed these changes in schedule contingencies appropriately, whereas the exposed monkeys did not. This learning deficit suggests that the methylmercury-exposed monkeys were insensitive to changes in the rules of their environment.

In contrast to these findings, methylmercury-treated monkeys were not impaired on other learning tasks (Rice, 1996a; Gilbert *et al.*, 1993). This suggests that the effects of methylmercury on cognition are not global in nature.

The doses in the studies with macaque monkeys (10-50 ug/kg/day to mother and/or offspring) resulted in blood mercury levels above those expected in human environmental exposure. The highest dose, the only dose administered in the studies of *in utero* only or postnatal only exposure, resulted in peak blood mercury levels during infancy of 0.8-1.2 ppm. In the study of pre- plus postnatal exposure, doses of 10, 25, or 50 ug/kg/day were given to the mother during pregnancy and the offspring from birth to 4 years of age. Unfortunately, only a single infant was born in the lowest dose group; the maternal blood level was 37 ug/L, and the infants' blood at birth was 46 ug/L (Rice, 1989a). The infant born at the 10 ug/kg/day dose was as impaired as individuals at higher doses. The effects observed on sensory systems were robust, although the monkeys appeared normal upon observation until middle age (see section on delayed toxicity). A no-effect level was not identified. Testing on many of these endpoints occurred years after cessation of dosing, indicating that the effects were permanent.

Behavioral effects in rodents

Methylmercury-induced neurotoxicity in the adult rodent is manifested mostly as impairment to motor systems. Methylmercury neurotoxicity as a result of developmental exposure was identified in the mouse by Spyker *et al.* (1972), who reported retarded growth and increased mortality in pups exposed *in utero*, with no obvious effect on motor function. Neurotoxicity was revealed when these mice were forced to swim, however, displayed as abnormal swimming movements and posture. A number of subsequent studies in rats or mice exposed to high doses of methylmercury during several days of gestation demonstrated gross neurological signs, changes in activity, or impairment on simple learning tasks, usually in conjunction with decreased maternal or pup weight, or increased pup mortality (Reviewed by Rice, 1996a).

Methylmercury has been chosen as a model agent for the validation of various test batteries and/or determination of inter-laboratory reliability because of its potent action as a neurotoxic agent in humans. In a collaborative study involving six laboratories in the United States, the effects of 2.0 or 6.0 mg/kg of methylmercury administered on gestational days 6-9 were studied on negative geotaxis, olfactory orientation, auditory startle habituation, activity, activity following a pharmacological challenge, and a visual discrimination task (Buelke-Sam *et al.*, 1985). Facilitation of auditory startle at the high dose of methylmercury was reliably observed across laboratories, with inconsistent or minimal effects on activity, pharmacological challenge, and the discrimination task, in the presence of overt signs such as decreased weight gain and delayed developmental landmarks. Additional research with a different battery of tests using a subset of the rats from the U.S. collaborative study revealed delayed righting and swimming ontogeny and decreased activity (Vorhees, 1985). Impairment was also observed on performance in a complex water maze, a task heavily dependent upon intact motor function. Most effects were observed only at the high dose.

In a collaborative study in Europe, dams were exposed to methylmercury in drinking water during pregnancy and lactation. Delayed sexual maturity and impaired righting and swimming ability were observed in the offspring (Suter and Schön, 1986). Assessment of complex learning measured by visual discrimination reversal and spatial delayed alternation performance revealed increased response latencies and an increased incidence of failure to respond during a trial, with no effect on accuracy of performance (Schreiner *et al.*, 1986; Elsner, 1986). In addition, the pattern of locomotor behavior in a complex activity monitor differed between control and methylmercury-treated offspring, with treated rats exhibiting less behavioral diversity. In a follow-up study involving five European laboratories, dams were exposed to methylmercury in doses of 0.0025-5.0 mg/kg/day on days 6-9 of gestation (Elsner *et al.*, 1988). This study in general confirmed results of the previous study with respect to the lack of effect on accuracy of performance in the visual discrimination and delayed alternation tasks. Methylmercury-treated offspring exhibited delayed vaginal opening, impaired swimming behavior, decreased locomotor activity, increased amplitude in auditory startle, and decreased activity on a variety of endpoints in the learning tasks. Most effects were observed only at the highest dose, while impaired swimming ability, increased auditory startle, and failure to respond on a spatial alternation task were observed at 0.5 mg/kg. Delayed vaginal opening was observed at 0.025 mg/kg, the lowest dose at which an effect was observed.

In another study in which methylmercury was used to validate a test battery, dams were dosed on days 6-15 to doses of 1, 2, or 6 mg/kg of methylmercury (Goldey *et al.*, 1994). No effects were observed on T-maze alternation, locomotor activity, amplitude or habituation of auditory startle, observational assessment, or olfactory discrimination at the lowest two doses. (The highest dose was lethal.)

In a pair of studies specifically designed to be sensitive to the known effects of methylmercury neurotoxicity in the rodent, rat dams were gavaged with methylmercury on days 6-9 of gestation at doses between 0.005 and 0.50 mg/kg (Musch *et al.*, 1978; Bornhausen *et al.*, 1980). Offspring were impaired in their ability to perform on a DRH schedule of reinforcement, in which a number of responses on a lever were required in a specified (short) period of time. Methylmercury-treated offspring performed normally when required to press a lever twice within one second to be reinforced (DRH 2/1), but not when the response requirement was incrementally increased to DRH 4/2 and then DRH 8/4. Both male and female rats were reliably affected at a dose of 0.01 mg/kg, the lowest dose at which effects have been observed in rodents. The robust effects observed on this paradigm may be the result of motor impairment, although cognitive deficits also may have contributed to the poorer performance of the treated rats.

Rats whose dams were exposed to 0.5 or 1.5 ppm methylmercury during gestation were trained as adults to press a small platform with a force between two defined limits (Elsner, 1991). The exposed rats were impaired on this task, which could reflect sensory and/or motor impairment. These rats also displayed impaired swimming ability, which could also result from both sensory and motor deficits. These results replicated previous findings (Elsner *et al.*, 1988). Some individuals had tremors, clearly a motor effect.

In a study of several aspects of behavior, mouse dams were exposed to 0, 4, 6, or 8 pm methylmercury in drinking water during gestation and lactation (Goulet *et al.*, 2003). Pups were tested on rotorod (a test of gross motor function), spatial alternation (a test of working memory), and locomotor activity. Working memory was impaired in females in the two highest dose groups on one of two tests of working memory, and locomotor activity was decreased in females

in all groups. This study reported cognitive effects in mice in the absence of gross motor impairment as measured by ability to stay on a rotating rod. Similar effects on working memory were observed in a previous study by this group of investigators (Doré *et al.*, 2001)..

In a study on the potential interaction of methylmercury and PCBs on behavior, rat dams were exposed during pregnancy to 0.5 ppm methylmercury in drinking water to postnatal day 16 (Widholm *et al.*, 2004). Offspring were tested on a spatial memory task (delayed spatial alternation) beginning at 110 days of age. Methylmercury-exposed rats were impaired on this task across all delay values, suggesting a cognitive deficit other than memory. There was not an interaction between methylmercury and PCBs in this study.

It is clear that the most salient effect of methylmercury exposure in the rodent is impairment of motor function, particularly on test batteries. Results of tests of cognitive function were largely negative or showed a very weak high-dose effect. However, testing on more sophisticated tasks revealed cognitive impairment. (See section on delayed neurotoxicity for description of other studies in which cognitive impairment in rodents was reported.) Little research has been performed in the rodent on the effects of methylmercury exposure on sensory system function. *In utero* exposure has been reported to result in changes in visual evoked potentials (Zenick, 1976; Dyer *et al.*, 1978). Goldey *et al.* (1994) found no effect on auditory threshold for pure tones.

Evidence for long-term and delayed effects

Effects in animals

The possibility that methylmercury may produce toxicity during old age was recognized early. Mice exposed to methylmercury *in utero* displayed abnormalities of various sorts as these animals aged not present earlier, including kyphosis, obesity, apparent immune impairment, and severe neuropsychological deficits (Spyker, 1975).

Evidence of delayed neurotoxicity as a result of developmental exposure to methylmercury has also been observed in monkeys in the Health Canada laboratory. When the group of monkeys exposed from birth to 7 years of age was 13 years old, it was noted incidentally by animal care staff that some of these individuals appeared clumsy and hesitant in the large exercise cages. This observation was considered to be particularly important in view of the possibility that these signs represented methylmercury-induced delayed neurotoxicity manifested many years after cessation of exposure. Observation of these monkeys in the large cages in which they had exercised and socialized since infancy revealed clumsiness in some treated individuals, a tendency for the hind feet to slip down the bars when climbing, and a preference for climbing from area to area rather than jumping. Assessment by a veterinarian revealed a higher incidence of failure to respond to a light touch or pin prick to the hands, feet, or tail (Rice, 1996b). In a test of fine motor control, treated monkeys retrieved raisins from recessed wells more slowly than controls, with some treated monkeys having difficulty removing the raisins from deep compartments. These monkeys had undergone routine clinical assessment of sensory and motor function from infancy to about four years of age, with no signs of toxicity noted. The observation of overt toxicity at age 13, six years after cessation of dosing, therefore represents delayed neurotoxicity as a consequence of methylmercury exposure. During old age, some of these individuals had protruding tongues, which was considered indicative of perioral hypoesthesia, a recognized effect of methylmercury poisoning. The group of monkeys exposed *in utero* to four years of age were also slower than controls to retrieve raisins from recessed

compartments, even though these monkeys were not overtly clumsy. While it was not possible to rule out motor damage in these groups of monkeys, it seemed reasonable to assume that the observed slowness and clumsiness was at least partly the result of somatosensory damage, based on the results of these relatively crude assessment procedures. Objective assessment of somatosensory function confirmed impairment in the ability of these monkeys to detect vibration in the fingers. (See section on behavioral effects in animals.)

The ability to detect pure tones over a range of frequencies was examined at 11 and 19 years of age in the group of monkeys exposed during gestation and continuing to four years of age (Rice, 1998). At the first assessment, monkeys in the high-dose group were impaired at higher frequencies, whereas at the second assessment, the high-dose group was impaired at more frequencies relative to controls, and the lower-dose individuals were also impaired. This represents delayed neurotoxicity for this functional domain, and demonstrates an interaction of aging and previous methylmercury exposure in these monkeys. Visual function was also reassessed in both cohorts of monkeys during old age (Rice and Hayward, 1999), and compared to results from assessment at younger ages. Visual function declined in all animals as a result of aging, with no differential effect produced by methylmercury. However, some treated individuals displayed mild constriction of visual fields that had not been present when younger. Constriction of visual fields is a hallmark of high exposure to methylmercury in adults.

The effect of methylmercury exposure was studied in mice exposed to 1 or 3 ppm perinatally or over the lifetime (Weiss *et al.*, 2005). Mice in all groups were impaired on landing foot splay (an assessment of gross motor integrity), wheel running, and delayed alternation. There was an interaction between performance and age at testing, which was different for different measures. These data provide additional evidence for the interaction of aging and methylmercury exposure on neurotoxicity.

Evidence for delayed neurotoxicity was documented in a study of rats exposed to methylmercury during gestation and until postnatal day 16 (Newland and Rasmussen, 2000), using the D̃RH schedule described above. This task requires a sustained motor response. Rats were tested beginning at about 120 days old and continued until they were more than 900 days of age. The rate of response declined in all groups, but declined at younger ages in methylmercury-exposed groups in a dose-dependent manner. These results indicate an interaction of aging and developmental methylmercury exposure.

The effect of gestational and lactation exposure to methylmercury on performance of aging rats was also explored in the concurrent random interval-random interval schedules of reinforcement (Newland *et al.*, 2004). Performance on this schedule was also assessed in monkeys, described above. The rate of each rat's ability to adapt was measured by determining how quickly the relative response rate changed following a change in the relative payoff on the two levers. There was no difference on this measure or other measures of performance in 1.7-year-old rats whose mothers were exposed to 0.5 or 6.4 ppm mercury in food. When their 2.3-year-old littermates were tested at 2.3 years of age, however, both groups of treated rats were slower to make the transition. These results demonstrate failure to adapt to new environmental contingencies (learning) in old rats exposed developmentally to methylmercury, but not in younger ones.

Effects in humans

There is also evidence for delayed neurotoxicity as a result of methylmercury exposure in humans. It was recognized early that the onset of Minamata disease was delayed in some individuals, by as long as several years, and that manifestations of disease became worse over time in some cases (Igata *et al.*, 1993; Tsubaki and Irukayama, 1977). Hundreds of cases were diagnosed in Niigata years after the presumed cessation of ingestion of contaminated fish, although some individuals may well have been ill before presenting themselves for diagnosis. Interestingly, the frequency of signs showed a different distribution compared to early-onset Minamata disease (Tsubaki and Irukayama, 1977): in particular, the lower incidence of constriction of visual fields observed in "late onset" Minamata disease. In patients diagnosed after 1974, the frequency was less than 5%. On the other hand, disturbances of somatosensory function were present in almost every individual. This is consistent with the somatosensory deficits observed in aging monkeys.

An important study of 1144 patients over the age of 40 with Minamata disease, representing over 90% of diagnosed patients, and an equal number of age and gender matched controls, was undertaken to determine the functional ability of people with Minamata disease as they aged (Kinjo *et al.*, 1993). Subjects completed a questionnaire of subjective complaints and ability to perform activities of daily living (ADLs) including eating, bathing, face washing, dressing, and using the toilet. People with Minamata disease had higher rates of response than controls in all 18 subjective complaints investigated in the study. Perhaps the most important finding, however, was that for ADLs, the relative deficit between controls and people with Minamata disease increased with increasing age in a statistically-significant manner. In other words, the interference of Minamata disease with the individual's ability to perform the necessities of daily life grew worse as the individual aged, even though exposure to methylmercury had ceased 20-30 years previously. These findings represent concrete evidence of "delayed neurotoxicity" in a human population as a result of exposure to an environmental neurotoxicant.

Individuals exposed to methylmercury in the Japanese poisoning episode reported paresthesias of the distal extremities 30 years after cessation of exposure (Ninomiya *et al.*, 2005). Increased touch thresholds were present in both proximal and distal extremities, as were two-point discrimination thresholds in forefingers and lips of 3 MD individuals. Similar effects were also found in 32 persons exposed to methylmercury but not officially diagnosed as having MD. Median hair mercury levels in the group not diagnosed with MD was 37 ppm in 1960, and 2.4 at the time of testing (the hair mercury levels of the control group was 2.8). For the group with MD, hair levels in 1960 were 39-65 ppm. Results were interpreted as indicative of damage to somatosensory cortex. This was also suggested as the underlying damage responsible for somatosensory deficits in the monkey studies (Rice, 1996b). A similar study of individuals with Minamata Disease 60-79 years of age assessed ability to detect abrasive papers of various grits (Takaoka *et al.*, 2004). Subjects included individuals with MD, a group from Minamata without numbness who were not diagnosed with MD, and a control group from another area. The ability to detect whether pairs of papers were different (difference threshold) was determined. The MD group had the biggest difference thresholds, and the group from Minamata without MD also had greater difference thresholds than controls. Many of the MD group also had other signs of MD, including ataxia and constriction of visual fields. Hair mercury levels were 2.8 ppm in controls 60-79, and 2.4 ppm in MD individuals. These studies do not definitively document delayed neurotoxicity, since it is unknown whether these individuals were impaired in the 1960s.

Nonetheless, it is clear that exposure to methylmercury four decades before evaluation resulted in permanent impairment.

Although the molecular mechanisms of delayed neurotoxicity remain unknown, there are a number of relatively obvious ways in which toxicity could continue to be expressed or even exacerbated (and which are not mutually exclusive): 1) mercury stores in the body, specifically in the nervous system, continue to exert a toxic influence, 2) damaged neurons or other nervous system cell types may die prematurely, or 3) normal cells, required to compensate for damaged or missing cells, may undergo accelerated aging. There are at least limited data relevant to the first suggestion. Approximately 8 months after cessation of chronic dosing with methylmercury in the monkey, and months after blood mercury levels decreased below the detection level, brain contained significant amounts of total mercury (Rice, 1989b). In a study examining speciation of mercury after chronic methylmercury exposure in the monkey (Vahter *et al.*, 1994, 1995), the proportion of inorganic mercury increased with duration of exposure, and was highest if a period of several months elapsed between cessation of exposure and autopsy. In fact, inorganic mercury levels remained relatively constant whereas methylmercury levels decreased drastically. These data suggest that the half-life of mercury in the brain is longer than in blood after methylmercury exposure, and that this is at least in part the result of conversion to inorganic mercury in brain. Inorganic mercury was concentrated in astrocyte and reactive glia following chronic low-level methylmercury or inorganic mercury exposure in the monkey (Charleston *et al.*, 1994, 1995). The authors suggest that these astrocytes and possibly microglia are the primary sources of demethylation of methylmercury. Astrocyte and/or microglia cell numbers decreased in various brain areas following methylmercury exposure in the absence of changes in neuronal cell numbers (Charleston *et al.*, 1994, 1995, 1996). The authors suggest that this may represent the proximal cause of neurotoxicity, although the degree to which these findings would extrapolate to lower exposures is unknown. The long-term consequences of methylmercury exposure in adults in Minamata is consistent with results from the monkey studies.

Mechanisms of toxicity

It is very clear from the episodes of human poisoning that the fetus and infant were more sensitive to the effects of methylmercury than the adult, and that effects were qualitatively as well as quantitatively different. In both the adult and developing organisms, methylmercury is found throughout the brain, so that differential distribution probably does not account for the different pattern of pathology.

The brain develops by a series of processes that are exquisitely choreographed both spatially and temporally. Most of these processes are unique to the developing brain; therefore toxicants can affect the developing brain in ways not possible in the adult brain. These processes include neurogenesis and proliferation, migration of neurons from their origin to their final locations in the brain, differentiation of the immature neurons to their final cell type, the formation of synapses (connections) between cells and thereby between brain areas, birth and differentiation of numerous supportive cell types responsible for maintenance of normal brain development and function, myelination (the wrapping of nerve processes in a protective sheath that increases the speed to communication between nerve cells), and apoptosis (the genetically-programmed death of cells and pruning of connections that is vital to normal brain functioning). All of these processes are affected by methylmercury exposure (Rice and Barone, 2000).

The control of brain development is orchestrated by a large assortment of molecules (signal transducers) that regulate the integration of genetic and epigenetic events. The effects of methylmercury on many of these systems has been investigated, and the mechanisms of methylmercury neurotoxicity are well characterized (Aschner and Syversen, 2005). Some of these mechanisms are relevant to adults, whereas others are particularly important during development.

An important mechanism is inhibition of glutamate uptake, and stimulation of its efflux, resulting in excitotoxic injury. Methylmercury inhibits uptake systems for cystine and cystine transport, compromising glutathione synthesis. This would result in increased susceptibility to reactive oxygen species (ROS). ROS are known to mediate methylmercury-induced neurotoxicity in a variety of experimental models. There has also been a substantial amount of research on the cascade of events leading to glutamate neurotoxicity produced by methylmercury.

The ability of methylmercury to interfere with neuronal migration, a salient feature of developmental methylmercury poisoning, is undoubtedly the result of interference with various microtubular elements, including N-CAM, astrotaction, and L1 (Aschner and Syversen, 2005). Methylmercury also interferes with mitosis (Rodier *et al.*, 1984), which would inhibit cell proliferation. It may be the case that at lower levels of exposure, inhibition of growth cone outgrowth, leading to decreased axonal and dendritic development, plays an important role in developmental neurotoxicity. Despite the relatively robust literature on the mechanisms of methylmercury-induced neurotoxicity, the reasons for differential pattern of neuropathological damage in the adult and developing brain are not understood.

Cardiovascular Effects

Studies in adults

There is evidence from several studies that increased methylmercury body burden is associated with cardiovascular or coronary disease, including heart attack and stroke. The potential for methylmercury to produce cardiovascular (CV) and coronary disease was identified as an important concern (EPA, 2001) that requires further analysis. Studies have identified effects at hair mercury levels within the range of exposures in the U.S. The relatively sensitivity of CV versus developmental neurotoxic effects is unknown, since the required dose-effect modeling has not bee performed for CV effects. The evidence has been recently reviewed (Stern, 2005).

In a study of 2500 men in Finland, acute myocardial infarction (AMI) and fatal coronary events were followed for an average of 6 years (Salonen *et al.*, 1995). Hair samples for mercury analysis and dietary data were obtained at the beginning of the study. The estimated mean dietary intake of methylmercury was 7.6 ug/day, about the same as that corresponding to the EPA reference dose of 7.0 ug/day for a 70 kg man. Mean hair mercury concentration was 1.9 ppm. Hair concentrations in the upper tertile (2 ppm) were associated with increased myocardial infarction (MI) (relative risk = 1.6). There were non-statistically significant associations between hair mercury concentration and death from coronary heart or CV disease. Fish intake of 30 g/day was also associated with these outcomes. A follow-up study (Rissanen *et al.*, 2000) examined the effects of methylmercury and omega-3 fatty acids on these same endpoints, the latter of which is believed to be protective against coronary disease. An interaction of serum omega-3 fatty acids (DHA + DPA) and methylmercury in hair was found. Men with hair mercury levels above 2 ppm

received less benefit from omega-3 fatty acids than those with lower levels, with no reduction in risk at all across the upper three quintiles of omega-3 fatty acid blood levels. This suggests that higher body burdens of methylmercury may negate the protective effects of fish oils. A further follow-up in this cohort was performed in 1871 men 42-60 years of age an average of 13.9 years after study initiation (Virtanen *et al.*, 2005). Men with the highest tertile of hair mercury levels were at significantly increased risk for acute coronary event (1.60-fold; CI, 1.24-2.06), CV disease (1.68-fold; CI, 1.05-2.44), CHD (1.56-fold; CI, 0.99-2.40), and any death (1.38-fold; CI, 1.15-1.66) compared with men in the lower two tertiles. As in the previous study, high hair mercury attenuated the beneficial effects of omega-3 fatty acids.

A study was performed by the same group of investigators on the progression of atherosclerosis in 1014 men from eastern Finland (Salonen *et al.*, 2000). This group was a subset of those studied by Salonen *et al.* (1995). The relationship between thickness of the carotid arteries and hair mercury was determined in 1014 men with an average age of 51.9 years during initial assessment, with a second measurement made 4 years later. The upper quintile of hair mercury was 2.8 ppm. The relationship between hair mercury and increase in carotid wall thickness was highly significant in a multivariate model; in fact, the mercury effect was second only to that for systolic blood pressure. There was no apparent effect across the first four quintiles, with significant thickening in men in the highest quintile, suggesting a threshold for this effect. In their earlier study, Salonen *et al.* reported an association between hair mercury concentrations and immune titers to oxidized low-density lipids (LDL), suggesting a mechanism for the association between mercury levels and atherosclerosis in this study.

A multicenter case-control study was performed in a total of 1408 men 70 years old or younger in eight European countries and Israel (Guallar *et al.*, 2002). Cases were defined as men hospitalized with a first MI, and age-matched controls were selected for the same geographical areas as cases. Mercury exposure was determined from toenail clippings, and DHA was determined in subcutaneous fat. After covariate adjustment, the mercury concentration in cases was significantly higher than in controls. After adjustment for center, age, DHA, cardiovascular risk factors, and antioxidants, the odds ratio (OR) was 2.16 (CI, 1.09-4.29) for the upper quintile compared to the lowest quintile. As in the Rissanen *et al.* (2000) study, the results suggest that mercury antagonized the protective effect of omega-3 fatty acids. Toenail mercury is a non-standard marker of exposure. Further, it is unknown to what extent inorganic mercury exposure may have contributed to toenail mercury levels. However, there was a reasonable correspondence between mercury and DHA levels ($r = .34$); this suggests that the main source of mercury was methylmercury from fish, since the main source of DHA would also presumably be fish.

A nested case-control study of the effects of mercury exposure on coronary heart disease (CHD) was conducted in U.S. male health professionals who were 40-75 years old at recruitment (Yoshizawa *et al.*, 2002). Each of 470 cases was matched with a control for age, smoking status, and time of sampling. Toenail mercury was higher than in the Guallar study, with the dentists having twice the mercury levels of other participants. This was presumably the result of exposure to mercury vapor in their dental practice. After adjusting for risk factors, mercury levels were not associated with risk of CHD. When dentists were eliminated from the analysis, a relative risk (RR) of 1.27 was found. After further adjustment for DHA and EPA levels, the RR was 1.70. These were not statistically significant, which may be a consequence of reduced statistical

power. These results suggest that it is methylmercury that is responsible for CV risk, rather than total mercury or inorganic mercury.

A small case-control study for first-time myocardial infarction (MI) including both men and women was performed in Sweden (Hallgren *et al.*, 2001). A total of 78 cases and an equal number of controls matched for sex, age, and geographical region were recruited over a 10-year period. Blood samples were presumably collected at recruitment, as much as 10 years before the MI. Mercury was measured in erythrocytes, and EPA and DHA were measured in blood plasma. The omega-3 fatty acid concentrations were associated with decreased risk, whereas there was no effect of mercury concentration. The lack of effect may have been the result of low power, although the study was of sufficient size to detect the beneficial effects of omega-3 fatty acids. It may also be the result of the inclusion of women, who may respond differently than men. The OR for the low-fatty-acid – high-mercury group was greater than 1.0, but consisted of only four cases.

The relationship between blood pressure and blood mercury concentration was determined in women 16-49 years of age in the NHANES (Vupputuri *et al.*, 2005). There was no overall relationship between mercury levels and blood pressure. However, when women were stratified by fish consumption, there was an interaction between fish consumption and mercury levels on blood pressure. In women who had not eaten fish in the last 30 days, there was an increase in blood pressure as a function of increasing mercury quintile. For every 1.3 ug/L (interquartile range) increase in mercury level, there was a covariate-adjusted 1.83 mm mercury increase in systolic blood pressure, and a 0.61 mm mercury (nonsignificant) increase in diastolic blood pressure. This relationship did not hold among individuals who had eaten fish in the last 30 days. The authors postulated that omega-3 fatty acids in fish were protective. However, the results are puzzling since fish was presumably the source of mercury in all women. The authors did not have fatty acid levels in the women, nor did they try to estimate intake from the fish species consumed. Perhaps the beneficial effects of omega-3 fatty acids were of shorter duration than the deleterious effects of methylmercury. The average half-life in blood for methylmercury is about 50 days, so that blood mercury levels represent fish intake as long as several months previously.

Studies in children

The Faroe Island investigators examined the relationship between methylmercury exposure and blood pressure and heart rate at 7 and 14 years of age. At 7 years, systolic and diastolic blood pressure, heart rate, and heart rate variability were assessed with respect to *in utero* methylmercury exposure (Sorenson *et al.*, 1999). Cord blood mercury concentration was significantly associated with increased systolic and diastolic pressure after control for covariates, whereas maternal hair mercury was a poorer predictor. Blood pressure increased linearly as a function of log cord blood from 1 to 10 ug/L, and did not increase thereafter. The effect was greater in babies with birth weights below the mean (20.9 and 20.4 mm mercury for systolic and diastolic blood pressure, respectively, compared to 14.6 and 13.9 mm for the group as a whole). There was no effect on heart rate *per se*, but cord blood mercury was associated with decrease in heart rate variability. In boys, there was a 47% decrease in heart rate variability as cord blood increased from 1 to 10 ug/L. This was interpreted as indicative of action on the parasympathetic nervous system producing effects on both blood pressure and heart rate variability.

When the Faroe Islands cohort was reassessed at 14 years of age, associations between blood pressure and heart rate with cord blood and children's hair mercury concentrations at 7 and 14 years were determined (Grandjean *et al.*, 2004). At this later age, there were no associations between methylmercury exposure and blood pressure. Cord blood mercury concentration was associated with several parameters of decreased heart rate variability. The child's hair mercury level at 14 years was associated with one measure of variability at 14 years, which decreased after control for results at 7 years. The change was greatest at cord blood concentrations between about 1 and 10 ug/L. The interpretation of these findings for public health is not entirely clear. Decreased heart rate variability in adults following an MI predicts sudden cardiac death; however, the applicability of these findings to other adults or children is unknown. On the other hand, it is indicative of an effect on control of the autonomic nervous system, and therefore provides additional evidence for an effect of methylmercury on nervous system function in this cohort.

Animal studies

There are limited experimental data on the effects of methylmercury on CV function. In a study in adult rats, doses that did not produce gross toxicity produced increased systolic blood pressure, which persisted throughout a 9-month post-dosing observation period (Wakita *et al.*, 1987). Blood pressure increased as much as 30 mm mercury. Tamashiro *et al.* (1986) exposed male and female spontaneously hypertensive rats to methylmercury for 26 days beginning at 7 weeks of age, at doses that produced overt toxicity. Blood pressure in females increased by about 20 mm mercury; all males died soon after cessation of dosing. In an *in vitro* study, inhibition of thrombin-mediated platelet aggregation by human umbilical vascular endothelial cells was reversed in a dose-dependent manner by methylmercury Cl (Ohno *et al.*, 1995). The authors suggest that this effect is mediated through inhibition of endothelium-derived relaxing factor, and suggests a mechanism for the effects of methylmercury on both vascular tension and atherosclerosis observed in human studies.

Summary

Overall, there is reasonable support for an association between methylmercury exposure and effects on CV function, including AMI. The study of Yoshizawa *et al.* (2002), which failed to find an association in primary analyses, was flawed by the inclusion of a large percentage of men exposed to mercury vapor in the control group. As discussed by Stern (2005), there is substantial opportunity for exposure misclassification in these studies, since mercury body burden may have changed substantially between exposure assessment and adverse event. Since this would bias results toward the null, the fact that studies identified associations provide evidence for a reasonably strong effect. The potential for prenatal exposure to methylmercury to contribute to later CV disease is unknown, but any such contribution could represent an important societal burden from methylmercury exposure.

Methylmercury levels in the U.S., and comparison to mercury levels associated with health effects

The cord blood level corresponding to U.S. EPA reference dose is 5.8 ug/L. However, the maternal blood level associated with a cord blood level of 5.8 ug/L is 3.4 ug/L, based on the fact that cord blood is 1.7 times higher than maternal blood, on average. The hair mercury level associated with 3.4 ug/L is about 0.65 ppm. Studies on the body burden of mercury in individuals in the U.S. have used different values as representing elevated exposure, which is

reflected in the studies of body burdens of mercury in the U.S. discussed below. In addition, the prospective study of the effect of methylmercury on behavior of infants in the U.S. dichotomized data as above or below 1.2 ppm maternal hair mercury in ancillary analyses.

Blood and urinary mercury levels are analyzed as part of the NHANES (CDC, 2005). Blood levels for 1999-2002 are available for children 1-5, females and males 16 and over, and females 16-49 years. For children, the median blood mercury level was 0.3 ug/L, with a 95th percentile of 2.3 (1999-2000) or 1.9 (2001-2002) ug/L. For women of childbearing age, the median was 1.02 and 0.83 ug/L for the two time periods, with 95th percentiles of 7.10 and 4.60 ug/L. The 95th percentile would correspond to hair mercury levels of approximately 1.3 or 0.9 ppm for the two time periods. Approximately 15.7% of women of childbearing age had total blood mercury levels >= 3.5 ug/L (Mahaffey *et al.*, 2004) in 1999-2000. For individuals who eat fish more than three times a week , the 95th percentile hair mercury was 2.00 ppm for children 1-5 years old, and 2.75 ppm for women of childbearing age in 1999-2000 (McDowell *et al.*, 2004).

Using the NHANES database, hair mercury levels were examined for various ethnic groups, including "other" (Asians, Pacific Islanders, Native Americans, and multiracial) women of childbearing age (Hightower *et al.*, 2006). The percentage of women with blood mercury levels greater than 5.8 ug/L, as well as above 3.5 ug/L, were determined. For whites, 11% were above 3.5 ug/L, and 5.8% were above 5.8 ug/L. For "other" races, 27% were above 3.5 ug/L, and 16.6% above 5.8 ug/L. These ethnic groups ate twice as many fish meals as whites or blacks, and three times as many as Mexican Americans.

The NHANES survey is designed to be representative of the U.S. population. However, this survey does not adequately sample high-end fish consumers. In a survey of volunteers from a random-dial survey of women of childbearing age in 12 states, mean hair mercury levels varied between states from 0.21 to 1.23 ppm, with higher levels in coastal states (Knobeloch *et al.*, 2005). Fifty percent of women in NJ had hair levels above 1 ppm, as did 41% of women in CT. The 95th percentile for all women who had eaten 20 fish meals in the last month was 2.29 ppm, whereas it was 0.19 ppm for women who had not eaten fish. In a study of pregnant women recruited through obstetric practices in NJ, about 10% had hair mercury levels above 1 ppm, with about 1% above 6 ppm (Stern *et al.*, 2001). Increased mercury levels were associated with increased fish intake.

A recent survey of volunteers recruited through environmental organizations reported hair mercury levels in 6503 individuals collected in 2004 and 2005, and the association between hair mercury concentrations and fish intake (Environmental Quality Institute, 2005). Children less than 1 year old had median hair mercury levels of 0.29 (girls) and 0.17 (boys) ppm, with 7.7 percent of girls having hair mercury levels greater than 1.0 ppm. For women of childbearing age, the median was 0.43 ppm, with 22.6% having hair levels above 1 ppm. Individuals over 50 also had a substantial percentage of people with hair mercury levels above 1 ppm (24 and 29% for females and males, respectively). Hair mercury levels were associated with higher tuna fish and total fish consumption, but not with dental amalgams. Since this was a self-selected population, the distribution of levels presumably is not representative of the U.S. population as a whole. Nonetheless, the study provides further evidence of a strong association between fish consumption, including canned tuna, and increased methylmercury body burden. The study also documents that at least for some populations, a substantial percentage of individuals have methylmercury body burdens greater than that associated with the RfD.

In a study in high-end fish consumers in a private medical practice, blood mercury levels ranged from 2.0 to 89.5 ug/L for 89 individuals (Hightower and Moore, 2003). Mercury levels of 7 children were determined in hair or blood, with the highest levels being 14.8 ug/g in hair for a 7-year-old, above the BMD from the Faroe Islands study for defined effects.

The average exposures in the three large longitudinal studies of neuropsychological effects in children were similar, based on maternal hair mercury concentrations. The geometric mean in the Faroe Islands study was 4.3 ppm (interquartile range 2.6-7.7 ppm), and in the Seychelles Islands study the median was 5.9 ppm (interquartile range 6.0 ppm). In the New Zealand study, the "high" exposure group were women with >6 ppm, and these were matched with three times as many children whose mothers had lower hair levels. The average exposures in these studies are higher than those observed in the U.S. However, the ranges overlap those of U.S. women. For example, the cord blood range in the Faroe Islands study was 0.90-351 ug/L, which would correspond to a maternal blood mercury level of 0.52-203 ug/L based on an average cord:maternal blood ratio of 1.7. The Faroe Islands population clearly includes women with higher exposures than those in the U.S., but the range overlaps that of U.S. women. There is no evidence for a threshold for adverse effects within the range of exposures in the Faroe Islands. In the recent MA study that documented adverse effects (Oken *et al.*, 2005), the mean maternal hair mercury was 0.55 ppm and the 90th percentile was 1.2 ppm. This would correspond to approximately maternal blood levels of 2.7 ug/L and 5.8 ug/L, respectively. The study by Jedrychowski *et al.* (2006) identified a significantly increased risk for developmental delay on the Bayley Scales of Infant Development at one-tenth the RfD, and at less than the median of blood mercury levels of women child-bearing age in the U.S. Therefore it appears that effects of exposure to methylmercury are present within the range of body burdens of U.S. women.

The body burdens of men in the studies on CV function and heart disease also overlap those in the U.S. The mean hair mercury concentration in the Salonen *et al.* (1995), Risanen *et al.*, (2000), and Virtanen *et al.* (2005) studies of about 2 ppm is equivalent to about the 95th percentile for women in NHANES (corresponding data for men are not available, but mercury levels are probably higher). This level was associated with an increased risk of adverse CV events, including MI. In the Yoshizawa *et al.* (2002) study, mean toenail mercury concentration in non-dentists was 0.45 ppm, which presumably represents levels in the U.S. The toenail mercury level associated with the highest quintile of exposure in the Guallar *et al.* (2002) study was 0.7 ppm, suggesting that exposures in that study, in which increased risk of MI was observed, is not much, if at all, different than exposures in the U.S.

Estimation of societal costs associated with methylmercury exposure in the U.S.

Of considerable importance is a recent analysis performed by Dr. Louise Ryan for the U.S. EPA of all three longitudinal studies reporting that, in fact, the results from the three studies modeled by the NRC are not discordant with respect to effects on IQ (Ryan, 2005; EPA, 2005). Ryan (2005) modeled results for IQ from the WISC-R at 6 years from the New Zealand study and the WISC-III at 9 years from the Seychelles study. The Faroe Islands study did not assess full-scale IQ at 7 years, but did measure performance on three subtests of WISC-R: Digit Spans, Similarities, and Block Design. These measures were combined using structural equations modeling (Budtz-Jørgensen *et al.*, 2002). Bellinger (2005) points out that the correlation between full-scale IQ and results on Similarities plus Block Design is 0.885. Adding the third subtest,

Digit Span, would presumably increase the correlation. This provides reassurance that combining the scores on these subtests is a valid estimate of full-scale IQ. The relationship between mercury hair levels and full-scale IQ was estimated for each study individually, and an integrative analysis was performed combining all three studies. For each 1 ppm increase in maternal hair mercury from 1 to 10 ppm, IQ in the offspring decreased by 0.13, 0.13, and 0.12 point for the New Zealand, Seychelles, and Faroe Islands studies, respectively. The integrative analysis of all three studies yielded a decrement of 0.13 IQ point for every 1 ppm increase in maternal hair mercury. This analysis provides evidence that the three longitudinal studies are in fact concordant with respect to effects on IQ. The Ryan/EPA analysis also modeled other functional domains from the three studies in addition to IQ, and found concordance for multiple domains.

A quantitative risk-benefit analysis was performed by the Harvard Center for Risk Analysis of changes in fish consumption in the U.S. population for several hypothetical scenarios. This exercise, sponsored by the fishing industry, focused on the potential benefits of omega-3 fatty acids on coronary heart disease (König *et al.*, 2005), stroke (Bouzen *et al.*, 2005), and cognitive development. The authors of the paper addressing heart disease did not include potential risks from methylmercury exposure. Four of the five authors of the paper on the benefits of omega-3 fatty acids (Cohen *et al.*, 2005a) also analyzed the risks of methylmercury exposure in a separate paper (Cohen *et al.*, 2005b). For the effects of mercury, the authors relied on the analyses of the three studies by the NRC. The various domains were weighted in the analysis, with a value of 1.0 to tests of general intelligence, 0.6 to language and learning/achievement, 0.3 for attention, and 0.2 for motor. In addition, each study was weighted on the basis of sample size and various considerations of the quality of each study. The weights were 1.0, 0.88, and 0.16 for the Faroe Islands, Seychelles, and New Zealand studies, respectively. All analyses were integrated into an overall risk-benefit analysis (Cohen *et al.*, 2005c). Scenarios for changes in fish consumption for women of childbearing age included (1) elimination of fish with "medium" and "high" mercury levels (defined as >= 0.14 ppm) and substitution of an equal amount of "low" mercury fish, (2) a decrease of total fish consumption by 17%, or (3) an increase of fish consumption by 50% without changing the species consumed. Under all scenarios, the loss of IQ associated with methylmercury intake was greater than the gain conferred by consumption of omega-3 fatty acids. Under the first scenario, the net quality-adjusted life years (QALYs) for methylmercury increased by 45,000, and for DHA 4,700. Under the second scenario, the methylmercury benefit was 17,000 QALYs, and the lost for DHA was –5,800, for a net gain of 11,000. Under the final scneario, nondiscriminate increase in fish intake, the methylmercury impact was –49,000, and the DHA benefit was 17,000, for a net loss of –32,000 QALYs.

Trasande *et al.* (2005) used data from the Faroe Islands study to estimate the cost associated with exposure to methylmercury, based on IQ loss in children. They considered a cord blood level of 5.8 ug/L to be that associated with no impairment, based on data from the Faroe Islands. A maternal blood mercury level of 4.84 ug/L was considered to be associated with this cord blood level using the cord:maternal blood ratio found in the Faroe Islands. A doubling in blood mercury concentration above 4.84 ug/L in maternal blood was considered to be associated with loss of 0.85 to 2.4 IQ points. A number of factors were varied in a sensitivity analysis. A 1 ug/L increase in hair mercury concentration was considered to be associated with a loss of 0.59 to 1.24 IQ points, and cord:maternal blood ratio was varied from 1:1 to 1.7:1. The upper bound

estimate assumed that children born to women with blood mercury levels of 3.5-4.84 ug/L suffer no loss in IQ, and the lower bound estimate assumed that children born to women with mercury concentrations of 4.84-5.8 ug/L suffer no loss in IQ. Using data on the association between IQ and lifetime earnings, the cost of the loss of IQ produced by methylmercury exposure was estimated to be $8.7 billion annually in 2000 US$ (range $2.2-$43.8 billion). They estimated that $1.3 billion (range $0.1-$6.5 billion) was attributable to mercury emission from U.S. power plants.

In a subsequent analysis, these authors estimated the cost of the increase in mental retardation as a result of environmental exposure to methylmercury (Trasande *et al.*, 2006). A downward shift in the IQ of the population would result in an increase in the number of individuals with mental retardation (MR), clinically defined as an IQ less than 70. The authors used the published data from Mahaffey *et al.* (2004) on the percentage of women in the U.S. population with blood mercury concentrations of 4.84-5.8, 5.8-7.13, 7.13-15, or 7.13-15.0, and > 15.0 ug/L from NHANES 1999-2000. As in the previous analysis, they assumed that all women within each category were at the lowest exposure. In the base-case analysis, a cord:maternal blood ratio of 1.7:1.0 was assumed, although in sensitivity analysis, a range of 1-1.7 was applied. Both linear and logarithmic models were applied, with a doubling in mercury concentration associated with 0.59-1.24 or 0.85-2.4 IQ points respectively, for a doubling in mercury concentration. Sensitivity analyses assumed that children of women with blood mercury concentrations below 5.8 or 4.84 ug/L suffered no IQ loss. They estimated that methylmercury exposure is associated with 1566 (range 376-14,293) excess cases of MR annually, or 3.2% of MR cases in the U.S. The cost of MR included direct costs, including medical costs, and excluded indirect costs such as lost wages. The cost was estimated at $2.0 billion/year (range $0.5-$17.9 billion). The fraction attributed to American power plants was $289 million (range $35 million-$2.6 billion).

The costs estimated in the two analyses should be added together to estimate the cost in lost IQ attributable to methylmercury exposure in the U.S. population. The Trasande *et al.* (2005, 2006) analyses relied on an analysis by Salkever (1995) for the relationship between IQ and lifetime earnings. This analysis was based on data from the National Longitudinal Survey of Youth (NYSY), conducted by the U.S. Department of Labor (http://www.bls.gov/nls/). The initial survey was begun in 1979, and has followed a stratified random sample of 12,656 individuals who were between the ages of 14 and 22 when first interviewed. A number of variables are included in the yearly longitudinal follow up. This database allows the determination of the association between IQ at 14-22 years of age and future earnings. As discussed by Weiss (2000), IQ predicts many other outcomes in addition to earnings. A 3% (3 point) increase in IQ is associated with a 12-28% reduction in children living in poverty in the first 3 years of life, out of wedlock births, low-weight births, welfare recipiency, children without parents, high school dropout rate, poverty rate, and males interviewed in jail, depending on the variable. A number of these effects could be monetized in a relatively straightforward manner.

Developmental methylmercury exposure produces neuropsychological effects in addition to decrements in IQ, and which are not directly assessed in IQ tests. In the Faroe Islands study, two of the most sensitive endpoints were the Boston Naming Test, which assesses word retrieval (expressive vocabulary), and the California Verbal Learning Test, which assesses processing and memory of information presented verbally. As discussed by Bellinger (2005), these abilities are not assessed by the WISC-R or the WISC-III, and yet defiicts on these abilities could put a child

at considerable disadvantage in the classroom. Similarly, deficits in attention, identified on the continuous performance task in the Faroe Islands study, would also make it difficult for a child to learn. Attention deficits are not associated with IQ. The consideration of only the effects of IQ, and only related to lost wages and increase in MR, undoubtedly substantially underestimates the cost of the effects of methylmercury exposure on the developing brain.

Also not included in the various monetization exercises is quantification of the CV and coronary effects of exposure to methylmercury in adults. MI, CV disease, and death were associated with increased hair mercury concentrations in a longitudinal study in Finland (Salonen *et al.*, 1995, 2000; Rissanen *et al.*, 2000; Virtanen *et al.*, 2005). An additional study identified an increased risk of MI and mercury body burden (Guallar *et al.*, 2002), as well as a study linking increased risk of CVD and methylmercury exposure after exclusion of dentists exposed to mercury vapor (Yoshizawa *et al.*, 2002). Exposures were within the range of the U.S. population, as discussed above. The shape of relationship between adverse outcome and methylmercury exposure has not been determined; however, the results from these studies suggest that there may be significant morbidity associated with methylmercury expsoure within the U.S. population. Any health-protective effects of omega-3 fatty acids are included in the analyses in these studies, since fish are the only source of methylmercury exposure. Any potential effects of methylmercury on blood pressure could also result in significant cost. On a population basis, small increases in blood pressure, even within the "normal" range, result in significant increases in MI and death. For example, in the Framingham study, there was a monotonic increase in MI and death from MI as diastolic blood pressure increased, starting as low as 70 mm mercury (EPA, 1985). In the EPA assessment on the health costs associated with lead exposure, the costs associated with CV effects were greater than that associated with lost wages as a result of decreased IQ (EPA, 1985). Whether this would also be the case for methylmercury is unknown. However, these effects could add significantly to the monetary burden produced by methylmercury exposure.

Finally, the potential for methylmercury to produce cognitive deficits in adults, or to accelerate the aging process, remains unaddressed. There is substantial evidence that relatively high exposure to methylmercury that is nonetheless insufficient to produce a diagnosis of MD results in sensorimotor impairment many years later, which may result in impairment of an elderly individual's ability to live independently. The degree to which this may be manifest in the U.S. population, or sub-population of high fish consumers, has not been studied. Similarly, cognitive effects have been observed in adults at body burdens that overlap those in the U.S. There is also anecdotal evidence that consumers of fish with high mercury levels in the U.S. suffer adverse health consequences (Hightower and Moore, 2003). These effects cannot be monetized at this time. However, recognition that these effects may be important consequences of methylmercury exposure underscores the fact that the monetary burden of methylmercury exposure in analyses performed to date is underestimated, perhaps substantially.

Table I. Tests modeled by NRC, functions assessed, and potential societal relevance

Study	Test	Domain/Function Assessed	Societal Relevance
Seychelles	Bender Copying Errors	Visuospatial	Math performance
	McCarthy GCI	Full-scale IQ	School performance, intelligence
	WJ Applied Problems	Ability to solve problems	Academic skills
	CBCL	Social and adaptive behavior	Antisocial behavior, need for therapeutic services
	Preschool Language Scale	Broad-based language	Learning, intelligence, school performance
	WJ letter/word recognition	Word recognition	Reading ability, school performance
Faroes	Finger Tapping	Motor performance	Motor speed/neuropathy
	CPT Reaction Time	Vigilance, attention, information processing speed	Intelligence, school behavior and performance
	Bender Copying Errors	Visuospatial	Math performance
	Boston Naming Test	Expressive vocabulary	Reading, school performance
	CVLT: Delayed Recall	Memory	Learning ability, school performance
New Zealand	TOLD Language Development	Broad-based language	Literacy skills, learning, school performance
	WISC-R: PIQ	Performance IQ, e.g. visuospatial, sustained attention, sequential memory	Learning, school performance
	WISC-R: FSIQ	Full-scale IQ, e.g. PIQ + verbal processing, expressive vocabulary	Learning, school performance
	McCarthy Perceptual Performance	Performance IQ, e.g. visuospatial, audition, memory	Learning, school performance
	McCarthy Motor Test	Gross and fine motor skills	Motor system integration

Abbreviations: WJ = Woodcock-Johnson Tests of Achievement; CBCL = Child Behavior Check List; CPT = Continuous Performance Test; CVLT = California Verbal Learning Test; TOLD = Test of Language Development; WISC-R:PIQ = Wechsler Intelligence Scale for Children-Revised Performance IQ; WISC-R:FSIQ = Wechsler Intelligence Scale for Children-Revised Full-Scale IQ.

From EPA, 2001, p. 4-51

Table II. BMDLs, ingested dose, and RfDs for various endpoints from the Faroes Islands, New Zealand, and the NRC integrative analysis[a]

Test[b]	BMDL ppb mercury cord blood	Ingested dose µg/kg/day[c]	RfD µg/kg/day[d]
BNT Faroes			
Whole cohort	58	1.081	0.1
PCB adjusted	71	1.323	0.1
Lowest PCB	40	0.745	0.1
CPT Faroes			
Whole cohort	46	0.857	0.1
PCB adjusted	49	0.913	0.1
Lowest PCB	28	0.522	0.05
CVLT Faroes			
Whole cohort	103	1.920	0.2
PCB adjusted	78	1.454	0.1
Lowest PCB	52	0.969	0.1
Finger Tap Faroes			
Whole cohort	79	1.472	0.1
PCB adjusted	66	1.230	0.1
Lowest PCB	24	0.447	0.05
Geometric mean Faroes			
Whole cohort	68	1.268	0.1
PCB adjusted	65	1.212	0.1
Lowest PCB	34	0.634	0.1
Smoothed values			
BNT Faroes	48	0.895	0.1
CPT Faroes	48	0.895	0.1
CVLT Faroes	60	1.118	0.1
Finger Tap Faroes	52	0.969	0.1
MCCPP New Zealand	28	0.522	0.05
MCMT New Zealand	32	0.596	0.1
Median values			
Faroes	48	0.895	0.1
New Zealand	24	0.447	0.05
Integrative			
All endpoints	32	0.596	0.1

[a]$BMDL_{05}$ s from NRC (2000), Tables 7-4, 7-5, 7-6. Total hair mercury was converted to blood mercury for the New Zealand and Seychelles Islands studies using a 250:1 ratio and an assumption of equivalent maternal and cord levels.
[b]Abbreviations: BNT = Boston Naming Test; CPT = Continuous Performance Test; CVLT = California Verbal Learning Test; MCCPP = McCarthy Perceived Performance; MCMT = McCarthy Motor Test.
[c] Calculated using a one-compartment model.
[d] Calculated using an UF of 10.
from U.S. EPA, 2001, p. 4-61.

Table III. BMD and BMDL estimates from the Faroe Islands study with and without adjustment for PCBs and in the subset of children in the lowest tertile with respect to PCB exposure (calculated using the *K*-power model)

Exposure	Endpoint	Full Cohort	Adjusted for PCBs	Low-PCB tertile
Maternal hair (ppm)	Finger Tapping	20 (12)	17 (9)	7 (4)
	CPT Reaction Time	18 (10)	27 (11)	13 (5)
	BNT	15 (10)	24 (10)	21 (6)
Cord Blood (ppb)	Finger Tapping	140 (79)	149 (66)	41 (24)
	CPT Reaction Time	72 (46)	83 (49)	53 (28)
	BNT	85 (58)	184 (71)	127 (40)
	CVLT: Delayed Recall	246 (103)	224 (78)	393 (52)

[a] BMDs are calculated under the assumption that 5% of the responses will be abnormal in unexposed subjects ($P_0 = 0.05$), assuming a doubling of the excess risk (BMR = 0.05).

CPT = Continuous Performance Test; BNT = Boston Naming Test; CVLT = California Verbal Learning Test

from NRC, 2000, Table 7-4, p. 289.

References

Altmann, L., Sveinsson, K., Krämer, U., Weishoff-Houben, M., Turfeld, M., Winneke, G., and Wiegand, H. Visual functions in 6-year-old children in relation to lead and mercury levels. Neurotoxicol. Teratol. 20:9-17, 1998.

Amin-Zaki, L., Elhassani, S., Majeed, M.A., Clarkson, T.W., Doherty, R.A., and Greenwood, M. Intra-uterine methylmercury poisoning in Iraq. Pediatr. 54:587-595, 1974.

Amorim, M.I.M, Mergler, D., Bahia, M.O., Dubeau, H., Miranda, D., Lebel, J., Burbano, R.R., and Lucotte, M. Cytogenetic damage related to low levels of methyl mercury contamination in the Brazilian Amazon. An. Acad. Bras. Ci. 72:497-506, 2000.

Aschner, M., and Syversen, T. Methylmercury – Recent advances in the understanding of its neurotoxicity. Ther. Drug. Monit. 27:278-283, 2005.

Axtell, C.D., Cox, C., Myers, G.J., Davidson, P.W., Choi, A.L., Cernichiari, E., Sloane-Reeves, J., Shamlaye, C.F., and Clarkson, T.W. Association between methylmercury exposure from fish consumption and child development at five and a half years of age in the Seychelles Child Development Study: an evaluation of nonlinear relationships. Environ. Res. 84:71-80, 2000.

Bellinger, D.C. Neurobehvaioral Assessments Conducted in the New Zealand, Faroe Islands, and Seychelles Islands Studies of Methylmercury Neurotoxicity in Children. Report to the U.S. Environmental Protection Agency, March 2005.

Beuter, A., de Geoffroy, A., and Edwards, R. Analysis of rapid alternating movements in Cree subjects exposed to methylmercury and in subjects with neurological deficits. Environ. Res. 80:64-79, 1999.

Beuter, A., and Edwards, R. Tremor in Cree subjects exposed to methylmercury: A preliminary study. Neurotoxicol. Teratol. 20:581-589, 1998.

Bornhausen, M., Musch, H.R., and Greim, H. Operant behavior changes in rats after prenatal methylmercury exposure. Toxicol. Appl. Pharmacol. 56:305-310, 1980.

Bouzan, C., Cohen, J.T., Connor, W.E., Kris-Etherton, P.M., Gray, G.M., König, A., Lawrence, R.S., Savitz, D.A., and Teutsch, S.M. A quantiative analysis of fish consumption and stroke risk. Am. J. Prev. Med. 29: 347-352, 2005.

Budtz-Jørgensen, E., Keiding, N., Grandjean, P., and Weihe P. Estimation of health effects of prenatal methylmercury exposure using structural equation models. Environ. Health 1: 2002. http://www.ehjournal.net/content/1/1/2

Budtz-Jørgensen, E., Grandjean, P., Keiding, N., White, R.F., and Weihe P. Benchmark dose calculations of methylmercury-associated neurobehavioural deficits. Toxicol Lett. 112-113:193-199, 2000.

Budtz-Jørgensen, E., Keiding, N.,Grandjean, P., White, R.F., and Weihe P. Methylmercury toxicity independent of PCB exposure. Environ. Health Perspect. 107: A236-237, 1999.

Buelke-Sam, J., Kimmel, C.A., Adams, J., Nelson, C.J., Vohees, C.V., Wright, D.C., St Omer, V., Korol, B.A., Butcher, R.E., Geyer, M.A., Holson, J.F., Kutscher, C.L., and Wayner, M.J. Collaborative behavioral teratology study: Results. Neurobehav. Toxicol. Teratol. 7:591-624, 1985.

Burbacher, T.M., Grant, K.S., Mayfield, D.B., Gilbert, S.G., and Rice, D.C. Prenatal methylmercury exposure affects spatial vision in adult monkeys. Toxicol. Appl. Pharmacol. 208:21-28, 2005.

Burbacher, T.M., Grant, K.S., and Mottet, N.K. Retarded object permanence development in methylmercury exposed *Macaca fascicularis* infants. Dev. Psychol. 22:771-776, 1988.

Burbacher, T.M., Rodier, P.M., and Weiss, B. Methylmercury developmental neurotoxicity: a comparison of effects in humans and animals. Neurotoxicol. Teratol. 12:191-202, 1990a.

Burbacher, T.M., Sackett, G.P., and Mottet, N.K. Methylmercury effects on the social behavior of *Macaca fascicularis* infants. Neurotoxicol Teratol. 12:65-71, 1990b.

Carta, P., Flore, C., Alinovi, R., Ibba, A., Tocco, M.G., Aru, G., Carta, R., Girei, E., Mutti, A., Lucchini, R., and Randaccio, F.S. Sub-clinical neurobehavioral abnormalities associated with low level of mercury exposure through fish consumption. Neurotoxicol. 24:617-623, 2003.

CDC (Centers for Disease Control and Prevention). Third National Report on Human Exposure to Environmental Chemicals. July 2005. Department of Health and Human Services, Centers for Disease Control and Prevention, NCEH Pub. No. 05-0570 http://www.cdc.gov/exposurereport/3rd/pdf/thirdreport.pdf

Charleston, J.S., Body, R.L., Bolender, R.P., Mottet, N.K., Vahter, M.E., and Burbacher, T.M. Changes in the number of astrocytes and microglia in the thalamus of the monkey *Macaca fascicularis* following long-term subclinical methylmercury exposure. Neurotoxicol. 17:127-138, 1996.

Charleston, J.S., Body, R.L., Mottet, N.K., Vahter, M.E., and Burbacher, T.M. Autometallographic determination of inorganic mercury distribution in the cortex of the calcarine sulcus of the monkey *Macaca fascicularis* following long-term subclinical exposure to methylmercury and mercuric chloride. Toxicol. Appl. Pharmacol. 132:325-333, 1995.

Charleston, J.S., Bolender, R.P., Mottet, N.K., Body, R.L., Vahter, M.E., and Burbacher, T.M. Increases in the number of reactive glia in the visual cortex of *Macaca fascicularis* following subclinical long-term methyl mercury exposure. Toxicol. Appl. Pharmacol. 129:196-206, 1994.

Cohen, J.T., Bellinger, D.C., Connor, W.E., Kris-Etherton, P.M., Lawrence, R.S., Savitz, D.A., Shaywitz, B.A., Teutsch, S.M., and Gray, G.M. A quantitative risk-benefit analysis of changes in population fish consumption. Am. J. Prev. Med. 29:325-334, 2005c.

Cohen, J.T., Bellinger, D.C., Connor, W.E., and Shaywitz, B.A. A quantitative analysis of prenatal intake of n-3 polyunsaturated fatty acids and cognitive development. Am. J. Prev. Med. 29:366-374, 2005a.

Cohen, J.T., Bellinger, D.C., and Shaywitz, B.A. A quantitative analysis of prenatal methyl mercury exposure and cognitive development. Am. J. Prev. Med. 29:353-365, 2005b.

Cordier, S., Garel, M., Mandereau, L., Morcel, H., Doineau, P., Gosme-Seguret, S., Josse, D., White, R., and Amiel-Tison, C. Neurodevelopmental investigations among methylmercury-exposed children in French Guiana. Environ. Res. 89:1-11, 2002.

Counter, S.A., Buchanan, L.H., Laurell, G., and Ortega, F. Blood mercury and auditory neuro-sensory responses in children and adults in the Nambija gold mining area of Ecuador. Neurotoxicol. 19:185-196, 1998.

Cox, C., Clarkson, T.W., Marsh, D.O., Amin-Zaki, L., Tikriti, S., and Myers, G.G. Dose-response analysis of infants prenatally exposed to methyl mercury: an application of a single compartment model to single-strand hair analysis. Environ. Res. 49:318-332, 1989.

Crump, K.S., Kjellström, T., Shipp, A.M., Silvers, A., and Stewart, A. Influence of prenatal mercury exposure upon scholastic and psychological test performance: benchmark analysis of a New Zealand cohort. Risk Anal. 18:701-713, 1998.

Davidson, P.W., Myers, G.J, Cox, C., Axtell, C., Shamlaye, C., Sloan-Reeves, J., Cernichiari, E., Needham, L., Choi, A., Wang, Y., Berlin, M., and Clarkson, T.W. Effects of prenatal and postnatal methylmercury exposure from fish consumption on neurodevelopment: outcomes at 66 months of age in the Seychelles child development study. JAMA 280:701-707, 1998.

Davidson, P.W., Palumbo, D., Myers, G.J., Cox, C., Shamlaye, C.F., Sloane-Reeves, J., Cernichiari, E., Wilding, G.E., and Clarkson, T.W. Environ. Res. 84:1-11, 2000.

Dolbec, J., Mergler, D., Sousa Passos, C.-J., Sousa de Morais, S., and Lebel, J. Methylmercury exposure affects motor performance of a riverine population of the Tapajós river, Brazilian Amazon. Int. Arch. Occup. Environ. Health 73:195-203, 2000.

Doré, F.Y., Goulet, S., Gallagher, A., Harvey, P.-O., Cantin, J.-F., D'Aigle, T., and Mirault, M.-E. Neurobehavioral changes in mice treated with methylmercury at two different stages of fetal development. Neurotoxicol. Teratol. 23:463-472, 2001.

Dyer, R.S., Eccles, C.U, and Annau, Z. Evoked potential alterations following prenatal methylmercury exposure. Pharmacol. Biochem. Behav. 8:135-141, 1978.

Elsner, J. Testing strategies in behavioral teratology: III. Microanalysis of behavior. Neurobehav. Toxicol. Teratol. 8:573-584, 1986.

Elsner, J. Tactile-kinesthetic system of rats as an animal model for minimal brain dysfunction. Arch. Toxicol. 65:465-473, 1991.

Elsner, J., Hodel, B., Suter, K.E., Oelke, D., Ulbrich, B., Schreiner, G., Cuomo, V., Cagiano, R., Rosengren, R.E., Karlsson, J.E., and Halid, K.G. Detection limits of different approaches in behavioral teratology, and correlation of effects with neurochemical parameters. Neurotoxicol. Teratol. 10:155-167, 1988.

EPA (Environmental Protection Agency). Costs and Benefits of Reducing Lead in Gasoline. Final Regulatory Impact Analysis. EPA-230-05-85-006, 1985.

yosemite.epa.gov/ee/epa/eerm.nsf/
a7a2ee5c6158cedd852563970080ee30/4242532644520FAB8525660400177383

EPA (Environemental Protection Agency). Integrated Risk Information System. Methylmercury. http:// www.epa.gov/iris/subst/0073.htm, 2001.

EPA (Environmental Protection Agency). Regulatory Impact Analysis of the Clear Air Mercury Rule. EPA-452/R-05-003. Research Triangle Park, NC: Office of Air Quality Planning and Standards, Air Quality Strategies and Standards Division. http://www.epa.gov/ttn/atw/utility/ria_final.pdf, 2005.

Environmental Quality Institute (Patch, S.C., Maas, R.P., and Sergent, K.R.) An investigation of factors related to levels of mercury in human hair. Technical Report #05-150, Environmental Quality Institute, University of North Carolina – Asheville, Asheville, NC, 2005.

Gilbert, S.G., Burbacher, T.M., and Rice, D.C. Effects of in utero methylmercury exposure on a spatial delayed alternation task in monkeys. Toxicol. Appl. Pharmacol. 123, 130-136, 1993.

Gilbert, S.G., and Grant-Webster, K.S. Neurobehavioral effects of developmental methylmercury exposure. Environ. Health Perspect. 103:135-142, 1995.

Gilbert, S.G., Rice, D.C., and Burbacher, T.M. Fixed interval/fixed ratio performance in adult monkeys exposed in utero to methylmercury. Neurotoxicol. Teratol. 18:539-546, 1996.

Goldey, E.S., O'Callaghan, J.P., Stanton, M.E., Barone, S., and Krofton, K.M. Developmental neurotoxicity: Evaluation of testing procedures with methylazoxymethanol and methylmercury. Fundam. Appl. Toxicol. 23:447-464, 1994.

Goulet, S., Doré, F.Y., and Mirault, M.-E. Neurobehavioral changes in mice chronically exposed to methylmercury during fetal and early postnatal development. Neurotoxicol. Teratol. 25:335-347, 2003.

Grandjean, P., Budtz-Jørgensen, E., Jørgensen, P., and Weihe, P. Umbilical cord mercury concentration as biomarker of prenatal exposure to methylmercury. Environ. Health Perspect. 113:905-908, 2005.

Grandjean, P., Murata, K., Budtz-Jørgensen, E., and Weihe, P. Cardiac autonomic activity in methylmercury neurotoxicity: 14-year follow-up of a Faroese birth cohort. J. Pediatr. 144:169-176, 2004.

Grandjean, P., Weihe, P., Burse, V.W., Needham, L.L., Storr-Hansen, E., Heinzow, B., Debes, F., Murata, K., Simonsen, H., Ellefsen, P., Budtz-Jørgensen, E., Keiding, N., and White, R.F. Neurobehavioral deficits associated with PCB in 7-year-old children prenatally exposed to seafood neurotoxicants. Neurotoxicol. Teratol. 23:305-317, 2001.

Grandjean, P., Weihe, P., Jørgensen, P.J., Clarkson, T., Cernichiari, E., and Viderø, T. Impact of maternal seafood diet on fetal exposure to mercury, selenium, and lead. Arch. Environ. Health 47:185-195, 1992.

Grandjean, P., Weihe, P., Needham, L.L., Burse, V.W., Patterson, D.G. Jr., Sampson, E.J., Jørgensen, P.J., and Vahter, M. Effect of a seafood diet n mercury, selenium, arsenic, and PCBs and other organochlorines in human milk. Environ. Res. 71:29-38, 1995.

Grandjean, P., Weihe, P., White, R.F., Debes, F., Araki, S., Yokoyama, K., Murata, K., Sørensen, N., Dahl, R., and Jørgensen, P.J. Cognitive deficit in 7-year-old children with prenatal exposure to methylmercury. Neurotoxicol. Teratol. 19:417-428, 1997.

Grandjean, P., White, R.F., Nielsen, A., Cleary, D., and de Oliviera Santos, E.C. Methylmercury neurotoxicity in Amazonian children downstream from gold mining. Environ. Health. Perspect. 107:587-591, 1999.

Grandjean, P., White, R.F., Weihe, P., Jørgensen, P.J. Neurotoxic risk caused by stable and variable exposure to methylmercury from seafood. Ambul. Pediatr. 3:18-23, 2003.

Guallar, E., Sanz-Gallardo, M.I., van't Veer, P., Bode, P., Aro, A., Gomez-Aracena, J., Kark, J.D., Riemersma, R.A., Martin-Moreno, J.M., Kok, F.J., and the Heavy Metals and Myocardial Infarction Study Group. Mercury, fish oils, and the risk of myocardial infarction. N. Engl. J. Med. 347:1747-1754, 2002.

Gunderson, V.M., Grant-Webster, K.S., Burbacher, T.M., and Mottet, N.K. Visual recognition memory deficits in methylmercury-exposed *Macaca facicularis* infants. Neurotoxicol. Teratol. 10:373-379, 1988.

Gunderson, V.M., Grant, K.S., Burbacher, T.M., Fagan III, J.F., and Mottet, N.K. The effect of low-level prenatal methylmercury exposure on visual recognitino memory in infant crab-eating macaques. Child Dev. 57:1076-1083, 1986.

Hallgren, C.G., Hallmans, G., Jansson, J.H., Marklund, S.L., Huhtasaari, G., Schutz, A., Stromberg, U., Vessby, B., and Skerfving, S. Markers of high fish intake are associated with decreased risk of a first myocardial infarction. Br. J. Nutr. 86:397-404, 2001.

Harada, M. Congenital Minamata Disease: intrauterine methylmercury poisoning. Teratol. 18:285-288, 1978.

Hightower, J.M., and Moore, D. Mercury levels in high-end consumers of fish. Environ. Health Perspect. 111:604-608, 2003.

Hightower, J.M, O'Hare, A., and Hernandez, G.T. Blood mercury reporting in NHANES: Identifying Asian, Pacific Islander, Native American, and multiracial groups. Environ. Health Perspect. 114:173-175, 2006.

Huang, L.-S., Cox, C., Myers, G.J., Davidson, P.W., Cernichiari, E., Shamlaye, C.F., Sloane-Reeves, J., and Clarkson, T.W. Exploring nonlinear association between prenatal methylmercury exposure from fish consumption and child development: evaluation of the Seychelles Child Development Study nine-year data using semiparametric additive models. Environ. Res. 97:100-108, 2005.

Igata, A. Epidemiological and clinical features of Minamata disease. Environ. Res. 63:157-169, 1993.

Jedrychowski, W., Jankowski, J., Flak, E., Skarupa, A., Mroz, E., Sochacka-Tatara, E., Lisowska-Miszczyk, I, Szpanowska-Wohn, A., Rauh, V., Skolicki, Z., Kaim, I., and Perera, F. Effects of prenatal exposure to mercury on cognitive and psychomotor function

in one-year-old infants: epidemiologic cohort study in Poland. Ann. Epidemiol. In press, 2006.

Kinjo, Y., Higashi, H., Nakano, A., Sakamoto, M., and Sakai, R. Profile of subjective complaints and activities of daily living among current patients with Minamata disease after 3 decades. Environ. Res. 63:241-251, 1993.

Kjellström, T., Kennedy, P., Wallis, S., and Mantell, C. Physical and mental development of children with prenatal exposure to mercury from fish. State 1: Preliminary test at age 4. National Swedish Environmental Protection Board Report 3080. Solna, Sweden: National Swedish Environmental Protection Board, 1986.

Kjellström, T., Kennedy, P., Wallis, S., & Mantell, C. Physical and Mental Development of Children with Prenatal Exposure to Mercury from Fish. Stage 2: Interviews and Psychological Tests at Age 6. National Swedish Environmental Protection Board Report 3642. Solna, Sweden: National Swedish Environmental Protection Board, 1989.

König, A., Bouzan, C., Cohen, J.T., Connor, W.E., Kris-Etherton, P.M., Gray, G.M., Lawrence, R.S., Savitz, D.A., and Teutsch, S.M. A quantitative analysis of fish consumption and coronary heart disease mortality. Am. J. Prev. Med. 29:335-346, 2005.

Knobeloch, L., Anderson, H.A., Imm, P., Peters, D., and Smith, A. Fish consumption, advisory awareness, and hair mercury levels among women of childbearing age. Environ. Res. 97:220-227, 2005.

Lebel, J., Mergler, D., Branches, F., Lucotte, M., Amorim, M., Larribe, F., and Dolbec, J. Neurotoxic effects of low-level methylmercury contamination in the Amazonian Basin. Environ. Res. 79:20-32, 1998.

Lebel, J., Roulet, M., Mergler, D., Lucotte, M., and Larribe, F. Fish diet and mercury exposure in a riparian Amazonian population. Water Air Soil Poll. 97:31-44, 1997.

Mahaffey, K.R., Clickner, R.P., and Bodurow, C.C. Blood organic mercury and dietary mercury intake: National Health and Nutrition Examination Survey, 1999 and 2000. Environ. Health Perspect. 112:562-570, 2004.

Marsh, D.O., Clarkson, T.W., Cox, C., Myers, G.J., Amin-Zaki, L., and Al-Tikriti, S. Fetal methylmercury poisoning. Relationship between concentration in single strands of maternal hair and child effects. Arch. Neurol. 44:1017-1022, 1987.

McDowall, M.A., Dillon, C.F., Osterloh, J., Bolger, P.M., Pellizzari, E., Fernando, R., Montes de Oca, R., Schober, S.E., Sinks, T., Jones, R.L., and Mahaffey, K.R. Hair mercury levels in U.S. children and women of childbearing age: reference range data from NHANES 1999-2000. Environ. Health Perspect. 112:1165-1171, 2004.

McKeown-Eyssen, G.E., Ruedy, J., and Neims, A. Methyl mercury exposure in northern Quebec. II. Neurologic findings in children. Am. J. Epidemiol. 118:470-279, 1983.

Murata, K., Weihe, P., Araki, S., Budtz-Jørgensen, E., and Grandjean, P. Evoked potentials in Faroese children prenatally exposed to methylmercury. Neurotoxicol. Teratol. 21:471-472, 1999a.

Murata, K., Weihe, P., Ronzoni, A., Debes, F., Vasconcelos, R., Zino, F., Araki, S., Jørgensen, P.J., White, R.F., and Grandjean, P.F. Delayed evoked potentials in children exposed to methylmercury from seafood. Neurotoxicol. Teratol. 21:343-348, 1999b.

Murata, K., Weihe, P., Budtz-Jørgensen, E., Jensen, P.J., and Grandjean, P. Delayed brainstem auditory evoked potential latencies in 14-year-old children exposed to methylmercury. J. Pediatr. 144:177-183, 2004.

Musch, H.R., Bornhausen, M., Kreigel, H., and Greim, H. Methylmercury chloride induces learning deficits in prenatally treated rats. Arch. Toxicol. 40:103-108, 1978.

Myers, G.J., Davidson, P.W., Cox, C., Shamlaye, D.F., Palumbo, D., Cernichiari, E., Sloane-Reeves, J., Wilding, G.E., Kost, J., Huang, L.-S., and Clarkson, T.W. Prenatal methylmercury exposure from ocean fish consumption in the Seychelles child development study. Lancet 361:1686-1692, 2003.

Myers, G.J., Marsh, D.O., Cox, C., Davidson, P.W., Shamlaye, C.F., Tanner, M.A., Choi, A., Cernichiari, E., Choisy, O., and Clarkson, T.W. A pilot neurodevelopmental study of Seychellois children following in utero exposure to methylmercury from a maternal fish diet. Neurotoxicol. 16:629-638, 1995.

Newland, M.C., and Paletz, E.M. Animal studies of methylmercury and PCBs: What do they tell us about expected effects in humans? Neurotoxicol. 21:1003-1028, 2000.

Newland, M.C., and Rasmussen, E.B. Aging unmasks adverse effects in gestational exposure to methylmercury in rats. Neurotoxicol. Teratol. 22:819-828, 2000.

Newland, M.C., Reile, P.A., and Langston, J.L. Gestational exposure to methylmercury retards choice in transition in aging rats. Neurotoxicol. Teratol. 26:179-194, 2004.

Newland, M.C., Yezhou, S., Logdberg, B., and Berlin, M. Prolonged behavioral effects of *in utero* exposure to lead or methyl mercury: reduced sensitivity to changes in reinforcement contingencies during behavioral transitions and in steady state. Toxicol. Appl. Pharmacol. 126:6-15, 1994.

NIEHS (National Institute of Environmental Health Sciences). Scientific issues relevant to assessment of health effects from exposure to methylmercury. Workshop organized by Committee on Environmental and Natural Resources (CENR) Office of Science and Technology Policy (OSTP), The White House, November 18-20, 1999, Raleigh, N.C. http://www.eurobc.org/Report%20of%20the%20Methylmercury%20Workshop.htm

Ninomiya, T., Imamura, K., Kuwahata, M., Kindaichi, M., Susa, M., and Ekino, S. Reappraisal of somatosensory disorders in methylmercury poisoning. Neurotoxicol. Teratol. 27:643-653, 2005.

NRC (National Research Council). Toxicological Effects of Methylmercury. National Academy Press, Washington, D.C., 2000. http://www.nap.edu/books/0309071402/html/index.html

Ohno, M., Kishimoto, T., and Tada, M. The effect of methylmercury (CH_3HgCl) on the production of endothelium-derived relaxing factor (EDRF) by cultured human umbilical

vascular endothelial cells based on its anti-aggregatory effect on human platelets. Cell Biol. Toxicol. 11:303-311, 1995.

Oken, E., Wright, R.O., Kleinman, K.P., Bellinger, D., Amarasiriwardena, C.J., Hu, H., Rich-Edwards, J.W., & Gillman, M.W. Maternal fish consumption, hair mercury, and infant cognition in a U.S. cohort. Environmental Health Perspectives online doi:10.1289/ehp.8041 (available at http://dx.doi.org), 2005.

Ramirez, G.B., Pagulayan, O., Akagi, H., Francisco Rivera, A., Lee, L.V., Berroya, A., Vince Cruz, C., and Casintahan, D. Tagum study II: follow-up study at two years of age after prenatal exposure to mercury. Pediatr. 111:e289-e295, 2003. http://www.pediatrics.org/cgi/content/full/111/3/e289

Reuhl, K.R., and Chang, L.W. Effects of methylmercury on the development of the nervous system: A review. Neurotoxicol. 1:21-55, 1979.

Rice, D.C. Blood mercury concentrations following methyl mercury exposure in adult and infant monkeys. Environ. Res. 49:115-126, 1989a.

Rice, D.C. Brain and tissue levels of mercury after chronic methylmercury exposure in the monkey. J. Toxicol. Environ. Health 27:189-198, 1989b.

Rice, D.C. Effects of pre- plus postnatal exposure to methylmercury in the monkey on fixed interval and discrimination reversal. Neurotoxicol. 13: 443-452, 1992.

Rice, D.C. Sensory and cognitive effects of developmental methylmercury exposure in monkeys, and a comparison to effects in rodents. Neurotoxicol. 17:139-154, 1996a.

Rice, D.C. Evidence for delayed neurotoxicity produced by methylmercury. Neurotoxicol. 17:583-596, 1996b.

Rice, D.C. Age-related increase in auditory impairment in monkeys exposed in utero plus postnatally to methylmercury. Toxicol. Sci. 44:191-196, 1998.

Rice, D.C. and Barone, S. Critical periods of vulnerability for the developing nervous system: Evidence from humans and animal models. Environ. Health Perspect. Supplement 3, 511-533, 2000.

Rice, D.C., and Gilbert, S.G. Early chronic low-level methylmercury poisoning in monkeys impairs spatial vision. Science 216:759-761, 1982

Rice, D.C., and Gilbert, S.G. Effects of developmental exposure to methylmercury on spatial and temporal visual function in monkeys. Toxicol. Appl. Pharmacol. 102:151-163, 1990.

Rice, D.C., and Gilbert, S.G. Exposure to methyl mercury from birth to adulthood impairs high-frequency hearing in monkeys. Toxicol. Appl. Pharmacol. 115:6-10, 1992.

Rice, D.C., and Gilbert, S.G. Effects of developmental methylmercury exposure or lifetime lead exposure on vibration sensitivity function in monkeys. Toxicol. Appl. Pharmacol. 134:161-169, 1995.

Rice, D.C., and Hayward, S. Comparison of visual function at adulthood and during aging in monkeys exposed to lead or methylmercury. Neurotoxicol. 20:767-784, 1999.

Rice, D.C., Shoney, R., and Mahaffey, K. Methods and rationale for derivation of a reference dose for methylmercury by the U.S. EPA. Risk Analysis 23:107-115, 2003.

Rissanen, T., Voutilainen, S., Nyssönen, K., Lakka, T.A., and Salonen, J.T. Fish oil-derived fatty acids, docosahexaenoic acid and docosapentaenoic acid, and the risk of acute coronary events. The Kuopio Ischaemic Heart Disease Risk Factor Study. Circulation 102:2677-2679, 2000.

Rodier, P., Aschner, M., and Sager, P. Mitotic arrest in the developing CNS after prenatal exposure to methylmercury. Neurobehav. Toxicol. Teratol. 6:379-385, 1984.

Ryan, L.M. Effects of Prenatal Mercury Exposure on Childhood IQ: A Synthesis of Three Studies. Report to the U.S. Environmental Protection Agency, March 2005.

Salkever, D.S. Updated estimates of earnings benefits from reduced exposure of children to environmental lead. Environ. Res. 70:1-6, 1995.

Salonen, J.T., Seppänen, K., Lakka, T.A., Salonen, R., and Kaplan, G.A. Mercury accumulation and accelerated progression of carotid atherosclerosis: a population-based prospective 4-year follow-up study in men in eastern Finland. Atherosclerosis 148:265-273, 2000.

Salonen, J.T., Seppänen, K., Nyyssönen, K., Korpela, H., Kauhanen, J., Kantola, M., Tuomilehto, J., Esterbauer, H., Tatzber, F., and Salonen, R. Intake of mercury from fish, lipid peroxidation, and the risk of myocardial infarction and coronary, cardiovascular, and any death in Eastern Finnish men. Circulation 91:645-655, 1995.

Schreiner, G., Ulbrich, B., and Bass, R. Testing strategies in behavioral teratology: II. Discrimination learning. Neurobehav. Toxicol. Teratol. 8:567-572, 1986.

Sørensen, N., Murata, K., Budtz-Jørgensen, E., Weihe, P., and Grandjean, P. Prenatal methylmercury exposure as a cardiovascular risk factor at seven years of age. Epidemiol. 10:370-375, 1999.

Spyker, J.M. Assessing the impact of low level chemicals on development: Behavioral and latent effects. Fed. Prco. 34:1835-1844, 1975.

Spyker, J.M., Sparber, S.B., and Goldberg, A.M. Subtle consequences of methylmercury exposure: Behavioral deviations in offspring of treated mothers. Science 177:621-623, 1972.

Stern, A.H. A review of the studies of the cardiovascular health effects of methylmercury with consideration of their suitability for risk assessment. Environ. Res. 98:133-142, 2005.

Stern, A.H., Gochfeld, M., Weisel, C., and Burger, J. Mercury and methylmercury exposure in the New Jersey pregnant population. Arch. Environ. Health 56:4-10, 2001.

Stern, A.H., and Smith, A.E. An assessment of the cord blood:maternal blood methylmercury ratio: Implications for risk assessment. Environ. Health Perspect. 111:1465-1470, 2003.

Suter, K.E., and Schön, H. Testing strategies in behavioral teratology: I. Testing battery approach. Neurobehav. Toxicol. Teratol. 8:561-566, 1986.

Takaoka, S., Fujino, T., Sekikawa, T., and Miyaoka, T. Psychophysical sensory examination in individuals with a history of methylmercury exposure. Environ. Res. 95:126-132, 2004.

Tamashiro, H., Arakaki, M., Akagi, H., Hirayama, K., Murao, K., and Smolensky, M.H. Sex differential of methylmercury toxicity in spontaneous hypertensive rats (SHR). Bull. Environ. Contam. Toxicol. 37:916-924, 1986.

Trasande, L., Landrigan, P.J., and Schechter, C. Public health and economic consequences of methyl mercury toxicity to the developing brain. Environ. Health Perspect. 113:590-596, 2005.

Trasande, L., Schechter, C.B., Haynes, K.A., and Landrigan, P.J. Mental retardation and prenatal methylmercury toxicity. Am. J. Indust. Med. 49:153-158, 2006.

Tsubaki, T., and Irukayama, K. Eds. Minamata Disease, Amsterdam, Elsevier, 1977

Vahter, M.E., Motet, N.K., Friberg, L., Lind, B., Shen, D.D. , and Burbacher, T. Speciation of mercury in the primate blood and brain following long-term exposure to methylmercury. Toxicol. Appl. Pharmacol. 124: 221-229, 1994.

Vahter, M.E., Mottet, N.K., Friberg, L.T., Lind, B., Charleston, J.S., and Burbacher, T.M. Demethylation of methyl mercury in different brain sites of *Macaca fascicularis* monkeys during long-term subclinical methyl mercury exposure. Toxicol. Appl. Pharmacol. 134:273-284, 1995.

Virtanen, J.K, Voutilainen, S., Rissanen, T.H., Mursu, J., Tuomainen, T.-P., Korhonen, M.J., Valkonen, V.-P., Seppänen, K., Laukkanen, J.A., and Salonen, J.T. Aerterioscler. Thromb. Vasc. Biol. 25:228-233, 2005.

Vorhees, C. Behavioral effects of prenatal methylmercury in rats: A parallel trial to the collaborative behavioral teratology study. Neurobehav. Toxicol. Teratol. 7:717-724, 1985.

Vupputuri, S., Longnecker, M.P., Daniels, J.L., Guo, X., and Sandler, D.P. Blood mercury level and blood pressure among U.S. women: results form the National Health and Nutrition Examination Survey 1999-2000. Environ. Res. 97:195-2000, 2005.

Wakita, Y. Hypertension induced by methyl mercury in rats. Toxicol. Appl. Pharmacol. 89:144-147, 1987.

Weil, M., Bressler, J., Parsons, P., Bolla, K., Glass, T., and Schwartz, B. Blood mercury levels and neurobehavioral function. J. Amer. Med. Assoc. 293:1875-1882, 2005.

Weiss, B. Vulnerability of children and the developing brain to neurotoxic hazards. Environ. Health Perspect. 108 Suppl 3:375-381, 2000.

Weiss, B., Stern, S., Cox, C., and Balys, M. Perinatal and lifetime exposure to methylmercury in the mouse: behavioral effects. Neurotoxicol. 26:675-690, 2005.

WHO (World Health Organization). Methylmercury. Environmental Health Criteria 101. Geneva: World Health Organization, 1990. Available online at http://www.inchem.org/documents/ehc/ehc/ehc101.htm

Widholm, J.J, Villareal, S., Seegal, R.F., and Schantz, S.L. Spatial alternation deficits following developmental exposure to Aroclor and/or methylmercury in rats. Toxicol. Sci. 82:577-589, 2004.

Yokoo, E.M., Valente, J.G., Grattan, L., Schmidt, S.L., Platt, I., and Silbergeld, E.K. Low level methylmercury exposure affects neuropsychological function in adults. Environ. Health 2:8, 2003 (http://www.ehjournal.net/content/2/1/8).

Yoshizawa, K., Rimm, E.B., Morris, J.S., Spate, V.I., Hsieh, C., Spiegelman, D., Stampfer, M.J., and Willett, W.C. Mercury and the risk of coronary heart disease in men. N. Engl. J. Med. 347:1755-1760, 2002.

Zenick, H. Evoked potential alterations in methylmercury chloride toxicity. Pharmacol. Biochem. Behav. 5:253-255, 1976.

Exhibit B

ATMOSPHERIC DEPOSITION OF MERCURY

Gerald J. Keeler, Ph.D.
University of Michigan, School of Public Health
Department of Environmental Health Sciences
Ann Arbor, MI

March 2006

INTRODUCTION

Mercury continues to be targeted as a pollutant of concern for source identification, reduction and/or elimination through a variety of state, federal and international efforts. Recently, the Council of Great Lakes Governors, a non-partisan partnership of the Governors of the eight Great Lakes States - Illinois, Indiana, Michigan, Minnesota, New York, Ohio, Pennsylvania, and Wisconsin, identified reducing the input of toxic substances to the lakes and reducing human health impacts as major priorities for restoration efforts in the Great Lakes. The atmosphere has been determined to be the most significant source of mercury (Hg) to Michigan's inland lakes and for some of the Great Lakes (Fitzgerald et al., 1991; Landis et al., 2002a). In 2003, the Great Lakes Commission, identified mercury monitoring as one of the most urgent priorities among the air toxic programs in the Great Lakes. The Great Lakes Commission is a binational agency that promotes development, use and conservation of the water and related natural resources of the Great Lakes basin and St. Lawrence River. Its members include the eight Great Lakes states and the Canadian provinces of Ontario and Québec.

On a global basis, it is estimated that between 50 to 75% of total atmospheric mercury emissions are of anthropogenic origin (Pirrone et al., 1996). Natural emissions are typically assumed to be elemental gaseous mercury (Hg^0) (Pacyna and Pacyna, 2002), however, a lack of measurement data make this assumption highly uncertain. Anthropogenic emissions are primarily Hg^0, divalent reactive gaseous mercury (RGM), and particulate mercury (Hg(p)). The dominant form of mercury in the atmosphere is Hg^0. Because it is relatively insoluble and deposits very inefficiently, the mean residence time for Hg^0 in the atmosphere is estimated to be approximately one year (Schroeder and Munthe, 1998) allowing for global redistribution. This lifetime was recently challenged, however, due to new insights on the atmospheric chemistry of mercury, and these studies suggest the lifetime of mercury will likely be much shorter. RGM directly emitted to the atmosphere is expected to deposit efficiently on a local or regional scale near major sources largely because of its solubility, as is the case for Hg(p). Atmospheric deposition at any particular location can, therefore, be a complex combination of local, regional, and global emissions and transport/ transformation processes (EPMAP, 1994).

Major anthropogenic mercury sources in the Great Lakes region and preliminary estimates of their annual emissions into the atmosphere have been described by Pirrone et al., (1996), and USEPA (1994). Sources include fossil fuel utility boilers, municipal and hospital waste incinerators, iron and steel production, coke production, lime production, hazardous waste recycling facilities, and secondary copper, petroleum refining, and mobile sources. The sources of mercury are numerous and many are not well characterized. An accurate emissions inventory that includes speciated anthropogenic as well as natural mercury sources is still not available.

Early mercury studies focused on the relative importance of urban/source areas, e.g. Detroit, Chicago/Gary on loadings to the Great Lakes. These regional-scale monitoring studies included the Lake Michigan Mass Balance Study (LMMBS) and the Atmospheric Exchange Over Lakes

and Oceans Study (AEOLOS). These developed methods for the measurement and analysis of samples collected in multi-site networks. The Great Lakes Atmospheric Mercury Assessment Project (GLAMAP) provided the first comprehensive regional atmospheric mercury measurements in the Great Lakes Region. This international study showed the importance of a regional approach to understanding mercury sources and transport. The LMMBS clearly identified the need for methods for the measurement of speciated gaseous mercury and for the accurate determination of mercury associated with size-segregated particulate matter.

This document provides a brief summary of several of the key studies performed in the Great Lakes region over the past 15+ years together with insights on the sources, transport, chemistry, and deposition of atmospheric mercury and discusses the implications of these studies. This is not an exhaustive review of the literature but a selection of findings that reflect our current state-of-the-art knowledge of atmospheric mercury levels and deposition in the Great Lakes Region. Only wet deposition data collected on an event-basis is discussed, as the focus of the research presented is related to source apportionment and meteorological analysis.

MERCURY LEVELS IN THE GREAT LAKES REGION

Ambient Mercury Measurements

The Lake Michigan Urban Air Toxics Study (LMUATS) performed in 1991 provided new insight on the levels and behavior of atmospheric mercury and other hazardous air pollutants in the southern Lake Michigan Basin (Keeler, 1994; Holsen et al., 1992; Pirrone and Keeler, 1993; Pirrone et al., 1995). Total mercury measurements were performed simultaneously at three sites as part of the month-long intensive study designed to observe the behavior of many different classes of compounds as they were advected from the urban/industrial source regions across Lake Michigan. Ambient mercury concentrations, both vapor and particulate phase, were significantly elevated in the Chicago urban/industrial area relative to the levels measured concurrently in surrounding areas. The levels of atmospheric mercury varied greatly from day to day at the urban Chicago location, and much less so at the more rural sites. In addition, the total

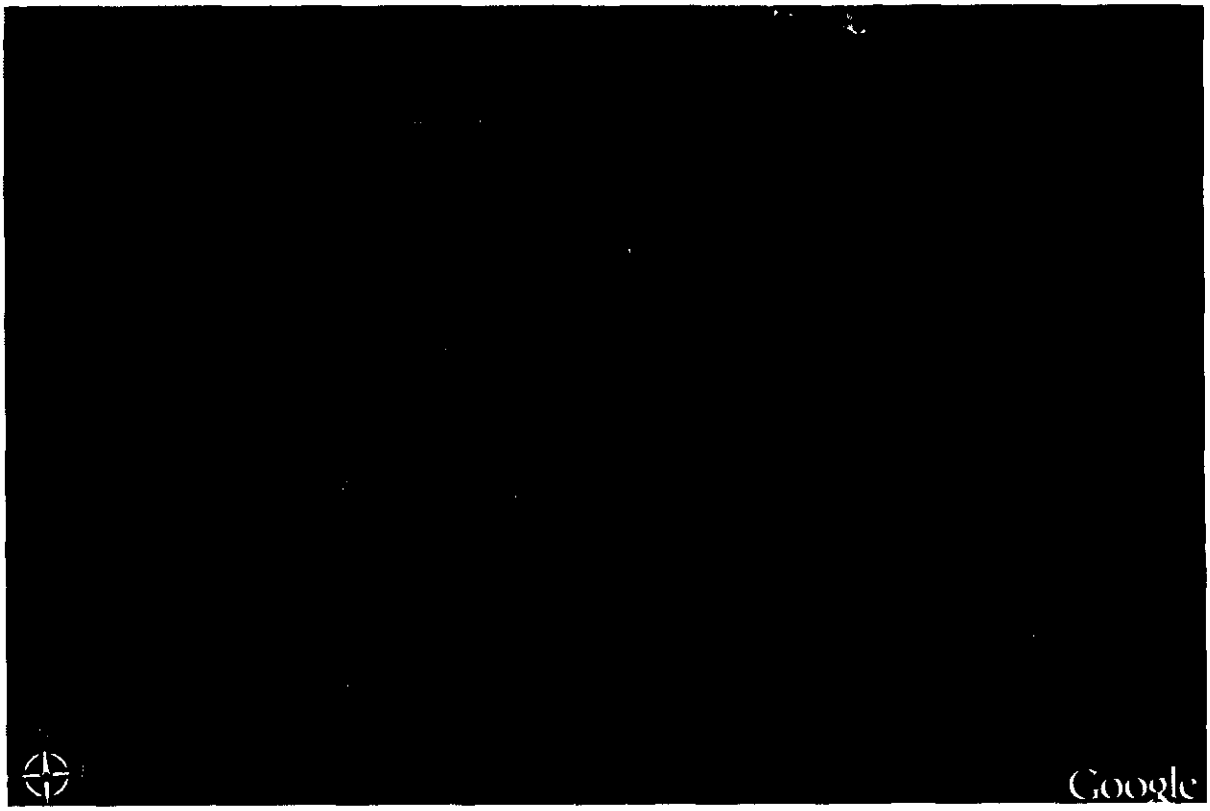

Figure 1. Great Lakes Atmospheric Mercury Monitoring Sites.

vapor phase mercury concentrations varied diurnally with the highest concentrations observed during the daytime.

The levels of particulate mercury during the LMUATS were significantly greater than those observed previously at rural sites in the Great Lakes Region, as much as 50 times greater. Particulate mercury was measured on coarse particles >2.5 μm in size as well as on fine particles

<2.5 μm. Furthermore, coarse particle mercury was measured in both urban and rural locations, and the chemical form and reactivity of the particulate mercury varied depending upon the source and meteorological conditions. Over-water measurements on Lake Michigan of mercury performed in the southern Lake Michigan Basin found particulate mercury concentrations >1 ng/m^3 (Keeler et al., 1994), and confirmed that particulate mercury was associated with both fine and coarse particulate matter. These findings suggested that dry deposition estimates for mercury had likely underestimated the mass loading of this toxic compound to both terrestrial and aquatic systems.

Some of the first multi-year atmospheric mercury data in the region included daily total vapor and particulate phase mercury samples and event wet deposition (discussed later) at three rural sites in Michigan (Pellston, South Haven and Dexter) over a two-year period (Hoyer et al., 1995). Regional and local–scale spatial gradients were identified for both the atmospheric concentrations and wet deposition of mercury. Meteorological analysis indicated that the elevated levels of mercury observed in the atmosphere were associated with transport from the urban/industrial area in Detroit as well as with transport from the Chicago/Gary corridor (Hoyer, 1995; Keeler and Hoyer, 1997). These findings revealed that source-receptor relationships for atmospheric mercury could be determined, and that short-duration ($\leq$daily) ambient sampling and event-precipitation sampling were critical for this determination.

The Great Lakes Atmospheric Mercury Assessment Project (GLAMAP) extended the mercury measurements performed in Michigan to a region-wide network of rural ambient sites in the Great Lakes Region aimed to determine the influence of the large anthropogenic source areas on mercury levels. The GLAMAP (1994-1996) provided a unique database for investigating source-receptor relationships for atmospheric mercury and included measurements of gas- and particle-phase mercury, as well as particulate trace elements, from 11 rural monitoring locations across the region (Burke, 1998). More than 1,300 sets of 24-hour measurements were collected from the 11 sites over the two-year period. Atmospheric mercury concentrations measured during GLAMAP were typical of rural locations, with daily mean concentrations ranging from 1.0 to 3.5 ng m^{-3} for gas-phase mercury and from 1 to 100 pg m^{-3} for particle-phase mercury.

Statistically significant spatial and seasonal differences were observed for both gas- and particle-phase mercury measured across the Great Lakes region. Sub-regions were identified (shown in Figure 2) within the region where the GLAMAP sites had similar trends in atmospheric mercury levels. These observations are discussed here in terms of their spatial and temporal trends.

Spatial and Temporal Trends for Atmospheric Mercury

Atmospheric mercury concentrations measured during GLAMAP were statistically different across the Great Lakes Region with average gas-phase mercury concentrations that differed by as much as 25% between sites (1.63 - 2.03 ng m^{-3}), while average particle-phase mercury levels differed by nearly a factor of three (8.7 - 24.5 pg m^{-3}). These differences were greater than previously reported spatial gradients for atmospheric mercury across smaller geographic scales (Keeler and Hoyer, 1997; Olmez et al., 1996; Keeler et al., 1995; Iverfeldt and Lindquist, 1986). Concentrations of both gas- and particle-phase mercury were consistently higher at the sites in the *east* and *south* sub-regions compared to the sites in the *north* and *west* sub-regions (see Figure 3 and 4). It was concluded that the spatial trends reflected the proximity of the sites to anthropogenic source areas for atmospheric mercury in the region. The concentrations of

particulate mercury measured at the Illinois Institute of Technology (IIT) site as part of the LMMBS are also shown in Figure 4. On average, the concentrations at this site were more than 3x higher than those measured concurrently at the more rural sites. Measurements performed during the AEOLOS at Washington High School in Indiana revealed even higher particulate mercury concentrations than those measured at IIT.

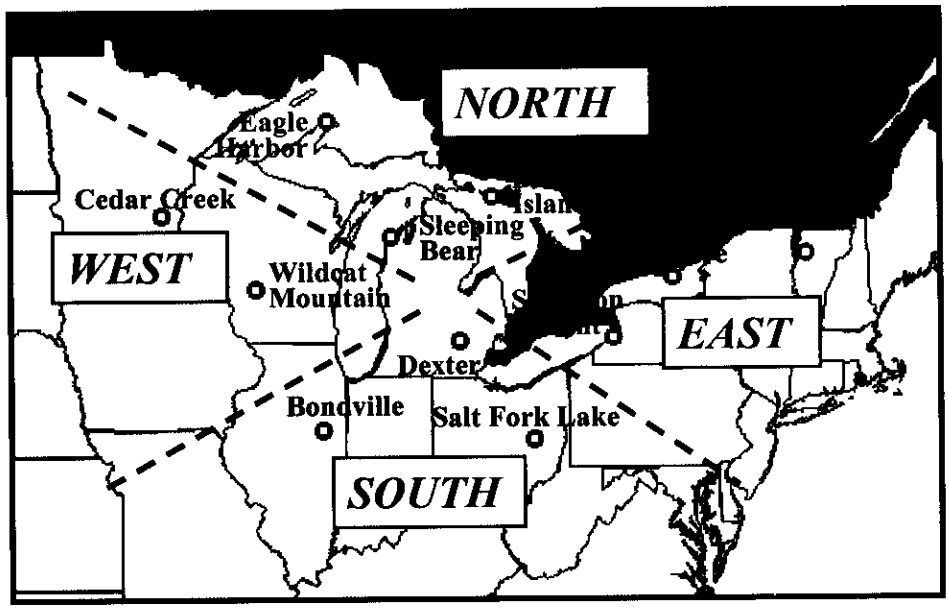

Figure 2. Location of GLAMAP Network Sites 1994-1996.

Although concentrations for both gas- and particle-phase mercury were not statistically different between the two sampling years at any of the GLAMAP sites, seasonal differences were statistically significant and the seasonal trends were different for the two forms of atmospheric mercury. Seasonally averaged gas-phase mercury concentrations were typically highest for the spring seasons and lowest for the autumn seasons during the study. This seasonal trend was consistent across most of the GLAMAP sites, indicating that regional-scale (or larger scale) processes were important for gas-phase mercury. In addition, the magnitude of the seasonal differences was significantly greater at the sites in the east and south parts of the Great Lakes region. Seasonally averaged particle-phase mercury concentrations were significantly higher for the winter season during GLAMAP, but only at the sites in the east and south. Particle-phase mercury concentrations were not statistically different between other seasons at these sites, or between all seasons at the sites to the north and west in the region.

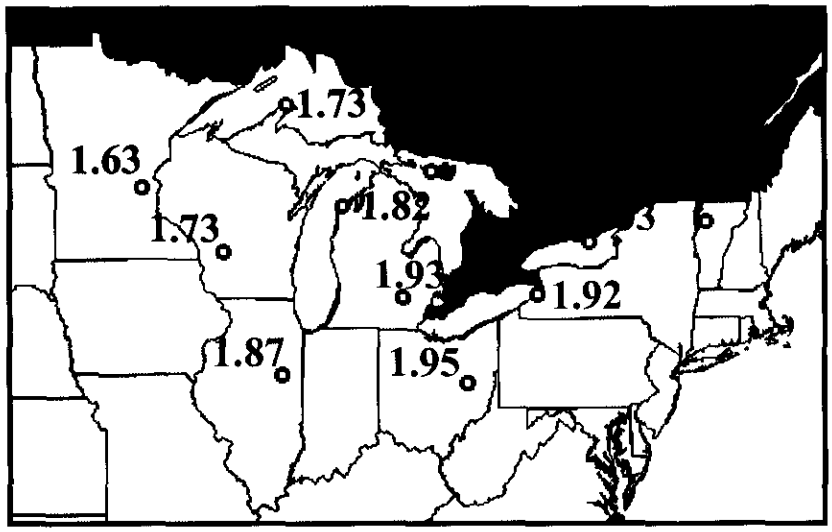

Figure 3. Average concentration of vapor-phase mercury measured from December 1994 to December 1996.

Meteorological factors were found to play a significant role in the seasonal trends for both gas- and particle-phase mercury. Specific synoptic-scale meteorological conditions were consistently associated with both above and below average concentrations of particle-phase mercury at the sites in the eastern and southern portions of the Great Lakes region. Periods with elevated atmospheric pressure across the region during the winter and autumn months with lower mixed-layer heights were associated with above average particle-phase mercury concentrations (30-50 pg m^{-3}). The highest particle-phase mercury concentrations were observed during wintertime high-pressure conditions with air mass transport from known anthropogenic source areas. Spatial differences in the seasonal behavior of mercury indicated that anthropogenic source influences also contributed to these trends. Distance from the major source areas for the region likely influenced the lower range of concentrations at the sites in the north sub-region compared to the other GLAMAP sites.

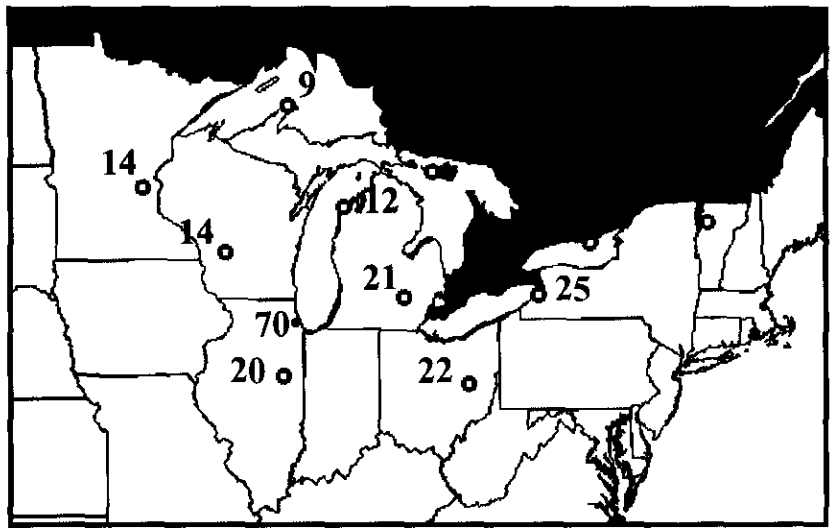

Figure 4. Average concentration of particle-bound mercury measured from 12/1994 to 12/1996.

Synoptic-scale meteorological features also influenced gas-phase mercury levels in the region but the significance of these relationships was not as strong as observed for particle-phase mercury. Periods with lower atmospheric pressure during the spring and summer seasons were associated with above average gas-phase mercury concentrations ($\geq$ 2.0 ng m^{-3}) at the sites in the east and south sub-regions (shown in red in Figure 3). Precipitation ahead of a frontal boundary typically associated with low-pressure systems also occurred with above average mercury concentrations at these sites. Below average gas-phase mercury concentrations (1.4-1.6 ng m^{-3}) occurred during the autumn season with strong pressure gradients between high and low pressure systems, and fast transport across the region (daily mean wind speeds $\geq$6 $msec^{-1}$). The highest concentrations of gas-phase mercury were observed with low-pressure conditions and air mass transport from known source areas. Thus, it was shown that source-receptor relationships for ambient mercury were strongly influenced by the distance from anthropogenic source regions and atmospheric transport that was controlled by synoptic-scale meteorology.

Figure 5 shows the average concentrations of sulfur (S) and slenium (Se) together with the measured mercury on PM samples collected over the two-year GLAMAP. The Se concentration was multiplied by 10, and the S concentration was divided by 100, both in units of ng/m^3 so that they could be simply plotted on the same scale with the particulate mercury in units of pg/m^3. The sites with the highest S and Se concentrations tended to also have the highest mercury concentrations across the network. Bondville, Illinois, Dexter, Michigan, Salt Fork Lake, Ohio, and Sturgeon Point, Ontario, all had relatively higher Se than S and higher particulate mercury as well. The sites farther to the north such as Eagle Harbor, Michigan, and Underhill, Vermont had relatively low and similar mercury, S, and Se concentrations over the two-years of measurement. Since both coal-fired utility boilers and municipal and medical waster incinerations were the dominant source categories at this time, the finding that particulate mercury was related to S and Se, as well as copper (Cu), zinc (Zn), and lead (Pb), indicated that these sources were contributing to the ambient mercury levels.

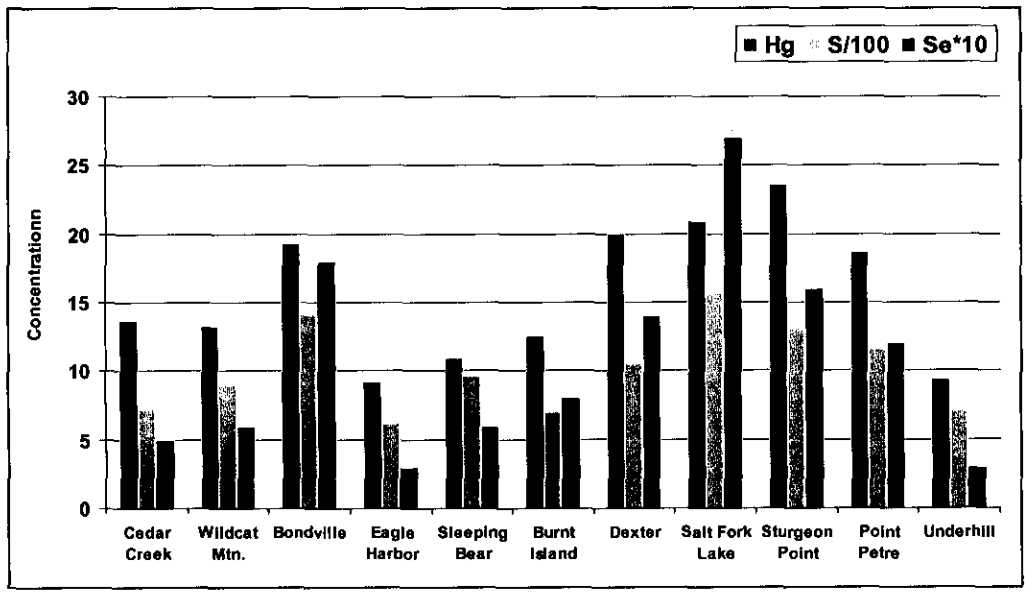

Figure 5. Average concentration of aerosol trace elements measured from December 1994 to December 1996 as part of the GLAMAP. Units for Hg (pg/m^3, and S, Se ng/m^3).

Wet Deposition

Event precipitation was collected from 1992 to 1994 at three Michigan sites: Dexter, South Haven, and Pellston (see Figure 1). This two-year data record clearly indicated a strong gradient in the wet deposition of mercury from the elevated levels in the south to the lower levels observed at the Pellston site (Hoyer et al; 1995). This study also found that air mass transport from source regions in summer often led to highly elevated mercury concentrations in precipitation, whereas in winter, a similar air mass trajectory resulted in extremely low levels of mercury in precipitation (~1.5 ng L^{-1}) if the precipitation fell as snow. The cloud microphysical processes, together with the atmospheric mercury speciation, were thought to be responsible for the strong seasonal variations that were observed in the event mercury concentrations and deposition.

The Lake Michigan Mass Balance Study (LMMBS) performed from July 1994 through October 1995 at five sites (Bondville, IL, Chicago, IL, Kenosha, WI, South Haven, MI, and Sleeping Bear Dunes, MI), found elevated concentrations of mercury in precipitation at the sites in the southern basin when compared to the northern site at Sleeping Bear Dunes (Landis et al. 2002a). The observed gradients in mercury wet deposition were similar to the gradients observed in ambient (gas and particle phase) mercury from the GLAMAP project, which were largely the result of anthropogenic point source emissions in the southern Great Lakes region (Landis and Keeler, 2002a). The annual wet deposition of mercury to Lake Michigan averaged over the entire

lake was 10.6 $\mu g\ m^{-2}$, or 895 kg to the lake (Figure 6). There was significant spatial and temporal variability in the mercury wet deposition flux over Lake Michigan. The summertime flux of mercury was much larger than the wintertime flux, due to the higher concentrations of mercury in rain than in snow and the greater precipitation amounts observed in the summer.

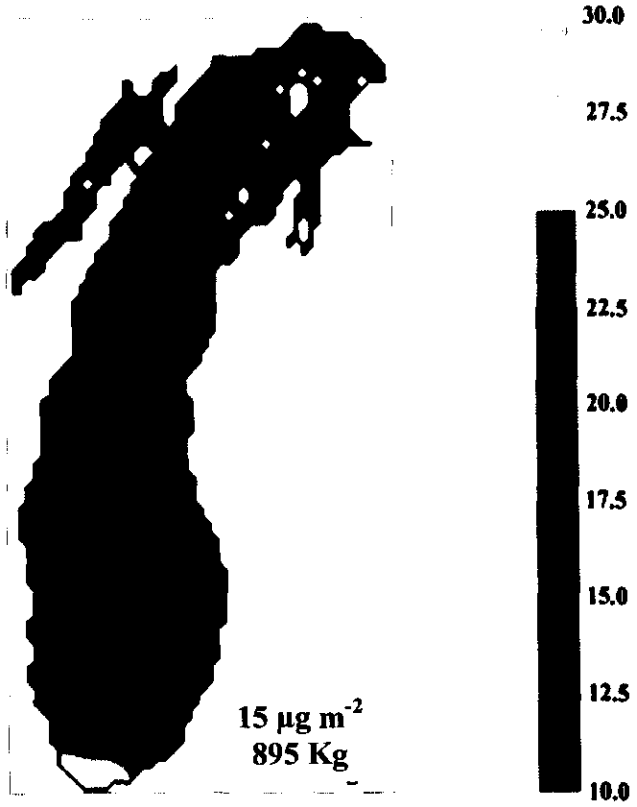

Figure 6. Estimated over-water wet Hg deposition flux (7/1/94-10/31/95).

The Atmospheric Exchange Over Lakes and Oceans Study (AEOLOS), conducted concurrently to the LMMBS, added an over-water measurement component using the USEPA research vessel *Lake Guardian* to the LMMBS network of land-based sites (Landis and Keeler, 2002). The AEOLOS conducted a meteorological cluster analysis (see Figure 7), which found the Chicago/Gary urban area had a significant impact on atmospheric mercury concentrations across the entire Lake Michigan Basin, and estimated that the urban/source area contributed almost 20% of the total deposition to Lake Michigan, and 14% to the wet deposition. In addition to the local source cluster contributing to the deposition to the lake, air mass transport to the south with regional sources in Illinois and Missouri also contributed to the elevated mercury concentrations and deposition measured. The total deposition due to the sources in the urban/industrial area would have been even greater had RGM deposition been considered in that analysis but, due to the lack of a reliable method, these measurements were not performed. The major sources contributing to the wet and dry deposition of mercury to the lake were iron-steel production, coal-fired utilities, and incineration (Landis, 1998).

The AEOLOS also investigated the importance of urban sources on deposition of mercury in Detroit, Michigan in 1996. Mercury event precipitation was collected as part of a study to

investigate the atmospheric contributions of mercury in urban runoff (Gildemeister et al., 2004). Mercury wet deposition measured in Detroit over the nine-month period was three times that measured at the Eagle Harbor site for the same period. At the conclusion of this study it was unclear how representative these findings were and whether this trend would continue after changes in mercury emissions. More recent data continue to show that levels in southern Michigan are 2-3 times those measured at the northern site at Eagle Harbor, but the investigation of the changes into the source contributions has not been performed at this time.

Figure 7. Trajectory clusters and associated volume-weighted mean Hg concentrations for event precipitation samples collected for the Lake Michigan Mass Balance Study (After Landis, 1998).

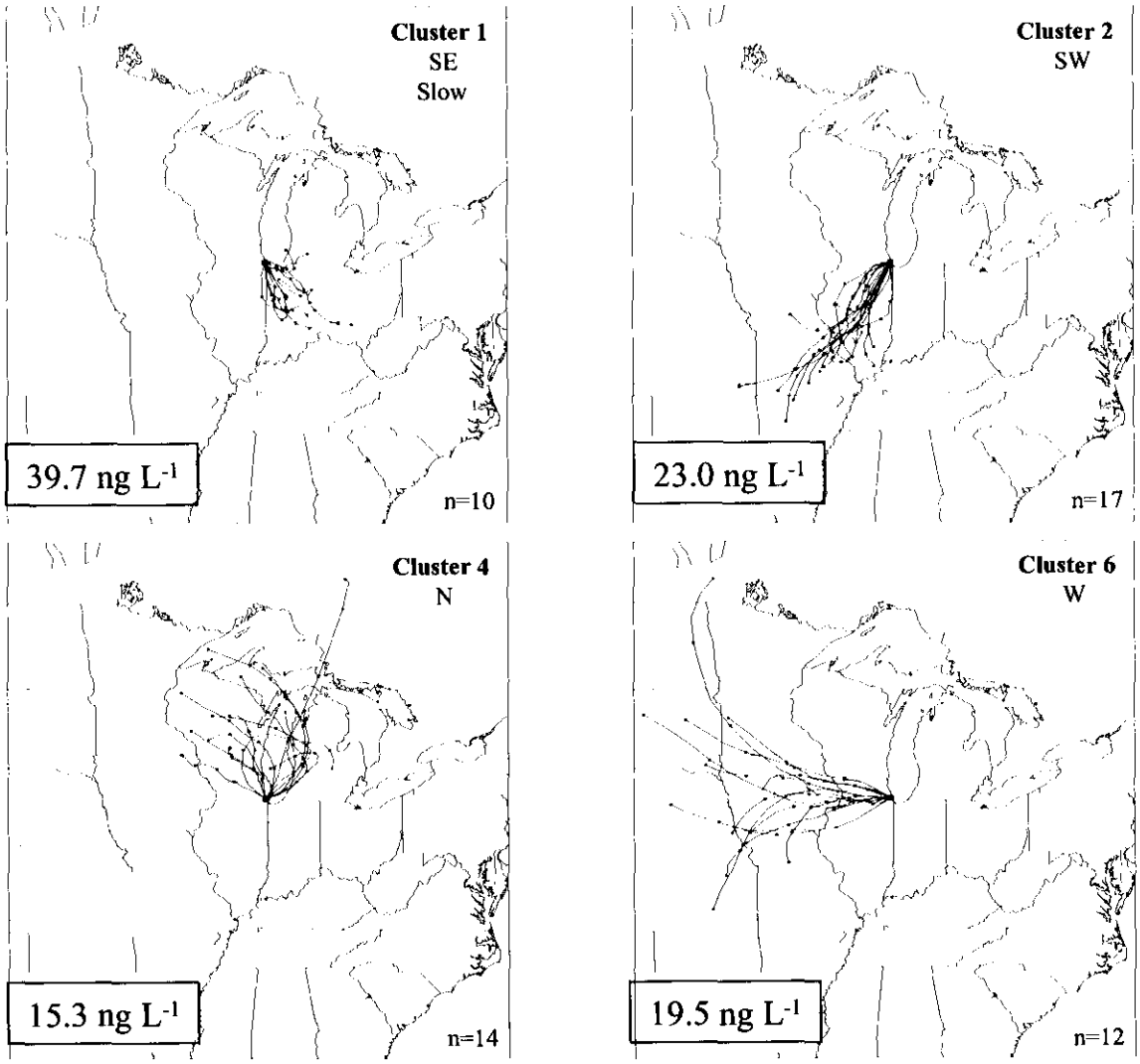

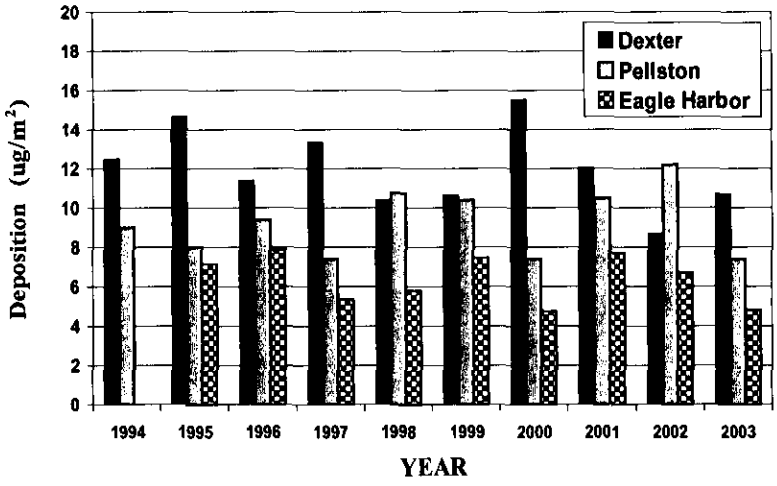

Figure 8. The annual wet deposition of mercury measured at three Michigan sites from 1994 to 2003.

Recognizing that long-term precipitation records are essential for establishing trends and understanding the impacts of changes in mercury emissions, a decade of event precipitation sampling has been conducted at three sites in Michigan (Dexter, Pellston, and Eagle Harbor, see site locations in Figure 1).

The annual mercury wet deposition measured at the three sites for the period 1994-2003 is shown in Figure 8. Over the 10-year deposition record, a clear decreasing gradient from south to north was observed. While the year-to-year variability in the deposition was on average 18% at each site, the 10-year total wet deposition sum at Dexter was 1.6 times the deposition collected at Pellston and 2.1 times that measured at the Eagle Harbor site. With the exception of the 2002 mercury deposition for Pellston (the maximum annual deposition over the 10 year record) the south to north decreasing gradient in deposition was observed each year. Futhermore, there was not an obvious trend, either increasing or decreasing, in the deposition rates at the three sites over the decade of measurements. This data illustrate the consistent long-term impact that anthropogenic sources in the southern part of the Great Lakes region have had on mercury deposition across the Great Lakes Basin.

To date, only a limited number of studies have been performed simultaneously in urban areas and in downwind areas impacted by the sources. Studies in both Chicago and south Florida have found as much as 2/3 of the mercury wet deposition to be of local anthropogenic origin (Landis and Keeler, 2002a; Dvonch et al., 1999). In light of this, a new urban mercury wet deposition network was recently established that added three urban sites, Detroit, Grand Rapids and Flint, to the long-term data collection at the three rural sites in Dexter, Pellston, and Eagle Harbor. These new sites will be used to assess the long-term influence of urban sources relative to background regional sources through the central region of the Great Lakes. In addition, a comprehensive monitoring site was established in Stuebenville, Ohio to specifically assess the impacts of coal-combustion emissions in the southern Great Lakes Region relative to other regional sources contributing to the mercury wet deposition at this site. A quantitative source apportionment of the mercury wet deposition measured in Stuebenville is presented later in this document.

Dry Deposition

During periods without precipitation, mercury can be removed from the atmosphere by particle deposition and by gas exchange between the air, water, and earth's surface. The importance of dry deposition as a source of mercury to the Great Lakes and inland aquatic environments was the focus of studies that pointed to the importance of mercury speciation on the deposition to both urban and remote areas of the region (Pirrone et al., 1993, 1995a,b; Rea et al., 2001, 2002; Landis et al., 2002a; Vette et al., 2002; Gildmeister et al., 2004).

Mercury dry deposition flux measurements were performed using surrogate surfaces techniques in Chicago, as part of the AEOLOS and LMMBS. The daily dry deposition fluxes measured in July 1994 are shown in Figure 9, with 52% of the dry deposition measured due to particulate mercury deposition and the remainder due to RGM deposition. In 1996, wet and dry deposition samples were collected at three sites in Detroit to investigate the atmospheric contributions of mercury to urban runoff (Gildemeister, 2001; Gildemeister et al., 2004). The monthly dry particulate mercury deposition flux for the April-October period was similar to the monthly wet mercury deposition flux (10.2 $\mu g\ m^{-2}$ vs 14.8 $\mu g\ m^{-2}$, respectively) at the Livernois site in Detroit. It is anticipated that the total dry deposition flux due to both particulate and gaseous mercury would have been greater than the wet deposition flux, based upon the earlier findings in Chicago which suggested that about half of the dry deposition was due to particulate mercury. The elevated levels of RGM and particulate mercury continue to be elevated in the urban areas and substantial dry deposition fluxes continue to be measured (Liu et al. 2006).

As part of a whole-ecosystem mercury cycling study, Rea et al. (2002) measured mercury in the foliage of deciduous trees in Pellston, Michigan over the course of the growing season and found that total foliar mercury accumulation was substantially less than vapor phase Hg^0 deposition estimated following Lindberg et al. (1992). Rea et al. (2001) determined that Hg(p) and RGM dry deposition were rapidly washed off foliar surfaces, and therefore foliar accumulation of mercury most likely represents vapor phase Hg^0 assimilation. In controlled pot and chamber studies with aspen, Ericksen et al. (2003) determined that all foliar accumulation of mercury was due to vapor uptake, regardless of soil mercury concentration.

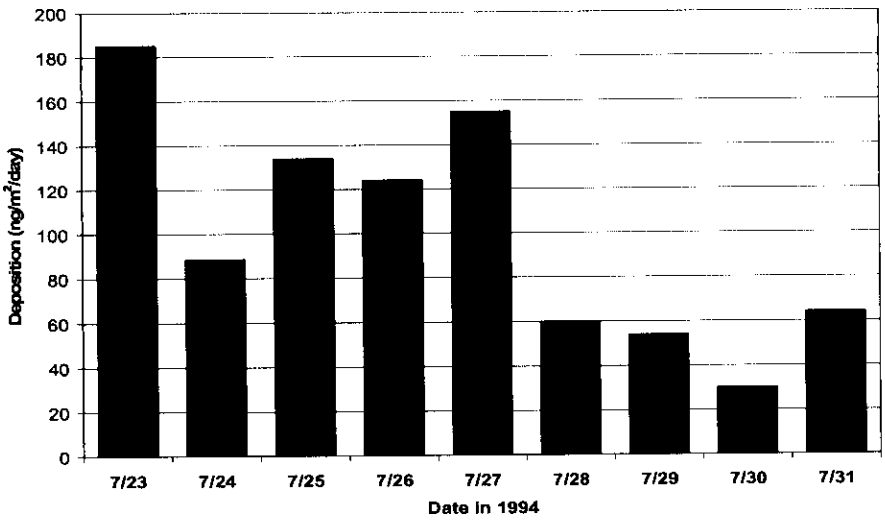

Figure 9. Total mercury dry deposition flux measured in Chicago using the UM aerodynamic mercury water surface sampler in 1994.

The rate of mercury accumulation in foliage was linear with no significant difference between accumulation rates measured by Rea et al. (2002) in two different forests, with significantly different meteorological conditions and modeled vapor phase Hg^0 deposition velocities at each site. Miller et al. (2004) suggested that the lack of difference in foliar accumulation rates for the two sites indicated that foliar mercury accumulation was limited by biological processes mediating sequestration of the mercury. Since the annual transfer of mercury from foliage to forest floor via leaf fall represented the net vapor phase Hg^0 deposition (Rea et al., 2002; Ericksen et al., 2003), Miller et al. (2004) developed an empirical method to estimate the accumulation of mercury in foliage of the study area, with the mercury content of deciduous foliage found to be a linear function of growing season length. To date, Hg^0 deposition and accumulation have not been adequately treated in mercury transport and deposition models and represent significant sources of uncertainty in our impact assessments. The elevated levels of Hg^0 observed in the southern and eastern portion of the Great Lakes region represent the contributions of the major anthropogenic sources in this region and therefore are likely the major contributor to the vapor phase Hg^0 deposition and accumulation in the foliage.

While it was evident that urban sources were impacting mercury deposition to downwind lakes and ecosystems, studies performed to date were limited by the lack of RGM measurements, which are essential for estimating the dry deposition of mercury and for identifying the source or sources of the mercury deposited.

ATMOSPHERIC CHEMISTRY AND SPECIATION

Mercury has been measured in the atmosphere in both gas and particle phases. Greater than 95% of global gaseous mercury may be in the elemental state (Hg^0). It is the divalent gaseous form of mercury (Hg^{2+}), as well as particulate mercury, however, that are the critical components in understanding mercury removal processes and deposition rates from the atmosphere because

these species are highly water soluble (Fitzgerald et al., 1991). That the gaseous forms of mercury interact in a complex way with particulate matter suggests that gas-particle partitioning of mercury also controls the deposition from the atmosphere. A large percentage (as much as 95%) of the mercury emitted by various source types was in a water soluble, reactive gaseous form (Prestbo and Bloom 1995; Dvonch et al., 1999; Lindberg and Stratton, 1998). While progress has been made in identifying and quantifying mercury emission sources, few field-based studies have attempted to identify the mechanisms and processes critical to enable predictive modeling of mercury transport, transformation, and deposition. These processes include the characterization of speciated mercury in emissions, ambient air, and ultimately deposition.

Local Source Impacts in Urban Areas

Measurements of speciated gaseous mercury were made in Detroit during each summer from 2000-2002. The sampling site was located in close proximity (within 4 km) to a large heavy industrial source complex (Dvonch et al., 2005), which included coal combustion, oil refineries, coke ovens, iron/steel mills, and sewage sludge incineration. Significant local source impacts were observed at the site with maximum hourly RGM values that reached 208 pg/m^3 and the Hg^0 values that exceeded 14 ng/m^3 on July 17, 2001. An analysis of the surface meteorological data collected on-site indicated that winds were from the southwest during this period, the direction of the nearby industrial source complex. These results provide evidence that RGM may remain in a divalent form downwind from the source. The maximum values observed in 2001 were quite similar to those measured in Detroit in 2000 and 2002 (Lynam and Keeler, 2002; Lynam and Keeler, 2004). The maximum RGM values in Detroit during these measurements were also similar to those previously measured in Baltimore in 1998, when levels reached 211 pg/m^3 after plume impaction at the measurement site by a nearby municipal waste incinerator (Dvonch et al., 2005). Elevated RGM may be expected immediately downwind of waste incinerators since previous in-stack measurements have shown that 75-95% of the mercury is emitted as RGM (Dvonch et al., 1999).

Production of RGM in Ambient Air

Speciated measurements of gaseous mercury were performed in Ann Arbor, Michigan, during the summer of 1999 (Dvonch et al., 2004). A clear diurnal pattern was observed in the RGM concentrations similar to that observed in Detroit, and this pattern was particularly pronounced on certain days, such as those shown in June and July 1999. The highest levels of RGM occurred during the daytime, after solar noon, as seen in Figure 10. A clear positive relationship between RGM and ozone (O_3) was also observed on these summer days, as RGM maximums exceeded 140 pg m^{-3} on both June 22 and June 23, 1999. Overall for the 16-week sampling period at Ann Arbor, Dvonch et al. (2004) determined the diurnal patterns observed in RGM were found to significantly co-vary with ambient O_3 ($r = 0.50$, $n = 916$, $\alpha = 0.01$). Since O_3 is a photochemically produced secondary pollutant that serves as an indicator of increased photochemistry and increased oxidant production, the positive relationship observed between with RGM points to the real-time production of RGM as a result of photochemical oxidants.

An analysis of concurrent Hg^0 concentrations provided additional evidence for the photochemical production of RGM. Overall for the 16-week sampling period at Ann Arbor, a significant negative correlation was found between Hg^0 and O_3 ($r = -0.18$, $n = 526$, $\alpha = 0.01$) (Dvonch et al., 2004).

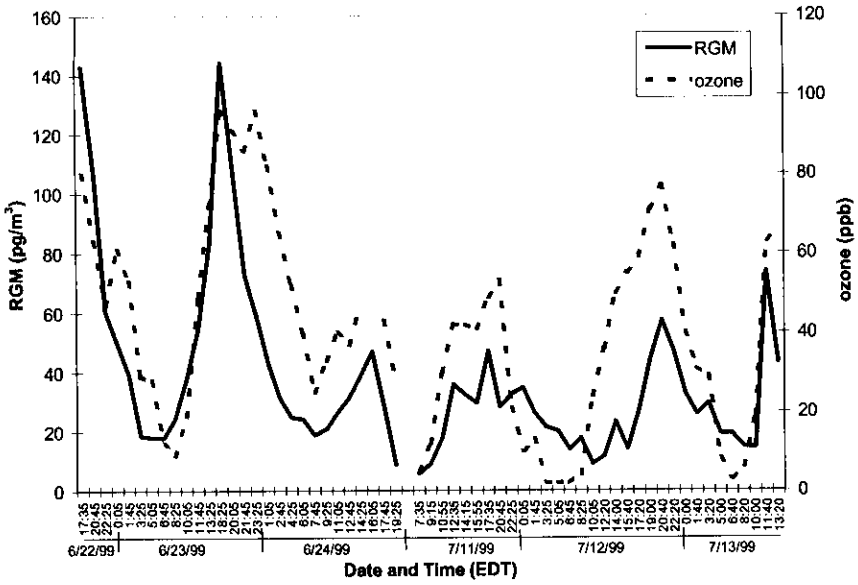

Figure 10. Reactive Gaseous Mercury and Ozone Measured at Ann Arbor, MI (June-July, 1999).

This relationship was particularly pronounced during periods of enhanced O_3, such as September 1-5, 1999 ($r = -0.77$, $n = 58$, $\alpha = 0.01$). A significant negative correlation between Hg^0 and RGM was also found during this period ($r = -0.35$, $n = 66$, $\alpha = 0.01$), as illustrated in Figure 5 by the sharp decrease in Hg^0 together with the increase in afternoon RGM and O_3.

The strong diurnal patterns observed provide additional evidence to suggest that RGM is produced via photochemical reactions. As part of the analysis, daily air mass back-trajectories from the site were calculated, which suggested that the diurnal RGM maximums observed at Ann Arbor were not due to local source impacts, but instead were a result of RGM production during transport of the air mass. It was also noted that while the increases in RGM represented roughly only 10% of the decreases in Hg^0 during periods of elevated O_3, a mass balance of the two species should not be expected given the high solubility of RGM relative to Hg^0 and the expected deposition during air mass transport.

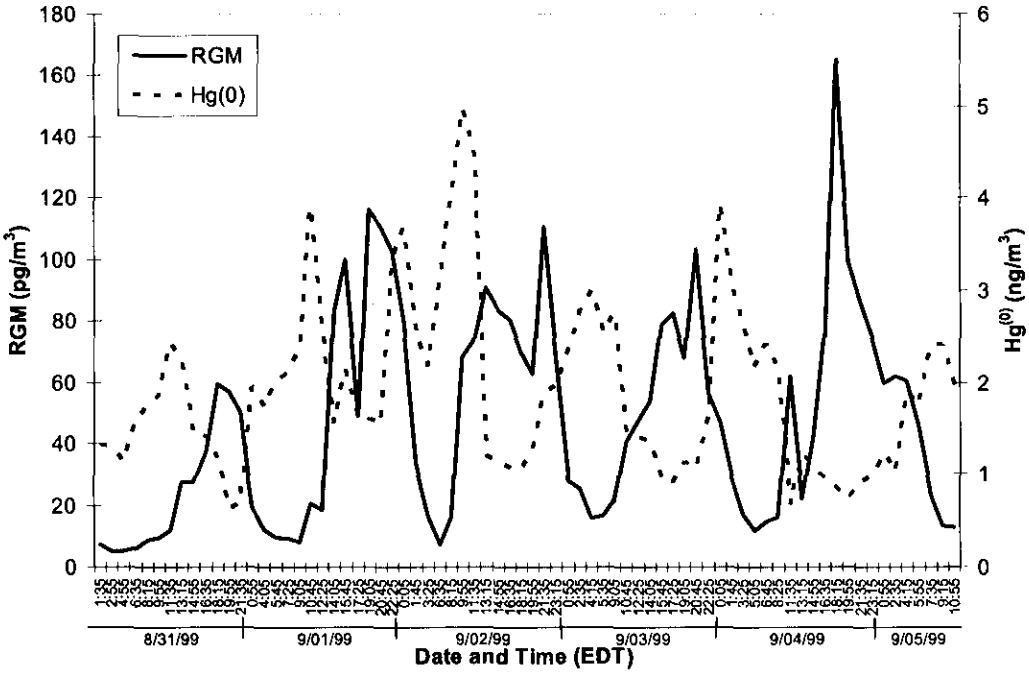

Figure 11. Speciated Gaseous Mercury Measured at Ann Arbor, MI (August-September, 1999).

While a small amount of field-based data have been published to date to assess atmospheric mercury oxidation in northern temperate climates, recent measurements along the west coast of Washington State identified that large and frequent Hg^0 losses occurred during summertime periods with increased O_3 (Weiss-Penzias et al., 2003), and measurements along the west coast of Ireland suggest BrO^- as responsible for Hg^0 oxidation (Munthe et al., 2003). The loss of Hg^0 and production of RGM on days with increased photochemistry observed in Michigan differ from the above investigations in that these measurements are far removed from influences of the marine environment. Because of this, reactive halogen species, which evolved from sea salt, would not be expected to be responsible for the observed Hg^0 oxidation. Species, such as the hydroxyl radical, are more likely to be important in temperate climates that are far removed from marine influences, and require further study in future investigations.

Long-Term Speciated Ambient Mercury Levels in Detroit

The intensive speciated mercury data collected in urban areas during 1998-2002 made clear the need for long-term measurements. In September 2002, a long-term speciated ambient mercury monitoring site in Detroit was established for the measurements of Hg^0, RGM, and particulate mercury utilizing the Tekran 2537A/1130/1135 Mercury Speciation System. Data are presented here for the first full year of data collection (thru September 2003). Mean levels (± standard deviation) of Hg^0, RGM, and particulate mercury were 2.4 ± 1.4 ng m^{-3}, 16.5 ± 28.9 pg m^{-3}, and 22 ± 30 pg m^{-3}, respectively. The University of Michigan Air Quality Laboratory (UMAQL) has established long-term speciated ambient mercury monitoring sites at a rural site in Dexter, Michigan, as well as at a regionally impacted site in Stuebenville, Ohio, to quantify

the source impacts and levels of speciated ambient mercury across the Great Lakes region. Maximum hourly concentrations of RGM and particulate mercury at the urban Detroit and source-impacted Ohio site reach near 1 ng/m^3 and are 5-10 fold higher than maximum levels observed at rural measurement sites.

SOURCES OF ATMOSPHERIC MERCURY DEPOSITION

Currently, emissions of mercury from coal burning utilities are the largest source category within the U.S., and new rules have been issued by the Federal Government to control these emissions (USEPA, 2005). Understanding all of the major sources of mercury is required to manage the risk to humans and vulnerable ecosystems. One approach to defining the sources of atmospheric mercury is the development of source receptor relationships that can be used to assess contributions from various sources based on observations made at sampling or receptor sites. Therefore, speciated mercury emissions rates from all the major sources that are likely to impact the receptor site are not required. Source receptor relationships have been developed for mercury in precipitation (Dvonch et al, 1999) and for particulate phase mercury (Ames et al, 1998; Gildemeister, 2001; Graney et al. 2004). These studies reveal that mercury in precipitation and in the particulate phase exhibit well defined source receptor relationships.

Recently, Lynam and Keeler (2006) reported the results from a field measurement program performed in Detroit. In this study, measurements of other criteria pollutants including ozone, carbon monoxide, sulfur dioxide nitrogen oxides, as well as meteorological parameters were made, in addition to measurements of speciated mercury. The combined short-duration measurement data were analyzed to develop source receptor relationships. The relationships between elemental mercury, RGM, and particulate phase mercury, chemical and meteorological variables were defined to apportion the sources of mercury observed at the Detroit monitoring site. They concluded that regional sources of RGM in photochemically active air masses as well source contributions from local coal combustion and motor vehicle emission sources were important in Detroit. This finding is applicable to other urban areas in the Great Lakes region that have a similar density of industrial and mobile sources contributing to the elevated levels measured in these areas.

Impact of Coal-fired Utilities

In a 1998 Report to Congress, the USEPA identified coal-fired utility boilers as the largest source of domestic anthropogenic mercury emissions to the atmosphere and provided evidence of a causal link between such releases and the presence of methylmercury in fish tissue. At that time, USEPA recognized that the Ohio River Valley contained a high density of coal-fired utility boilers and that no monitoring of atmospheric mercury deposition was being conducted in the area. In 2002, USEPA initiated a mercury monitoring and source apportionment study to investigate the impact of local and regional coal combustion sources on atmospheric mercury deposition in the Ohio River Valley.

The relative importance of domestic coal combustion sources to atmospheric mercury deposition in the U.S., and the efficacy of the USEPA's Clean Air Mercury Rule (CAMR) cap and trade approach to decrease mercury in fish, are topics in an ongoing debate in the scientific community. At the center of this debate is the question of the relative importance of mercury emissions from domestic coal-fired utility boilers to atmospheric deposition into sensitive

aquatic and terrestrial ecosystems. As part of the CAMR development process, USEPA used the Community Multi-scale Air Quality model (CMAQ), an Eulerian dispersion model, to estimate the impact of domestic mercury sources on atmospheric deposition for CY2001. While extremely useful, all contemporary deterministic models (e.g., CMAQ) are limited by the currently large uncertainties in emission inventories, atmospheric mercury chemistry, and wet and dry deposition parameterizations. Receptor models differ from deterministic models in that they are statistical methods for which implementation relies only upon observations of deposition at a location or receptor. Deterministic and receptor modeling source apportionment approaches are independent and complementary.

Multivariate statistical receptor models, such as principal component analysis (PCA), have been successfully used to apportion the sources of mercury deposited in southern Florida (Dvonch et al. 1999) and the sources of other chemical compounds elsewhere (Anderson et al. 2002). More recently, statistical techniques such as Unmix (Lewis et al. 2003) and positive matrix factorization (PMF) have been developed to improve upon the earlier techniques using uncertainties in the data matrix (Paaterro et al. 1994; Anttila et al. 1995) as well as through constraining the solutions to non-negative solutions. Both techniques have the advantage of not requiring prior measurements of source profiles or emission inventories. PMF and Unmix were applied to the precipitation chemistry data collected at Steubenville, Ohio, to determine the sources contributing to mercury in wet deposition.

Six source factors were identified with similar composition and mercury contributions, with the factor identified as coal combustion (S, As, Se, and NO_3^-) clearly dominant in terms of explaining the mercury deposition (~70%). Atmospheric Se is often associated with the burning of fossil fuels such as coal (Biegalski et al. 1998) and Se in the absence of significant Ni and V was determined to be an appropriate tracer of coal combustion in Steubenville (Grahme and Hidy, 2004). There are several large steel manufacturing facilities in the Steubenville–Wheeling, West Virginia area as well as plants to the east in Pittsburgh, but iron-steel production (Fe, V, and Cr) was not a significant contributor to mercury deposition (< 1%). An unidentified phosphorous source (P, Mg, Mn, Fe, and Sr) and an oil combustion/incineration source (Pb, Cl, V, Zn) were found to be minor contributors to mercury deposition (2 and 6% respectively). The elements Zn, Pb, Cu, and Cl have been used to identify municipal waste incinerator emissions (Greenberg et al. 1978), and the elements Ni and V are commonly used tracers to identify oil combustion (Kitto, 1993). A meteorological analysis corroborates that a substantial amount of the mercury deposition found at the Steubenville site is due to local and regional sources (Keeler et al. 2006).

The large temporal variability and range of concentrations among the event samples in Steubenville (4.0 to 78.9 ng L^{-1}) also indicates a strong local and/or regional source influence. Only 9.5% of the variability in concentration could be accounted for by precipitation amount alone. In addition, a large range was found in mercury concentrations among samples with a similar precipitation depth: 4.3 to 78.9 ng L^{-1} for low precipitation depth samples (< 1 cm) and 4.2 to 22.1 ng L^{-1} for high precipitation depth samples (>5 cm). Previous studies have shown that a large range in concentration for similar rainfall amounts can be attributed to variability in impacts by local sources and to the variation in distance between the sources and the receptor site (Dvonch et al. 2005). Because the multivariate statistical analysis points to ~70% of the mercury in the wet deposition as originating from a coal combustion source, all analysis indicate the major contribution from local and regional coal-burning sources.

The importance of coal combustion on the levels of particulate mercury was also quantified as part of the GLAMAP (Burke, 1998). The major sources contributing to the ambient mercury were located in the large urban/industrial areas and along the Ohio River Valley. This is consistent with the findings from the study of the sources of wet deposition in Steubenville discussed above.

SUMMARY

Our understanding of the environmental cycle of mercury has drastically improved over the past two decades. The importance of urban/industrial areas on the levels and deposition of mercury in these areas has been documented, and dry deposition in urban areas likely exceeds wet deposition due to the importance of mercury bound to large particles, and the direct emissions of reactive gaseous mercury (RGM) and its role in the total loading of this contaminant. Deposition of Hg^0 and its subsequent accumulation in plant materials results in significant fluxes of mercury to vegetated ecosystems. Elevated RGM was observed during periods of enhanced photochemical activity with high ozone, warm temperatures, and high solar insolation, which indicated that RGM was produced in the atmosphere during atmospheric transport. Changes in the form of both vapor and particulate phase mercury in response to regional changes in atmospheric chemistry suggest that more research is needed to understand the chemical reactions controlling the deposition of this persistent bioaccumulative pollutant.

Some of the highest concentrations of mercury in precipitation, and in the ambient air in vapor and particulate forms, have been observed in the Midwest. This is consistent with our understanding of the emissions density in the major urban/source areas in the region. Significant south to north gradients in the levels and deposition of mercury have been observed, and air mass transport from known source areas could explain the majority of the variability in the mercury deposition recorded. Local air mass stagnation and synoptic-scale meteorological transport strongly influenced the day-to-day variability in the mercury levels and deposition.

Source-receptor studies indicate that coal-fired utilities contributed ~70% of the mercury wet deposition measured at a site in eastern Ohio. This finding is not unexpected as the Steubenville site was selected due to its close proximity to a number of large coal-fired power plants. The deposition of mercury at this site was heavily influenced by several large precipitation events that contributing significantly (~10%) to the annual deposition, and these events were associated with emissions from local/regional sources. The ambient levels of RGM and particulate mercury are elevated above the levels observed at the more rural sites in Michigan and also reflect the local impact of sources in the vicinity of the site similarly to the levels observed in Detroit. This would suggest that the levels of dry deposition at this site are comparable to those in Detroit and would be similar in magnitude to the wet deposition. Thus, reductions in emissions from coal combustion sources in the region would have a significant impact on the amount of mercury deposited via both wet and dry deposition.

REFERENCES

Burke, J. An Investigation of source-receptor relationships for atmospheric mercury in the Great Lakes Region using receptor modeling techniques. Ph.D. Thesis, University of Michigan, 1998.

Burke, J., Hoyer, M., Keeler, G., Scherbatskoy, T. Wet deposition of mercury and ambient mercury concentrations at a site in the Lake Champlain basin. *Water, Air Soil Pollut.*, 80, 353-362, 1995.

Dvonch, J.T., Graney, J.R., Marsik, F.J., Keeler, G.J., Stevens, R.K. Use of elemental tracers to source apportion mercury in south Florida precipitation. *Env. Sci. Technol.*, 33, 4522-4527, 1999.

Dvonch, J.T., Keeler, G.J., Lynam, M.M., Marsik, F.J., Barres, J.A. The production of reactive gaseous mercury (RGM) in ambient air and its removal by precipitation. *J. Environ. Monit.* (submitted) 2005.

Ericksen, J., Gustin, M.S., Schorran, D., Johnson, D., Lindberg, S., Coleman J. Accumulation of atmospheric mercury in forest foliage. *Atmos. Envir.*, 37, 1613-1622, 2003.

Expert Panel on Mercury Atmospheric Processes (EPMAP). Mercury Atmospheric Processes: A Synthesis Report. EPRI/TR-104214, 1994.

Fitzgerald, W., Gill G. Sub-nanogram determination of mercury by two-stage gold amalgamation and vapor phase detection applied to atmospheric analysis. *Anal. Chem.* 15, 1714, 1979.

Fitzgerald, W.F., Mason, R.P., Vandal, G.M. Atmospheric cycling and air-water exchange of mercury over mid-continental lacustrine regions. *Water, Air Soil Pollut.*, 56, 745, 1991.

Gildemeister, A.E Urban Atmospheric Mercury: The Impact of Local Sources on Deposition and Ambient Concentration in Detroit, Michigan. Ph.D. Thesis, University of Michigan, 2001.

Gildemeister, A.E, Keeler, G.J.and Graney, J.R. Source proximity reflected in spatial and temporal variability in particle and vapor phase Hg concentrations in Detroit, MI. *Atmos. Environ.*, 39, 353-358, 2005.

Graney, J.R., Dvonch, J.T. and Keeler, G.J. Use of elemental tracers to source apportion mercury in south Florida aerosols. *Atmos. Environ.* **38**, 1715-1726. 2004.

Holsen, T.M., Noll, K.E., Fang, G.C., Lee, W.J., Lin, J.M. and Keeler, G.J. Dry Deposition and particle size distributions measured during Lake Michigan Urban Air Toxics study. *Env. Sci. Technol.*, 27, 1141-1150, 1992.

Hoyer, M.E., Burke, J.B., Keeler, G.J. Atmospheric sources, transport and deposition of mercury in Michigan: two years of event precipitation. *Water, Air Soil Pollut.*, 80, 199-208, 1995.

Iverfeldt, A., Lindqvist, O. Atmospheric oxidation of elemental mercury by ozone in the aqueous phase. *Atmos. Environ.*, 20, 1567-1573, 1986;.

Keeler, G.J. Atmospheric Monitoring for the Lake Michigan Mass Balance and the Lake Michigan and Lake Superior Loading Studies: Quality Assurance Project Plan, submitted to the U.S. EPA Great Lakes National Program Office, Chicago, IL: 1994.

Keeler, G., Glinsorn, G., Pirrone, N. Particulate mercury in the atmosphere: its significance, transport, transformation and sources. *Water Air Soil Pollut.*, 80, 159-168, 1995.

Keeler, G. J., Hoyer, M. "Recent measurements of atmospheric mercury in the Great Lakes region." In Atmospheric Deposition of Contaminants to the Great Lakes and Coastal Waters. J.E. Baker, ed. Pensacola, FL: SETAC Press, 1997.

Keeler, G.J., Hoyer, M.E., Lamborg, C.H. Measurements of atmospheric mercury in the Great Lakes basin. Mercury Pollution: Integration and Synthesis. Lewis Publishers, Boca Raton, FL, 231-241, 1994.

Keeler, G.J., Christainson, E.M., Dvonch, J.T., Landis, M. Norris, G. Source of mercury wet deposition in Eastern Ohio, USA. Submitted to *Environ. Sci. Technol.*, 2005.

Keeler, G.J., Gratz, L. and Al-Wali, K. Influences on the Long-term Atmospheric Mercury Wet Deposition at Underhill, Vermont. *Ecotoxicology,* **14**, 71-83. 2005.

Keeler, G.J. and Dvonch, J.T. Atmospheric Mercury: A Decade of Observations in the Great Lakes. *In:* Dynamics of Mercury Pollution on Regional and Global Scales: Atmospheric Processes and Human Exposures around the World. N. Pirrone and K. Mahaffey Eds. Kluwer Ltd. 2005.

Landis, M.S. Keeler, G.J. Critical evaluation of a modified automatic wet-only precipitation collector for mercury and trace element determinations. *Env. Sci. Technol.*, 29, 2123-2132, 1997.

Landis, M.S., Keeler, G.J. Atmospheric mercury deposition to Lake Michigan during the Lake Michigan Mass Balance Study. *Env. Sci. Technol.*, 36, 4518-4524, 2002.

Landis, M.S., Stevens, R.K., Schaedlich, F., Prestbo, E. Development and characterization of an annular denuder methodology for the measurement of divalent inorganic reactive gaseous mercury in ambient air. *Env. Sci. Technol.*, 36, 3000-3009, 2002.

Landis, M.S., Vette, A., Keeler, G.J. Atmospheric mercury in the Lake Michigan Basin: influence of the Chicago/Gary urban area. *Env. Sci. Technol.*, 36, 4508-4517, 2002.

Landis, M.S., Keeler, G.J., Al-Wali, K.I., Stevens, R.K. Divalent inorganic reactive gaseous mercury emissions from a mercury cell chlor-alkali plant and its impact on near-field atmospheric dry deposition. *Atmos. Environ.*, 38, 613-622, 2004.

Lindberg, S.E., Meyers, T.P., Taylor, G.E., Turner, R.R., Schroeder, W.H. Atmosphere-surface exchange of mercury in a forest: Results of modeling and gradient approaches. *J. Geophys. Res.*, 97, 2519-2528, 1992.

Lindberg, S.E., Stratton, W.J. Atmospheric mercury speciation: concentrations and behavior of reactive gaseous mercury in ambient air. *Env. Sci. Technol.*, 32, 49-57, 1998.

Lynam, M.M., Keeler, G.J. Comparison of methods for particulate phase mercury: sampling and analysis. *Anal. Bioanal. Chem.*, 374, 1009-1014, 2002.

Lynam, M.M. and Keeler, G.J. Automated speciated mercury measurements in Michigan, *Environ. Sci. Technol.* **39,** 3289-3299, 2005.

Lynam, M.M. and Keeler, G.J. Source-receptor relationships for elemental and reactive gaseous mercury in Detroit, Michigan. In Press, *Environ. Sci. Technol.*, 2006.

Mierle, G. Aqueous inputs of mercury to precambrian shield lakes in Ontario. *Environ. Tox. and Chem.*, 9, 843-851, 1990.

Miller, E.K., Van Arsdale A., Keeler, G.J., Chalmers, A., Poissant, L. Kammen, N. Estimation and Mapping of Wet and Dry Mercury Deposition Across Northeastern North America. *Ecotoxicology*, (in Press) 2004.

Munthe, J., Wangberg, I., Iverfeldt, A., Lindqvist, O., Stromberg, D., Sommar, J., Gardfeldt, K., Petersen, G., Ebinghaus, R., Prestbo, E., Larjava, K., Siemens, V. Distribution of atmospheric mercury species in Northern Europe: final results from the MOE project. *Atmos. Environ.*, 37 (S1), 9-20, 2003.

Olmez, I. M.R. Ames, G. Gullu, J. Che, J.K. Gone. Upstate New York trace metals program Vol. I. "Mercury" MIT Report No. MITNRL-064, 1996.

Pacyna, E.G., Pacyna, J.M. Global emission of mercury from anthropogenic sources in 1995. *Water Air Soil Pollut.*, 137, 149-165, 2002.

Pirrone, N., Keeler, G.J. Deposition of trace metals in urban and rural areas in the Lake Michigan Basin. *Water Sci. & Technol.*, 28, 261-271, 1993.

Pirrone, N., Keeler, G.J., Holsen, T.M. Dry Deposition of semivolatile organic compounds to Lake Michigan. *Env. Sci. Technol.*, 29, 2123-2132, 1995.

Pirrone, N., Keeler, G.J. and Holsen, T.M. Dry Deposition of trace elements over Lake Michigan: A hybrid-receptor deposition modeling approach. *Env. Sci. Technol.*, 29, 2112-2122, 1995.

Pirrone, N., Keeler, G.J., Nriagu, J.O. Regional differences in worldwide emissions of mercury to the atmosphere. *Atmos. Environ.*, 30, 2981-2987, 1996.

Prestbo, E.M., Bloom, N.S. Mercury speciation adsorption method (MESA) method for combustion flue gas: methodology, artifacts, intercomparison, and atmospheric implications. *Water, Air Soil Pollut.*, 80, 145-158, 1995.

Rea, A.W., Lindberg, S.E., Keeler, G.J. Assessment of dry deposition and foliar leaching of mercury and selected trace elements based on washed foliar and surrogate surfaces. *Env. Sci. Technol.*, 34, 2418-2425, 2000.

Rea, A.W., Lindberg, S.E., Keeler, G.J. Dry deposition and foliar leaching of mercury and selected trace elements in deciduous forest throughfall. *Atmos. Environ.*, 35, 3453-3462, 2001.

Rea, A.W., Lindberg, S.E., Scherbatskoy, T. Keeler, G.J. Mercury accumulation over time in two northern mixed-hardwood forests. *Water, Air Soil Pollut.*, 133, 49-67, 2002.

Schroeder, W. H., Munthe. J. Atmospheric Mercury - An Overview. *Atmos. Environ.*, 32:809-822, 1998.

Sofuoglu, S.C., Paode, R.D., Sivadechathep, J., Noll K.E., Holsen, T.M., Keeler, G.J. Dry Deposition Fluxes and Atmospheric Size Distributions of Mass, Al, and Mg Measured in Southern Lake Michigan during AEOLOS. *Aerosol Sci. Technol.*, 29, 4, 281-293, 1998.

U.S. EPA Office of Air Quality Planning and Standards, Deposition of Air of Pollutants to the Great Waters. First Report to Congress. Research Triangle Park, NC: GEPA-453/R-93-055, 1994.

U.S. EPA, Compendium of Methods for the Determination of Inorganic Compounds in Ambient Air, IO-5, Sampling and Analysis for Vapor and Particle Phase Mercury Utilizing Cold Vapor Atomic Fluorescence Spectrometry. U.S. EPA National Risk Management Research Laboratory, Cincinnati, OH: EPA-625/R-96-010a, 1999.

U.S. Environmental Protection Agency. *Mercury Study Report to Congress*; EPA-452/R-97-005 Office of Air Quality Planning and Standards, Office of Research and Development: Washington, DC, **1997**.

U.S. Environmental Protection Agency, 2005, Clean Air Mercury Rule, www.epa.gov/mercuryrule/

Vette, A.F., Landis, M.S., Keeler, G.J. Deposition and emission of gaseous mercury to and from Lake Michigan during the Lake Michigan Mass Balance Study. *Env. Sci. Technol.*, 36, 4525-4532, 2002.

Weiss-Penzias, P., Jaffe, D.A., McClintick, A., Prestbo, E.M., Landis, M.S. Gaseous elemental mercury in the marine boundary layer: evidence for rapid removal in anthropogenic pollution. *Env. Sci. Technol.*, 37, 3755-3763, 2003.

Yee, Lin Wu, Davidson, Cliff I., Lindberg, S., Armistead, E. Russell, G. Resuspension of particulate chemical species at forested sites. *Env. Sci. Technol.*, 26, 2428-2435, 1992.

Yi, S.M., Holsen, T.M., Noll, K.E. Development of a novel water surface sampler for dry deposition. *Env. Sci. Technol.*, 36, 2815-2821, 2002.

Exhibit C

ICF CONSULTING

Analysis of the Proposed Illinois Mercury Rule

Prepared for:
Illinois Environmental Protection Agency
Division of Air Quality

Prepared by:
ICF Resources, LLC

Under contract to:
Lake Michigan Air Directors Consortium (LADCO)

March 10, 2006

powered by perspective

Table of Contents

List of Exhibits

Appendices

This report is prepared for the Illinois Environmental Protection Agency (IEPA) and analyzes the cost impacts of the proposed Illinois Mercury Rule[1] using ICF's Integrated Planning Model (IPM®). This study focuses on the impacts of the mercury rule in terms of costs to the power sector and costs to electricity consumers. National level and state level results are presented. In addition, the study highlights the effects on generation, coal consumption, control equipment, and emissions.

Scenarios Examined

ICF examined three cases (or scenarios) using IPM as requested by IEPA:

(i) A Base Case with no additional Federal air regulations in place beyond existing regulations including the Title IV SO_2 program, the NO_x SIP Call requirements, and other state regulations in place (the Base Case)

(ii) A Case based upon the run above, but also including the Final Clean Air Interstate Rule (CAIR) and the Clean Air Mercury Rule (CAMR) as put forth by the U.S. EPA (the "CAIR/CAMR" case)

(iii) A case with the Clean Air Interstate Rule in place, the Clean Air Mercury Rule in place for all states but Illinois, and the proposed Illinois Mercury Rule (described below) for Illinois' affected sources. The CAMR mercury emission limit is adjusted downward by the level of the Illinois budget under CAMR.

The difference between a base case and any air regulatory policy case represents the impact of that policy. In this study, differences between the second and first case represents the cost of the CAIR/CAMR rule based on the assumptions underlying this study. The difference between the third and the first run represents the cost of the Illinois Mercury rule, based on those same assumptions. A comparison of these two *cost impact estimates* reflects the incremental cost of Illinois' mercury policy over the CAIR/CAMR case. Note that, mathematically, this impact is the same as the difference between the third and second run. This report focuses on that difference (iii vs. ii). Appendix A summarizes the full results for all three cases and provides comparison of case ii vs. case i, and case iii vs. case i.

The Illinois Mercury Rule

This study uses the IPM model to determine the impacts of the Illinois mercury rule on coal plants in Illinois. The Illinois rule is summarized as follows:

Phase 1 of the rule begins in July 2009. It requires:

- The plant-wide average emissions of coal units: 75-percent reduction of input mercury or 0.020 lbs Hg/GWh.
- The system-wide average emissions of coal units: 90–percent reduction of input mercury or 0.0080 lbs Hg/GWh.

[1] See Title 35: Environmental Protection, Subtitle B: Air Pollution, Chapter I: Pollution Control Board, Subchapter C: Emission Standards And Limitations For Stationary Sources, Part 225, Control Of Emissions From Large Combustion Sources, Draft 03/03/06, as provided by J. Ross, IEPA.

Phase 2 of the rule begins January 1, 2013:

- Plant-wide average emissions of all coal units: 90-percent reduction of input mercury or 0.0080 lbs/GWh.

Given the short time frame for the modeling exercise, ICF was not able to model the rule exactly as it is summarized in the referenced document. Based on discussions with IEPA, and given the available time for this analysis, we structured the analysis as follows:

- First, it is assumed that Phase I of the rule is initiated at the start of 2009.
- Second, rather than model unit level emission rate limits for existing units, ICF simulated unit level emission *rate limits* based on unit level emissions *caps* calculated by IEPA. For subbituminous units, this cap was based on a 90 reduction in emissions from historic levels. For bituminous plants, the cap reflects the rate limit and a fixed generation level. IPM model plant level emissions caps are the sum of the individual unit caps. Note that using caps to simulate a rate limit is a more restrictive policy. Under a rate limit policy, a unit would be able to increase generation and emissions so long as it remained under the rate. Under a cap, emissions do not increase over time.
- The rate limits that are specified above (i.e., 0.020 or 0.0080) were implemented for all potential coal and potential IGCC units in IPM's MANO region (Illinois capacity consists of 88 percent of MANO region's capacity).
- In addition to the plant level caps implemented across the two phases, a system level emissions limit was imposed that reflected the 90 percent reduction requirements of Phase I. This was calculated based on the 0.008 lbs/GWh emission rate limit. This system cap was applied to all Illinois affected units, which is a less restrictive requirement than the proposed rule.

These scenarios were examined using IPM under the assumptions developed and described in this report. IPM is a capacity planning and dispatch model that simulates the operation of the electric power system based upon engineering and economic fundamentals. It is supported by a detailed set of data and assumptions that characterize the current generation and transmission system; fuel markets; demand; environmental requirements; and system constraints. Additional inputs include new technology (including pollution control equipment) costs, current environmental laws and regulations, and any potential future policies being modeled. More information on IPM is provided in Appendix B.

The results that come from the model are dependent on these input assumptions. The starting point for modeling assumptions the Illinois mercury rule for this study is the EPA IPM Base Case 2004 (v.2.1.9) used for analysis of the Clean Air Rules along with modifications made during previous work for the VISTAS, CENRAP, and LADCO Regional Planning Organizations (RPO). Subsequent to this RPO work, ICF was directed to make additional changes by IEPA, including unit level changes for the Illinois units and modifications to mercury control costs. These changes are described further in Appendix C. The results described herein reflect these assumptions.

Results

This section summarizes the results of the analysis focusing on the incremental impacts of the Illinois rule, as represented by the differences between cases (iii) the Illinois rule described above and (ii) the CAIR/CAMR rules. Additional tables and information are provided in the remainder of this report. Full summaries of all cases are presented in Appendix A.

Table 1-1 shows the changes in emissions for mercury, SO_z and NO_X for Illinois and at the national level. Due to the more stringent nature of the mercury rule in Illinois relative to Illinois' allocations under CAMR, emissions of mercury in Illinois are lower by 4,726 lbs in 2009. This is an 85 percent reduction in Illinois mercury emissions relative to the Base and CAMR Cases.

Emissions levels decrease in Illinois over time under the Illinois mercury rule reflecting increased stringency of the emissions constraints and reduced flexibility in compliance. Emissions in Illinois from all units total 883 lbs in 2009 falling to 799 lbs in 2018. This represents a reduction of 4,726 pounds and 1127 pounds in 2009 and 2018, respectively. Note that under the CAIR/CAMR case, Illinois is a net purchaser of mercury emission allowances in 2018 given that its state budget under CAMR is 1,258 pounds of mercury.

The SO_2 and NO_x emissions in Illinois are also lower under the Illinois rule relative to CAIR/CAMR. This results from reductions in coal-fired generation and an increase in scrubber installations in 2009 as a result of the Illinois rule. The mercury emissions are also lower nation-wide, reflecting the reductions from Illinois units.

Table 1-1
Emissions (thousand Tons or Lbs)

	(iii) Policy Case with IL Rule			(ii) Base Case with CAIR/CAMR			Delta (iii - ii)		
Pollutant	2009	2015	2018	2009	2015	2018	2009	2015	2018
IL State									
Hg [1]	883	789	799	5,609	2,463	1,926	(4,726)	(1,674)	(1,127)
SO_2 (Title IV)	232	212	206	309	268	266	(77)	(56)	(60)
NOx (SIP Call)	63	62	61	67	68	68	(4)	(6)	(7)
National									
Hg [1]	81,822	59,828	56,676	86,201	61,552	57,914	(4,379)	(1,724)	(1,238)
SO_2 (Title IV)	6,725	5,204	4,795	6,765	5,195	4,815	(40)	9	(20)
NOx (SIP Call)	2,514	2,366	2,272	2,516	2,365	2,268	(2)	1	4

1. Mercury emissions are reported in pounds; all other pollutants are reported in short tons.

Table 1-2 shows the changes in generation in Illinois and nationally. The total generation in Illinois is lower by 2 percent in 2009 relative to the CAIR/CAMR case. By 2015 and 2018, total generation has decreased by 7 and 5 percent, respectively, relative to the CAMR case.

This reduction is driven by reductions in coal-fired generation in Illinois. Illinois is a net exporter of energy – that is, it generates more than is required to meet its internal demand. Under the CAMR rule, Illinois coal fired generation is reduced somewhat – by 2 percent in 2009, and 6 percent in 2018. However, under the Illinois mercury rule, the impact is more pronounced with reductions in coal-fired generation in 2009, 2015, and 2018 of 4 percent, 15 percent, and 10 percent, respectively, relative to the CAMR rule. With more stringent regulations in place in Illinois, the Illinois coal plants are less competitive, and thus, have fewer opportunities to export coal-fired generation.

The projected decrease in coal generation is slightly compensated by an increase in generation for the oil and natural gas-fired units in Illinois. However, the bulk of the displaced Illinois generation is made up in the rest of MANO and in neighboring regions. Illinois remains a net exporter, but to a lesser degree. Thus, decreases in generation from Illinois units result in a net decline in exports of energy from the MANO region. Total generation decreases overall at the national level, reflecting marginal changes in losses, pumped storage activity and transmission.

Table 1-2
Generation (GWh)

	(iii) Policy Case with IL Rule			(ii) Base Case with CAIR/CAMR			Delta (iii - ii)		
Generation	2009	2015	2018	2009	2015	2018	2009	2015	2018
IL State									
Coal	102,514	93,733	98,375	107,327	109,692	109,523	(4,813)	(15,958)	(11,148)
Hydro	92	92	92	92	92	92	-	-	-
Nuclear	95,092	95,259	96,575	95,092	95,259	96,575	-	-	-
Oil/Natural Gas	3,693	7,528	8,648	3,367	5,815	7,908	326	1,713	739
Other	166	166	166	166	166	166	-	-	-
Renewables	589	1,097	1,097	589	1,097	1,097	-	-	-
Grand Total	202,146	197,875	204,953	206,633	212,120	215,361	(4,487)	(14,245)	(10,408)
National									
Coal	2,187,043	2,448,517	2,650,066	2,189,406	2,448,364	2,640,484	(2,362)	153	9,582
Hydro	287,113	290,063	288,249	287,218	290,205	289,165	(104)	(142)	(916)
Nuclear	796,715	810,065	807,698	796,715	810,065	807,698	-	-	-
Oil/Natural Gas	889,675	1,023,427	1,063,795	887,468	1,023,775	1,073,736	2,207	(348)	(9,940)
Other	44,066	51,731	49,497	44,066	51,731	49,497	-	-	-
Renewables	81,947	101,232	108,330	81,947	101,178	108,361	-	54	(31)
Grand Total	4,286,560	4,725,036	4,967,636	4,286,820	4,725,318	4,968,941	(260)	(283)	(1,305)

Tables 1-3 shows the impact on total production costs due to the Illinois rule as compared to the CAMR. Production costs shown are the total going forward costs for meeting electricity demand, including fuel, VOM costs, FOM costs, and annualized capital costs (including costs for new capacity and retrofits). As can be seen, the total costs at the national level are higher under the Illinois rule by $147 to $267 million per year over the time frame analyzed. These are very small impacts relative to total national costs (about two-tenths of a percent).

In Illinois, production costs are higher in 2009, by about half the national level ($68 million). This reflects a mix of increased capital costs and variable O&M due to additional controls required, partially offset by displaced fuel consumption from lost generation.
In later years under Phase II of the Illinois rule, production costs are *lower* in all years (by $188 and $53 million, in 2015 and 2018, respectively). This reduction in costs reflects the lower level of generation that occurs in Illinois due to the rule (which is down by between 5-7 percent in these years), offset by increased cost of retrofit decisions. Capital costs are up in these years; however, these costs are offset by the reduced fuel and net decreases in VOM costs.

Note that these costs are production costs and do not reflect the opportunity costs (i.e., lost revenues and associated profits) of the lost exports. Generation in Illinois is sufficient to meet internal load and export power to neighboring regions (this assumes that Illinois generators share proportionally in the exports). Under the Illinois mercury rule, this remains true; however, the level of exports declines, with attendant loss of revenues from these sales. We have not quantified these lost revenues.

Table 1-3
Total Production Costs (1999 million dollars) Impacts of the Illinois Rule

	(iii) Policy Case with IL Rule			(ii) Base Case with CAIR/CAMR			Delta (iii - ii)		
Plant Type	2009	2015	2018	2009	2015	2018	2009	2015	2018
IL State									
Variable O&M	357	340	355	306	372	382	51	(32)	(27)
Fixed O&M	2,030	2,137	2,316	2,003	2,134	2,300	28	3	16
Fuel Total	1,931	1,908	1,963	1,995	2,069	2,102	(63)	(162)	(140)
Capital	84	105	295	32	101	198	53	3	97
Total Cost	4,403	4,488	4,929	4,335	4,676	4,982	68	(188)	(53)
National									
Variable O&M	7835	9495	10549	7780	9496	10511	56	(2)	38
Fixed O&M	28926	31772	33432	28910	31749	33388	16	23	44
Fuel Total	61818	65527	68945	61759	65480	69139	59	47	(194)
Capital	2574	13256	19167	2558	13057	18807	16	199	360
Total Cost	101,153	120,049	132,094	101007	119782	131846	147	267	248

Table 1-4 shows the changes in total costs, generation, and average production costs in Illinois and nationally under the two policy cases. Despite lower overall production costs in Illinois (due to lower generation levels), average production costs increase because of the mercury rule. They increase by $0.80 per MWh in 2009, $0.64 per MWh in 2015, and $0.92 per MWh in 2018. Thus, average production costs in Illinois increase by 4 percent, 3 percent, and 4 percent in 2009, 2015 and 2018, respectively. The increase at the national level is minimal (less than two-tenths of a percent) in all years.

The decrease in <u>total</u> costs in Illinois is a result of the decrease in generation levels from Illinois units offset by increased costs for compliance. In these years, these reductions outweigh the increase in production costs due to the mercury rule. Though the decrease in generation leads to a decrease in the exports of energy, the MANO region is still a net exporter of energy. However, the region must import capacity in order to meet summer peak reserve requirements,

Table 1-4
Total Costs (Millions of $) and Average Production Costs (1999 $/MWh)

	(iii) Policy Case with IL Rule			(ii) Base Case with CAIR/CAMR			Delta (iii - ii)		
Plant Type	2009	2015	2018	2009	2015	2018	2009	2015	2018
IL State									
Total Costs (MM$)	4,403	4,488	4,929	4,335	4,676	4,982	68	(188)	(53)
Total Generation (GWh)	202,146	197,875	204,953	206,633	212,120	215,361	(4,487)	(14,245)	(10,408)
Average Costs ($/MWh)	21.78	22.68	24.05	20.98	22.04	23.13	0.80	0.64	0.92
National									
Total Costs (MM$)	101,153	120,049	132,094	101,007	119,782	131,846	147	267	248
Total Generation (GWh)	4,286,560	4,725,036	4,967,636	4,286,820	4,725,318	4,968,941	(260)	(283)	(1,305)
Average Costs ($/MWh)	23.60	25.41	26.59	23.56	25.35	26.53	0.04	0.06	0.06

Table 1-5 shows the changes in firm wholesale electricity prices. The firm price is made of two components: marginal energy and marginal capacity prices. Firm prices in Illinois increase by $0.50/MWh in 2009, by $1.46/MWh in 2015, and $1.00/MWh in 2018. Marginal energy prices reflect the production costs of the marginal plant – the last plant to be dispatched in each hour. The mercury rule causes an increase in production costs and increases the costs of the marginal unit, and thus increases the marginal energy prices over CAMR levels. This in turn leads to higher firm prices for all the years. The rule has a negligible impact on firm electricity prices nation-wide -- $0.07-0.15/MWh across the study horizon.

Table 1-5
Wholesale Firm Electricity Price (1999 $/MWh)

	(iii) Policy Case with IL Rule			(ii) Base Case with CAIR/CAMR			Delta (iii - ii)		
Region	2009	2015	2018	2009	2015	2018	2009	2015	2018
IL (MANO)	27.40	41.08	50.29	26.90	39.62	49.29	0.50	1.46	1.00
National	37.73	39.33	45.45	37.66	39.23	45.31	0.07	0.10	0.14

** The firm wholesale price represents the sum of marginal energy costs and marginal capacity price, spread across all generation. The prices are energy weighted segmental prices.
** Wholesale marginal energy and capacity prices in IPM are forecast at the IPM model region level for each run-year, season, and segment. The wholesale prices for MANO are presented as representative of Illinois.

IPM is a wholesale power market model. As such, its outputs include estimates of increased generation system costs (and hence average cost increases) and impacts on marginal energy and capacity costs. It does not provide projections of retail rates or retail price impacts. Therefore, it is necessary to estimate retail rate impacts based on the available outputs of the model.

Final retail rates depend on the nature of the market in each state (deregulated or not) and the ratemaking process, including how cost increases are allocated among sectors, what returns are ultimately allowed, among a host of other factors. In Illinois, an auction process was recently established that allows for the procurement of electricity at wholesale by Ameren and ComEd for delivery to Illinois retail consumers requiring supply service from their local distribution utility beginning in 2007.

The estimate of retail rate impacts estimated here reflects an assumption that retail rates over the study horizon would increase by the increase in wholesale energy prices. Given the competitive nature of wholesale markets in Illinois, this is not an unreasonable assumption.

A number of other inputs and assumptions are required to calculate the retail rate impact. It is assumed that the increase is applied equally across all sectors -- that is, all sectors bear the same incremental per kWh wholesale cost increases. Second, a forecast of baseline retail rates is required to which to add this increase. For this purpose, we obtained from the DOE's Energy Information Agency's (EIA) Annual Energy Outlook (AEO) 2006 a forecast of sectoral retail electricity rates over the study horizon for the MAIN (Mid-America Interconnected Network) region. The underlying assumption is that forecast retail rates for MAIN are applicable to the state of Illinois. The AEO 2006 scenario from which this rate is taken is comparable to the CAIR/CAMR rule in that those two rules are assumed to be in place in the AEO analysis. However, it is important to note that the two cases may differ on other aspects.

Table 1-6 shows the changes in retail electricity prices by sector. We calculated the retail electricity prices by applying the IPM projected increase in firm wholesale electricity prices resulting from the Illinois rule to the retail sectoral rates obtained from AEO 2006 (adjusted to be consistent year dollars). The policy causes an increase in the production costs and thus energy prices. This in turn leads to higher retail prices for all the sectors.

Price increases range from 0.05 cents per kWh to 0.15 cents per kWh over the study horizon. These represent increases of one to two percent in the residential and industrial sectors and one to 3.5 percent in the commercial sector. Under this methodology, increases in the commercial and industrial sectors are proportionately higher given the lower starting base rates.

Tables 1-6
Estimated Impacts on Retail Electricity Prices in Illinois
(1999 cents per kWh)*

	(iii) Policy Case with IL Rule			(ii) Base Case with CAIR/CAMR			Delta (iii - ii)		
Region	2009	2015	2018	2009	2015	2018	2009	2015	2018
[illegible]				IL State					
Residential	7.43	7.67	7.75	7.38	7.52	7.65	0.05	0.15	0.10
Industrial	6.50	6.50	6.65	6.44	6.35	6.55	0.05	0.15	0.10
Commercial	4.58	4.32	4.45	4.53	4.17	4.35	0.05	0.15	0.10

*Retail prices are estimated by adding the incremental increase in Firm Wholesale Electricity Prices (shown in Table 1-5) between the cases to the retail prices by sector. Retail prices by sector were obtained from EIA's AEO 2006 data. Refer to Table 62: Electric Power Projections by EMM region". Data for the "MAIN" region was used to estimate prices for the Illinois state.

Tables 1-7 and 1-8 show the changes in total expenditures for each sector on an annual and monthly basis. In 2009, residential customer expenditures increase by $28 million; industrial expenditures for electricity increase by $31 million while commercial expenditures increase by $27 million. In 2015, increased expenditures total $87, $101, and $83 million for the residential, commercial, and industrial sectors, respectively. On a monthly basis, the average household will pay $0.49, $1.50 and $1.06 more in 2009, 2015 and 2018, respectively, as a result of incremental impact of the Illinois mercury rule. These numbers are the increase in monthly expenditures in the residential sector in Table 1-8 divided by the number of households in Illinois. The number of households in Illinois was estimated based on forecasts of total population and an estimate of current persons per households, based on Census data.

Tables 1-7
Total Expenditures for Electricity by Sector (1999 million dollars)

	(iii) Policy Case with IL Rule			(ii) Base Case with CAIR/CAMR			Delta (iii - ii)		
Region	2009	2015	2018	2009	2015	2018	2009	2015	2018
IL State									
Residential	4,109	4,569	4,786	4,081	4,482	4,724	28	87	62
Industrial	4,038	4,482	4,848	4,007	4,382	4,775	31	101	73
Commercial	2,488	2,449	2,570	2,461	2,366	2,512	27	83	58

Total bill payments for each sector are calculated as follows. First, an estimate of sales to each sector in Illinois is made based the AEO 2006 projections of each sector's share of total retail sales (for the MAIN region). For example, if AEO projects that in 2010 residential customers will account for x percent of total retail electricity sales, we assume the same share. We estimate Illinois sales based on the assumption that Illinois sales as a proportion of total Illinois generation are the same as that of the MANO region. Finally, the retail prices estimated in Table 1-6 are multiplied by generation to derive total annual expenditures for electricity by sector.

Table 1-8
Impacts on Monthly Expenditures for Electricity by Sector
(1999 million dollars)

	(iii) Policy Case with IL Rule			(ii) Base Case with CAIR/CAMR			Delta (iii - ii)		
Region	2009	2015	2018	2009	2015	2018	2009	2015	2018
IL State									
Residential	342	381	399	340	374	394	2	7	5
Industrial	336	374	404	334	365	398	3	8	6
Commercial	207	204	214	205	197	209	2	7	5

These costs are calculated by dividing the annual payments in 1-7 by 12.

Table 1-9 shows the changes in control technology retrofits between the two policy cases. The proposed mercury rule in Illinois requires an additional 11 GW of ACI controls and 2 GW of FGD controls by 2009. The incremental level of retrofits required by the Illinois rule shrinks by 2018 as the difference between the stringency of the Illinois and CAMR rule shrinks. By 2018, the level of scrubber retrofits required is *lower* than that predicted under CAIR/CAMR, and the least-cost response to the Illinois rule is to add some scrubbers earlier. Similarly, for ACI, the least-cost response is to add about 8 GW of ACI earlier than would be the case under CAIR/CAMR. By 2018, the incremental level of ACI retrofits in Illinois is 2 GW. Note that incremental ACI retrofits occur in the rest of the nation (an additional 1.5 GW by 2015). This is due to the increased level of generation in the rest of the nation that makes up for lost exports from Illinois.

Table 1-9
Control Technology Retrofits (Cumulative MW)

	(iii) Policy Case with IL Rule				(ii) Base Case with CAIR/CAMR				Delta (iii - ii)		
Technology	2009	2015	2018		2009	2015	2018		2009	2015	2018
IL State											
FGD	2,556	2,762	2,762		387	2,836	2,836		2,168	(74)	(74)
SCR	1,748	1,826	1,826		1,799	2,121	2,121		(51)	(295)	(295)
SNCR	-	-	-		-	-	-		-	-	-
ACI	10,590	10,727	11,023		-	7,185	8,498		10,590	3,542	2,525
National											
FGD	38,578	72,100	85,019		36,948	73,530	85,543		1,630	(1,431)	(525)
SCR	34,362	51,042	64,747		34,223	51,213	65,181		139	(171)	(434)
SNCR	2,039	2,575	2,925		2,041	2,578	3,106		(3)	(3)	(181)
ACI	18,493	63,788	72,423		7,934	58,723	67,672		10,559	5,065	4,751

Table 1-10 summarizes the changes in coal consumption between the two cases. It also provides a full comparison of the Illinois rule vs. a Base Case without CAIR/CAMR (second section of the table), and the CAIR /CAMR vs. a case with neither rule in place (third section).

Under CAIR/CAMR, bituminous coal consumption falls by about 18 to 68 TBtu (or about 8 to 24 percent over the study horizon). Under the Illinois Rule, bituminous fuel consumption rises by 48 TBtu in 2009. It falls slightly in 2018 (18 TBtu or 10 percent) under the Illinois rule, but by a much lesser amount than under CAIR. Hence, relative to CAMR, the proposed mercury rule in Illinois leads to an increase in use of bituminous coal and a decrease in the use of subbituminous coal in Illinois units. This reflects the incremental use of scrubbers in early years. These decreases in subbituminous coal consumption are substantially offset by increases in the rest of the nation. Coal prices are not affected by the Illinois rule.

Table 1-10
Coal Consumption (TBtu)

Comparison of Two Policy Cases										
	(iii) Policy Case with IL Rule			(ii) Base Case with CAIR/CAMR			Delta (iii - ii)		
Coal Type	2009	2015	2018	2009	2015	2018	2009	2015	2018
IL State									
Bituminous	268	254	262	201	214	212	67	40	50
Subbituminous	808	728	751	924	942	942	(116)	(214)	(191)
Lignite	-	-	-	-	-	-	-	-	-
Total	1,077	982	1,013	1,126	1,156	1,154	(49)	(174)	(141)
National									
Bituminous	12,940	14,114	15,153	12,945	14,070	15,068	(5)	44	86
Subbituminous	8,990	9,995	10,680	8,990	10,053	10,701	-	(58)	(21)
Lignite	774	774	774	792	792	792	(18)	(18)	(18)
Total	22,704	24,882	26,607	22,727	24,915	26,560	(23)	(32)	47
Impact of the Illinois Rule									
	(iii) Policy Case with IL Rule			(i) Base Case without CAIR/CAMR			Delta (iii - i)		
IL State									
Bituminous	268	254	262	220	243	280	48	11	(18)
Subbituminous	808	728	751	920	938	936	(112)	(211)	(185)
Lignite	-	-	-	-	-	-	-	-	-
Total	1,077	982	1,013	1,140	1,181	1,215	(63)	(200)	(202)
National									
Bituminous	12,940	14,114	15,153	13,117	13,570	14,418	(177)	544	735
Subbituminous	8,990	9,995	10,680	8,989	10,813	11,683	1	(818)	(1,003)
Lignite	774	774	774	801	801	801	(27)	(27)	(27)
Total	22,704	24,882	26,607	22,908	25,184	26,902	(203)	(302)	(295)
Impact of CAIR/CAMR									
	(ii) Base Case with CAIR/CAMR			(i) Base Case without CAIR/CAMR			Delta (ii - i)		
IL State									
Bituminous	201	214	212	220	243	280	(18)	(29)	(68)
Subbituminous	924	942	942	920	938	936	4	3	6
Lignite	-	-	-	-	-	-	-	-	-
Total	1,126	1,156	1,154	1,140	1,181	1,215	(14)	(26)	(62)
National									
Bituminous	12,945	14,070	15,068	13,117	13,570	14,418	(172)	500	650
Subbituminous	8,990	10,053	10,701	8,989	10,813	11,683	1	(760)	(981)
Lignite	792	792	792	801	801	801	(10)	(10)	(10)
Total	22,727	24,915	26,560	22,908	25,184	26,902	(180)	(269)	(341)

Table 1-11 summarized coal plant retirements resulting from the rule. IPM retires units when it is uneconomic for them to continue operation, in comparison to the alternatives of running existing units harder, building new units, and when considering whether their continued operation is required for reserve margin purposes. This decision reflects the situation over the entire study horizon. Relative to the CAIR/CAMR, the proposed rule causes a small amount of coal-fired capacity to be uneconomic and thus retire (252 MW). These plants are Hutsonville Units 5 and 6 (partial) and Meredosia Units 1-4. These units are currently 50 years old or older. In practice, units that become uneconomic when the rule takes effect may be "mothballed" until fuel prices or other conditions change, they may retire, or kept in service for grid reliability purposes.

Table 1-11
Cumulative Coal Plant Retirements (MW)

	(iii) Policy Case with IL Rule			(ii) Base Case with CAIR/CAMR			Delta (iii - ii)		
Plant Type	2009	2015	2018	2009	2015	2018	2009	2015	2018
IL State									
Coal	597	597	597	345	345	345	252	252	252
National									
Coal	2,085	2,788	2,788	1,880	2,585	2,585	205	203	203

* Retirement figures are cumulative.

Conclusions

The principal findings of this study are:

- The mercury rule reduces coal-fired generation in Illinois by 15 percent in 2015 (7 percent reduction in total generation). This generation lowers exports to neighboring regions.
- Total production cost in the region increase by about 2 percent in the first year of the policy. However, in subsequent years, costs fall as exports fall and associated production costs offset compliance costs increases. This also implies that revenues from exports fall.
- Average production costs in Illinois increase by 2 to 3 percent as a result of the rule. Marginal prices increase by 2 to 4 percent across the study period.
- Mercury emissions drop to 883 pounds of mercury by 2009, 84 percent below levels under the CAMR. By 2018, they fall to 799 pounds, 58 percent below CAMR levels.
- The retail electricity prices and expenditures across all sectors (residential, industrial and commercial) are higher as a result of the rule relative to the CAMR, but by only a small percentage – 1 to 3.5 percent over the study horizon. On an average bill basis, residential customers pay less than $1.50 per month more under the Illinois rule relative to CAMR across the study horizon.

ICF CONSULTING

Analysis of the Proposed Illinois Mercury Rule

Appendix A: Summary Results Tables

Prepared for:
Illinois Environmental Protection Agency
Division of Air Quality

Prepared by:
ICF Resources, LLC

Under contract to:
Lake Michigan Air Directors Consortium (LADCO)

March 10, 2006

powered by perspective

List of Exhibits

Exhibit A.1
Comparison of Emissions (thousand Tons)

	(iii) Policy Case with IL Rule			(ii) Base Case with CAIR/CAMR			Delta (iii - ii)		
Pollutant	**2009**	**2015**	**2018**	**2009**	**2015**	**2018**	**2009**	**2015**	**2018**
IL State									
Hg [1]	883	789	799	5,609	2,463	1,926	(4,726)	(1,674)	1,127)
SO_2 (Title IV)	232	212	206	309	268	266	(77)	(56)	(60)
NOx (SIP Call)	63	62	61	67	68	68	(4)	(6)	(7)
National									
Hg [1]	81,822	59,828	56,676	86,201	61,552	57,914	(4,379)	(1,724)	(1,238)
SO_2 (Title IV)	6,725	5,204	4,795	6,765	5,195	4,815	(40)	9	(20)
NOx (SIP Call)	2,514	2,366	2,272	2,516	2,365	2,268	(2)	1	4

	(iii) Policy Case with IL Rule			(i) Base Case without CAIR/CAMR			Delta (iii - i)		
Pollutant	**2009**	**2015**	**2018**	**2009**	**2015**	**2018**	**2009**	**2015**	**2018**
IL State									
Hg [1]	883	789	799	5,803	5,638	5,648	(4,920)	(4,849)	(4,848)
SO_2 (Title IV)	232	212	206	344	342	346	(111)	(131)	(140)
NOx (SIP Call)	63	62	61	135	141	142	(72)	(79)	(81)
National									
Hg [1]	81,822	59,828	56,676	107,563	108,298	111,403	(25,741)	(48,470)	(54,728)
SO_2 (Title IV)	6,725	5,204	4,795	10,119	9,101	8,876	(3,393)	(3,897)	(4,081)
NOx (SIP Call)	2,514	2,366	2,272	3,732	3,744	3,788	(1,219)	(1,379)	(1,515)

	(ii) Base Case with CAIR/CAMR			(i) Base Case without CAIR/CAMR			Delta (ii - i)		
Pollutant	**2009**	**2015**	**2018**	**2009**	**2015**	**2018**	**2009**	**2015**	**2018**
IL State									
Hg [1]	5,609	2,463	1,926	5,803	5,638	5,648	(194)	(3,174)	(3,722)
SO_2 (Title IV)	309	268	266	344	342	346	(35)	(74)	(80)
NOx (SIP Call)	67	68	68	135	141	142	(68)	(73)	(74)
National									
Hg [1]	86,201	61,552	57,914	107,563	108,298	111,403	21,362)	(46,746)	(53,490)
SO_2 (Title IV)	6,765	5,195	4,815	10,119	9,101	8,876	(3,353)	(3,906)	(4,061)
NOx (SIP Call)	2,516	2,365	2,268	3,732	3,744	3,788	(1,217)	(1,379)	(1,520)

1. Mercury emissions are reported in pounds; all others are short tons

Exhibit A.2
Generation (GWh)

	(iii) Policy Case with IL Rule			(ii) Base Case with CAIR/CAMR			Delta (iii - ii)		
Generation	2009	2015	2018	2009	2015	2018	2009	2015	2018
IL State									
Coal	102,514	93,733	98,375	107,327	109,692	109,523	(4,813)	(15,958)	(11,148)
Hydro	92	92	92	92	92	92	-	-	-
Nuclear	95,092	95,259	96,575	95,092	95,259	96,575	-	-	-
Oil/Natural Gas	3,693	7,528	8,648	3,367	5,815	7,908	326	1,713	739
Other	166	166	166	166	166	166	-	-	-
Renewables	589	1,097	1,097	589	1,097	1,097	-	-	-
Grand Total	202,146	197,875	204,953	206,633	212,120	215,361	(4,487)	(14,245)	(10,408)
National									
Coal	2,187,043	2,448,517	2,650,066	2,189,406	2,448,364	2,640,484	(2,362)	153	9,582
Hydro	287,113	290,063	288,249	287,218	290,205	289,165	(104)	(142)	(916)
Nuclear	796,715	810,065	807,698	796,715	810,065	807,698	-	-	-
Oil/Natural Gas	889,675	1,023,427	1,063,795	887,468	1,023,775	1,073,736	2,207	(348)	(9,940)
Other	44,066	51,731	49,497	44,066	51,731	49,497	-	-	-
Renewables	81,947	101,232	108,330	81,947	101,178	108,361	-	54	(31)
Grand Total	4,286,560	4,725,036	4,967,636	4,286,820	4,725,318	4,968,941	(260)	(283)	(1,305)

	(iii) Policy Case with IL Rule			(i) Base Case without CAIR/CAMR			Delta (iii - i)		
Generation	2009	2015	2018	2009	2015	2018	2009	2015	2018
IL State									
Coal	102,514	93,733	98,375	108,482	111,883	115,910	(5,968)	(18,150)	(17,535)
Hydro	92	92	92	92	92	92	-	-	-
Nuclear	95,092	95,259	96,575	95,092	95,259	96,575	-	-	-
Oil/Natural Gas	3,693	7,528	8,648	3,152	5,982	6,725	541	1,546	1,923
Other	166	166	166	166	166	166	-	-	-
Renewables	589	1,097	1,097	583	589	1,097	7	507	-
Grand Total	202,146	197,875	204,953	207,567	213,971	220,565	(5,421)	(16,097)	(15,612)
National									
Coal	2,187,043	2,448,517	2,650,066	2,208,601	2,477,667	2,680,544	(21,558)	(29,150)	(30,478)
Hydro	287,113	290,063	288,249	288,494	291,785	292,094	(1,381)	(1,721)	(3,844)
Nuclear	796,715	810,065	807,698	796,715	810,065	807,698	-	-	-
Oil/Natural Gas	889,675	1,023,427	1,063,795	869,402	996,033	1,035,789	20,273	27,394	28,006
Other	44,066	51,731	49,497	44,066	51,731	49,497	-	-	-
Renewables	81,947	101,232	108,330	81,652	100,739	107,949	295	492	381
Grand Total	4,286,560	4,725,036	4,967,636	4,288,930	4,728,021	4,973,571	(2,370)	(2,985)	(5,935)

Exhibit A.2 (continued)
Generation (GWh)

	(ii) Base Case with CAIR/CAMR			(i) Base Case without CAIR/CAMR			Delta (ii - i)		
Generation	**2009**	**2015**	**2018**	**2009**	**2015**	**2018**	**2009**	**2015**	**2018**
IL State									
Coal	107,327	109,692	109,523	108,482	111,883	115,910	(1,155)	(2,192)	(6,387)
Hydro	92	92	92	92	92	92	0	0	0
Nuclear	95,092	95,259	96,575	95,092	95,259	96,575	0	0	0
Oil/Natural Gas	3,367	5,815	7,908	3,152	5,982	6,725	215	(167)	1,184
Other	166	166	166	166	166	166	0	0	0
Renewables	589	1,097	1,097	583	589	1097	7	507	0
Grand Total	206,633	212,120	215,361	207,567	213,971	220,565	(933)	(1,851)	(5,204)
National									
Coal	2,189,406	2448364	2,640,484	2,208,601	2,477,667	2,680,544	(19,196)	(29,304)	(40,061)
Hydro	287,218	290205	289,165	288,494	291,785	292,094	(1,277)	(1,579)	(2,929)
Nuclear	796,715	810065	807,698	796,715	810,065	807,698	0	0	0
Oil/Natural Gas	887,468	1023775	1,073,736	869,402	996,033	1,035,789	18,066	27,742	37,946
Other	44,066	51731	49,497	44,066	51,731	49,497	0	0	0
Renewables	81,947	101178	108,361	81,652	100,739	107,949	295	438	412
Grand Total	4,286,820	4725318	4,968,941	4,288,930	4,728,021	4,973,571	(2,111)	(2,702)	(4,630)

Exhibit A.3
Comparison of Wholesale Firm Electricity Prices (1999 Mills/kWh)

	(iii) Policy Case with IL Rule				(ii) Base Case with CAIR/CAMR				Delta (iii - ii)		
Region	2009	2015	2018		2009	2015	2018		2009	2015	2018
IL	27.40	41.08	50.29		26.90	39.62	49.29		0.50	1.46	1.00
National	37.73	39.33	45.45		37.66	39.23	45.31		0.07	0.10	0.14

	(iii) Policy Case with IL Rule				(i) Base Case without CAIR/CAMR				Delta (iii - i)		
Region	2009	2015	2018		2009	2015	2018		2009	2015	2018
IL	27.40	41.08	50.29		25.55	38.82	47.09		1.85	2.26	3.20
National	37.73	39.33	45.45		36.73	38.86	44.90		1.00	0.47	0.55

	(ii) Base Case with CAIR/CAMR				(i) Base Case without CAIR/CAMR				Delta (ii - i)		
Region	2009	2015	2018		2009	2015	2018		2009	2015	2018
IL[1]	26.90	39.62	49.29		25.55	38.82	47.09		1.36	0.80	2.20
National	37.66	39.23	45.31		36.73	38.86	44.90		0.93	0.37	0.41

1. Representative of IPM's MANO regional prices

Exhibit A.4
Retail Electricity Prices (1999 mills/kWh)

	(iii) Policy Case with IL Rule			(ii) Base Case with CAIR/CAMR			Delta (iii - ii)		
Region	2009	2015	2018	2009	2015	2018	2009	2015	2018
IL State									
Residential	74.32	76.70	77.47	73.81	75.25	76.47	0.50	1.46	1.00
Industrial	64.95	64.98	66.55	64.45	63.52	65.55	0.50	1.46	1.00
Commercial	45.75	43.16	44.47	45.25	41.70	43.47	0.50	1.46	1.00
National									
Residential	75.76	73.69	74.02	75.69	73.59	73.88	0.07	0.10	0.14
Industrial	69.07	65.85	66.41	69.01	65.75	66.27	0.07	0.10	0.14
Commercial	49.14	45.49	46.17	49.07	45.39	46.04	0.07	0.10	0.14

	(iii) Policy Case with IL Rule			(i) Base Case with out CAIR/CAMR			Delta (iii - ii)		
Region	2009	2015	2018	2009	2015	2018	2009	2015	2018
IL State									
Residential	74.32	76.70	77.47	72.46	74.45	74.27	1.85	2.26	3.20
Industrial	64.95	64.98	66.55	63.10	62.72	63.35	1.85	2.26	3.20
Commercial	45.75	43.16	44.47	43.90	40.90	41.27	1.85	2.26	3.20
National									
Residential	75.76	73.69	74.02	74.76	73.22	73.47	1.00	0.47	0.55
Industrial	69.07	65.85	66.41	68.07	65.38	65.86	1.00	0.47	0.55
Commercial	49.14	45.49	46.17	48.14	45.02	45.62	1.00	0.47	0.55

	(ii) Base Case with CAIR/CAMR			(i) Base Case with out CAIR/CAMR			Delta (iii -a ii)		
Region	2009	2015	2018	2009	2015	2018	2009	2015	2018
IL State									
Residential	73.81	75.25	76.47	72.46	74.45	74.27	1.35	0.80	2.20
Industrial	64.45	63.52	65.55	63.10	62.72	63.35	1.35	0.80	2.20
Commercial	45.25	41.70	43.47	43.90	40.90	41.27	1.35	0.80	2.20
National									
Residential	75.69	73.59	73.88	74.76	73.22	73.47	0.93	0.37	0.41
Industrial	69.01	65.75	66.27	68.07	65.38	65.86	0.93	0.37	0.41
Commercial	49.07	45.39	46.04	48.14	45.02	45.62	0.93	0.37	0.41

Note: *Retail price are estimated by adding the incremental increase in Firm Wholesale Electricity Prices between the cases to the retail prices by sector. Retail prices by sector were obtained from EIA's AEO 2006 data. Refer to Table 62: Electric Power Projections by EMM region". Data for the "MAIN" region was used to estimate prices for the Illinois state. See main report.

Exhibit A.5
Annual Expenditures for Electricity by Sector (1999 million dollars)

	(iii) Policy Case with IL Rule			(ii) Base Case with CAIR/CAMR			Delta (iii - ii)		
Region	2009	2015	2018	2009	2015	2018	2009	2015	2018
IL State									
Residential	4,109	4,569	4,786	4,081	4,482	4,724	28	87	62
Industrial	4,038	4,482	4,848	4,007	4,382	4,775	31	101	73
Commercial	2,488	2,449	2,570	2,461	2,366	2,512	27	83	58
National									
Residential	119,218	127,672	134,274	119,111	127,502	134,022	107	171	252
Industrial	105,790	115,234	124,221	105,686	115,062	123,961	104	172	260
Commercial	56,660	55,149	57,860	56,582	55,029	57,686	79	119	174

	(iii) Policy Case with IL Rule			(i) Base Case with out CAIR/CAMR			Delta (iii - ii)		
Region	2009	2015	2018	2009	2015	2018	2009	2015	2018
IL State									
Residential	4,109	4,569	4,786	4,007	4,435	4,588	102	135	198
Industrial	4,038	4,482	4,848	3,923	4,326	4,615	115	156	233
Commercial	2,488	2,449	2,570	2,387	2,321	2,385	101	128	185
National									
Residential	119,218	127,672	134,274	117,645	126,857	133,274	1,573	816	1,000
Industrial	105,790	115,234	124,221	104,259	114,411	123,190	1,531	824	1,031
Commercial	56,660	55,149	57,860	55,507	54,578	57,169	1,153	571	691

	(ii) Base Case with CAIR/CAMR			(i) Base Case with out CAIR/CAMR			Delta (iii - ii)		
Region	2009	2015	2018	2009	2015	2018	2009	2015	2018
IL State									
Residential	4,081	4,482	4,724	4,007	4,435	4,588	75	48	136
Industrial	4,007	4,382	4,775	3,923	4,326	4,615	84	55	160
Commercial	2,461	2,366	2,512	2,387	2,321	2,385	73	45	127
National									
Residential	119,111	127,502	134,022	117,645	126,857	133,274	1,466	645	748
Industrial	105,686	115,062	123,961	104,259	114,411	123,190	1,427	652	772
Commercial	56,582	55,029	57,686	55,507	54,578	57,169	1,074	451	517

Note: Total bill payments for each sector are calculated as follows. First, an estimate of sales to each sector in Illinois is made based the AEO 2006 projections of each sector's share of total retail sales (for the MAIN region). For example, if AEO projects that in 2010 residential customers will account for x percent of total retail electricity sales, we assume the same share. We estimate Illinois sales based on the assumption that Illinois sales as a proportion of total Illinois generation are the same as that of the MANO region. Finally, the retail prices estimated are multiplied by generation to derive total annual expenditures for electricity by sector. See main report

Exhibit A.6
Monthly Expenditures for Electricity by Sector (1999 million dollars)

	(iii) Policy Case with IL Rule			(ii) Base Case with CAIR/CAMR			Delta (iii - ii)		
Region	2009	2015	2018	2009	2015	2018	2009	2015	2018
IL State									
Residential	342	381	399	340	374	394	2	7	5
Industrial	336	374	404	334	365	398	3	8	6
Commercial	207	204	214	205	197	209	2	7	5
National									
Residential	9,935	10,639	11,189	9,926	10,625	11,169	9	14	21
Industrial	8,816	9,603	10,352	8,807	9,589	10,330	9	14	22
Commercial	4,722	4,596	4,822	4,715	4,586	4,807	7	10	15

	(iii) Policy Case with IL Rule			(i) Base Case with out CAIR/CAMR			Delta (iii - ii)		
Region	2009	2015	2018	2009	2015	2018	2009	2015	2018
IL State									
Residential	342	381	399	334	370	382	9	11	16
Industrial	336	374	404	327	361	385	10	13	19
Commercial	207	204	214	199	193	199	8	11	15
National									
Residential	9,935	10,639	11,189	9,804	10,571	11,106	131	68	83
Industrial	8,816	9,603	10,352	8,688	9,534	10,266	128	69	86
Commercial	4,722	4,596	4,822	4,626	4,548	4,764	96	48	58

	(ii) Base Case with CAIR/CAMR			(i) Base Case with out CAIR/CAMR			Delta (iii - ii)		
Region	2009	2015	2018	2009	2015	2018	2009	2015	2018
IL State									
Residential	340	374	394	334	370	382	6	4	11
Industrial	334	365	398	327	361	385	7	5	13
Commercial	205	197	209	199	193	199	6	4	11
National									
Residential	9,926	10,625	11,169	9,804	10,571	11,106	122	54	62
Industrial	8,807	9,589	10,330	8,688	9,534	10,266	119	54	64
Commercial	4,715	4,586	4,807	4,626	4,548	4,764	90	38	43

Exhibit A.7
Total Production Costs (1999 million dollars)

	(iii) Policy Case with IL Rule			(ii) Base Case with CAIR/CAMR			Delta (iii - ii)		
Plant Type	**2009**	**2015**	**2018**	**2009**	**2015**	**2018**	**2009**	**2015**	**2018**
IL State									
Variable O&M	357	340	355	306	372	382	51	(32)	(27)
Fixed O&M	2,030	2,137	2,316	2,003	2,134	2,300	28	3	16
Fuel Total	1,931	1,908	1,963	1,995	2,069	2,102	(63)	(162)	(140)
Capital	84	105	295	32	101	198	53	3	97
Total Cost	4,403	4,488	4,929	4,335	4,676	4,982	68	(188)	(53)
National									
Variable O&M	7835	9495	10549	7780	9496	10511	56	(2)	38
Fixed O&M	28926	31772	33432	28910	31749	33388	16	23	44
Fuel Total	61818	65527	68945	61759	65480	69139	59	47	(194)
Capital	2574	13256	19167	2558	13057	18807	16	199	360
Total Cost	101,153	120,049	132,094	101007	119782	131846	147	267	248

	(iii) Policy Case with IL Rule			(i) Base Case without CAIR/CAMR			Delta (iii - i)		
Plant Type	**2009**	**2015**	**2018**	**2009**	**2015**	**2018**	**2009**	**2015**	**2018**
IL State									
Variable O&M	357	340	355	286	324	343	71	15	13
Fixed O&M	2,030	2,137	2,316	2,009	2,121	2,303	22	16	13
Fuel Total	1,931	1,908	1,963	1,986	2,098	2,130	(54)	(190)	(167)
Capital	84	105	295	28	72	271	57	32	24
Total Cost	4,403	4,488	4,929	4,308	4,615	5,047	95	(126)	(118)
National									
Variable O&M	7835	9495	10549	7,078	8,274	9,106	757	1,221	1,443
Fixed O&M	28926	31772	33432	28,739	31,163	32,710	187	608	722
Fuel Total	61818	65527	68945	60,877	65,309	69,069	941	217	(124)
Capital	2574	13256	19167	1,885	11,059	16,564	689	2,197	2,603
Total Cost	101,153	120,049	132,094	98,579	115,806	127,449	2,574	4,243	4,645

	(ii) Base Case with CAIR/CAMR			(i) Base Case without CAIR/CAMR			Delta (ii - i)		
Plant Type	**2009**	**2015**	**2018**	**2009**	**2015**	**2018**	**2009**	**2015**	**2018**
IL State									
Variable O&M	306	372	382	286	324	343	20	48	39
Fixed O&M	2,003	2,134	2,300	2,009	2,121	2,303	(6)	13	(3)
Fuel Total	1,995	2,069	2,102	1,986	2,098	2,130	9	(28)	(28)
Capital	32	101	198	28	72	271	4	29	(74)
Total Cost	4,335	4,676	4,982	4,308	4,615	5,047	27	61	(65)
National									
Variable O&M	7,780	9,496	10,511	7,078	8,274	9,106	702	1,222	1,405
Fixed O&M	28,910	31,749	33,388	28,739	31,163	32,710	171	586	679
Fuel Total	61,759	65,480	69,139	60,877	65,309	69,069	882	170	70
Capital	2,558	13,057	18,807	1,885	11,059	16,564	672	1,998	2,243
Total Cost	101,007	119,782	131,846	98,579	115,806	127,449	2,428	3,976	4,397

Exhibit A.8
Average Production Costs (1999 mills/kWh)

	(iii) Policy Case with IL Rule			(ii) Base Case with CAIR/CAMR			Delta (iii - ii)		
Plant Type	**2009**	**2015**	**2018**	**2009**	**2015**	**2018**	**2009**	**2015**	**2018**
IL State									
Total Costs (MM$)	4,403	4,488	4,929	4,335	4,676	4,982	68	(188)	(53)
Total Generation (GWh)	202,146	197,875	204,953	206,633	212,120	215,361	(4,487)	(14,245)	(10,408)
Average Costs (mills/kWh)	21.78	22.68	24.05	20.98	22.04	23.13	0.80	0.64	0.92
National									
Total Costs (MM$)	101,153	120,049	132,094	101,007	119,782	131,846	147	267	248
Total Generation (GWh)	4,286,560	4,725,036	4,967,636	4,286,820	4,725,318	4,968,941	(260)	(283)	(1,305)
Average Costs (mills/kWh)	23.60	25.41	26.59	23.56	25.35	26.53	0.04	0.06	0.06

	(iii) Policy Case with IL Rule			(i) Base Case without CAIR/CAMR			Delta (iii - i)		
Plant Type	**2009**	**2015**	**2018**	**2009**	**2015**	**2018**	**2009**	**2015**	**2018**
IL State									
Total Costs (MM$)	4,403	4,488	4,929	4,308	4,615	5,047	95	(126)	(118)
Total Generation (GWh)	202,146	197,875	204,953	207,567	213,971	220,564	(5,421)	(16,097)	(15,612)
Average Costs (mills/kWh)	21.78	22.68	24.05	20.76	21.57	22.88	1.03	1.12	1.17
National									
Total Costs (MM$)	101,153	120,049	132,094	101,007	119,782	131,846	2,574	4,243	4,645
Total Generation (GWh)	4,286,560	4,725,036	4,967,636	4,288,930	4,728,021	4,973,571	(2,370)	(2,985)	(5,935)
Average Costs (mills/kWh)	23.60	25.41	26.59	23.55	25.33	26.51	0.05	0.07	0.08

	(ii) Base Case with CAIR/CAMR			(i) Base Case without CAIR/CAMR			Delta (ii - i)		
Plant Type	**2009**	**2015**	**2018**	**2009**	**2015**	**2018**	**2009**	**2015**	**2018**
IL State									
Total Costs (MM$)	4,335	4,676	4,982	4,308	4,615	5,047	27	61	(65)
Total Generation (GWh)	206,633	212,120	215,361	207,567	213,971	220,564	(933)	(1,851)	(5,203)
Average Costs (mills/kWh)	20.98	22.04	23.13	20.76	21.57	22.88	0.22	0.48	0.25
National									
Total Costs (MM$)	101,007	119,782	131,846	98,579	115,806	127,449	2,428	3,976	4,397
Total Generation (GWh)	4,286,820	4,725,318	4,968,941	4,288,930	4,728,021	4,973,571	(2,111)	(2,702)	(4,630)
Average Costs (mills/kWh)	23.56	25.35	26.53	22.98	24.49	25.63	0.58	0.86	0.91

Exhibit A.9
Comparison of Retrofits (Cumulative MWs)

	(iii) Policy Case with IL Rule			(ii) Base Case with CAIR/CAMR			Delta (iii - ii)		
Technology	2009	2015	2018	2009	2015	2018	2009	2015	2018
IL State									
FGD	2,556	2,762	2,762	387	2,836	2,836	2,168	(74)	(74)
SCR	1,748	1,826	1,826	1,799	2,121	2,121	(51)	(295)	(295)
SNCR	-	-	-	-	-	-	-	-	-
ACI	10,590	10,727	11,023	-	7,185	8,498	10,590	3,542	2,525
National									
FGD	38,578	72,100	85,019	36,948	73,530	85,543	1,630	(1,431)	(525)
SCR	34,362	51,042	64,747	34,223	51,213	65,181	139	(171)	(434)
SNCR	2,039	2,575	2,925	2,041	2,578	3,106	(3)	(3)	181)
ACI	18,493	63,788	72,423	7,934	58,723	67,672	10,559	5,065	4,751

	(iii) Policy Case with IL Rule			(i) Base Case without CAIR/CAMR			Delta (iii - i)		
Technology	2009	2015	2018	2009	2015	2018	2009	2015	2018
IL State									
FGD	2,556	2,762	2,762	391	2,530	2,530	2,164	231	231
SCR	1,748	1,826	1,826	1,500	1,762	1,762	248	64	64
SNCR	-	-	-	-	416	416	-	(416)	(416)
ACI	10,590	10,727	11,023	-	-	-	10,590	10,727	11,023
National									
FGD	38,578	72,100	85,019	10,040	15,446	16,897	28,538	56,653	68,122
SCR	34,362	51,042	64,747	21,556	27,657	28,291	12,806	23,385	36,456
SNCR	2,039	2,575	2,925	7,481	10,085	13,590	(5,442)	(7,509)	(10,664)
ACI	18,493	63,788	72,423	8,896	8,896	8,896	9,597	54,892	63,526

	(ii) Base Case with CAIR/CAMR			(i) Base Case without CAIR/CAMR			Delta (ii - i)		
Technology	2009	2015	2018	2009	2015	2018	2009	2015	2018
IL State									
FGD	387	2,836	2,836	391	2,530	2,530	(4)	305	305
SCR	1,799	2,121	2,121	1,500	1,762	1,762	299	359	359
SNCR	-	-	-	-	416	416	-	(426)	(426)
ACI	-	7,185	8,498	-	-	-	-	7,185	8,498
National									
FGD	36,948	73,530	85,543	10,040	15,446	16,897	26,909	58,084	68,647
SCR	34,223	51,213	65,181	21,556	27,657	28,291	12,667	23,556	36,890
SNCR	2,041	2,578	3,106	7,481	10,085	13,590	(5,439)	(7,507)	(10,484)
ACI	7,934	58,723	67,672	8,896	8,896	8,896	(962)	49,827	58,776

Exhibit A.10
Comparison of Mine Mouth Coal Prices (1999 $/MMBtu)

	(iii) Policy Case with IL Rule			(ii) Base Case with CAIR/CAMR			Delta (iii - ii)		
Coal Region	2009	2015	2018	2009	2015	2018	2009	2015	2018
Appalachia	1.07	1.07	1.08	1.07	1.07	1.07	0.00	(0.00)	0.00
Interior	1.04	1.05	1.05	1.04	1.05	1.05	(0.00)	(0.00)	(0.00)
West	0.51	0.50	0.51	0.51	0.51	0.51	(0.01)	(0.01)	0.00
National	0.77	0.77	0.77	0.77	0.77	0.77	(0.00)	(0.00)	0.00

	(iii) Policy Case with IL Rule			(i) Base Case without CAIR/CAMR			Delta (iii - i)		
Coal Region	2009	2015	2018	2009	2015	2018	2009	2015	2018
Appalachia	1.07	1.07	1.08	1.09	1.09	1.11	(0.02)	(0.02)	(0.04)
Interior	1.04	1.05	1.05	1.06	1.02	1.02	(0.01)	0.03	0.03
West	0.51	0.50	0.51	0.48	0.51	0.52	0.03	(0.00)	(0.01)
National	0.77	0.77	0.77	0.78	0.77	0.78	(0.01)	0.00	(0.00)

	(ii) Base Case with CAIR/CAMR			(i) Base Case without CAIR/CAMR			Delta (ii - i)		
Coal Region	2009	2015	2018	2009	2015	2018	2009	2015	2018
Appalachia	1.07	1.07	1.07	1.09	1.09	1.11	(0.02)	(0.02)	(0.04)
Interior	1.04	1.05	1.05	1.06	1.02	1.02	(0.01)	0.03	0.03
West	0.51	0.51	0.51	0.48	0.51	0.52	0.04	0.00	(0.01)
National	0.77	0.77	0.77	0.78	0.77	0.78	(0.01)	0.01	(0.00)

Exhibit A.11
Comparison of Coal Usage (TBtu)

	(iii) Policy Case with IL Rule			(ii) Base Case with CAIR/CAMR			Delta (iii - ii)		
Coal Type	2009	2015	2018	2009	2015	2018	2009	2015	2018
IL State									
Bituminous	268	254	262	201	214	212	67	40	50
Subbituminous	808	728	751	924	942	942	(116)	(214)	(191)
Lignite	-	-	-	-	-	-	-	-	-
Total	1,077	982	1,013	1,126	1,156	1,154	(49)	(174)	(141)
National									
Bituminous	12,940	14,114	15,153	12,945	14,070	15,068	(5)	44	86
Subbituminous	8,990	9,995	10,680	8,990	10,053	10,701	-	(58)	(21)
Lignite	774	774	774	792	792	792	(18)	(18)	(18)
Total	22,704	24,882	26,607	22,727	24,915	26,560	(23)	(32)	47

	(iii) Policy Case with IL Rule			(i) Base Case without CAIR/CAMR			Delta (iii - i)		
Coal Type	2009	2015	2018	2009	2015	2018	2009	2015	2018
IL State									
Bituminous	268	254	262	220	243	280	48	11	(18)
Subbituminous	808	728	751	920	938	936	(112)	(211)	(185)
Lignite	-	-	-	-	-	-	-	-	-
Total	1,077	982	1,013	1,140	1,181	1,215	(63)	(200)	(202)
National									
Bituminous	12,940	14,114	15,153	13,117	13,570	14,418	(177)	544	735
Subbituminous	8,990	9,995	10,680	8,989	10,813	11,683	1	(818)	(1,003)
Lignite	774	774	774	801	801	801	(27)	(27)	(27)
Total	22,704	24,882	26,607	22,908	25,184	26,902	(203)	(302)	(295)

	(ii) Base Case with CAIR/CAMR			(i) Base Case without CAIR/CAMR			Delta (ii - i)		
Coal Type	2009	2015	2018	2009	2015	2018	2009	2015	2018
IL State									
Bituminous	201	214	212	220	243	280	(18)	(29)	(68)
Subbituminous	924	942	942	920	938	936	4	3	6
Lignite	-	-	-	-	-	-	-	-	-
Total	1,126	1,156	1,154	1,140	1,181	1,215	(14)	(26)	(62)
National									
Bituminous	12,945	14,070	15,068	13,117	13,570	14,418	(172)	500	650
Subbituminous	8,990	10,053	10,701	8,989	10,813	11,683	1	(760)	(981)
Lignite	792	792	792	801	801	801	(10)	(10)	(10)
Total	22,727	24,915	26,560	22,908	25,184	26,902	(180)	(269)	(341)

Exhibit A.12
Comparisons of Coal Power Plant Retirements (MW)

	(iii) Policy Case with IL Rule			(ii) Base Case with CAIR/CAMR			Delta (iii - ii)		
Plant Type	2009	2015	2018	2009	2015	2018	2009	2015	2018
IL State									
Coal	597	597	597	345	345	345	252	252	252
National									
Coal	2,085	2,788	2,788	1,880	2,585	2,585	205	203	203

	(iii) Policy Case with IL Rule			(i) Base Case without CAIR/CAMR			Delta (iii - i)		
Plant Type	2009	2015	2018	2009	2015	2018	2009	2015	2018
IL State									
Coal	597	597	597	148	148	148	449	449	449
National									
Coal	2,085	2,788	2,788	330	551	551	1,755	2,237	2,237

	(ii) Base Case with CAIR/CAMR			(i) Base Case without CAIR/CAMR			Delta (ii - i)		
Plant Type	2009	2015	2018	2009	2015	2018	2009	2015	2018
IL State									
Coal	345	345	345	148	148	148	197	197	197
National									
Coal	1,880	2,585	2,585	330	551	551	1,550	2,034	2,034

Note: Retirement figures are cumulative

ICF CONSULTING

Analysis of the Proposed Illinois Mercury Rule

Appendix B: Overview of Modeling Framework

Prepared for:
Illinois Environmental Protection Agency
Division of Air Quality

Prepared by:
ICF Resources, LLC
Under contract to:

Lake Michigan Air Directors Consortium (LADCO)

March 10, 2006

powered by perspective

Table of Contents

Overview of IPM and Core Modeling Assumptions

The analysis underlying this report was performed using the Integrated Planning Model (IPM®) -- a sophisticated energy modeling system that simulates the deregulated wholesale market for electricity. This appendix provides an overview of IPM as well as the underlying assumptions and inputs. As noted in the report, the underlying basis of this analysis is developed by EPA for its Base Case (v. 2.1.9). This appendix describes the core model with reference to the EPA 2.1.9 Base Case assumptions. This document is not meant to be an exhaustive description of that case as it is extensively documented by EPA on its website. See *Standalone Documentation for EPA Base Case 2004 (V. 2.1.9) Using the Integrated Planning Model, September 2005, at* http://www.epa.gov/airmarkets/epa-ipm/.

Subsequent to the EPA 2.1.9 base case being made available, several data and modeling parameter changes were implemented by the VISTAS Regional Planning Organization (RPO) during a two-phase modeling effort during 2004 and 2005 (of which LADCO and Illinois EPA were participants). For this study, Illinois EPA made additional changes. A separate appendix describes subsequent changes made relative to the EPA 2.1.9 case and implemented in this case.

IPM Overview

ICF's IPM® model has been applied over the past 30 years for a wide range of clients. IPM is used by the U.S. Environmental Protection Agency (EPA) as well as other government and industry entities for the analysis of wholesale power markets, environmental policies and compliance decisions, based on fundamentals relating to supply and demand. IPM models all major facets of energy markets such as fuel prices, emission markets, environmental compliance costs and operating constraints.

EPA has used IPM in the analysis of the U.S. EPA's recent Clean Air Rules (including the Clean Air Interstate Rule, the Clean Air Mercury Rule, and the Clean Air Visibility Rule) and the NOx SIP Call. Regional Planning Organizations (RPOs) -- including WRAP, VISTAS, LADCO, and CENRAP -- have used the IPM for analyses in support of their state implementation plans (SIPs) development process. The model has been used by the Regional Greenhouse Gas Initiative (RGGI) working group to analyze proposed carbon policies in the northeast. IPM has also been used extensively on behalf of utilities, the financial community and developers of generation assets to evaluate environmental compliance strategies for electricity, as well as to generate forward price curves and value power plant assets. Finally, the model has also been used by the Federal Energy Regulatory Commission (FERC) to assess the potential emission impact of open access transmission policies and to develop an Environmental Assessment of the Regional Transmission Organization (RTO) Proposed Rulemaking.

Model Structure and Formulation

IPM is a capacity planning and dispatch model for the electric power sector based upon engineering and economic fundamentals. IPM simulates the operations of every generator in the continental U.S. with regional detail. The model determines the least-cost method of meeting national level energy and peak demand requirements for a specific period of time. In its solution, the model takes into consideration several operating regulatory, market and engineering constraints, such as emission limits, transmission capabilities, fuel market constraints, regional reserve margin constraints and system operating constraints. The model is a national implementation with regional details. Given a specified set of inputs and constraints, IPM develops an optimal capacity expansion plan, dispatch order, and air emissions compliance plan for the power generation system based on factors such as fuel prices, capital costs and operation and maintenance (O&M) costs of power generation, among others.

The IPM is an optimization model that has as its objective function to minimize the total, discounted net present value of the costs of meeting electricity demand, recognizing power system constraints, and environmental requirements over the entire planning horizon. The objective function represents the summation of all the going-forward costs incurred by the electricity sector in meeting future demand. It does not include embedded (or sunk) costs such as carrying charges associated with existing units, fixed transmission system costs, or general and administrative costs.

The total resulting cost is expressed as the net present value of all the component costs. These costs include the cost of new plant and pollution control construction, fixed and variable operating and maintenance costs (O&M) for existing plants, and fuel costs. The applicable discount rates are applied to derive the net present value for the entire planning horizon from the costs obtained for all years in the planning horizon.

IPM is a multi-region model. The model regions representing the U.S. power market in the EPA Base Case (and in this study) correspond broadly to regions and sub-regions that constitute the North American Electric Reliability Council (NERC) regions. Figure B1 shows the IPM modeling regions for this study. In this study, Illinois lies within what is called the "MANO" region in IPM and corresponds to the southern region of the Mid America Interconnected Network (MAIN). Illinois makes up the majority of

Figure B2 IPM and Model Regions

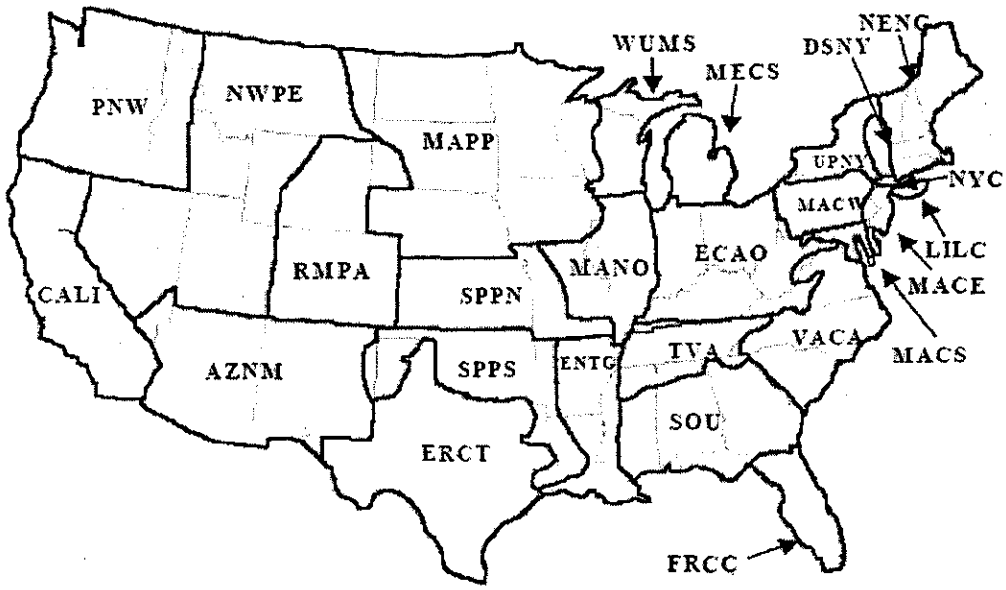

the MANO region. In terms of capacity, the share of the MANO region's total capacity that lies in Illinois is 88 percent.

Given the objective of minimizing overall system wide costs, IPM solves for certain decision variables. These decision variables are the model's "outputs" and they characterize the optimal or least-cost solution for meeting the given set of constraints. Some of the key decision variables represented in IPM are: generation dispatch (in GWh), capacity (in MW), new capacity additions, retrofit decisions, transmission

flows (in TWh), emissions, emission allowance prices (in $/Ton for capped pollutants), and fuel prices and consumption.

The model finds this optimal solution recognizing certain constraints such as:

- *Reserve Margin Constraints*: This constraint represents system reliability requirements. Each IPM model region must have a minimum level of reserve margin capacity (in terms of MW). If in a given year, total capacity (existing as well as planned) is less than the requirement, the model will add additional capacity.
- *Demand Constraints*: Each region's annual electricity energy and peak demand levels are specified as inputs to the model. These energy demands are further defined by load shapes represented as winter and summer seasonal load duration curves. The LDC is the minimum amount of generation required to meet the region's electrical demand for a specific season.
- *Equivalent Availability Constraints*: This constraint specifies the maximum amount of electricity that a plant can generate, given its net dependable capacity available, forced outage rates, and seasonal maintenance requirements.
- *Turndown/area protection constraints*: This constraint represents the operating characteristics of peaking, cycling and base load units.
- *Emission constraints*: IPM has the capability of modeling a variety of emission constraints for each of the pollutants such as SO_2, NO_x, mercury and CO_2. These constraints are implemented at the unit level, regional level or system-wide and are defined either in terms of a total tonnage cap (e.g., tons of NO_x SO_2 per year or season) or a maximum emission rate (e.g., lbs/MMBtu of NOx). The emission constraints can be customized as per user specification and thus vary from analysis to analysis.
- *Transmission constraints*: IPM models several power regions simultaneously and each model region is linked with another through transmission lines. The constraints define either a maximum capacity on each link or a maximum level of transmission on two or more (i.e., joint limits) links to different regions.
- *Fuel Supply constraints*: In IPM, each model plant is designed to obtain a certain type of fuel from a specific supply region.

Figure B2 below shows the various IPM components and data structure.

Figure B2
Modeling and Data Structure of IPM

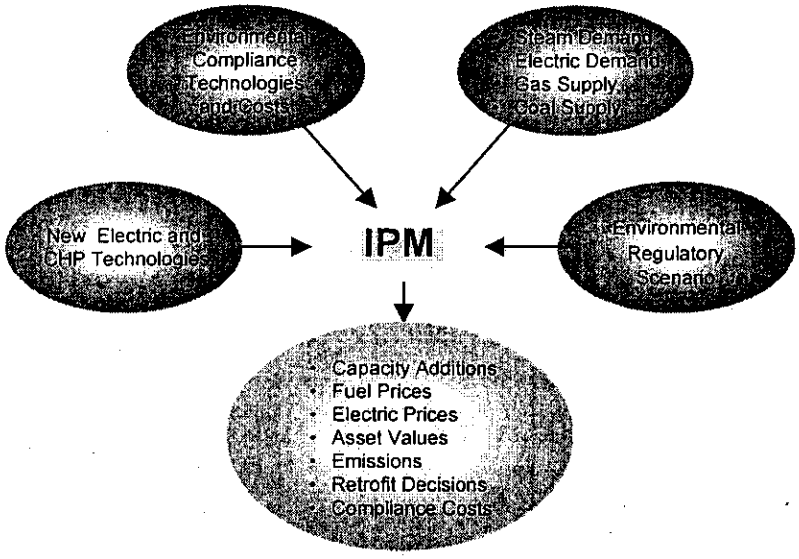

Two other characteristics of IPM are those regarding perfect competition and perfect foresight. The former implies that IPM models all activity in the wholesale electric markets as perfectly competitive and any market imperfections such as market power, transaction costs or informational asymmetry are not explicitly treated in the model. However, market imperfections can be estimated by doing sensitivity analyses or redefining model inputs. There are no assumptions on retail deregulation in IPM since it is a wholesale market model.

Perfect foresight implies that in IPM all economic agents know precisely the nature and timing of the constraints that will be imposed in the future as well as future fuel supply availability and pricing. For example, under IPM there is complete foreknowledge of the levels, timings and regulatory design of emission limits that will be imposed throughout the modeling time horizon.

It is important to note that IPM simulates the electric power markets through an engineering economic framework that is completely flexible with respect to the core data and underlying inputs, assumptions, policy inputs and other system and unit constraints. Therefore, the results are influenced by the user-specified inputs.

Model Outputs

IPM produces a variety of reports ranging from very detailed reports that show results for each model plant and run year to the broader summary reports which present data on a state, regional and national level. Key outputs of the model include:

- *Generation* –the total amount of electric energy produced by a generating unit in GWh. Generation is forecast by the model based on the economics of the units, given all constraints and other inputs.
- *Capacity Mix* – the model forecast total capacity (in terms of MW) by plant type such as combined cycle, combustion turbine, Oil/gas steam, scrubbed coal, hydro, pumped storage, IGCC, nuclear, cogen, biomass and geothermal. In addition to the existing capacity mix for a given region, the output shows the amount and type of new capacity that is added in each run year as well as capacity that is retired, repowered, or retrofitted with emission controls equipment.
- *Capacity prices* – Capacity price is one of the two components of the firm electricity price and is expressed in terms of $/KW. The capacity price is determined by several factors such as the reserve margins in different regions, cost of building new capacity, fixed costs of existing units and transmission.
- *Firm Wholesale electricity prices* – The firm electricity price is the sum of the electrical energy price and capacity price. It is expressed in terms of $/MWh. In each hour, the electric energy price is determined by the short-run marginal cost of production of the most expensive unit in that hour. Marginal energy prices for each region and model run year are reported at the seasonal and segmental level.
- *Production Costs* – All production costs derived in IPM represent wholesale production costs. The model costs represent the "going-forward" costs and do not consider embedded (or sunk) costs such as carrying charges of existing units, transmission and distribution charges, and general and administrative costs. For each region and each run year, the model projects the total production costs such as variable O&M, fixed O&M costs, fuel costs and capital costs.
- *Fuel consumption and prices* – The model projects total fuel consumption by region and price. Prices for fuels such as coal and natural gas are endogenously determined by the model via supply curves – a set of price-quantity relationships that reflect the underlying fundamentals of the market. The model determines the optimal level of supply.
- *Emissions (NOx, SO_2, Co_2 and Hg)* – the model forecasts the level of emissions for NO_x (in terms of thousands of Tons), SO_2 (in terms of thousands of tons), CO_2 (in terms of millions of tons) and Mercury (in terms of tons).
- *Allowance prices* – For each emission constraint that is defined the model determines allowance prices (can be thought of as the shadow price of the pollutant constraint) for pollutants such as NOx, SO_2 and mercury. The allowance prices are expressed either terms of $/Ton or $/lb.
- *Retrofits* – All existing units are given the option to retrofit with several pollution control technologies such as scrubbers, SCR, SNCR and ACI controls based on the applicability of the technology and the unit characteristics. Two states of retrofit are possible (e.g. Scrubber followed by SCR in a later year). Combinations of options are allowed in each year.

NEEDS Database and Other Unit Data

The core set of data for IPM describes the characteristics and specific operating parameters of all existing and planned generating units. For EPA Base Case 2004(V.2.1.9), the data used is EPA's National Electric Energy Data System (NEEDS) database. This source contains unit-level information on each steam boiler and generator including its location, net dependable capacity, plant type, pollution control equipment for SO2, NOx and particulate matter, boiler configurations, and the emission rates or emission

rate limits. NEEDS is developed from large number of data sources including EIA and NERC data, DOE data, EPA Emission Tracking System Data among other sources. This database, the rules for populating the data, and key summary statistics are described in EPA's documentation: *Standalone Documentation for EPA Base Case 2004 (V. 2.1.9) Using the Integrated Planning Model, September 2005, at* http://www.epa.gov/airmarkets/epa-ipm/.

The NEEDS database represents every generating unit in the country. It is possible, but impractical to run IPM at this level of disaggregation. Run times would be very long and model size would be an issue. Therefore, "model plants" are constructed from the NEEDs data set to represent the power system. For existing units, model plants represent aggregations of existing generating units. Logical aggregation algorithms are developed to group units with similar characteristics into model plants. These model plans have characteristics that reflect these combinations, for example, capacity is the sum of all units' capacities while heat rate is a weighted-average value. Note that coal plants are highly disaggregated in the model, with approximately only 2-3 boilers aggregated into a typical model plant. Key aggregation criteria are boiler rate, unit size, heat rate, environmental controls, allowed fuel types, among many others.

Model Run Years

IPM uses model run years to represent the span of the planning horizon being modeled. Each year of the planning horizon is mapped into a representative model run year. This run year mapping also prevents the model size from becoming too large. Although, IPM reports results only for the model run years, costs for all years of the planning horizon are taken into consideration in the algorithm. To avoid boundary distortions or "end-year effect" characteristic of optimization models, IPM includes a final model run year that is not reported in the results. This technique reduces the likelihood that later year results will be skewed due to the modeling artifact of having to specify an end point in the planning horizon, whereas, in reality, economic decisions are likely to persist beyond that end point.

In this study, (i.e., for the 3 cases: Base Case without CAIR/CAMR rule, base case with CAIR/CAMR and the policy run with CAIR, IL mercury rule for Illinois plants and CAMR for non-Illinois plants), the IPM model was run for seven run years.

New Unplanned Units

IPM also allows new generation capacity to be built during a model run. All the model plants that can be potentially built are pre-defined at set-up, differentiated by type of technology, regional location, and the on-line date when the plants can become available. IPM makes the decision to "build" new capacity in a given region based on the economics and costs of the new technology options as well as regional variations in capital costs over time. All the potential units represent new capacity and are pre-defined at set-up to differentiate by type of technology, regional location, and years available.

Retrofit, Repowering and Retirement Options

IPM also explicitly represents the retrofit, repowering, and retirement options that are available to existing units. For example, plants can retrofit with pollution control equipment, repower, or retire early. The options available to each model plant are defined during model set-up (as per client specifications). In the EPA Base Case 2004 as well as this study, every existing model plant is given the option to retrofit with a pollution control, repower or retire early. Every plant is allowed a maximum of two stages of retrofit options. For example, an existing model plant may be retrofit with a scrubber in one model run year (stage 1) and with an SCR in the same or subsequent run year (stage 2).

Environmental Assumptions

IPM is designed to take into consideration the complex nature of emission regulations involving banking, trading and progressive flow control of emission allowances as well as command-and-control emission policies. This study incorporates existing SO_2, NOx, mercury and CO_2 environmental regulations as per Federal and state regulations. The regulations are implemented in IPM via system-wide and unit-level emission constraints.

Title IV SO_2 Regulations: The broadest system-wide environmental regulation modeled is the SO_2 allowance trading program established under Title IV of the CAAA. The program became operational in year 2000 and affects all SO_2 emitting electric generating units greater than 25 MW.

NO_X Regulations: NOx regulations are modeled through a combination of state and unit-level NOx limits. The following NOx regulations are modeled in this case: NOx SIP Call trading program, Title IV unit specific rate limits and Clean Air Act Reasonable Available Control Technology (RACT) requirements for controlling NOx emissions from electric generating units in ozone non-attainment areas or in the Ozone Transport Regions[1] (OTR). The NOx SIP Call program is also implemented in this case.

State Specific Environmental Regulations: This study incorporates state laws and regulations that affect the electricity sector emissions of sulfur dioxide, nitrogen oxides, mercury and carbon dioxide. For example, it represents environmental regulations for 12 states, including Connecticut, Massachusetts, Missouri, New Hampshire, North Carolina, Texas, Wisconsin, Illinois, Maine, Minnesota, New York and Oregon.

Parsed Files and Outputs

IPM produces output at the model plant level. In order to do air quality modeling and understand impacts at the state, county or plant level, it is necessary to relate model plants into units. This is done by "parsing" the outputs in order to get unit level results.

In the context of IPM, "parsing" refers to the methodology used to allocate IPM model plant projections of fuel use and emissions to individual electricity generating units (EGUs) or other individual entities (such as cogenerators) that constitute the model plants in IPM.

The IPM model aggregates individual entities into model plants of similar characteristics, and assigns each aggregated model plant a weighted average heat rate, a weighted average emission rate, and appropriate cost parameters based on that model plant's underlying units characteristics. As a result, IPM projections such as fuel consumption and air emissions are for aggregated model plants. To determine the fuel use and the air emissions of individual EGUs and other entities that constitute "a model plant," the total fuel consumed by, and the air emissions from, each model plant are allocated (or parsed) to each constituent EGU, industrial boiler, or other entity, by applying a series of algorithms.

A parsed file includes much of the unit level input data given to IPM as well as outputs of IPM allocated to the unit level.

[1] The OTR consists of the following states: Maine, New Hampshire, Vermont, Massachusetts, Rhode Island, Connecticut, New York, New Jersey, Pennsylvania, Delaware, Maryland, District of Columbia and northern Virginia.

Overview of Key Modeling Assumptions

The section below provides a brief summary of the input assumptions used in IPM for the EPA 2.1.9 Base Case. Changes to these assumptions for the current work are described separately. This is provided to help the reader understand how these key inputs influence IPM

Fuel Assumptions

IPM includes fuels such as coal, natural gas, oil, nuclear fuel, and biomass for electric generation. Coal, natural gas and biomass price assumptions are represented via supply curves, whereas oil and nuclear fuel prices are exogenously determined and entered in the model during model set-up as a constant price point that is applicable at all levels of supply.

IPM is capable of modeling the full range of fuels used for electric power generation including the price, supply and even the quality of fuels included, such as the average mercury or sulfur content of coal mined from a specific region. Based on grades of fuel used IPM determines the emissions resulting from the combustion of that fuel.

Coal is modeled endogenously. There is a distinct coal supply curve for each IPM coal supply region and coal type within that region. The supply curve shows the relationship between coal supply and the mine-mouth price of coal and depicts changes in prices associated with a change in quantity. The market price of coal is determined endogenously in IPM and is the price at which the supply of a certain coal type from a specific coal supply region satisfies demand in a given model run year. Hence all plants purchasing the same coal type from a supply region get the same mine-mouth clearing price (an equilibrium price).

The equilibrium mine-mouth price excludes the transportation costs of moving coal from the supply region to the demand region. There is however, a transportation link between a coal demand region and supply region that is based on the distance and transport mode for that link.

As in the case of coal, natural gas prices are determined endogenously in IPM, using supply and demand curves. The gas supply curves are determined using ICF's North American Natural Gas Analysis System (NANGAS) model. This is a detailed natural gas market optimization model. The supply curves are generated through a series of NANGAS model runs wherein natural gas supply, demand and transportation are equilibrated under varying electricity growth rate assumptions. Supply and demand curves are created for each run year to find market clearing price and quantity of natural gas. There is however only one regional price and quantity calculated and that is at the Henry Hub. From this vantage point transportation differentials are included to the cost of natural gas prices at Henry Hub to find what individual plants will be subject to in their region. For this study, gas supply curves that were intended to represent EIA/AEO forecasts were used.

Consistent with the endogenous price determination of coal and natural gas, biomass fuels are also determined by supply and demand curves created for each region and run year. Unlike coal and natural gas, biomass does not allow for inter-regional trading, but does account for transportation costs within a region.

For nuclear and fuel oil, prices are derived exogenously. The oil price assumptions are derived from crude oil prices in EIA's Annual Energy Outlook (AEO) 2004. The nuclear fuel price used in the EPA Base Case 2004 is from AEO 2004.

Demand

Net energy for load and net internal demand are exogenous inputs to IPM and together represent the total grid wide demand for electricity. The former is the projected annual electric grid-demand before accounting for transmission and distribution losses and the latter is the maximum hourly demand in a given year net of interruptible load. The regional net energy for load is derived from the national net energy for load based on the regional demand distribution from the NERC ES&D (North American Electric Reliability Council: Electric Demand and Supply) forecasts. Net internal demand for the various IPM model regions is based on regional load shapes (obtained by summing up the load for control areas within a given region). The average annual growth rate assumptions for energy and peak demand are based on U.S. EIA's (Energy Information Agency) "Annual Energy Outlook 2004 with Projections to 2025" (AEO 2004).

As opposed to chronological load curves (i.e., 8,760 hours of the year), IPM uses load duration curves (LDCs) for dispatching units. The LDCs are created by rearranging the chronological load curve from the highest to lowest (MW) value. The EPA Base Case 2004 uses two LDCs - one for the winter season (October – April) and one for the summer season (May – September). These load shapes are created using chronological hourly data for normal weather years. The chronological hourly data in turn are derived by aggregating individual utility load curves as reported by the FERC (Federal Energy Regulatory Commission).

Within IPM, LDCs are represented by discrete load segments, or generation blocks. The load segment depicts time in terms of hours (on the x-axis) and the capacity produced in terms of MW (on the y-axis). The EPA Base Case 2004 uses five load segments, with segment one representing all hours when load is at peak demand levels. Segments 2 through 5 represent hourly loads at progressively lower levels of demand. All plants in the model are dispatched to meet load in the five segments based on their operating costs. Plants with the lowest operating costs will run for the maximum hours of the LDC and are referred to as the baseload units (such as nuclear and coal units).

Control Costs and Retrofit Assumptions

IPM can model specific SO_2, NO_X, and mercury (Hg) emission control technology options for meeting existing and potential federal, regional and state SO_2, NO_X and Hg emission limits. Each control has VOM, FOM and capital costs associated with operation and an emission reduction factor for having this technology enabled. There can be multiple options for each broad technology (e.g., for sulfur dioxide, Limestone Forced Oxidation (LFO), Magnesium Enhanced Lime (MEL) and Lime Spray Dryer (LSD)). There are specific characteristics that a plant must have to adopt one of these options, but each option gives a reduction in SO_2, along with appropriate heat rate penalties and costs.

Emission control technologies can have co-benefits. For example, in the EPA Base Case 2004, units that install SO_2 and NO_X controls reduce mercury emissions as a byproduct of these SO_2 and NO_X retrofits. A plant can also specifically target mercury by using Activated Carbon Injection (ACI). The efficiency of Hg removal is subject to the coal type and how much mercury needs to be contained. The IPM system will decide which controls are the most cost effective in meeting governmental emission constraints keeping in mind the cost of controls and fuels made available by these controls.

Capital costs for building a new unit are specified including adjustments for regional differences in labor, material and construction costs and derive regional capital costs. Costs include overnight capital, interest during construction, FOM, and VOM.

Financial Assumptions

The discount rate and the capital charge rate are the key variables in IPM's financial decision-making process for investment options. The discount rate is necessary for calculation of net present value (NPV). This enables accurate cost comparisons across the whole time horizon and accounts for the time value of money. Annualized capital payments for retrofit or potential investments are computed using the capital charge rate, which takes into account the cost of debt, return on equity, taxes and depreciation.

The EPA Base Case 2004 includes different technologies that have varying methods of operation, financing, revenue streams, depreciation schedules and risk profiles. These differences will categorize the unit into a risk profile of low, medium or high risk. For example, baseload units such as combined cycles and coal plants have a low risk compared to peaking units such as combustion turbines that are more risky.

ICF CONSULTING

Analysis of the Proposed Illinois Mercury Rule

Appendix C: Data Changes and Updates

Prepared for:
Illinois Environmental Protection Agency
Division of Air Quality

Prepared by:
ICF Resources, LLC

Under contract to:
Lake Michigan Air Directors Consortium (LADCO)

March 10, 2006

Table of Contents

OVERVIEW

The EPA Base Case (known as the EPA Base Case 2004, v.2.1.9) was developed by ICF under the direction of the U.S. Environmental Protection Agency (EPA). It serves as the starting point for the analysis presented in this report. Subsequent to its release the VISTAS Regional Planning Organization initiated a two-phase study using IPM. Starting as the EPA 2.1.9 as a base, VISTAS, along with study participants from CENRAP and LADCO RPOs, made several changes to the underlying datasets and modeling assumptions. The starting point for this study was work from the VISTAS study. Subsequent to this RPO work, ICF was directed to make additional changes by IEPA, including unit level changes for the Illinois units and modifications to mercury control costs. These changes are described in detail below.

Summary of Changes to EPA Base Case by Vistas

VISTAS and its workgroup initiated a review of NEEDs and recommended a large number of changes to the data. This occurred in two phases. The tables that follow this section documents those changes. Changes made by IEPA are described at the end of the section.

In addition to unit level changes, VISTAS and its workgroup made a number of global changes that re reflected in this case. These are briefly described below:

- Demand forecast were changed to reflect unadjusted EIA AEO 2005 national electricity and peak demand values
- The natural gas supply curve and pricing forecasts were scaled in such a manner that IPM would solve for AEO 2005 gas prices when the power sector gas demand in IPM is consistent with AEO 2005 power sector gas demand projections. In instances where the power sector gas demand in IPM is lower than that of AEO 2005 projections, IPM would project gas prices that are lower than that in AEO 2005 and vice versa.
- Coal supply curves also involved scaling due to the fact that the coal grades and supply regions between AEO 2005 and the EPA 2.1.9 are not directly comparable. This initiated an approximate approach that was performed in an iterative fashion but did not involve updating the coal transportation matrix with EIA assumptions due to significant differences between the EPA 2.1.9 and EIA AEO 2005 coal supply and coal demand regions. The overall effect is IPM coal prices that reflect EIA AEO 2005 prices.
- EIA AEO 2005 oil price forecasts were also applied under VISTAS.
- AEO 2005 data was used for all assumptions regarding new builds or potential units. The cost and performance assumptions for these units were as per the AEO 2005 documentation, while assumptions for renewable capacity were the same as those used in the EPA Base Case 2004 v.2.1.9.
- Preserved the EPA Base Case 2004 v.2.1.9 assumptions regarding pollution control cost and performance for retrofits, but excluded constraints on new build capacity types (i.e. no new coal).
- For nuclear units, used the same IPM configuration as in the EPA Base Case 2004 v.2.1.9, but with updated EIA AEO 2005 incurrence cost (~27/Kw) for continued operation.
- Set the 2007 SO2 banking value for 4.99 million tons.

- Used North Carolina Clean Smoke Stacks data for 2009 in determining "must run" units.

- The renewable portfolio standards (RPS) is modeled based on the most recent RGGI documentation using a single RPS region for Massachusetts (MA), Rhode Island (RI), New York (NY), New Jersey (NJ), Maryland (MD) and Connecticut (CT). The RPS requirements within these states can be met by renewable generation from New England, New York and PJM. EPA Base Case 2004 v.2.1.9 methodology and EIA AEO 2004 projected renewable builds were used for the rest of the regions.

VISTAS Changes to EPA 2.1.9 – Detailed Tables

The following tables show changes made by VISTAS and other RPOs during 2004 and 2005 during the VISTAS modeling project. Two series of changes were made during that work. Appendix 1 shows VISTAS phase I changes and Appendix 2 shows VISTAS phase II changes. Vistas phase I changes are implemented on top of NEEDS NODA database (i.e., NEEDS v2.1.9 database) to develop the NEEDS Vistas I database. Vistas II changes are implemented on top of NEEDS Vistas I database and the resulted NEEDS Vistas II database formed the foundation of the Vistas phase II runs which forms the starting point for this study. All data was provided by the VISTAS technical director or stakeholder participants.

Phase I Changes

Existing Unit Level NOx Control Technology Assumptions

Exhibit C1.1: Revisions to NO_x Post Combustion Control Installations in Vistas Phase I

Plant Name	Unique ID	Post Combustion NO_x Control (NEEDS NODA)	Post Combustion NO_x Control (VISTAS Phase I)
ASHEVILLE	2706_B_1	SNCR	None
BARRY	3_B_1	SNCR	None
BARRY	3_B_2	SNCR	None
BARRY	3_B_3	SNCR	None
BARRY	3_B_4	SNCR	None
Barry	3_G_A1	None	SCR
Barry	3_G_A2ST	None	SCR
MT STORM	3954_B_3	None	SCR
PLEASANTS	6004_B_1	None	SCR
PLEASANTS	6004_B_2	None	SCR
Victor J Daniel Jr	6073_G_3	None	SCR
Victor J Daniel Jr	6073_G_3CT	None	SCR
Victor J Daniel Jr	6073_G_4CT	None	SCR

Unit Level NOx Emission Rate Changes

Exhibit C1.2: Changes made to NO_x Emission Rates (lbs/MMBtu) in Vistas Phase I

Plant Name	Unique ID	Mode1 Rate (VISTAS I)	Mode2 Rate (VISTAS I)	Mode3 Rate (VISTAS I)	Mode4 Rate (VISTAS I)
GREENE COUNTY	10_B_1	0.718	0.718	0.468	0.468
GREENE COUNTY	10_B_2	0.416	0.416	0.380	0.380
Greene County	10_G_GT10	0.090	0.090	0.090	0.090
Greene County	10_G_GT2	0.090	0.090	0.090	0.090
Greene County	10_G_GT3	0.090	0.090	0.090	0.090
Greene County	10_G_GT4	0.090	0.090	0.090	0.090
Greene County	10_G_GT5	0.090	0.090	0.090	0.090
Greene County	10_G_GT6	0.090	0.090	0.090	0.090
Greene County	10_G_GT7	0.090	0.090	0.090	0.090
Greene County	10_G_GT8	0.090	0.090	0.090	0.090
Greene County	10_G_GT9	0.090	0.090	0.090	0.090
CROSS	130_B_1	0.100	0.100	0.100	0.100
CROSS	130_B_2	0.100	0.100	0.100	0.100
EATON	2046_B_1	0.280	0.280	0.280	0.280
EATON	2046_B_2	0.280	0.280	0.280	0.280
EATON	2046_B_3	0.280	0.280	0.280	0.280
Chevron Oil	2047_G_1	0.320	0.320	0.320	0.320
Chevron Oil	2047_G_2	0.320	0.320	0.320	0.320
Chevron Oil	2047_G_3	0.320	0.320	0.320	0.320
Chevron Oil	2047_G_4	0.320	0.320	0.320	0.320
Chevron Oil	2047_G_5	0.064	0.064	0.064	0.064
SWEATT	2048_B_1	0.280	0.280	0.280	0.280
SWEATT	2048_B_2	0.280	0.280	0.280	0.280
Sweatt	2048_G_A	0.320	0.320	0.320	0.320
JACK WATSON	2049_B_1	0.280	0.280	0.280	0.280
JACK WATSON	2049_B_2	0.280	0.280	0.280	0.280
JACK WATSON	2049_B_3	0.280	0.280	0.280	0.280
JACK WATSON	2049_B_4	0.470	0.470	0.415	0.415
JACK WATSON	2049_B_5	0.590	0.590	0.415	0.415
Jack Watson	2049_G_A	0.880	0.880	0.880	0.880
E C GASTON	26_B_1	0.473	0.473	0.473	0.473
E C GASTON	26_B_2	0.473	0.473	0.473	0.473
E C GASTON	26_B_3	0.457	0.457	0.457	0.457
E C GASTON	26_B_4	0.457	0.457	0.457	0.457
E C GASTON	26_B_5	0.429	0.060	0.429	0.060
E C Gaston	26_G_GT4	0.880	0.880	0.880	0.880
ASHEVILLE	2706_B_1	0.491	0.319	0.491	0.319
CLIFFSIDE	2721_B_5	0.294	0.070	0.294	0.070
BARRY	3_B_1	0.500	0.500	0.500	0.500
BARRY	3_B_2	0.500	0.500	0.500	0.500
BARRY	3_B_3	0.300	0.300	0.300	0.300
BARRY	3_B_4	0.290	0.290	0.290	0.290
BARRY	3_B_5	0.380	0.380	0.380	0.380
Barry	3_G_A1	0.013	0.013	0.013	0.013
Barry	3_G_A1CT	0.013	0.013	0.013	0.013
Barry	3_G_A1ST	0.013	0.013	0.013	0.013
Barry	3_G_A2C1	0.013	0.013	0.013	0.013
Barry	3_G_A2C2	0.013	0.013	0.013	0.013
Barry	3_G_A2ST	0.013	0.013	0.013	0.013
W S LEE	3264_B_1	0.393	0.393	0.250	0.250
W S LEE	3264_B_2	0.415	0.415	0.250	0.250
W S Lee	3264_G_4	0.320	0.320	0.320	0.320
W S Lee	3264_G_5	0.320	0.320	0.320	0.320
W S Lee	3264_G_6	0.320	0.320	0.320	0.320
MCMEEKIN	3287_B_MCM1	0.350	0.350	0.350	0.350
MCMEEKIN	3287_B_MCM2	0.350	0.350	0.350	0.350
MT STORM	3954_B_3	0.604	0.060	0.604	0.060
JAMES H MILLER JR	6002_B_1	0.275	0.060	0.275	0.060
JAMES H MILLER JR	6002_B_2	0.247	0.060	0.247	0.060
JAMES H MILLER JR	6002_B_3	0.306	0.070	0.306	0.070

Plant Name	Unique ID	Mode1 Rate (VISTAS I)	Mode2 Rate (VISTAS I)	Mode3 Rate (VISTAS I)	Mode4 Rate (VISTAS I)
JAMES H MILLER JR	6002_B_4	0.275	0.070	0.275	0.070
PLEASANTS	6004_B_1	0.302	0.060	0.302	0.060
PLEASANTS	6004_B_2	0.335	0.060	0.335	0.060
WANSLEY	6052_B_1	0.405	0.070	0.405	0.070
WANSLEY	6052_B_2	0.390	0.070	0.390	0.070
Wansley	6052_G_5A	0.880	0.880	0.880	0.880
VICTOR J DANIEL JR.	6073_B_1	0.310	0.310	0.310	0.310
VICTOR J DANIEL JR.	6073_B_2	0.350	0.350	0.350	0.350
Victor J Daniel Jr	6073_G_3	0.013	0.013	0.013	0.013
Victor J Daniel Jr	6073_G_3CT	0.013	0.013	0.013	0.013
Victor J Daniel Jr	6073_G_3ST	0.013	0.013	0.013	0.013
Victor J Daniel Jr	6073_G_4	0.013	0.013	0.013	0.013
Victor J Daniel Jr	6073_G_4CT	0.013	0.013	0.013	0.013
Victor J Daniel Jr	6073_G_4ST	0.013	0.013	0.013	0.013
MCINTOSH	6124_B_1	0.613	0.613	0.410	0.410
McIntosh	6124_G_CT1	0.090	0.090	0.090	0.090
McIntosh	6124_G_CT2	0.090	0.090	0.090	0.090
McIntosh	6124_G_CT3	0.090	0.090	0.090	0.090
McIntosh	6124_G_CT4	0.090	0.090	0.090	0.090
McIntosh	6124_G_CT5	0.090	0.090	0.090	0.090
McIntosh	6124_G_CT6	0.090	0.090	0.090	0.090
McIntosh	6124_G_CT7	0.090	0.090	0.090	0.090
McIntosh	6124_G_CT8	0.090	0.090	0.090	0.090
WINYAH	6249_B_1	0.100	0.100	0.100	0.100
WINYAH	6249_B_2	0.120	0.120	0.120	0.120
WINYAH	6249_B_3	0.120	0.120	0.120	0.120
WINYAH	6249_B_4	0.120	0.120	0.120	0.120
SCHERER	6257_B_1	0.450	0.450	0.150	0.150
SCHERER	6257_B_2	0.450	0.450	0.150	0.150
SCHERER	6257_B_3	0.300	0.300	0.150	0.150
SCHERER	6257_B_4	0.300	0.300	0.150	0.150
Wilson	6258_G_5A	0.880	0.880	0.880	0.880
Wilson	6258_G_5B	0.880	0.880	0.880	0.880
Wilson	6258_G_5C	0.880	0.880	0.880	0.880
Wilson	6258_G_5D	0.880	0.880	0.880	0.880
Wilson	6258_G_5E	0.880	0.880	0.880	0.880
Wilson	6258_G_5F	0.880	0.880	0.880	0.880
Wilson	6258_G_IC1	0.880	0.880	0.880	0.880
CRIST	641_B_2	0.280	0.280	0.280	0.280
CRIST	641_B_3	0.280	0.280	0.280	0.280
CRIST	641_B_4	0.400	0.400	0.240	0.240
CRIST	641_B_5	0.400	0.400	0.240	0.240
CRIST	641_B_7	0.482	0.060	0.482	0.060
SCHOLZ	642_B_1	0.540	0.540	0.320	0.320
SCHOLZ	642_B_2	0.570	0.570	0.320	0.320
SMITH	643_B_1	0.490	0.490	0.240	0.240
SMITH	643_B_2	0.410	0.410	0.410	0.410
Lansing Smith	643_G_CT1	0.880	0.880	0.880	0.880
GADSDEN	7_B_1	0.544	0.544	0.544	0.544
GADSDEN	7_B_2	0.544	0.544	0.544	0.544
Atkinson	700_G_5A	0.320	0.320	0.320	0.320
Atkinson	700_G_5B	0.320	0.320	0.320	0.320
BOWEN	703_B_1BLR	0.405	0.070	0.405	0.070
BOWEN	703_B_2BLR	0.405	0.070	0.405	0.070

Plant Name	Unique ID	Mode1 Rate (VISTAS I)	Mode2 Rate (VISTAS I)	Mode3 Rate (VISTAS I)	Mode4 Rate (VISTAS I)
BOWEN	703_B_3BLR	0.409	0.070	0.409	0.070
BOWEN	703_B_4BLR	0.419	0.070	0.419	0.070
Bowen	703_G_6	0.880	0.880	0.880	0.880
HAMMOND	708_B_1	0.800	0.800	0.410	0.410
HAMMOND	708_B_2	0.800	0.800	0.410	0.410
HAMMOND	708_B_3	0.800	0.800	0.410	0.410
HAMMOND	708_B_4	0.404	0.070	0.404	0.070
HARLLEE BRANCH	709_B_1	0.800	0.800	0.519	0.519
HARLLEE BRANCH	709_B_2	0.800	0.800	0.374	0.374
HARLLEE BRANCH	709_B_3	0.800	0.800	0.381	0.381
HARLLEE BRANCH	709_B_4	0.800	0.800	0.381	0.381
JACK MCDONOUGH	710_B_MB1	0.450	0.450	0.230	0.230
JACK MCDONOUGH	710_B_MB2	0.450	0.450	0.230	0.230
Jack McDonough	710_G_3A	0.320	0.320	0.320	0.320
Jack McDonough	710_G_3B	0.320	0.320	0.320	0.320
MCMANUS	715_B_1	0.310	0.310	0.310	0.310
MCMANUS	715_B_2	0.310	0.310	0.310	0.310
McManus	715_G_3A	0.880	0.880	0.880	0.880
McManus	715_G_3B	0.880	0.880	0.880	0.880
McManus	715_G_3C	0.880	0.880	0.880	0.880
McManus	715_G_4A	0.880	0.880	0.880	0.880
McManus	715_G_4B	0.880	0.880	0.880	0.880
McManus	715_G_4C	0.880	0.880	0.880	0.880
McManus	715_G_4D	0.880	0.880	0.880	0.880
McManus	715_G_4E	0.880	0.880	0.880	0.880
McManus	715_G_4F	0.880	0.880	0.880	0.880
McManus	715_G_IC1	3.200	3.200	3.200	3.200
MITCHELL	727_B_3	0.625	0.625	0.625	0.625
Mitchell	727_G_4A	0.880	0.880	0.880	0.880
Mitchell	727_G_4B	0.880	0.880	0.880	0.880
Mitchell	727_G_4C	0.880	0.880	0.880	0.880

Mode 1 Rate (Uncontrolled Base Rate) – This emission rate reflects current configuration of combustion controls. If a post combustion NOx control such as a SCR or a SNCR exists, it is assumed that it is not operating.
Mode 2 Rate (Controlled Base Rate) – This emission rate reflects current configuration of combustion. If a post combustion NOx control such as a SCR or a SNCR exists, it is assumed that it is operating.
Mode 3 Rate (Uncontrolled Policy Rate) – This emission rate reflects a state of the art configuration of combustion controls. If a post combustion NOx control such as a SCR or a SNCR exists, it is assumed that it is not operating.
Mode 4 Rate (Controlled Policy Rate) – This emission rate reflects a state of the art configuration of combustion controls. If a post combustion NOx control such as a SCR or a SNCR exists, it is assumed that it is operating.

For more details on the development of these rates please refer to http://www.epa.gov/airmarkets/epa-ipm/section3powsysop.pdf

Existing Unit Level SO2 Control Technology Assumptions

Exhibit C1.3: Changes made to SO_2 Scrubber Installations in Vistas Phase I

Plant Name	Unique ID	Scrubber Installation (NEEDS NODA)	Scrubber Installation (VISTAS Phase 1)
NORTH BRANCH POWER STATION	7537_B_1A	Dry Scrubber	-
NORTH BRANCH POWER STATION	7537_B_1B	Dry Scrubber	-
Morgantown Energy Facility	10743_G_GEN1	Dry Scrubber	-

Existing Unit Level Emission Rate Assumptions

Exhibit C1.4: Changes made to SO_2 Emission Rate Limits (lbs/MMBtu) in Vistas Phase I

Plant Name	Unique ID	SO_2 Rate (NEEDS NODA)	SO_2 Rate (VISTAS Phase I)
GREENE COUNTY	10_B_1	4.000	1.197
GREENE COUNTY	10_B_2	4.000	1.197
EATON	2046_B_1	4.800	0.001
EATON	2046_B_2	4.800	0.001
EATON	2046_B_3	4.800	0.001
SWEATT	2048_B_1	4.800	0.001
SWEATT	2048_B_2	4.800	0.001
JACK WATSON	2049_B_1	4.800	0.001
JACK WATSON	2049_B_2	4.800	0.001
JACK WATSON	2049_B_3	4.800	0.001
JACK WATSON	2049_B_4	4.800	0.885
JACK WATSON	2049_B_5	4.800	0.885
E C GASTON	26_B_1	3.800	1.667
E C GASTON	26_B_2	3.800	1.667
E C GASTON	26_B_3	3.800	1.667
E C GASTON	26_B_4	3.800	1.667
E C GASTON	26_B_5	3.800	1.667
BUCK	2720_B_5	2.300	1.630
BUCK	2720_B_6	2.300	1.630
BUCK	2720_B_7	2.300	1.630
BUCK	2720_B_8	2.300	1.630
BUCK	2720_B_9	2.300	1.630
CLIFFSIDE	2721_B_1	2.300	2.200
CLIFFSIDE	2721_B_2	2.300	2.200
CLIFFSIDE	2721_B_3	2.300	2.200
CLIFFSIDE	2721_B_4	2.300	2.200
CLIFFSIDE	2721_B_5	2.300	2.200
DAN RIVER	2723_B_1	2.300	1.810
DAN RIVER	2723_B_2	2.300	1.810
DAN RIVER	2723_B_3	2.300	1.810
BARRY	3_B_1	1.800	1.197
BARRY	3_B_2	1.800	1.197
BARRY	3_B_3	1.800	1.197
BARRY	3_B_4	1.800	1.197
BARRY	3_B_5	1.800	1.197
JAMES H MILLER JR	6002_B_1	1.800	0.795
JAMES H MILLER JR	6002_B_2	1.800	0.795

Plant Name	Unique ID	SO_2 Rate (NEEDS NODA)	SO_2 Rate (VISTAS Phase I)
JAMES H MILLER JR	6002_B_3	1.800	0.795
JAMES H MILLER JR	6002_B_4	1.800	0.795
VICTOR J DANIEL JR.	6073_B_1	4.800	0.885
VICTOR J DANIEL JR.	6073_B_2	4.800	0.885
SCHERER	6257_B_1	1.200	0.796
SCHERER	6257_B_2	1.200	0.796
SCHERER	6257_B_3	1.200	0.796
SCHERER	6257_B_4	1.200	0.796
CRIST	641_B_2	0.740	0.001
CRIST	641_B_3	0.740	0.001
CRIST	641_B_4	5.900	1.197
CRIST	641_B_5	5.900	1.197
CRIST	641_B_6	5.900	1.197
CRIST	641_B_7	5.900	1.197
SCHOLZ	642_B_1	6.170	1.200
SCHOLZ	642_B_2	6.170	1.200
SMITH	643_B_1	6.170	1.197
SMITH	643_B_2	6.170	1.197
GADSDEN	7_B_1	4.000	2.500
GADSDEN	7_B_2	4.000	2.500
BOWEN	703_B_1BLR	4.580	1.667
HAMMOND	708_B_1	4.580	1.667
HAMMOND	708_B_2	4.580	1.667
HAMMOND	708_B_3	4.580	1.667
HAMMOND	708_B_4	4.580	1.667
HARLLEE BRANCH	709_B_1	4.580	1.667
HARLLEE BRANCH	709_B_2	4.580	1.667
HARLLEE BRANCH	709_B_3	4.580	1.667
HARLLEE BRANCH	709_B_4	4.580	1.667
JACK MCDONOUGH	710_B_MB1	4.580	1.667
JACK MCDONOUGH	710_B_MB2	4.580	1.667
MCMANUS	715_B_1	3.159	2.620
MCMANUS	715_B_2	3.159	2.620
MITCHELL	727_B_3	4.580	2.500
YATES	728_B_Y2BR	4.580	1.667
YATES	728_B_Y3BR	4.580	1.667
YATES	728_B_Y4BR	4.580	1.667
YATES	728_B_Y5BR	4.580	1.667
KRAFT	733_B_1	4.580	1.270
KRAFT	733_B_2	4.580	1.270
KRAFT	733_B_3	4.580	1.270
KRAFT	733_B_4	0.800	0.001
RIVERSIDE	734_B_11	2.632	0.001
RIVERSIDE	734_B_12	3.159	0.001
RIVERSIDE	734_B_4	2.632	0.001
RIVERSIDE	734_B_5	2.632	0.001
RIVERSIDE	734_B_6	2.632	0.001
GORGAS	8_B_10	4.000	1.667
GORGAS	8_B_6	4.000	2.500
GORGAS	8_B_7	4.000	2.500

Plant Name	Unique ID	SO_2 Rate (NEEDS NODA)	SO_2 Rate (VISTAS Phase I)
GORGAS	8_B_8	4.000	1.667
GORGAS	8_B_9	4.000	1.667

Existing Unit Level PM Control Assumptions

Exhibit C1.5: Changes made to Particulate Matter (PM) Control Installations in Vistas Phase I

Plant Name	Unique ID	PM Control (NEEDS NODA)	PM Control (VISTAS)
G G ALLEN	2718_B_3	Hot-side ESP	Cold-side ESP
G G ALLEN	2718_B_5	Hot-side ESP	Cold-side ESP
WESTON	4078_B_3	Hot-side ESP + Fabric Filter	Fabric Filter

Existing Unit Characteristics - Summer Net Dependable

Exhibit C1.6: Changes made to Summer Net Dependable Capacity (MW) in Vistas Phase I

Plant Name	Unique ID	Capacity (NEEDS NODA)	Capacity (VISTAS Phase I)
VACA_SC_Combined Cycle	077_C_077	1317	807
CRIST	641_B_1	24	0 **
Lansing Smith	A274_G_A274	500	530
Atkinson	700_G_5A	32	15.3
Atkinson	700_G_5B	32	15.3
Dahlberg	7709_G_10	75	80
Dahlberg	7709_G_9	75	80
FRANKLIN	A7840_G_A331	570	630
Mill Creek	A294_G_A294	320	326.8
Mill Creek	A295_G_A295	240	245.1
Mill Creek	A296_G_A296	80	81.7
SCE&G Hardeeville	3286_C_2		170
SCE&G Hardeeville	3286_C_3		170
SCE&G Hardeeville	3286_C_4		170
Cross 3	130_C_3		660

** Zero capacity denotes that unit was retired in 2002.

Existing Unit Heat Rate Data

Exhibit C1.7: Changes made to Heat Rate (Btu/kWh) in Vistas Phase I

Plant Name	Unique ID	Heat Rate (NEEDS NODA)	Heat Rate (VISTAS Phase I)
ALLEN S KING	1915_B_1	8879	9229

Existing Unit Unit ID

Exhibit C1.8: Unit ID Changes in Vistas Phase I

Plant Name	Unique ID	Unit ID (NEEDS NODA)	Unit ID (VISTAS Phase I)
Talbot County Energy	A397_G_A397	397	1
Talbot County Energy	A398_G_A398	398	2
Talbot County Energy	A399_G_A399	399	3-4
Talbot County Energy	A400_G_A400	400	5-6
Mill Creek	A294_G_A294	294	1-4
Mill Creek	A295_G_A295	295	5-7
Mill Creek	A296_G_A296	296	8

Committed Units - Control Decisions

Exhibit C1.9: Duke and Progress Energy SO_2 Control Plan for North Carolina Clean Smokestacks Rule in Vistas Phase I

Unit	Technology	Operation Date	Company
Asheville 1	Scrubber	2005	Progress Energy
Asheville 2	Scrubber	2006	Progress Energy
Cape Fear 5	Scrubber	2012	Progress Energy
Cape Fear 6	Scrubber	2011	Progress Energy
Mayo 1	Scrubber	2008	Progress Energy
Roxboro 1	Scrubber	2009	Progress Energy
Roxboro 2	Scrubber	2007	Progress Energy
Roxboro 3	Scrubber	2007	Progress Energy
Roxboro 4	Scrubber	2007	Progress Energy
Sutton 3	Scrubber	2012	Progress Energy
Allen 1	Scrubber	2011	Duke Power
Allen 2	Scrubber	2011	Duke Power
Allen 3	Scrubber	2011	Duke Power
Allen 4	Scrubber	2012	Duke Power
Allen 5	Scrubber	2012	Duke Power
Belews Creek 1	Scrubber	2008	Duke Power
Belews Creek 2	Scrubber	2008	Duke Power
Cliffside 5	Scrubber	2009	Duke Power
Marshall 1	Scrubber	2007	Duke Power
Marshall 2	Scrubber	2007	Duke Power
Marshall 3	Scrubber	2006	Duke Power
Marshall 4	Scrubber	2006	Duke Power

Exhibit C1.10: Duke and Progress Energy NO_x Control Plan for North Carolina Clean Smokestacks Rule in Vistas Phase I

Unit	Technology	Operation Date	Company
Asheville 1	SCR	2009	Progress Energy
Lee 2	ROFA	2007	Progress Energy
Lee 3	SCR	2010	Progress Energy
Sutton 2	ROFA	2006	Progress Energy
Allen 1	SNCR	2003	Duke Power
Allen 2	SNCR	2007	Duke Power
Allen 3	SNCR	2005	Duke Power
Allen 4	SNCR	2006	Duke Power
Allen 5	SNCR	2008	Duke Power
Belews Creek 1	SCR	2003	Duke Power
Belews Creek 2	SCR	2004	Duke Power
Buck 3	SNCR	2009	Duke Power
Buck 4	SNCR	2008	Duke Power
Buck 5	SNCR	2006	Duke Power
Buck 6	SNCR	2007	Duke Power
Cliffside 1	SNCR	2009	Duke Power
Cliffside 2	SNCR	2009	Duke Power
Cliffside 3	SNCR	2008	Duke Power
Cliffside 4	SNCR	2008	Duke Power
Cliffside 5	SCR	2002	Duke Power
Dan River 1	SNCR	2009	Duke Power
Dan River 2	SNCR	2009	Duke Power
Dan River 3	SNCR	2007	Duke Power
Marshall 1	SNCR	2007	Duke Power
Marshall 2	SNCR	2006	Duke Power
Marshall 3	SNCR	2005	Duke Power
Marshall 4	SNCR	2008	Duke Power
Riverbend 4	SNCR	2007	Duke Power
Riverbend 5	SNCR	2008	Duke Power
Riverbend 6	SNCR	2008	Duke Power
Riverbend 7	SNCR	2007	Duke Power

Source: Gregory Stella, VISTAS Technical Advisor for Emissions Inventories.

Phase II Changes

Potential Units Characteristics – Cost and Heat Rate

Exhibit C2.1: Default Cost and Heat Rate for Potential Units in Vistas Phase II

Plant Type	Heat rate (Btu/Kwh)	VOM_1999/MWh	FOM_1999/kW-yr	Capital Costs_1999/kW
Coal Steam	8670	3.75	22.49	1104.27
IGCC	7517	2.38	31.59	1260.31
Combined Cycle	6857	1.69	10.19	516.12
Turbine	10450	2.92	9.90	360.09
ACT	8550	2.59	8.60	332.39
ACC	6393	1.63	9.56	501.35

Existing Unit Characteristics - Capacity

Exhibit C2.2: Capacity Changes by Unit in Vistas Phase II

Exhibit C2.2 Plant Name	Unique ID	Capacity From Phase I (MW)	Capacity for Phase II (MW)
FLINT CREEK	6138_B_1	480.0	528.0
Indianola	1150_G_1	0.6	0.3
Indianola	1150_G_2	1.2	1.1
Indianola	1150_G_3	0.8	1.0
Indianola	1150_G_5	3.5	3.6
Indianola	1150_G_7	18.5	18.1
MUSCATINE	1167_B_7	25.6	0.0
MUSCATINE	1167_B_8	76.3	35.0
MUSCATINE	1167_B_9	161.0	147.0
PELLA	1175_B_7	20.1	12.8
PELLA	1175_B_8	2.8	15.0
PELLA	1175_B_6	15.6	15.0
Summit Lake	1206_G_IC1	0.9	1.1
Summit Lake	1206_G_1	6.9	6.0
Summit Lake	1206_G_2	7.0	6.4
Summit Lake	1206_G_3	7.6	7.1
Summit Lake	1206_G_GT1	31.0	30.9
Summit Lake	1206_G_GT2	30.0	31.2
EARL F WISDOM	1217_B_1	38.5	37.5
FAIR STATION	1218_B_1	23.4	23.4
LA CYGNE	1241_B_1	682.0	724.0
LA CYGNE	1241_B_2	668.0	674.0
Fredonia	1277_G_3	0.3	1.4
Fredonia	1277_G_4	0.5	2.5
Fredonia	1277_G_2	1.3	1.4
EAST 12TH STREET	7013_B_4	28.7	25.8
Osawatomie	A324_G_A324	84.0	77.0
West Gardner	A429_G_A429	334.0	308.0
Russell Energy Cntr	A374_G_A374	15.0	12.8
Erie	1276_G_4	1.5	1.1
Erie	1276_G_1	0.6	1.1
Erie	1276_G_3	1.0	1.1
ARSENAL HILL	1416_B_5A	120.0	110.0
LIEBERMAN	1417_B_2	26.0	25.0
LIEBERMAN	1417_B_3	110.0	111.0
LIEBERMAN	1417_B_4	111.0	109.0
WATERFORD #3 NUCLEAR	4270_B_W3-1N	1159.0	1075.0
RIVER BEND NUCLEAR	6462_B_1N	997.0	936.0
NRG Sterlington Power LLC	55099_G_03	18.0	25.0
NRG Sterlington Power LLC	55099_G_04	18.0	25.0
NRG Sterlington Power LLC	55099_G_06	18.0	25.0
NRG Sterlington Power LLC	55099_G_07	18.0	25.0
NRG Sterlington Power LLC	55099_G_08	18.0	25.0
Bayou Cove Peaking Power	A55433_G_A112	320.0	300.0
Perryville	A328_G_A328	558.0	637.0

Exhibit C2.2 Plant Name	Unique ID	Capacity From Phase I (MW)	Capacity for Phase II (MW)
ASBURY	2076_B_1	211.0	213.0
HAWTHORN	2079_B_9	120.4	137.0
Hawthorn	2079_G_7	73.1	77.0
Hawthorn	2079_G_8	73.1	77.0
HAWTHORN	2079_B_5	550.0	565.0
MONTROSE	2080_B_1	155.0	170.0
MONTROSE	2080_B_2	153.0	164.0
MONTROSE	2080_B_3	161.0	176.0
LABADIE	2103_B_1	574.0	600.0
LABADIE	2103_B_2	574.0	597.0
LABADIE	2103_B_3	576.0	612.0
LABADIE	2103_B_4	576.0	612.0
MERAMEC	2104_B_1	132.0	114.0
MERAMEC	2104_B_2	132.0	114.0
MERAMEC	2104_B_3	277.0	272.0
MERAMEC	2104_B_4	336.0	321.0
State Line Combined Cycle	7296_G_2-1	129.0	250.0
Columbia	55447_G_CT01	31.6	35.0
Columbia	55447_G_CT02	31.6	35.0
Columbia	55447_G_CT03	31.6	35.0
Columbia	55447_G_CT04	31.6	35.0
WHELAN ENERGY CENTER	60_B_1	72.0	76.3
NORTH DENVER	2244_B_5	20.0	22.0
Kearney	2268_G_1	1.0	1.3
Jones Street	2290_G_1	54.7	59.0
Jones Street	2290_G_2	54.7	59.0
NORTH OMAHA	2291_B_1	75.6	79.0
NORTH OMAHA	2291_B_2	110.5	111.0
NORTH OMAHA	2291_B_3	110.5	111.0
NORTH OMAHA	2291_B_4	133.2	138.0
NORTH OMAHA	2291_B_5	214.7	224.0
Sarpy County	2292_G_1	51.4	55.0
Sarpy County	2292_G_2	51.4	55.0
Sarpy County	2292_G_3	105.5	106.0
Sarpy County	2292_G_BSD	3.4	3.0
Sarpy County	2292_G_4	47.5	48.0
Sarpy County	2292_G_5	47.5	48.0
NEBRASKA CITY	6096_B_1	584.9	646.0
COOPER NUCLEAR	8036_B_1N	758.0	778.0
Cass County	A138_G_A138	330.0	320.0
NORTHEASTERN	2963_B_3302	485.0	480.0
NORTHEASTERN	2963_B_3313	460.0	450.0
Northeastern	2963_B_3301A	163.0	157.0
Weleetka	2966_G_4	53.0	55.0
Weleetka	2966_G_6	47.0	54.0
Riverside	4940_G_IC1	3.0	2.8
OKLAUNION	127_B_1	676.0	690.0
LIMESTONE	298_B_LIM1	720.0	836.0
LIMESTONE	298_B_LIM2	720.0	766.0

Exhibit C2.2c Plant Name	Unique ID	Capacity From Phase I (MW)	Capacity for Phase II (MW)
P H ROBINSON	3466_B_PHR4	739.0	737.0
T H Wharton	3469_G_33	48.0	57.0
T H Wharton	3469_G_34	48.0	57.0
T H Wharton	3469_G_41	48.0	57.0
W A PARISH	3470_B_WAP8	555.0	610.0
WILKES	3478_B_3	343.0	348.0
PAINT CREEK	3524_B_4	117.0	118.0
Rio Pecos	3526_G_4	3.0	5.0
RIO PECOS	3526_B_5	36.0	38.0
San Angelo	3527_G_1	22.0	21.0
SAM SEYMOUR	6179_B_1	580.0	598.0
SAM SEYMOUR	6179_B_2	580.0	598.0
SAM SEYMOUR	6179_B_3	435.0	445.0
PIRKEY	7902_B_1	580.0	675.0
Sweeny Cogeneration Facility	55015_G_GEN1	84.0	115.0
Sweeny Cogeneration Facility	55015_G_GEN2	84.0	115.0
Sweeny Cogeneration Facility	55015_G_GEN3	84.0	115.0
Sweeny Cogeneration Facility	55015_G_GEN4	81.1	115.0
Lost Pines I	55154_G_CTA	155.7	162.0
Lost Pines I	55154_G_CTB	155.7	162.0
Lost Pines I	55154_G_ST	163.9	176.0
PRESQUE ISLE	1769_B_5	87.0	88.0
PRESQUE ISLE	1769_B_6	90.0	88.0
PRESQUE ISLE	1769_B_7	85.0	88.0
PRESQUE ISLE	1769_B_8	85.0	88.0
Elgin Energy Center	A191_G_A191	117.0	107.0
Elgin Energy Center	A194_G_A194	117.0	107.0
Grand Tower	862_G_1-3	213.2	325.0
NEWTON	6017_B_1	555.0	557.0
NEWTON	6017_B_2	555.0	569.0
MONROE	1733_B_1	750.0	770.0
MONROE	1733_B_2	750.0	785.0
MONROE	1733_B_3	750.0	795.0
MONROE	1733_B_4	750.0	775.0
ST CLAIR	1743_B_1	163.0	153.0
ST CLAIR	1743_B_2	162.0	162.0
ST CLAIR	1743_B_3	163.0	171.0
ST CLAIR	1743_B_4	162.0	158.0
ST CLAIR	1743_B_6	294.0	321.0
Lakefield Junction	7925_G_4	72.3	87.0
Lakefield Junction	7925_G_5	72.3	87.0
Lakefield Junction	7925_G_6	72.3	87.0
M L HIBBARD	1897_B_3	36.9	33.3
M L HIBBARD	1897_B_4	13.9	15.3
OWATONNA	2003_B_6	19.9	14.0
De Pere Energy Center	55029_G_CT01	186.1	183.0
PULLIAM	4072_B_3	28.6	26.0
PULLIAM	4072_B_4	27.0	29.0
PULLIAM	4072_B_5	50.2	51.0

Exhibit C2.2 Plant Name	Unique ID	Capacity From Phase I (MW)	Capacity for Phase II (MW)
PULLIAM	4072_B_6	70.9	69.0
PULLIAM	4072_B_7	86.7	82.0
PULLIAM	4072_B_8	143.5	132.0
Pulliam	A338_G_A338	83.0	74.0
BLOUNT STREET	3992_B_7	23.7	22.4
BLOUNT STREET	3992_B_8	49.4	49.0
BLOUNT STREET	3992_B_9	48.8	48.2
Concord	7159_G_1	83.0	94.0
Concord	7159_G_2	83.0	94.0
Concord	7159_G_3	83.0	94.0
Concord	7159_G_4	83.0	94.0
Paris	7270_G_1	83.0	100.0
Paris	7270_G_2	83.0	100.0
Paris	7270_G_3	83.0	100.0
Paris	7270_G_4	83.0	100.0
PLEASANT PRAIRIE	6170_B_1	600.0	617.0
PLEASANT PRAIRIE	6170_B_2	600.0	617.0
Pleasant Prairie	6170_G_3	2.0	2.0
WESTON	4078_B_1	61.5	62.0
WESTON	4078_B_2	81.8	86.0
WESTON	4078_B_3	334.3	338.0
Weston	4078_G_31	19.3	20.0
Weston	4078_G_32	48.6	47.0
West Marinette	4076_G_31	40.4	43.0
West Marinette	4076_G_32	41.4	43.0
West Marinette	4076_G_33	80.2	75.0
West Marinette	7799_G_34	79.5	79.5
South Oak Creek	4041_G_9	20.0	18.0
VALLEY	4042_B_1	69.6	70.0
VALLEY	4042_B_2	70.4	70.0
VALLEY	4042_B_3	71.0	70.0
VALLEY	4042_B_4	69.0	70.0
Valley	4042_G_3	3.0	3.0
Germantown	6253_G_1	53.0	63.0
Germantown	6253_G_3	53.0	63.0
Germantown	6253_G_4	53.0	63.0
Germantown	6253_G_5	72.6	93.0
AES Warrior Run Cogeneration Facility	10678_G_GEN1	204.3	180.0
C P CRANE	1552_B_1	190.0	200.0
C P CRANE	1552_B_2	190.0	200.0
Riverside	1559_G_8	22.0	17.0
Riverside	1559_G_GT7	22.0	17.0
Rockspring Generating	A366_G_A366	113.3	190.0
Rockspring Generating	A367_G_A367	113.3	190.0
Rockspring Generating	A368_G_A368	226.7	190.0
Rockspring Generating	A369_G_A369	226.7	190.0
St Albans	3726_G_IC1	1.1	1.3
St Albans	3726_G_IC2	1.1	1.3
MONTVILLE	546_B_6	402.0	407.4

Exhibit C2-28 Plant Name	Unique ID	Capacity From Phase II (MW)	Capacity for Phase II (MW)
BRIDGEPORT HARBOR	568_B_BHB2	170.0	372.0
Bridgeport Harbor	568_G_4	14.6	9.9
Branford	540_G_10	14.9	16.2
Algonquin Power Windsor Locks LLC(fka Dexter)	10567_G_GTG	31.6	26.0
Bridgeport Energy	55042_G_GEN1	169.4	0.0
Capital District Energy Center Cogen Ass	50498_G_GTG	41.0	31.9
Lake Road	55149_G_U1	177.3	232.1
AES Thames Incorporated	10675_G_GEN1	194.8	181.0
Cos Cob	542_G_10	17.9	17.9
Cos Cob	542_G_11	17.1	18.2
Cos Cob	542_G_12	16.4	18.4
Franklin Drive	561_G_19	17.2	15.4
Middletown	562_G_10	17.2	17.1
Norwalk Harbor	548_G_10	11.8	11.9
Bridgeport Energy	55042_G_GEN2	169.4	224.0
Bridgeport Energy	55042_G_GEN3	178.5	224.0
New Milford Gas Recovery	50564_G_GEN1	2.4	3.0
Wallingford	55517_G_CTG1	29.0	44.5
Wallingford	55517_G_CTG2	29.0	38.5
Wallingford	55517_G_CTG3	29.0	44.9
Wallingford	55517_G_CTG4	29.0	42.2
Wallingford	55517_G_CTG5	29.0	39.9
Hartford Landfill	55163_G_UNT1	0.9	0.8
Hartford Landfill	55163_G_UNT2	0.9	0.8
Hartford Landfill	55163_G_UNT3	0.9	0.8
Montville	546_G_10	2.8	2.7
Montville	546_G_11	2.8	2.7
Torrington	565_G_10	17.2	15.8
Tunnel	557_G_10	16.9	15.9
South Meadow	563_G_12	39.0	37.7
South Meadow	563_G_13	39.0	38.3
South Meadow	563_G_14	39.0	37.4
Capital District Energy Center Cogen Ass	50498_G_STG	31.7	19.8
Algonquin Power Windsor Locks LLC(fka Dexter)	10567_G_STG	12.6	12.0
Lake Road	55149_G_U2	177.3	227.0
NEW HAVEN HARBOR	6156_B_NHB1	447.0	447.9
Devon	544_G_12	30.5	29.8
Devon	544_G_13	30.8	33.3
Devon	544_G_14	31.8	29.6
Clement Dam Hydroelectric LLC	10276_G_49	2.4	0.9
Lochmere Hydroelectric Plant	54572_G_UNT1	0.3	0.1
Lochmere Hydroelectric Plant	54572_G_UNT2	0.3	0.1
Lochmere Hydroelectric Plant	54572_G_UNT3	0.3	0.1
Lochmere Hydroelectric Plant	54572_G_UNT4	0.3	0.1
Pinetree Power Tamworth Inc	50739_G_GEN1	22.7	21.0
White Lake	2369_G_GT1	17.7	16.2
Errol Hydroelectric Project	10570_G_1	3.0	2.5
Lost Nation	2362_G_GT1	13.7	15.0
Whitefield Power and Light Co	10839_G_GEN1	14.5	14.4

Exhibit C2.2 Plant Name	Unique ID	Capacity From Phase I (MW)	Capacity for Phase II (MW)
Bridgewater Power Company LP	10290_G_GEN1	18.1	15.8
Newfound Hydroelectric Company	50324_G_1	0.8	0.4
Newfound Hydroelectric Company	50324_G_2	0.8	0.4
Pinetree Power Incoporated Bethlehem	50208_G_GEN1	16.4	15.8
Dunbarton Energy PartnersL P	50347_G_MA15	0.7	0.6
Four Hills Nashua Landfill	55006_G_UNT1	2.1	0.5
Four Hills Nashua Landfill	55006_G_UNT2	0.7	0.5
Gregg Falls	50384_G_1	2.2	0.0
Hillsborough Hosiery	10036_G_GEN1	0.6	0.1
Hillsborough Hosiery	10036_G_GEN2	0.6	0.1
Jackman	2360_G_1	3.6	3.6
Bio Energy Corporation	52041_G_GEN1	11.4	0.0
Briar Hydro Assoc Penacook Upper Falls F	50414_G_1	3.4	0.9
Briar Hydro Associates Rolfe Canal Facil	50351_G_1	4.3	1.1
Wheelabrator Concord Facility	50873_G_GEN1	12.5	12.5
EHC West Hopkinton	54384_G_GEN1	1.0	0.5
Franklin Industrial Complex	10109_G_1	0.4	0.3
Franklin Industrial Complex	10109_G_2	0.2	0.3
Merrimack	2364_G_GT1	16.3	16.8
Pembroke Hydro	50312_G_1	2.7	0.5
Mine Falls Ltd Partnership	10183_G_GEN1	2.9	0.0
NEWINGTON	8002_B_1	406.0	400.2
SCHILLER	2367_B_5	49.6	47.2
SCHILLER	2367_B_6	48.0	47.9
Milton Hydro	10519_G_2	0.4	0.1
Milton Hydro	10519_G_3	0.3	0.1
Milton Hydro	10519_G_4	0.5	0.1
Rollinsford	54418_G_GEN1	0.8	0.3
Rollinsford	54418_G_GEN2	0.8	0.3
Somersworth Lower Great Dam	50704_G_GEN1	1.3	0.5
Hemphill Power and Light Company	10838_G_GEN1	14.3	14.1
Fore River Generating Station	A199_G_A199	687.5	775.0
INDIAN RIVER	594_B_1	89.0	91.0
INDIAN RIVER	594_B_2	89.0	91.0
INDIAN RIVER	594_B_3	162.0	165.0
INDIAN RIVER	594_B_4	403.0	420.0
Indian River	594_G_10	17.0	20.0
Lewes	600_G_7	0.9	0.9
Lewes	600_G_8	0.9	0.9
Seaford	601_G_7	1.1	1.1
Hay Road	7153_G_1	112.0	100.0
Hay Road	7153_G_2	112.0	100.0
Hay Road	7153_G_3	112.0	100.0
Van Sant Station	7318_G_1	39.0	40.0
Stone Container Corporation Hopewell Mil	50813_G_GEN1	4.8	47.6
Cogentrix Hopewell	10377_G_GEN1	39.1	54.6
Cogentrix Hopewell	10377_G_GEN2	39.1	54.6
Reusens	3779_G_1	10.4	2.5
Smith Mountain	3780_G_1	70.0	66.0

Exhibit C2.2 Plant Name	Unique ID	Capacity From Phase I (MW)	Capacity for Phase II (MW)
Smith Mountain	3780_G_2	160.0	174.0
Smith Mountain	3780_G_3	105.0	106.0
Smith Mountain	3780_G_4	160.0	174.0
Smith Mountain	3780_G_5	70.0	66.0
Leesville	3777_G_1	17.3	25.0
Leesville	3777_G_2	17.3	25.0
Buck	3772_G_1	8.6	2.8
Buck	3772_G_2	2.8	2.8
Buck	3772_G_3	2.8	2.8
Byllesby	3773_G_1	4.3	4.3
Byllesby	3773_G_2	4.3	4.3
Byllesby	3773_G_3	4.3	4.3
Byllesby	3773_G_4	4.3	4.3
Claytor	3774_G_1	16.4	18.8
Claytor	3774_G_2	16.4	18.8
Claytor	3774_G_3	16.4	18.8
Claytor	3774_G_4	16.4	18.8
Niagara	3778_G_1	2.6	1.2
Niagara	3778_G_2	1.2	1.2
KANAWHA RIVER	3936_B_2	195.0	205.0
London	6560_G_1	13.8	4.8
London	6560_G_2	4.8	4.8
London	6560_G_3	4.8	4.8
Marmet	6561_G_1	13.8	4.8
Marmet	6561_G_2	4.8	4.8
Marmet	6561_G_3	4.8	4.8
KAMMER	3947_B_1	200.0	205.0
KAMMER	3947_B_2	200.0	205.0
KAMMER	3947_B_3	200.0	205.0
PHILIP SPORN	3938_B_51	440.0	445.0
Winfield	6562_G_1	16.4	4.9
Winfield	6562_G_2	4.9	4.9
Winfield	6562_G_3	4.9	4.9
PLEASANTS	6004_B_1	614.0	639.0
PLEASANTS	6004_B_2	614.0	639.0
Wrightsville Power Facility	A446_G_A446	67.8	74.0
Wrightsville Power Facility	A445_G_A445	161.7	74.0
Wrightsville Power Facility	A444_G_A444	30.1	16.5
Wrightsville Power Facility	A443_G_A443	20.9	16.5
Wrightsville Power Facility	A442_G_A442	65.2	74.0
Wrightsville Power Facility	A441_G_A441	155.3	74.0
Wrightsville Power Facility	A440_G_A440	28.9	16.5
Wrightsville Power Facility	A439_G_A439	20.1	17.4
Evangeline Power Station	55305_G_U7CT	186.4	155.0
Evangeline Power Station	55305_G_U72	186.4	155.0
Evangeline Power Station	55305_G_U6CT	186.4	157.0
Evangeline Power Station	55305_G_7ST	240.1	178.0
Evangeline Power Station	55305_G_6ST	112.3	104.0
Buchanan	1754_G_1	1.7	0.4

Exhibit C2.2 Plant Name	Unique ID	Capacity From Phase I (MW)	Capacity for Phase II (MW)
Hay Road	A7153_G_A435	500.0	179.0
MAPP_IA_Turbine	045_C_045	170.0	0.0
ENTG_LA_Combined Cycle	021_C_021	1409.0	509.0
MACW_PA_Combined Cycle	038_C_038	1150.0	550.0
ERCT_TX_Combined Cycle	027_C_027	255.0	0.0
ERCT_TX_Turbine	025_C_025	220.0	180.0
WUMS_WI_Combined Cycle	081_C_081	1390.0	845.0
ELK RIVER	2039_B_1	11.3	7.8
ELK RIVER	2039_B_2	9.3	7.5
ELK RIVER	2039_B_3	19.2	14.5
State Line Combined Cycle	7296_G_2	152.0	250.0
Cayuga	1001_G_4	99.0	106.0
Connersville	1002_G_1	42.0	43.0
Walter C Beckjord	2830_G_GT1	46.6	51.0
Walter C Beckjord	2830_G_GT3	46.6	51.0
Walter C Beckjord	2830_G_GT4	46.6	51.0
Woodsdale	7158_G_GT1	77.0	83.0
Woodsdale	7158_G_GT2	77.0	83.0
Woodsdale	7158_G_GT3	77.0	83.0
Woodsdale	7158_G_GT4	77.0	83.0
Woodsdale	7158_G_GT5	77.0	83.0
Woodsdale	7158_G_GT6	77.0	83.0
Concord Facility	50873_G_GEN1	12.5	6.3
Anita	1123_G_6	1825.0	1.8

Cogeneration Flag

Exhibit C2.3: Cogeneration Flag Revision by Unit in Vistas Phase II

Plant Name	Unique ID	Cogen Flag from Phase I	Cogen Flag for Phase II
MUSCATINE	1167_B_8	No	Yes
VALLEY	4042_B_1	No	Yes
VALLEY	4042_B_2	No	Yes
VALLEY	4042_B_3	No	Yes
VALLEY	4042_B_4	No	Yes
Bio Energy Corporation	52041_G_GEN1	Yes	No
Indeck Pepperell Power Facility	10522_G_GEN1	No	Yes
Indeck Pepperell Power Facility	10522_G_GEN2	No	Yes
BLACKSTONE STREET	1594_B_11	No	Yes
BLACKSTONE STREET	1594_B_12	No	Yes
BLACKSTONE STREET	1594_B_5	No	Yes
BLACKSTONE STREET	1594_B_6	No	Yes
KENDALL SQUARE	1595_B_1	No	Yes
KENDALL SQUARE	1595_B_2	No	Yes
KENDALL SQUARE	1595_B_3	No	Yes
CANAL	1599_B_1	Yes	No
Pittsfield Generating Company L P	50002_G_GEN2	No	Yes
Pittsfield Generating Company L P	50002_G_GEN3	No	Yes
Pittsfield Generating Company L P	50002_G_GEN4	No	Yes
Kendall Square	A259_G_A259	No	Yes

Existing Unit Emissions Controls

Exhibit C2.4: NOx Combustion Control Changes by Unit in Vistas Phase II

Plant Name	Unique ID	Combustion Control from Vistas Phase I	Combustion Control for Vistas Phase II
	2709_B_2	Combustion Modification	Combustion Modification; add LNB in 2006
MONROE	1448_B_11	-	Flue Gas Recirculation
Empire Energy Center	A184_G_A184	-	Water Injection
Empire Energy Center	A185_G_A185	-	Water Injection
SABINE	3459_B_3	Low NOx Burner Technology with Separated OFA (Tangentially-fired units only)	OFA
SABINE	3459_B_4	Combustion Modification	Flue Gas Recirculation
SABINE	3459_B_5	Low NOx Burner Technology with Close-coupled OFA (Tangentially-fired units only)	OFA
ROCKPORT	6166_B_MB1	Low NOx Burner Technology (Dry Bottom boilers only)	LNB & OFA
ROCKPORT	6166_B_MB2	Low NOx Burner Technology (Dry Bottom boilers only)	LNB & OFA
CONESVILLE	2840_B_1	-	OFA
CONESVILLE	2840_B_2	-	OFA
CONESVILLE	2840_B_4	Other	LNB + OFA + BOOS
CONESVILLE	2840_B_5	Overfire Air	LNB+OFA
CONESVILLE	2840_B_6	Overfire Air	LNB+OFA
Exeter Energy Project	50736_G_GEN1	-	thermal de-NOx (urea injection)
GLEN LYN	3776_B_51	Other	LNB
GLEN LYN	3776_B_52	Other	LNB
KANAWHA RIVER	3936_B_1	Low NOx Burner Technology (Dry Bottom boilers only)	OFA + CANALIS
KANAWHA RIVER	3936_B_2	Low NOx Burner Technology (Dry Bottom boilers only)	OFA + CANALIS
PHILIP SPORN	3938_B_11	Low NOx Burner Technology (Dry Bottom boilers only)	OFA
PHILIP SPORN	3938_B_21	Low NOx Burner Technology (Dry Bottom boilers only)	OFA
PHILIP SPORN	3938_B_31	Low NOx Burner Technology (Dry Bottom boilers only)	OFA
PHILIP SPORN	3938_B_41	Low NOx Burner Technology (Dry Bottom boilers only)	OFA
BIG SANDY	1353_B_BSU1	Low NOx Burner Technology (Dry Bottom boilers only)	LNB+OFA

Existing Unit Characteristics – Location Codes

Exhibit C2.5: Plant Location Revisions by Unit in Vistas Phase II

Plant Name	Unique ID	County Name from Phase I	County Name for Phase II	County Code from Phase I	County Code for Phase II
Gilliam South	7857_G_1	GUTHRIE	ADAIR	77	1
Lenox Wind Turbine	ZZ351_C_1		TAYLOR		173
Mulvane	1308_G_2	SEDGWICK	SUMNER	173	191
Mulvane	1308_G_1	SEDGWICK	SUMNER	173	191
Mulvane	1308_G_4	SEDGWICK	SUMNER	173	191
Mulvane	1308_G_3	SEDGWICK	SUMNER	173	191
Mulvane	1308_G_5	SEDGWICK	SUMNER	173	191
Mulvane	1308_G_6	SEDGWICK	SUMNER	173	191
Bayou Cove Peaking Power	A55433_G_A112	JEFFERSON DAVIS	ACADIA	53	1
Bergen	2398_G_1SC	HUDSON	BERGEN	17	3
Bergen	2398_G_1ST	HUDSON	BERGEN	17	3
Bergen	2398_G_3	HUDSON	BERGEN	17	3
Bergen	A121_G_A121	HUDSON	BERGEN	17	3
Essex Junction Wastewater Trea	ZZ133_C_1	-	CHITTENDEN	-	7
Bradford	ZZ118_C_1	-	BRADFORD	-	15
Humbolt Industries, Energy Unl	ZZ480_C_1	-	LUZERNE	-	79
Meyersdale Wind Power Project	ZZ382_C_1	-	SOMERSET	-	111
Rolling Hills	55884_C_N01	-	BERKS	-	11
Rolling Hills	55884_C_N02	-	BERKS	-	11
Reusens	3779_G_1	CAMPBELL	BEDFORD	31	19
Reusens	3779_G_2	CAMPBELL	BEDFORD	31	19
Reusens	3779_G_3	CAMPBELL	BEDFORD	31	19
Reusens	3779_G_4	CAMPBELL	BEDFORD	31	19
Reusens	3779_G_5	CAMPBELL	BEDFORD	31	19
Smith Mountain	3780_G_1	FRANKLIN	BEDFORD	67	19
Smith Mountain	3780_G_2	FRANKLIN	BEDFORD	67	19
Smith Mountain	3780_G_3	FRANKLIN	BEDFORD	67	19
Smith Mountain	3780_G_4	FRANKLIN	BEDFORD	67	19
Smith Mountain	3780_G_5	FRANKLIN	BEDFORD	67	19
Winfield	6562_G_1	KANAWHA	PUTNAM	39	79
Winfield	6562_G_2	KANAWHA	PUTNAM	39	79
Winfield	6562_G_3	KANAWHA	PUTNAM	39	79
North Plant	7922_C_10	-	POWESHIEK	-	157

Existing Unit Characteristics – Firing Type

Exhibit C2.6: Firing Type Revisions by Unit in Vistas Phase II

Plant Name	Unique ID	Firing from Phase I	Firing For Phase II
HARVEY COUCH	169_B_1	-	Wall
HARVEY COUCH	169_B_2	-	Wall
LAKE CATHERINE	170_B_3	-	Wall
LAKE CATHERINE	170_B_4	-	Tangential
ROBERT E RITCHIE	173_B_1	-	Cyclone
ROBERT E RITCHIE	173_B_2	-	Tangential
FAIR STATION	1218_B_1	-	wall
CIMARRON RIVER	1230_B_1	-	wall
JUDSON LARGE	1233_B_4	-	wall
ARTHUR MULLERGREN	1235_B_3	-	wall
GORDON EVANS	1240_B_1	-	wall
GORDON EVANS	1240_B_2	-	wall
MURRAY GILL	1242_B_1	-	wall
MURRAY GILL	1242_B_2	-	wall
MURRAY GILL	1242_B_3	-	wall
MURRAY GILL	1242_B_4	-	wall
HUTCHINSON	1248_B_1	-	wall
HUTCHINSON	1248_B_2	-	wall
HUTCHINSON	1248_B_3	-	wall
R S NELSON	1393_B_3	-	tangential
R S NELSON	1393_B_4	-	wall
WILLOW GLEN	1394_B_1	-	tangential
WILLOW GLEN	1394_B_2	-	tangential
WILLOW GLEN	1394_B_3	-	wall
WILLOW GLEN	1394_B_4	-	wall
WILLOW GLEN	1394_B_5	-	tangential
TECHE	1400_B_1	-	front firing
TECHE	1400_B_2	-	front firing
TECHE	1400_B_3	-	opposed
LITTLE GYPSY	1402_B_1	-	wall
LITTLE GYPSY	1402_B_2	-	wall
LITTLE GYPSY	1402_B_3	-	wall
NINEMILE POINT	1403_B_1	-	wall
NINEMILE POINT	1403_B_2	-	wall
NINEMILE POINT	1403_B_3	-	wall
NINEMILE POINT	1403_B_4	-	tangential
NINEMILE POINT	1403_B_5	-	tangential
STERLINGTON	1404_B_10	-	wall
MICHOUD	1409_B_1	-	wall
MICHOUD	1409_B_2	-	wall
MICHOUD	1409_B_3	-	wall
ARSENAL HILL	1416_B_5A	-	tang
LIEBERMAN	1417_B_3	-	tang
LIEBERMAN	1417_B_4	-	tang
CHAMOIS	2169_B_1	-	cyclone
LEWIS CREEK	3457_B_1	-	wall
LEWIS CREEK	3457_B_2	-	wall

Plant Name	Unique ID	Firing from Phase I	Firing For Phase II
SABINE	3459_B_1	-	tangential
SABINE	3459_B_2	-	tangential
SABINE	3459_B_3	-	tangential
SABINE	3459_B_4	-	wall
SABINE	3459_B_5	-	tangential
San Angelo	3527_G_1	-	other
SAN ANGELO	3527_B_2	-	wall
SAM SEYMOUR	6179_B_1	wall	tangential
MONROE	1733_B_1	wall	cell
MONROE	1733_B_2	wall	cell
MONROE	1733_B_3	wall	cell
MONROE	1733_B_4	wall	cell
GREENWOOD	6035_B_1	-	wall
BEACON HEATING	1724_B_1	-	wall
BEACON HEATING	1724_B_2	-	wall
BEACON HEATING	1724_B_3	-	wall
BEACON HEATING	1724_B_4	-	wall
CONNERS CREEK	1726_B_15	-	wall
CONNERS CREEK	1726_B_16	-	wall
GEN J M GAVIN	8102_B_1	wall	cell
GEN J M GAVIN	8102_B_2	wall	cell
CARDINAL	2828_B_1	wall	cell
CARDINAL	2828_B_2	wall	cell
MUSKINGUM RIVER	2872_B_5	wall	cell
BLOUNT STREET	3992_B_7	wall	other
DEVON	544_B_7	-	FF
DEVON	544_B_8	-	FF
NORWALK HARBOR	548_B_1	-	TF
NORWALK HARBOR	548_B_2	-	TF
MIDDLETOWN	562_B_2	-	FF
MONTVILLE	546_B_5	-	TF
MONTVILLE	546_B_6	-	TF
MIDDLETOWN	562_B_4	-	TF
MIDDLETOWN	562_B_3	-	CY
BRIDGEPORT HARBOR	568_B_BHB2	-	CY
Occum	582_G_1	other	
Bantam	6457_G_1	other	
NEW HAVEN HARBOR	6156_B_NHB1	-	TF
Robertsville	549_G_1	other	
Robertsville	549_G_2	other	
NEWINGTON	8002_B_1	-	Tangential
EDGE MOOR	593_B_5	-	Wall
MCKEE RUN	599_B_1	-	wall
MCKEE RUN	599_B_2	-	wall
MCKEE RUN	599_B_3	-	wall
M L HIBBARD	1897_B_3	-	stoker
M L HIBBARD	1897_B_4	-	stoker
MERRIMACK	2364_B_1	cyclone	wall

Exhibit C2.7: Bottom Type Revisions by Unit in Vistas Phase II

Plant Name	Unique ID	Bottom Type (Phase I)	Bottom Type (Phase II)
FAIR STATION	1218_B_1	-	Dry
CIMARRON RIVER	1230_B_1	-	Dry
JUDSON LARGE	1233_B_4	-	Dry
ARTHUR MULLERGREN	1235_B_3	-	dry
GORDON EVANS	1240_B_1	-	dry
GORDON EVANS	1240_B_2	-	dry
MURRAY GILL	1242_B_1	-	dry
MURRAY GILL	1242_B_2	-	dry
MURRAY GILL	1242_B_3	-	dry
MURRAY GILL	1242_B_4	-	dry
HUTCHINSON	1248_B_1	-	dry
HUTCHINSON	1248_B_2	-	dry
HUTCHINSON	1248_B_3	-	dry
CHAMOIS	2169_B_1	-	wet
BRIDGEPORT HARBOR	568_B_BHB3	dry	wet
EDGE MOOR	593_B_5	-	dry
MCKEE RUN	599_B_1	-	dry
MCKEE RUN	599_B_2	-	dry
MCKEE RUN	599_B_3	-	dry

Existing Units Heat Rate

Exhibit C2.8: Heat Rate Revisions by Unit in Vistas Phase II

Plant Name	Unique ID	Heat Rate from Phase I (Btu/KWh)	Heat Rate for Phase II (Btu/KWh)
CECIL LYNCH	167_B_2	12740	12566
HAMILTON MOSES	168_B_1	12154	12188
HAMILTON MOSES	168_B_2	12154	11818
HARVEY COUCH	169_B_1	12154	13725
HARVEY COUCH	169_B_2	14416	11372
LAKE CATHERINE	170_B_1	11537	13356
LAKE CATHERINE	170_B_2	11372	13226
LAKE CATHERINE	170_B_3	12435	12208
LAKE CATHERINE	170_B_4	11007	11870
Mabelvale	171_G_3	15243	13999
ROBERT E RITCHIE	173_B_1	13002	10372
ROBERT E RITCHIE	173_B_2	11666	9931
Robert E Ritchie	173_G_GT1	12688	14250
FLINT CREEK	6138_B_1	10042	10300
INDEPENDENCE	6641_B_1	10619	10549
INDEPENDENCE	6641_B_2	11150	10442
Indianola	1150_G_1	15130	10500
Indianola	1150_G_2	15130	10500
Indianola	1150_G_3	15130	10500
Indianola	1150_G_4	15130	10500
Indianola	1150_G_5	15130	10500
Indianola	1150_G_6	15130	10500
Indianola	1150_G_7	15130	12979
Lake Mills	1154_G_5	11649	9700
Lake Mills	1154_G_6	12666	9050
MUSCATINE	1167_B_7	11344	14114
MUSCATINE	1167_B_8	12029	15279
MUSCATINE	1167_B_9	11499	10740
Summit Lake	1206_G_1	10041	10500
Summit Lake	1206_G_2	10041	10500
Summit Lake	1206_G_3	10041	10500
Summit Lake	1206_G_GT1	14245	13500
Summit Lake	1206_G_GT2	14245	13500
EARL F WISDOM	1217_B_1	13380	12200
FAIR STATION	1218_B_1	12067	11691
FAIR STATION	1218_B_2	12067	10609
LA CYGNE	1241_B_1	12050	10518
LA CYGNE	1241_B_2	10383	10740
Erie	1276_G_4	11990	9655
Erie	1276_G_1	11990	10057
Erie	1276_G_3	11990	10057
DOLET HILLS	51_B_1	10765	10674
R S NELSON	1393_B_3	12531	10476
R S NELSON	1393_B_4	11152	10419
WILLOW GLEN	1394_B_1	12039	10431
Cos Cob	542_G_11	11829	12700

Plant Name	Unique ID	Heat Rate from Phase I (Btu/KWh)	Heat Rate for Phase II (Btu/KWh)
Cos Cob	542_G_12	11829	12700
Devon	544_G_10	9586	13300
Franklin Drive	561_G_19	11829	13300
Middletown	562_G_10	10592	13300
Norwalk Harbor	548_G_10	9708	14650
New Milford Gas Recovery	50564_G_GEN1	11805	17053
Wallingford	55517_G_CTG1	10888	9000
Wallingford	55517_G_CTG2	10888	9000
Wallingford	55517_G_CTG3	10888	9000
Wallingford	55517_G_CTG4	10888	9000
Wallingford	55517_G_CTG5	10888	9000
Montville	546_G_10	11829	11050
Montville	546_G_11	11829	11050
Torrington	565_G_10	11829	13300
Devon	544_G_11	9586	9771
Devon	544_G_12	12341	9771
Devon	544_G_13	12341	9771
Devon	544_G_14	12341	9771
MERRIMACK	2364_B_1	10252	11672
MERRIMACK	2364_B_2	10180	10411
AES Granite Ridge Energy	A093_G_A093	7056	18680
NEWINGTON	8002_B_1	12361	14336
Newington Power Facility	A311_G_A311	7056	8402
SCHILLER	2367_B_4	12866	13896
SCHILLER	2367_B_5	12808	13498
SCHILLER	2367_B_6	12688	12518
Christiana	591_G_11	12666	15789
Christiana	591_G_14	12666	16848
Delaware City	592_G_10	16500	15317
EDGE MOOR	593_B_3	9512	13668
EDGE MOOR	593_B_4	10116	9569
EDGE MOOR	593_B_5	10131	11070
Edge Moor	593_G_10	11829	18050
West Substation	597_G_1	11829	18146
MCKEE RUN	599_B_3	9903	12116
Lewes	600_G_7	9932	9967
Lewes	600_G_8	9932	9967
Seaford	601_G_1	11270	10404
Seaford	601_G_2	11270	10404
Seaford	601_G_3	10597	10379
Seaford	601_G_7	10000	10379
Seaford	601_G_6	9861	10445
Hay Road	7153_G_3	8500	15122
BIG SANDY	1353_B_BSU1	9627	10140
BIG SANDY	1353_B_BSU2	10720	9412
GLEN LYN	3776_B_51	12275	12427
GLEN LYN	3776_B_52	9484	12427
GLEN LYN	3776_B_6	9484	9434
CLINCH RIVER	3775_B_1	9638	9671
CLINCH RIVER	3775_B_2	9504	9784

Plant Name	Unique ID	Heat Rate from Phase I (Btu/KWh)	Heat Rate for Phase II (Btu/KWh)
CLINCH RIVER	3775_B_3	9445	9571
KANAWHA RIVER	3936_B_1	9781	9861
KANAWHA RIVER	3936_B_2	9866	9834
KAMMER	3947_B_1	9652	10389
KAMMER	3947_B_2	9609	10368
KAMMER	3947_B_3	9418	10362
MITCHELL	3948_B_1	9737	9876
MITCHELL	3948_B_2	9634	9793
PHILIP SPORN	3938_B_11	10366	10317
PHILIP SPORN	3938_B_21	10273	10000
PHILIP SPORN	3938_B_31	9646	9930
PHILIP SPORN	3938_B_41	9850	9779
PHILIP SPORN	3938_B_51	9594	9775
MOUNTAINEER	6264_B_1	10472	9264
JOHN E AMOS	3935_B_1	10477	9683
JOHN E AMOS	3935_B_2	10477	9802
JOHN E AMOS	3935_B_3	10477	9751
HARRISON	3944_B_1	10477	9918
HARRISON	3944_B_2	10477	9994
HARRISON	3944_B_3	10477	10069
RIVESVILLE	3945_B_7	11344	18031
RIVESVILLE	3945_B_8	11344	12648
FORT MARTIN	3943_B_1	9698	9584
FORT MARTIN	3943_B_2	9663	9470
WILLOW ISLAND	3946_B_1	12020	12684
WILLOW ISLAND	3946_B_2	10413	10953
PLEASANTS	6004_B_1	9858	10441
PLEASANTS	6004_B_2	9696	10162
ALBRIGHT	3942_B_1	10994	12516
ALBRIGHT	3942_B_2	12161	12516
ALBRIGHT	3942_B_3	10341	10788
Bridgeport Energy	55042_G_GEN1	8700	7251
ALLEN S KING	1915_B_1	9229	8879
ELK RIVER	2039_B_1	14500	14800
ELK RIVER	2039_B_2	14500	14800
ELK RIVER	2039_B_3	14500	14800
Blackhawk	4048_B_3	12154	15840
CAYUGA	1001_B_1	9979	10019
CAYUGA	1001_B_2	9915	9874
EAST BEND	6018_B_2	10472	9945
EDWARDSPORT	1004_B_7-1	13207	12727
EDWARDSPORT	1004_B_7-2	13207	12727
EDWARDSPORT	1004_B_8-1	13207	12754
R GALLAGHER	1008_B_1	11344	10328
R GALLAGHER	1008_B_2	11344	10139
R GALLAGHER	1008_B_3	10720	10186
R GALLAGHER	1008_B_4	10720	10328
GIBSON	6113_B_1	10477	9622
GIBSON	6113_B_2	10477	9785
GIBSON	6113_B_3	10477	9869

Plant Name	Unique ID	Heat Rate from Phase I (Btu/KWh)	Heat Rate for Phase II (Btu/KWh)
GIBSON	6113_B_4	10477	9910
GIBSON	6113_B_5	10472	10113
MIAMI FORT	2832_B_6	10013	9415
MIAMI FORT	2832_B_7	10436	9894
MIAMI FORT	2832_B_8	10477	9691
Noblesville	A313_G_A313	7056	7670
WABASH RIVER	1010_B_2	10816	10340
WABASH RIVER	1010_B_3	10540	10456
WABASH RIVER	1010_B_4	11118	10456
WABASH RIVER	1010_B_5	10204	10747
WABASH RIVER	1010_B_6	10362	10274
WALTER C BECKJORD	2830_B_1	11477	10260
WALTER C BECKJORD	2830_B_2	11164	9806
WALTER C BECKJORD	2830_B_3	10519	9598
WALTER C BECKJORD	2830_B_4	10862	9290
WALTER C BECKJORD	2830_B_5	10215	9634
WALTER C BECKJORD	2830_B_6	10514	9680
W H ZIMMER	6019_B_1	9579	9624
Cayuga	1001_G_4	13195	10160
Connersville	1002_G_1	13628	11814
Connersville	1002_G_2	13628	11814
Dicks Creek	2831_G_1	15139	14544
Walter C Beckjord	2830_G_GT4	11567	11563
Woodsdale	7158_G_GT1	16492	12545
Woodsdale	7158_G_GT2	16492	12545
Woodsdale	7158_G_GT3	16492	12545
Woodsdale	7158_G_GT4	16492	12545
Woodsdale	7158_G_GT5	16492	12545
Woodsdale	7158_G_GT6	16492	12545
Wabash River 1	1010_G_1A	11175	9000
MIAMI FORT	2832_B_5-1	12684	12206
MIAMI FORT	2832_B_5-2	12684	12206
Weston	4078_G_31	14265	13949
Weston	4078_G_32	14265	13949
West Marinette	4076_G_31	14147	15040
West Marinette	4076_G_32	14147	15040
West Marinette	4076_G_33	14147	14489
West Marinette	7799_G_34	14314	14314
SOUTH OAK CREEK	4041_B_5	9899	9857
SOUTH OAK CREEK	4041_B_6	10074	9907
SOUTH OAK CREEK	4041_B_7	9914	9821
SOUTH OAK CREEK	4041_B_8	10124	9604
South Oak Creek	4041_G_9	11502	13428
VALLEY	4042_B_1	10720	13428
VALLEY	4042_B_2	10720	13199
VALLEY	4042_B_3	10700	13199
VALLEY	4042_B_4	10720	14749
BLACKHAWK	4048_B_4	12154	22416
ROCK RIVER	4057_B_1	13431	14435

Plant Name	Unique ID	Heat Rate from Phase I (Btu/KWh)	Heat Rate for Phase II (Btu/KWh)
ROCK RIVER	4057_B_2	13262	12169
Rock River	4057_G_3	13782	12614
Rock River	4057_G_5	13782	14265
Rock River	4057_G_6	13782	14158
Sheepskin	4059_G_1	12466	19469
EDGEWATER	4050_B_3	11685	11281
EDGEWATER	4050_B_4	10165	9924
EDGEWATER	4050_B_5	10070	10128
Germantown	6253_G_1	12961	13774
Germantown	6253_G_2	12961	13924
Germantown	6253_G_3	12961	14876
Germantown	6253_G_4	12961	19184
Germantown	6253_G_5	13209	13148
DEVON	544_B_7	10676	10710
DEVON	544_B_8	10908	10710
NORWALK HARBOR	548_B_1	10212	9756
NORWALK HARBOR	548_B_2	10286	9706
MIDDLETOWN	562_B_2	9725	9698
MONTVILLE	546_B_5	11309	9870
MONTVILLE	546_B_6	11982	10937
MIDDLETOWN	562_B_4	12712	10830
MIDDLETOWN	562_B_3	10643	8995
BRIDGEPORT HARBOR	568_B_BHB2	11093	11664
BRIDGEPORT HARBOR	568_B_BHB3	9831	10116
Bridgeport Harbor	568_G_4	9406	14497
Branford	540_G_10	14250	12700
Bridgeport Resco	50883_G_GEN1	11000	9652
Cos Cob	542_G_10	11829	12700

Existing Units NOx Emission Rates by Mode

Exhibit C2.9: NOx Emission Rate Revisions by Unit in Vistas Phase II

Plant Name	Unique ID	Mode1 Rate (VISTAS I)	Mode2 Rate (VISTAS I)	Mode3 Rate (VISTAS I)	Mode4 Rate (VISTAS I)
CECIL LYNCH	167_B_2	0.27	0.27	0.26	0.26
CECIL LYNCH	167_B_3	0.18	0.18	0.17	0.17
Cecil Lynch	167_G_4	0.23	0.23	0.23	0.23
HAMILTON MOSES	168_B_1	0.18	0.18	0.17	0.17
HAMILTON MOSES	168_B_2	0.14	0.14	0.13	0.13
HARVEY COUCH	169_B_1	0.14	0.14	0.14	0.21
HARVEY COUCH	169_B_2	0.09	0.09	0.09	0.09
LAKE CATHERINE	170_B_1	0.34	0.34	0.30	0.30
LAKE CATHERINE	170_B_2	0.42	0.42	0.42	0.47
LAKE CATHERINE	170_B_3	0.17	0.17	0.17	0.17
LAKE CATHERINE	170_B_4	0.13	0.13	0.13	0.16
Mabelvale	171_G_3	0.23	0.23	0.23	0.23
ROBERT E RITCHIE	173_B_1	0.14	0.14	0.12	0.12
Robert E Ritchie	173_G_GT1	0.23	0.23	0.23	0.23
WHITE BLUFF	6009_B_1	0.34	0.34	0.15	0.15
WHITE BLUFF	6009_B_2	0.34	0.34	0.13	0.13
FLINT CREEK	6138_B_1	0.26	0.26	0.20	0.26
INDEPENDENCE	6641_B_1	0.21	0.21	0.21	0.22
INDEPENDENCE	6641_B_2	0.29	0.29	0.28	0.28
DUBUQUE	1046_B_6	0.83	0.83	0.83	0.93
DUBUQUE	1046_B_5	0.85	0.85	0.26	0.26
DUBUQUE	1046_B_1	0.64	0.64	0.24	0.24
LANSING	1047_B_1	0.33	0.33	0.32	0.32
LANSING	1047_B_2	0.35	0.35	0.32	0.32
LANSING	1047_B_3	0.72	0.72	0.35	0.35
LANSING	1047_B_4	0.39	0.39	0.20	0.20
MILTON L KAPP	1048_B_2	0.14	0.14	0.12	0.12
SIXTH STREET	1058_B_2	0.42	0.42	0.41	0.41
SIXTH STREET	1058_B_3	0.49	0.49	0.49	0.53
SIXTH STREET	1058_B_4	0.35	0.35	0.35	0.41
SIXTH STREET	1058_B_5	0.34	0.34	0.34	0.42
PRAIRIE CREEK	1073_B_3	0.51	0.51	0.22	0.22
PRAIRIE CREEK	1073_B_4	0.40	0.40	0.37	0.37
SUTHERLAND	1077_B_1	0.38	0.38	0.22	0.22
SUTHERLAND	1077_B_2	0.35	0.35	0.22	0.22
SUTHERLAND	1077_B_3	0.64	0.64	0.57	0.57
RIVERSIDE	1081_B_6	0.27	0.27	0.27	0.32
RIVERSIDE	1081_B_7	0.27	0.27	0.27	0.32
RIVERSIDE	1081_B_8	0.27	0.27	0.27	0.32
RIVERSIDE	1081_B_9	0.27	0.27	0.20	0.26
COUNCIL BLUFFS	1082_B_1	0.47	0.47	0.22	0.22
COUNCIL BLUFFS	1082_B_2	0.36	0.36	0.14	0.14
COUNCIL BLUFFS	1082_B_3	0.43	0.43	0.26	0.26
GEORGE NEAL NORTH	1091_B_1	0.92	0.92	0.49	0.49

Exhibit C2.9 (continued): Heat Rate Revisions by Unit in Vistas Phase II

Plant Name	Unique ID	Mode1 Rate (VISTAS I)	Mode2 Rate (VISTAS I)	Mode3 Rate (VISTAS I)	Mode4 Rate (VISTAS I)
GEORGE NEAL NORTH	1091_B_2	0.41	0.41	0.27	0.27
GEORGE NEAL NORTH	1091_B_3	0.20	0.20	0.20	0.20
BURLINGTON	1104_B_1	0.14	0.14	0.14	0.16
MUSCATINE	1167_B_7	0.44	0.44	0.44	0.44
MUSCATINE	1167_B_8	0.92	0.92	0.92	0.92
MUSCATINE	1167_B_9	0.30	0.30	0.13	0.40
EARL F WISDOM	1217_B_1	0.57	0.57	0.59	0.59
FAIR STATION	1218_B_2	0.41	0.41	0.46	0.46
OTTUMWA	6254_B_1	0.33	0.33	0.20	0.20
LOUISA	6664_B_101	0.20	0.20	0.20	0.20
Lime Creek	7155_G_1	0.35	0.35	0.35	0.35
Lime Creek	7155_G_2	0.32	0.32	0.32	0.32
GEORGE NEAL SOUTH	7343_B_4	0.34	0.34	0.21	0.21
Greater Des Moines	A207_G_A207	0.07	0.01	0.07	0.01
LA CYGNE	1241_B_1	0.98	0.98	0.98	0.98
LA CYGNE	1241_B_2	0.34	0.34	0.22	0.22
Hutchinson	1248_G_GT4	0.03	0.03	0.03	0.03
Baldwin	1262_G_6	0.11	0.11	0.11	0.11
Belleville	1263_G_1	0.11	0.11	0.11	0.11
Belleville	1263_G_2	0.11	0.11	0.11	0.11
Belleville	1263_G_3	0.11	0.11	0.11	0.11
Belleville	1263_G_4	0.11	0.11	0.11	0.11
Belleville	1263_G_5	0.11	0.11	0.11	0.11
Belleville	1263_G_6	0.11	0.11	0.11	0.11
Belleville	1263_G_7	0.11	0.11	0.11	0.11
Beloit	1264_G_5	0.11	0.11	0.11	0.11
Beloit	1264_G_1	0.11	0.11	0.11	0.11
Beloit	1264_G_2	0.11	0.11	0.11	0.11
Beloit	1264_G_3	0.11	0.11	0.11	0.11
Beloit	1264_G_4	0.11	0.11	0.11	0.11
Beloit	1264_G_6	0.11	0.11	0.11	0.11
Beloit	1264_G_7	0.11	0.11	0.11	0.11
Burlingame	1265_G_3	0.11	0.11	0.11	0.11
Burlingame	1265_G_4	0.11	0.11	0.11	0.11
Burlingame	1265_G_1	0.11	0.11	0.11	0.11
Burlingame	1265_G_5	0.11	0.11	0.11	0.11
Colby	1272_G_5	0.11	0.11	0.11	0.11
Colby	1272_G_4	0.11	0.11	0.11	0.11
Colby	1272_G_3	0.11	0.11	0.11	0.11
Colby	1272_G_8	0.11	0.11	0.11	0.11
Colby	1272_G_6	0.11	0.11	0.11	0.11
Colby	1272_G_7	0.11	0.11	0.11	0.11
Ellinwood	1274_G_3	0.11	0.11	0.11	0.11
Ellinwood	1274_G_4	0.11	0.11	0.11	0.11

Exhibit C2.9 (continued): Heat Rate Revisions by Unit in Vistas Phase II

Plant Name	Unique ID	Mode1 Rate (VISTAS I)	Mode2 Rate (VISTAS I)	Mode3 Rate (VISTAS I)	Mode4 Rate (VISTAS I)
Ellinwood	1274_G_2	0.11	0.11	0.11	0.11
Ellinwood	1274_G_1	0.11	0.11	0.11	0.11
Ellinwood	1274_G_5	0.11	0.11	0.11	0.11
Fredonia	1277_G_3	0.11	0.11	0.11	0.11
Fredonia	1277_G_4	0.11	0.11	0.11	0.11
Fredonia	1277_G_1	0.11	0.11	0.11	0.11
Fredonia	1277_G_2	0.11	0.11	0.11	0.11
Fredonia	1277_G_IC5	0.11	0.11	0.11	0.11
Fredonia	1277_G_IC6	0.11	0.11	0.11	0.11
Fredonia	1277_G_IC7	0.11	0.11	0.11	0.11
Fredonia	1277_G_IC8	0.11	0.11	0.11	0.11
Fredonia	1277_G_IC9	0.11	0.11	0.11	0.11
Holton	1287_G_6	0.11	0.11	0.11	0.11
Holton	1287_G_7	0.11	0.11	0.11	0.11
Holton	1287_G_8	0.11	0.11	0.11	0.11
Holton	1287_G_10	0.11	0.11	0.11	0.11
Holton	1287_G_9	0.11	0.11	0.11	0.11
Holton	1287_G_11	0.11	0.11	0.11	0.11
Hugoton 1	1289_G_6	0.11	0.11	0.11	0.11
Jetmore	1292_G_3	0.11	0.11	0.11	0.11
Jetmore	1292_G_2	0.11	0.11	0.11	0.11
Jetmore	1292_G_1	0.11	0.11	0.11	0.11
Jetmore	1292_G_4	0.11	0.11	0.11	0.11
Jetmore	1292_G_5	0.11	0.11	0.11	0.11
La Crosse	1297_G_1	0.11	0.11	0.11	0.11
La Crosse	1297_G_2	0.11	0.11	0.11	0.11
La Crosse	1297_G_5	0.11	0.11	0.11	0.11
La Crosse	1297_G_6	0.11	0.11	0.11	0.11
Meade	1306_G_2	0.11	0.11	0.11	0.11
Meade	1306_G_3	0.11	0.11	0.11	0.11
Meade	1306_G_4	0.11	0.11	0.11	0.11
Meade	1306_G_5	0.11	0.11	0.11	0.11
Meade	1306_G_6	0.11	0.11	0.11	0.11
Mulvane	1308_G_4	0.11	0.11	0.11	0.11
Mulvane	1308_G_5	0.11	0.11	0.11	0.11
Mulvane	1308_G_6	0.11	0.11	0.11	0.11
Neodesha	1309_G_5	0.11	0.11	0.11	0.11
Neodesha	1309_G_6	0.11	0.11	0.11	0.11
Neodesha	1309_G_7	0.11	0.11	0.11	0.11
Neodesha	1309_G_8	0.11	0.11	0.11	0.11
Oakely	1311_G_3	0.11	0.11	0.11	0.11
Oakely	1311_G_4	0.11	0.11	0.11	0.11
Oakely	1311_G_1	0.11	0.11	0.11	0.11
Oakely	1311_G_5	0.11	0.11	0.11	0.11

Exhibit C2.9 (continued): Heat Rate Revisions by Unit in Vistas Phase II

Plant Name	Unique ID	Mode1 Rate (VISTAS I)	Mode2 Rate (VISTAS I)	Mode3 Rate (VISTAS I)	Mode4 Rate (VISTAS I)
Oakely	1311_G_6	0.11	0.11	0.11	0.11
Osage City	1313_G_1	0.11	0.11	0.11	0.11
Osage City	1313_G_2	0.11	0.11	0.11	0.11
Osage City	1313_G_4	0.11	0.11	0.11	0.11
Osage City	1313_G_5	0.11	0.11	0.11	0.11
Osage City	1313_G_IC6	0.11	0.11	0.11	0.11
Osage City	1313_G_7	0.11	0.11	0.11	0.11
Osage City	1313_G_10	0.11	0.11	0.11	0.11
Osawatomie	1314_G_4	0.11	0.11	0.11	0.11
Osawatomie	1314_G_2	0.11	0.11	0.11	0.11
Osawatomie	1314_G_5	0.11	0.11	0.11	0.11
Osborne	1315_G_3	0.11	0.11	0.11	0.11
Osborne	1315_G_2	0.11	0.11	0.11	0.11
Osborne	1315_G_1	0.11	0.11	0.11	0.11
Pratt	1317_G_IC1	0.11	0.11	0.11	0.11
Sabetha	1320_G_3	0.11	0.11	0.11	0.11
Sabetha	1320_G_4	0.11	0.11	0.11	0.11
Sabetha	1320_G_2	0.11	0.11	0.11	0.11
Sabetha	1320_G_5	0.11	0.11	0.11	0.11
Sabetha	1320_G_6	0.11	0.11	0.11	0.11
Sabetha	1320_G_7	0.11	0.11	0.11	0.11
Sabetha	1320_G_8	0.11	0.11	0.11	0.11
Sabetha	1320_G_IC9	0.11	0.11	0.11	0.11
Sabetha	1320_G_IC10	0.11	0.11	0.11	0.11
Sabetha	1320_G_11	0.11	0.11	0.11	0.11
St John	1322_G_3	0.11	0.11	0.11	0.11
St John	1322_G_4	0.11	0.11	0.11	0.11
St John	1322_G_5	0.11	0.11	0.11	0.11
Stafford	1325_G_1	0.11	0.11	0.11	0.11
Stafford	1325_G_2	0.11	0.11	0.11	0.11
Stafford	1325_G_4	0.11	0.11	0.11	0.11
Stafford	1325_G_5	0.11	0.11	0.11	0.11
Sterling	1326_G_2	0.11	0.11	0.11	0.11
Sterling	1326_G_4	0.11	0.11	0.11	0.11
Sterling	1326_G_1	0.11	0.11	0.11	0.11
Sterling	1326_G_3	0.11	0.11	0.11	0.11
Washington	1329_G_5	0.11	0.11	0.11	0.11
Washington	1329_G_2	0.11	0.11	0.11	0.11
Washington	1329_G_1	0.11	0.11	0.11	0.11
Washington	1329_G_6	0.11	0.11	0.11	0.11
Washington	1329_G_3	0.11	0.11	0.11	0.11
Washington	1329_G_IC4	0.11	0.11	0.11	0.11
JEFFREY ENERGY CENTE	6068_B_3	0.15	0.15	0.15	0.15
Johnson	6579_G_5	0.11	0.11	0.11	0.11

Exhibit C2.9 (continued): Heat Rate Revisions by Unit in Vistas Phase II

Plant Name	Unique ID	Mode1 Rate (VISTAS I)	Mode2 Rate (VISTAS I)	Mode3 Rate (VISTAS I)	Mode4 Rate (VISTAS I)
Johnson	6579_G_4	0.11	0.11	0.11	0.11
Johnson	6579_G_1	0.11	0.11	0.11	0.11
Johnson	6579_G_2	0.11	0.11	0.11	0.11
Johnson	6579_G_7	0.11	0.11	0.11	0.11
Johnson	6579_G_IC6	0.11	0.11	0.11	0.11
Hugoton 2	7011_G_7	0.11	0.11	0.11	0.11
Hugoton 2	7011_G_8	0.11	0.11	0.11	0.11
Hugoton 2	7011_G_10	0.11	0.11	0.11	0.11
Hugoton 2	7011_G_9A	0.11	0.11	0.11	0.11
Hugoton 2	7011_G_11	0.11	0.11	0.11	0.11
Hugoton 2	7011_G_12	0.11	0.11	0.11	0.11
Chanute 3	7018_G_9	0.11	0.11	0.11	0.11
Chanute 3	7018_G_10	0.11	0.11	0.11	0.11
Chanute 3	7018_G_11	0.11	0.11	0.11	0.11
Gardner	7281_G_CT1	0.11	0.11	0.11	0.11
Gardner	7281_G_CT2	0.11	0.11	0.11	0.11
DOLET HILLS	51_B_1	0.46	0.46	0.20	0.20
LOUISIANA 2	1392_B_11	0.16	0.16	0.16	0.18
R S NELSON	1393_B_4	0.11	0.11	0.11	0.13
WILLOW GLEN	1394_B_4	0.22	0.22	0.13	0.13
WILLOW GLEN	1394_B_5	0.10	0.10	0.10	0.14
TECHE	1400_B_1	0.27	0.27	0.27	0.27
TECHE	1400_B_2	0.22	0.22	0.22	0.22
TECHE	1400_B_3	0.19	0.19	0.19	0.19
LITTLE GYPSY	1402_B_1	0.17	0.17	0.17	0.20
LITTLE GYPSY	1402_B_2	0.10	0.10	0.10	0.11
LITTLE GYPSY	1402_B_3	0.22	0.22	0.22	0.24
NINEMILE POINT	1403_B_2	0.14	0.14	0.12	0.12
NINEMILE POINT	1403_B_5	0.28	0.28	0.28	0.33
STERLINGTON	1404_B_10	0.19	0.19	0.19	0.27
Sterlington	1404_G_7A	0.42	0.42	0.42	0.42
Sterlington	1404_G_7B	0.42	0.42	0.42	0.42
A B PATERSON	1407_B_3	0.19	0.19	0.17	0.17
A B Paterson	1407_G_5	0.23	0.23	0.23	0.23
MICHOUD	1409_B_1	0.11	0.11	0.10	0.10
MICHOUD	1409_B_3	0.24	0.24	0.24	0.38
ARSENAL HILL	1416_B_5A	0.14	0.14	0.14	0.14
LIEBERMAN	1417_B_1	0.15	0.15	0.15	0.15
LIEBERMAN	1417_B_2	0.13	0.13	0.13	0.13
LIEBERMAN	1417_B_3	0.17	0.17	0.17	0.17
LIEBERMAN	1417_B_4	0.15	0.15	0.15	0.15
MONROE	1448_B_11	0.08	0.08	0.08	0.18
MONROE	1448_B_12	0.10	0.10	0.10	0.18
RODEMACHER	6190_B_1	0.18	0.18	0.18	0.18

Exhibit C2.9 (continued): Heat Rate Revisions by Unit in Vistas Phase II

Plant Name	Unique ID	Mode1 Rate (VISTAS I)	Mode2 Rate (VISTAS I)	Mode3 Rate (VISTAS I)	Mode4 Rate (VISTAS I)
RODEMACHER	6190_B_2	0.40	0.40	0.20	0.20
WATERFORD 1 & 2	8056_B_1	0.18	0.18	0.18	0.20
WATERFORD 1 & 2	8056_B_2	0.18	0.18	0.17	0.17
Georgia Gulf Corporation Plaquemine Divi	55051_G_X773	0.22	0.22	0.22	0.22
Georgia Gulf Corporation P. Divi	55051_G_X774	0.22	0.22	0.22	0.22
Georgia Gulf Corporation P. Divi	55051_G_X775	0.22	0.22	0.22	0.22
NRG Sterlington Power LLC	55099_G_01	0.22	0.22	0.22	0.22
NRG Sterlington Power LLC	55099_G_02	0.22	0.22	0.22	0.22
NRG Sterlington Power LLC	55099_G_09	0.22	0.22	0.22	0.22
NRG Sterlington Power LLC	55099_G_03	0.22	0.22	0.22	0.22
NRG Sterlington Power LLC	55099_G_04	0.22	0.22	0.22	0.22
NRG Sterlington Power LLC	55099_G_06	0.22	0.22	0.22	0.22
NRG Sterlington Power LLC	55099_G_07	0.22	0.22	0.22	0.22
NRG Sterlington Power LLC	55099_G_08	0.22	0.22	0.22	0.22
Perryville	A328_G_A328	0.02	0.02	0.02	0.02
ASBURY	2076_B_1	0.72	0.72	0.72	0.77
Hawthorn	2079_G_7	0.03	0.03	0.03	0.03
Hawthorn	2079_G_8	0.02	0.02	0.02	0.02
MONTROSE	2080_B_1	0.29	0.29	0.28	0.28
MONTROSE	2080_B_2	0.33	0.33	0.33	0.35
MONTROSE	2080_B_3	0.33	0.33	0.33	0.35
MERAMEC	2104_B_1	0.20	0.20	0.15	0.15
MERAMEC	2104_B_2	0.17	0.17	0.15	0.15
MERAMEC	2104_B_3	0.39	0.39	0.23	0.23
MERAMEC	2104_B_4	0.18	0.18	0.18	0.18
SIOUX	2107_B_1	0.36	0.23	0.36	0.23
SIOUX	2107_B_2	0.31	0.20	0.31	0.20
James River	2161_G_GT1	0.15	0.15	0.15	0.15
James River	2161_G_GT2	0.15	0.15	0.15	0.15
THOMAS HILL	2168_B_MB1	0.56	0.56	0.51	0.51
THOMAS HILL	2168_B_MB2	0.56	0.56	0.51	0.51
CHAMOIS	2169_B_1	0.98	0.98	0.49	0.98
IATAN	6065_B_1	0.35	0.35	0.33	0.33
Southwest	6195_G_GT1	0.15	0.15	0.15	0.15
Empire Energy Center	6223_G_1	0.12	0.12	0.12	0.12
Empire Energy Center	6223_G_2	0.14	0.14	0.14	0.14
Empire Energy Center	A184_G_A184	0.10	0.10	0.10	0.10
Empire Energy Center	A185_G_A185	0.10	0.10	0.10	0.10
Stateline	7296_G_1	0.07	0.07	0.07	0.07
Stateline	7296_G_2	0.02	0.02	0.02	0.02
State Line Combined Cycle	7296_G_2-1	0.02	0.02	0.02	0.02
Columbia	55447_G_CT01	0.04	0.04	0.04	0.04
Columbia	55447_G_CT02	0.06	0.06	0.06	0.06
Columbia	55447_G_CT03	0.07	0.07	0.07	0.07

Exhibit C2.9 (continued): Heat Rate Revisions by Unit in Vistas Phase II

Plant Name	Unique ID	Mode1 Rate (VISTAS I)	Mode2 Rate (VISTAS I)	Mode3 Rate (VISTAS I)	Mode4 Rate (VISTAS I)
Columbia	55447_G_CT04	0.06	0.06	0.06	0.06
NORTH OMAHA	2291_B_1	0.31	0.31	0.15	0.15
NORTH OMAHA	2291_B_2	0.31	0.31	0.15	0.15
NORTH OMAHA	2291_B_3	0.31	0.31	0.15	0.15
NORTH OMAHA	2291_B_4	0.33	0.33	0.16	0.16
NORTH OMAHA	2291_B_5	0.31	0.31	0.16	0.16
Sarpy County	2292_G_3	0.07	0.07	0.07	0.07
Sarpy County	2292_G_BSD	0.06	0.06	0.06	0.06
Sarpy County	2292_G_4	0.09	0.09	0.09	0.09
Sarpy County	2292_G_5	0.08	0.08	0.08	0.08
NEBRASKA CITY	6096_B_1	0.41	0.41	0.21	0.21
Cass County	A138_G_A138	0.06	0.06	0.06	0.06
GRDA	165_B_1	0.38	0.38	0.38	0.38
GRDA	165_B_2	0.35	0.35	0.35	0.35
NORTHEASTERN	2963_B_3302	0.46	0.46	0.46	0.46
NORTHEASTERN	2963_B_3313	0.39	0.39	0.26	0.39
NORTHEASTERN	2963_B_3314	0.39	0.39	0.26	0.39
Northeastern	2963_B_3301A	0.03	0.03	0.03	0.03
SOUTHWESTERN	2964_B_801N	0.17	0.17	0.17	0.17
SOUTHWESTERN	2964_B_801S	0.14	0.14	0.14	0.14
SOUTHWESTERN	2964_B_8002	0.23	0.23	0.23	0.23
SOUTHWESTERN	2964_B_8003	0.31	0.31	0.31	0.31
TULSA	2965_B_1402	0.27	0.27	0.27	0.27
TULSA	2965_B_1403	0.27	0.27	0.27	0.27
TULSA	2965_B_1404	0.29	0.29	0.29	0.29
RIVERSIDE	4940_B_1501	0.25	0.25	0.25	0.25
RIVERSIDE	4940_B_1502	0.30	0.30	0.30	0.30
COMANCHE	8059_B_7251	0.45	0.45	0.45	0.45
COMANCHE	8059_B_7252	0.47	0.47	0.47	0.47
OKLAUNION	127_B_1	0.33	0.33	0.24	0.33
LIMESTONE	298_B_LIM1	0.19	0.19	0.17	0.17
LIMESTONE	298_B_LIM2	0.19	0.19	0.17	0.17
LEWIS CREEK	3457_B_1	0.16	0.03	0.16	0.03
LEWIS CREEK	3457_B_2	0.16	0.04	0.16	0.04
SABINE	3459_B_1	0.17	0.17	0.17	0.17
SABINE	3459_B_2	0.16	0.16	0.16	0.16
SABINE	3459_B_3	0.19	0.19	0.19	0.19
SABINE	3459_B_4	0.26	0.26	0.26	0.26
SABINE	3459_B_5	0.11	0.11	0.11	0.11
CEDAR BAYOU	3460_B_CBY1	0.11	0.03	0.11	0.03
CEDAR BAYOU	3460_B_CBY2	0.10	0.03	0.10	0.03
GREENS BAYOU	3464_B_GBY5	0.06	0.06	0.06	0.06
Greens Bayou	3464_G_73	0.20	0.20	0.20	0.20
Greens Bayou	3464_G_74	0.20	0.20	0.20	0.20

Exhibit C2.9 (continued): Heat Rate Revisions by Unit in Vistas Phase II

Plant Name	Unique ID	Mode1 Rate (VISTAS I)	Mode2 Rate (VISTAS I)	Mode3 Rate (VISTAS I)	Mode4 Rate (VISTAS I)
Greens Bayou	3464_G_81	0.20	0.20	0.20	0.20
Greens Bayou	3464_G_82	0.20	0.20	0.20	0.20
Greens Bayou	3464_G_83	0.20	0.20	0.20	0.20
Greens Bayou	3464_G_84	0.20	0.20	0.20	0.20
Hiram Clarke	3465_G_5	0.31	0.31	0.31	0.31
Hiram Clarke	3465_G_6	0.31	0.31	0.31	0.31
Hiram Clarke	3465_G_GT1	0.31	0.31	0.31	0.31
Hiram Clarke	3465_G_GT2	0.31	0.31	0.31	0.31
Hiram Clarke	3465_G_GT3	0.31	0.31	0.31	0.31
Hiram Clarke	3465_G_GT4	0.31	0.31	0.31	0.31
SAM BERTRON	3468_B_SRB2	0.13	0.13	0.13	0.13
SAM BERTRON	3468_B_SRB1	0.18	0.18	0.18	0.18
SAM BERTRON	3468_B_SRB3	0.14	0.14	0.14	0.14
SAM BERTRON	3468_B_SRB4	0.10	0.10	0.10	0.10
Sam Bertron	3468_G_GT1	0.20	0.20	0.20	0.20
Sam Bertron	3468_G_GT2	0.24	0.24	0.24	0.24
T H Wharton	3469_G_G1	0.24	0.24	0.24	0.24
T H Wharton	3469_G_31	0.08	0.08	0.08	0.08
T H Wharton	3469_G_32	0.07	0.07	0.07	0.07
T H Wharton	3469_G_33	0.07	0.07	0.07	0.07
T H Wharton	3469_G_34	0.08	0.08	0.08	0.08
T H Wharton	3469_G_41	0.07	0.07	0.07	0.07
T H Wharton	3469_G_42	0.07	0.07	0.07	0.07
T H Wharton	3469_G_43	0.07	0.07	0.07	0.07
T H Wharton	3469_G_44	0.05	0.05	0.05	0.05
T H Wharton	3469_G_51	0.02	0.02	0.02	0.02
T H Wharton	3469_G_52	0.02	0.02	0.02	0.02
T H Wharton	3469_G_53	0.02	0.02	0.02	0.02
T H Wharton	3469_G_54	0.02	0.02	0.02	0.02
T H Wharton	3469_G_55	0.02	0.02	0.02	0.02
T H Wharton	3469_G_56	0.02	0.02	0.02	0.02
W A PARISH	3470_B_WAP1	0.13	0.13	0.13	0.13
W A PARISH	3470_B_WAP2	0.09	0.09	0.09	0.09
W A PARISH	3470_B_WAP3	0.15	0.15	0.15	0.15
W A Parish	3470_G_GT1	0.24	0.24	0.24	0.24
W A PARISH	3470_B_WAP4	0.10	0.10	0.10	0.10
W A PARISH	3470_B_WAP5	0.03	0.03	0.03	0.03
W A PARISH	3470_B_WAP6	0.03	0.03	0.03	0.03
W A PARISH	3470_B_WAP7	0.05	0.05	0.05	0.05
W A PARISH	3470_B_WAP8	0.04	0.04	0.04	0.04
KNOX LEE	3476_B_4	0.40	0.40	0.40	0.40
KNOX LEE	3476_B_5	0.14	0.14	0.14	0.14
WILKES	3478_B_1	0.14	0.14	0.14	0.14
WILKES	3478_B_2	0.13	0.13	0.13	0.13

Exhibit C2.9 (continued): Heat Rate Revisions by Unit in Vistas Phase II

Plant Name	Unique ID	Mode1 Rate (VISTAS I)	Mode2 Rate (VISTAS I)	Mode3 Rate (VISTAS I)	Mode4 Rate (VISTAS I)
WILKES	3478_B_3	0.11	0.11	0.11	0.11
San Angelo	3527_G_1	0.20	0.20	0.20	0.20
SAN ANGELO	3527_B_2	0.20	0.20	0.20	0.20
SIM GIDEON	3601_B_1	0.13	0.13	0.13	0.13
SIM GIDEON	3601_B_2	0.08	0.08	0.08	0.08
SIM GIDEON	3601_B_3	0.09	0.09	0.09	0.09
T C FERGUSON	4937_B_1	0.18	0.18	0.18	0.18
FORT PHANTOM	4938_B_1	0.25	0.25	0.25	0.25
FORT PHANTOM	4938_B_2	0.09	0.09	0.09	0.09
WELSH	6139_B_1	0.17	0.17	0.17	0.17
WELSH	6139_B_2	0.34	0.34	0.34	0.34
WELSH	6139_B_3	0.20	0.20	0.20	0.20
SAM SEYMOUR	6179_B_1	0.10	0.10	0.10	0.17
SAM SEYMOUR	6179_B_2	0.15	0.15	0.12	0.17
SAM SEYMOUR	6179_B_3	0.32	0.32	0.17	0.17
PIRKEY	7902_B_1	0.18	0.18	0.18	0.18
Sweeny Cogeneration Facility	55015_G_GEN1	0.07	0.01	0.07	0.01
Sweeny Cogeneration Facility	55015_G_GEN2	0.07	0.01	0.07	0.01
Sweeny Cogeneration Facility	55015_G_GEN3	0.07	0.07	0.07	0.07
Sweeny Cogeneration Facility	55015_G_GEN4	0.07	0.07	0.07	0.07
Lost Pines I	55154_G_CTA	0.02	0.02	0.02	0.02
Lost Pines I	55154_G_CTB	0.02	0.02	0.02	0.02
Lost Pines I	55154_G_ST	0.00	0.00	0.00	0.00
PRESQUE ISLE	1769_B_1	0.63	0.63	0.32	0.32
PRESQUE ISLE	1769_B_2	0.63	0.63	0.27	0.27
PRESQUE ISLE	1769_B_3	0.37	0.37	0.27	0.27
PRESQUE ISLE	1769_B_4	0.37	0.37	0.27	0.27
PRESQUE ISLE	1769_B_5	0.37	0.37	0.29	0.29
PRESQUE ISLE	1769_B_6	0.39	0.39	0.31	0.31
PRESQUE ISLE	1769_B_7	0.42	0.42	0.32	0.32
PRESQUE ISLE	1769_B_8	0.38	0.38	0.29	0.29
PRESQUE ISLE	1769_B_9	0.40	0.40	0.31	0.31
ST CLAIR	1743_B_1	0.25	0.25	0.25	0.25
COLUMBIA	8023_B_1	0.13	0.13	0.13	0.13
COLUMBIA	8023_B_2	0.13	0.13	0.13	0.13
NELSON DEWEY	4054_B_1	0.30	0.30	0.30	0.30
NELSON DEWEY	4054_B_2	0.30	0.30	0.30	0.30
PLEASANT PRAIRIE	6170_B_2	0.07	0.07	0.07	0.07
EDGEWATER	4050_B_3	0.30	0.30	0.30	0.30
EDGEWATER	4050_B_4	0.26	0.26	0.26	0.26
EDGEWATER	4050_B_5	0.13	0.13	0.13	0.13
Elgin Energy Center	A191_G_A191	0.07	0.07	0.07	0.07
Elgin Energy Center	A192_G_A192	0.07	0.07	0.07	0.07
Elgin Energy Center	A193_G_A193	0.08	0.08	0.08	0.08

Exhibit C2.9 (continued): Heat Rate Revisions by Unit in Vistas Phase II

Plant Name	Unique ID	Mode1 Rate (VISTAS I)	Mode2 Rate (VISTAS I)	Mode3 Rate (VISTAS I)	Mode4 Rate (VISTAS I)
Elgin Energy Center	A194_G_A194	0.07	0.07	0.07	0.07
Grand Tower	862_G_1-3	0.08	0.08	0.08	0.08
HUTSONVILLE	863_B_05	0.37	0.37	0.24	0.24
HUTSONVILLE	863_B_06	0.36	0.36	0.24	0.24
Kinmundy	55204_G_1	0.11	0.11	0.11	0.11
Kinmundy	55204_G_2	0.08	0.08	0.08	0.08
MEREDOSIA	864_B_05	0.29	0.29	0.29	0.29
MEREDOSIA	864_B_06	0.09	0.09	0.09	0.09
Pinckneyville	55202_G_5	0.10	0.10	0.10	0.10
Pinckneyville	55202_G_6	0.11	0.11	0.11	0.11
Pinckneyville	55202_G_7	0.10	0.10	0.10	0.10
Pinckneyville	55202_G_8	0.10	0.10	0.10	0.10
Pinckneyville	7980_G_1	0.06	0.06	0.06	0.06
Pinckneyville	7980_G_2	0.06	0.06	0.06	0.06
Pinckneyville	7980_G_3	0.06	0.06	0.06	0.06
Pinckneyville	7980_G_4	0.05	0.05	0.05	0.05
Venice	913_G_GT1	0.10	0.10	0.10	0.10
Venice	A913_G_A422	0.09	0.09	0.09	0.09
HARBOR BEACH	1731_B_1	0.50	0.50	0.32	0.50
ST CLAIR	1743_B_3	0.25	0.25	0.25	0.25
ST CLAIR	1743_B_4	0.25	0.25	0.25	0.25
CLIFTY CREEK	983_B_1	0.89	0.09	0.89	0.09
CLIFTY CREEK	983_B_2	0.89	0.09	0.89	0.09
CLIFTY CREEK	983_B_3	0.89	0.09	0.89	0.09
CLIFTY CREEK	983_B_4	0.95	0.09	0.95	0.09
CLIFTY CREEK	983_B_5	0.95	0.09	0.95	0.09
CLIFTY CREEK	983_B_6	0.95	0.95	0.95	0.95
TANNERS CREEK	988_B_U1	0.37	0.37	0.37	0.37
TANNERS CREEK	988_B_U2	0.37	0.37	0.37	0.37
TANNERS CREEK	988_B_U3	0.37	0.37	0.37	0.37
TANNERS CREEK	988_B_U4	0.38	0.38	0.38	0.38
ROCKPORT	6166_B_MB1	0.21	0.21	0.21	0.21
ROCKPORT	6166_B_MB2	0.21	0.21	0.21	0.21
CONESVILLE	2840_B_1	0.89	0.89	0.89	0.89
CONESVILLE	2840_B_2	0.89	0.89	0.89	0.89
CONESVILLE	2840_B_3	0.55	0.55	0.55	0.55
CONESVILLE	2840_B_4	0.58	0.58	0.58	0.58
CONESVILLE	2840_B_5	0.53	0.53	0.53	0.53
CONESVILLE	2840_B_6	0.53	0.53	0.53	0.53
GEN J M GAVIN	8102_B_1	0.65	0.07	0.65	0.07
GEN J M GAVIN	8102_B_2	0.68	0.06	0.68	0.06
CARDINAL	2828_B_1	0.54	0.07	0.54	0.07
CARDINAL	2828_B_2	0.50	0.06	0.50	0.06
CARDINAL	2828_B_3	0.60	0.05	0.60	0.05

Exhibit C2.9 (continued): Heat Rate Revisions by Unit in Vistas Phase II

Plant Name	Unique ID	Mode1 Rate (VISTAS I)	Mode2 Rate (VISTAS I)	Mode3 Rate (VISTAS I)	Mode4 Rate (VISTAS I)
PICWAY	2843_B_9	0.52	0.52	0.52	0.52
MUSKINGUM RIVER	2872_B_1	0.74	0.74	0.74	0.74
MUSKINGUM RIVER	2872_B_2	0.74	0.74	0.74	0.74
MUSKINGUM RIVER	2872_B_3	0.74	0.74	0.74	0.74
MUSKINGUM RIVER	2872_B_4	0.74	0.74	0.74	0.74
MUSKINGUM RIVER	2872_B_5	0.54	0.06	0.54	0.44
KYGER CREEK	2876_B_1	0.80	0.10	0.80	0.10
KYGER CREEK	2876_B_2	0.80	0.10	0.80	0.10
KYGER CREEK	2876_B_3	0.80	0.10	0.80	0.10
KYGER CREEK	2876_B_4	0.80	0.10	0.80	0.10
KYGER CREEK	2876_B_5	0.80	0.10	0.80	0.10
MINNESOTA VALLEY	1918_B_4	0.36	0.36	0.19	0.19
BLACK DOG	1904_B_3	0.79	0.79	0.23	0.23
BLACK DOG	1904_B_4	0.79	0.79	0.23	0.23
Black Dog	A461_G_A461	0.03	0.03	0.03	0.03
RIVERSIDE	1927_B_6	0.76	0.76	0.23	0.23
RIVERSIDE	1927_B_7	0.76	0.76	0.23	0.23
RIVERSIDE	1927_B_8	0.95	0.95	0.49	0.49
Lakefield Junction	7925_G_1	0.05	0.05	0.05	0.05
Lakefield Junction	7925_G_2	0.05	0.05	0.05	0.05
Lakefield Junction	7925_G_3	0.04	0.04	0.04	0.04
Lakefield Junction	7925_G_4	0.04	0.04	0.04	0.04
Lakefield Junction	7925_G_5	0.04	0.04	0.04	0.04
Lakefield Junction	7925_G_6	0.04	0.04	0.04	0.04
Fergus Control Ctr	7505_G_1	3.40	3.40	3.40	3.40
HIGH BRIDGE	1912_B_5	0.60	0.60	0.23	0.23
HIGH BRIDGE	1912_B_6	0.60	0.60	0.23	0.23
SHERBURNE COUNTY	6090_B_1	0.22	0.22	0.16	0.22
SHERBURNE COUNTY	6090_B_2	0.22	0.22	0.22	0.22
SHERBURNE COUNTY	6090_B_3	0.35	0.35	0.23	0.23
ALLEN S KING	1915_B_1	0.70	0.07	0.49	0.49
JOLIET 9	874_B_5	0.52	0.52	0.34	0.34
POWERTON	879_B_51	0.61	0.61	0.56	0.56
POWERTON	879_B_52	0.61	0.61	0.56	0.56
POWERTON	879_B_61	0.61	0.61	0.56	0.56
POWERTON	879_B_62	0.61	0.61	0.56	0.56
WAUKEGAN	883_B_17	0.64	0.64	0.61	0.61
De Pere Energy Center	55029_G_CT01	0.08	0.08	0.08	0.08
Oneida Casino	7602_G_1	3.20	3.20	3.20	3.20
Oneida Casino	7602_G_2	3.20	3.20	3.20	3.20
PULLIAM	4072_B_3	0.76	0.76	0.21	0.21
PULLIAM	4072_B_4	0.76	0.76	0.21	0.21
PULLIAM	4072_B_5	0.81	0.81	0.23	0.23
PULLIAM	4072_B_6	0.81	0.81	0.23	0.23

Exhibit C2.9 (continued): Heat Rate Revisions by Unit in Vistas Phase II

Plant Name	Unique ID	Mode1 Rate (VISTAS I)	Mode2 Rate (VISTAS I)	Mode3Rate (VISTAS I)	Mode4 Rate (VISTAS I)
PULLIAM	4072_B_7	0.34	0.34	0.22	0.22
PULLIAM	4072_B_8	0.29	0.29	0.22	0.22
Pulliam	A338_G_A338	0.04	0.04	0.04	0.04
BLOUNT STREET	3992_B_7	0.52	0.52	0.32	0.32
BLOUNT STREET	3992_B_8	0.39	0.39	0.32	0.32
BLOUNT STREET	3992_B_9	0.44	0.44	0.34	0.34
South Fond Du Lac	7203_G_CT1	0.06	0.06	0.06	0.06
South Fond Du Lac	7203_G_CT2	0.08	0.08	0.08	0.08
South Fond Du Lac	7203_G_CT3	0.06	0.06	0.06	0.06
South Fond Du Lac	7203_G_CT4	0.07	0.07	0.07	0.07
Concord	7159_G_1	0.08	0.08	0.08	0.08
Concord	7159_G_2	0.10	0.10	0.10	0.10
Concord	7159_G_3	0.11	0.11	0.11	0.11
Concord	7159_G_4	0.11	0.11	0.11	0.11
Paris	7270_G_1	0.09	0.09	0.09	0.09
Paris	7270_G_2	0.07	0.07	0.07	0.07
Paris	7270_G_3	0.09	0.09	0.09	0.09
Paris	7270_G_4	0.08	0.08	0.08	0.08
WESTON	4078_B_1	0.73	0.73	0.20	0.20
WESTON	4078_B_2	0.40	0.40	0.18	0.18
WESTON	4078_B_3	0.25	0.25	0.16	0.16
West Marinette	7799_G_34	0.03	0.03	0.03	0.03
SOUTH OAK CREEK	4041_B_7	0.14	0.14	0.14	0.14
SOUTH OAK CREEK	4041_B_8	0.14	0.14	0.12	0.14
VALLEY	4042_B_1	0.36	0.36	0.29	0.29
VALLEY	4042_B_2	0.36	0.36	0.29	0.29
VALLEY	4042_B_3	0.38	0.38	0.30	0.30
VALLEY	4042_B_4	0.38	0.38	0.30	0.30
Combined Locks Energy Center	A156_G_A156	0.01	0.01	0.01	0.01
BLACKHAWK	4048_B_3	0.28	0.28	0.21	0.21
BLACKHAWK	4048_B_4	0.28	0.28	0.21	0.21
ROCK RIVER	4057_B_1	0.30	0.30	0.30	0.30
ROCK RIVER	4057_B_2	0.31	0.31	0.23	0.23
Rock River	4057_G_3	0.32	0.32	0.32	0.32
Rock River	4057_G_4	0.32	0.32	0.32	0.32
Rock River	4057_G_5	0.43	0.43	0.43	0.43
Rock River	4057_G_6	0.43	0.43	0.43	0.43
Sheepskin	4059_G_1	0.32	0.32	0.32	0.32
Eagle River	4062_G_1	3.20	3.20	3.20	3.20
Eagle River	4062_G_2	3.20	3.20	3.20	3.20
Germantown	6253_G_1	0.70	0.70	0.70	0.70
Germantown	6253_G_2	0.70	0.70	0.70	0.70
Germantown	6253_G_3	0.70	0.70	0.70	0.70
Germantown	6253_G_4	0.70	0.70	0.70	0.70

Exhibit C2.9 (continued): Heat Rate Revisions by Unit in Vistas Phase II

Plant Name	Unique ID	Mode1 Rate (VISTAS I)	Mode2 Rate (VISTAS I)	Mode3 Rate (VISTAS I)	Mode4 Rate (VISTAS I)
Germantown	6253_G_5	0.03	0.03	0.03	0.03
Mirant Neenah Generation Facility	55135_G_CT01	0.03	0.03	0.03	0.03
Mirant Neenah Generation Facility	55135_G_CT02	0.03	0.03	0.03	0.03
Ascutney	3708_G_GT4	0.89	0.89	0.89	0.89
Rutland	3723_G_GT5	0.89	0.89	0.89	0.89
St Albans	3726_G_IC1	3.20	3.20	3.20	3.20
St Albans	3726_G_IC2	3.20	3.20	3.20	3.20
Colchester 16	3735_G_GT1	0.89	0.89	0.89	0.89
Essex Junction 19	3737_G_IC5	3.20	3.20	3.20	3.20
Essex Junction 19	3737_G_IC6	3.20	3.20	3.20	3.20
Essex Junction 19	3737_G_IC7	3.20	3.20	3.20	3.20
Essex Junction 19	3737_G_IC8	3.20	3.20	3.20	3.20
Burlington GT	3754_G_GT1	0.60	0.60	0.60	0.60
Vergennes 9	6519_G_5	3.20	3.20	3.20	3.20
Vergennes 9	6519_G_6	3.20	3.20	3.20	3.20
Ryegate Power Station	51026_G_GEN1	0.08	0.08	0.08	0.08
J C MCNEIL	589_B_1	0.11	0.11	0.11	0.11
DEVON	544_B_7	0.12	0.12	0.12	0.12
DEVON	544_B_8	0.12	0.12	0.12	0.12
NORWALK HARBOR	548_B_1	0.14	0.14	0.15	0.15
NORWALK HARBOR	548_B_2	0.14	0.14	0.15	0.15
MIDDLETOWN	562_B_2	0.18	0.18	0.18	0.18
MONTVILLE	546_B_5	0.18	0.18	0.18	0.18
MONTVILLE	546_B_6	0.20	0.20	0.20	0.20
MIDDLETOWN	562_B_4	0.25	0.25	0.25	0.25
MIDDLETOWN	562_B_3	0.30	0.30	0.15	0.15
BRIDGEPORT HARBOR	568_B_BHB2	0.34	0.34	0.34	0.34
BRIDGEPORT HARBOR	568_B_BHB3	0.14	0.14	0.14	0.15
Bridgeport Harbor	568_G_4	0.66	0.66	0.66	0.66
Branford	540_G_10	0.80	0.80	0.80	0.80
Bridgeport Energy	55042_G_GEN1	0.02	0.02	0.02	0.02
Lake Road	55149_G_U1	0.01	0.01	0.01	0.01
Bridgeport Resco	50883_G_GEN1	0.43	0.32	0.43	0.32
Exeter Energy Project	50736_G_GEN1	0.12	0.12	0.12	0.12
Riley Energy Sys of Lisbon Wheelabrator	54758_G_GEN1	0.45	0.28	0.45	0.28
Wallingford Resource Recovery	50664_G_GEN1	0.27	0.27	0.27	0.27
Cos Cob	542_G_10	0.80	0.80	0.80	0.80
Cos Cob	542_G_11	0.80	0.80	0.80	0.80
Cos Cob	542_G_12	0.80	0.80	0.80	0.80
Devon	544_G_10	0.74	0.74	0.74	0.74
Franklin Drive	561_G_19	0.80	0.80	0.80	0.80
Middletown	562_G_10	0.67	0.67	0.67	0.67
Norwalk Harbor	548_G_10	0.52	0.52	0.52	0.52
Bridgeport Energy	55042_G_GEN2	0.02	0.02	0.02	0.02

Exhibit C2.9 (continued): Heat Rate Revisions by Unit in Vistas Phase II

Plant Name	Unique ID	Mode1Rate (VISTAS I)	Mode2 Rate (VISTAS I)	Mode3Rate (VISTAS I)	Mode4 Rate (VISTAS I)
Bridgeport Energy	55042_G_GEN3	0.02	0.02	0.02	0.02
New Milford Gas Recovery	50564_G_GEN1	0.12	0.12	0.12	0.12
Wallingford	55517_G_CTG1	0.01	0.01	0.01	0.01
Wallingford	55517_G_CTG2	0.01	0.01	0.01	0.01
Wallingford	55517_G_CTG3	0.01	0.01	0.01	0.01
Wallingford	55517_G_CTG4	0.01	0.01	0.01	0.01
Wallingford	55517_G_CTG5	0.01	0.01	0.01	0.01
North Main Street	581_G_5	0.57	0.57	0.57	0.57
Montville	546_G_10	3.11	3.11	3.11	3.11
Montville	546_G_11	2.96	2.96	2.96	2.96
Torrington	565_G_10	0.80	0.80	0.80	0.80
Tunnel	557_G_10	0.54	0.54	0.54	0.54
South Meadow	563_G_11	0.75	0.75	0.75	0.75
South Meadow	563_G_12	0.78	0.78	0.78	0.78
South Meadow	563_G_13	0.71	0.71	0.71	0.71
South Meadow	563_G_14	0.72	0.72	0.72	0.72
Lake Road	55149_G_U2	0.01	0.01	0.01	0.01
NEW HAVEN HARBOR	6156_B_NHB1	0.15	0.15	0.15	0.15
Pinetree Power Tamworth Inc	50739_G_GEN1	0.18	0.18	0.18	0.18
White Lake	2369_G_GT1	0.08	0.08	0.08	0.08
Lost Nation	2362_G_GT1	0.08	0.08	0.08	0.08
Whitefield Power and Light Co	10839_G_GEN1	0.08	0.08	0.08	0.08
Bridgewater Power Company LP	10290_G_GEN1	0.19	0.19	0.19	0.19
Pinetree Power Incoporated Bethlehem	50208_G_GEN1	0.19	0.19	0.19	0.19
Plymouth State-College Cogeneration	54803_G_A	0.29	0.29	0.29	0.29
Dunbarton Energy PartnersL P	50347_G_MA15	0.70	0.70	0.70	0.70
Four Hills Nashua Landfill	55006_G_UNT1	0.14	0.14	0.14	0.14
Four Hills Nashua Landfill	55006_G_UNT2	0.14	0.14	0.14	0.14
Bio Energy Corporation	52041_G_GEN1	0.25	0.25	0.25	0.25
MERRIMACK	2364_B_1	0.92	0.09	0.92	0.09
MERRIMACK	2364_B_2	0.37	0.06	0.37	0.06
Merrimack	2364_G_GT1	0.90	0.90	0.90	0.90
Merrimack	2364_G_GT2	0.90	0.90	0.90	0.90
AES Granite Ridge Energy	A093_G_A093	0.01	0.01	0.01	0.01
Foss Hampton Facility	10108_G_GEN8	0.10	0.10	0.10	0.10
NEWINGTON	8002_B_1	0.35	0.35	0.35	0.35
Newington Power Facility	A311_G_A311	0.01	0.01	0.01	0.01
SCHILLER	2367_B_4	0.43	0.28	0.43	0.28
SCHILLER	2367_B_5	0.40	0.26	0.40	0.26
SCHILLER	2367_B_6	0.35	0.23	0.35	0.23
Schiller	2367_G_GT1	0.83	0.83	0.83	0.83
Wheelabrator Claremont Facility	50872_G_GEN1	0.53	0.53	0.53	0.53
Hemphill Power and Light Company	10838_G_GEN1	0.16	0.16	0.16	0.16
Christiana	591_G_11	0.63	0.63	0.63	0.63

Exhibit C2.9 (continued): Heat Rate Revisions by Unit in Vistas Phase II

Plant Name	Unique ID	Mode1 Rate (VISTAS II)	Mode2 Rate (VISTAS I)	Mode3 Rate (VISTAS I)	Mode4 Rate (VISTAS I)
Christiana	591_G_14	0.63	0.63	0.63	0.63
Delaware City	592_G_10	0.53	0.53	0.53	0.53
EDGE MOOR	593_B_3	0.17	0.11	0.17	0.11
EDGE MOOR	593_B_4	0.22	0.18	0.22	0.18
EDGE MOOR	593_B_5	0.31	0.31	0.31	0.31
Edge Moor	593_G_10	0.48	0.48	0.48	0.48
INDIAN RIVER	594_B_1	0.38	0.38	0.38	0.38
INDIAN RIVER	594_B_2	0.33	0.33	0.33	0.33
Indian River	594_G_10	0.63	0.63	0.63	0.63
West Substation	597_G_1	0.47	0.47	0.47	0.47
MCKEE RUN	599_B_1	0.34	0.34	0.34	0.34
MCKEE RUN	599_B_2	0.29	0.29	0.29	0.29
MCKEE RUN	599_B_3	0.35	0.35	0.35	0.35
Hay Road	7153_G_1	0.06	0.06	0.06	0.06
Van Sant Station	7318_G_1	0.15	0.15	0.15	0.15
NA1	A7962_G_A424	0.02	0.02	0.02	0.02
GLEN LYN	3776_B_51	0.41	0.41	0.41	0.41
GLEN LYN	3776_B_52	0.36	0.36	0.36	0.36
GLEN LYN	3776_B_6	0.47	0.47	0.47	0.47
CLINCH RIVER	3775_B_1	0.50	0.50	0.50	0.50
CLINCH RIVER	3775_B_2	0.50	0.50	0.50	0.50
CLINCH RIVER	3775_B_3	0.47	0.47	0.47	0.47
KANAWHA RIVER	3936_B_1	0.39	0.39	0.39	0.39
KANAWHA RIVER	3936_B_2	0.39	0.39	0.39	0.39
KAMMER	3947_B_1	0.76	0.76	0.76	0.76
KAMMER	3947_B_2	0.76	0.76	0.76	0.76
KAMMER	3947_B_3	0.76	0.76	0.76	0.76
MITCHELL	3948_B_1	0.66	0.07	0.66	0.48
MITCHELL	3948_B_2	0.66	0.07	0.66	0.48
PHILIP SPORN	3938_B_11	0.34	0.34	0.34	0.34
PHILIP SPORN	3938_B_21	0.34	0.34	0.34	0.34
PHILIP SPORN	3938_B_31	0.34	0.34	0.34	0.34
PHILIP SPORN	3938_B_41	0.34	0.34	0.34	0.34
PHILIP SPORN	3938_B_51	0.40	0.40	0.40	0.40
MOUNTAINEER	6264_B_1	0.47	0.06	0.47	0.06
JOHN E AMOS	3935_B_1	0.62	0.06	0.62	0.48
JOHN E AMOS	3935_B_2	0.62	0.06	0.62	0.06
JOHN E AMOS	3935_B_3	0.84	0.09	0.84	0.09
FORT MARTIN	3943_B_1	0.65	0.29	0.65	0.42
FORT MARTIN	3943_B_2	0.47	0.26	0.47	0.21
PLEASANTS	6004_B_1	0.34	0.05	0.34	0.06
PLEASANTS	6004_B_2	0.37	0.10	0.37	0.06
McCartney	A288_G_A288	0.10	0.10	0.10	0.10
HAWTHORN	2079_B_9	0.02	0.02	0.02	0.02

Exhibit C2.9 (continued): Heat Rate Revisions by Unit in Vistas Phase II

Plant Name	Unique ID	Mode1 Rate (VISTAS I)	Mode2 Rate (VISTAS I)	Mode3 Rate (VISTAS I)	Mode4 Rate (VISTAS I)
SOUTH OAK CREEK	4041_B_5	0.17	0.17	0.17	0.17
SOUTH OAK CREEK	4041_B_6	0.17	0.17	0.17	0.17
Wheelabrator Concord Facility	50873_G_GEN1	0.35	0.35	0.35	0.35
Gibson City	7979_G_1	0.10	0.10	0.10	0.10
Gibson City	7979_G_2	0.10	0.10	0.10	0.10
ELK RIVER	2039_B_1	0.22	0.22	0.22	0.22
ELK RIVER	2039_B_2	0.23	0.23	0.23	0.23
ELK RIVER	2039_B_3	0.20	0.20	0.20	0.20
BIG SANDY	1353_B_BSU2	0.56	0.06	0.56	0.06
BAY FRONT	3982_B_5	0.49	0.49	0.49	0.49
ALMA	4140_B_B1	0.32	0.32	0.32	0.32
ALMA	4140_B_B2	0.32	0.32	0.32	0.32
ALMA	4140_B_B3	0.32	0.32	0.32	0.32
ALMA	4140_B_B4	0.32	0.32	0.32	0.32
ALMA	4140_B_B5	0.32	0.32	0.32	0.32
J P MADGETT	4271_B_B1	0.18	0.18	0.18	0.18
Cayuga 1	1001_B_1	0.27	0.27	0.27	0.28
Cayuga 2	1001_B_2	0.28	0.28	0.28	0.29
East Bend 2	6018_B_2	0.33	0.06	0.33	0.06
Edwardsprt 71	1004_B_7-1	0.69	0.69	0.34	0.34
Edwardsprt 72	1004_B_7-2	0.69	0.69	0.33	0.33
Edwardsport 8	1004_B_8-1	0.69	0.69	0.32	0.32
Gallagher 1	1008_B_1	0.30	0.30	0.30	0.40
Gallagher 2	1008_B_2	0.34	0.34	0.34	0.40
Gallagher 3	1008_B_3	0.35	0.35	0.35	0.40
Gallagher 4	1008_B_4	0.30	0.30	0.30	0.40
Gibson 1	6113_B_1	0.38	0.06	0.38	0.06
Gibson 2	6113_B_2	0.35	0.06	0.35	0.06
Gibson 3	6113_B_3	0.43	0.06	0.41	0.06
Gibson 4	6113_B_4	0.37	0.06	0.37	0.06
Gibson 5	6113_B_5	0.37	0.06	0.37	0.06
MIAMI FORT	2832_B_5-1	1.08	1.08	0.49	0.49
MIAMI FORT	2832_B_5-2	1.08	1.08	0.49	0.49
Miami Fort 6	2832_B_6	0.46	0.46	0.28	0.28
Miami Fort 7	2832_B_7	0.46	0.07	0.46	0.06
Miami Fort 8	2832_B_8	0.48	0.07	0.48	0.06
Noblesville 1	A313_G_A313	0.03	0.03	0.02	0.02
Wabash River 1	1010_G_1A	0.06	0.06	0.06	0.18
Wabash River 2	1010_B_2	0.49	0.49	0.32	0.48
Wabash River 3	1010_B_3	0.65	0.65	0.48	0.48
Wabash River 4	1010_B_4	0.65	0.65	0.48	0.48
Wabash River 5	1010_B_5	0.64	0.64	0.48	0.48
Wabash River 6	1010_B_6	0.26	0.26	0.26	0.48
W.C. Beckjord 1	2830_B_1	0.58	0.58	0.27	0.27

Exhibit C2.9 (continued): Heat Rate Revisions by Unit in Vistas Phase II

Plant Name	Unique ID	Mode1 Rate** (VISTAS I)	Mode2 Rate** (VISTAS I)	Mode3 Rate** (VISTAS I)	Mode4 Rate** (VISTAS I)
W.C. Beckjord 2	2830_B_2	0.61	0.61	0.25	0.25
W.C. Beckjord 3	2830_B_3	1.02	1.02	0.41	0.41
W.C. Beckjord 4	2830_B_4	0.56	0.56	0.27	0.27
W.C. Beckjord 5	2830_B_5	0.33	0.33	0.33	0.40
W.C. Beckjord 6	2830_B_6	0.29	0.29	0.29	0.30
W.H. Zimmer 1	6019_B_1	0.42	0.06	0.42	0.06
Cayuga CT4	1001_G_4	0.15	0.15	0.09	0.09
Connersville CT 1	1002_G_1	0.85	0.85	0.22	0.22
Connersville CT 2	1002_G_2	0.85	0.85	0.22	0.22
Dicks Creek CT1	2831_G_1	0.15	0.15	0.08	0.08
W.C. Beckjord CT1	2830_G_GT1	0.85	0.85	0.09	0.09
W.C. Beckjord CT2	2830_G_GT2	0.85	0.85	0.09	0.09
W.C. Beckjord CT3	2830_G_GT3	0.85	0.85	0.09	0.09
W.C. Beckjord CT4	2830_G_GT4	0.85	0.85	0.09	0.09
Woodsdale CT1	7158_G_GT1	0.15	0.15	0.12	0.12
Woodsdale CT2	7158_G_GT2	0.15	0.15	0.14	0.14
Woodsdale CT3	7158_G_GT3	0.15	0.15	0.13	0.13
Woodsdale CT4	7158_G_GT4	0.15	0.15	0.13	0.13
Woodsdale CT5	7158_G_GT5	0.15	0.15	0.13	0.13
Woodsdale CT6	7158_G_GT6	0.15	0.15	0.13	0.13

**

Mode 1 Rate (Uncontrolled Base Rate) – This emission rate reflects current configuration of combustion controls. If a post combustion NOx control such as a SCR or a SNCR exists, it is assumed that it is not operating.
Mode 2 Rate (Controlled Base Rate) – This emission rate reflects current configuration of combustion. If a post combustion NOx control such as a SCR or a SNCR exists, it is assumed that it is operating.
Mode 3 Rate (Uncontrolled Policy Rate) – This emission rate reflects a state of the art configuration of combustion controls. If a post combustion NOx control such as a SCR or a SNCR exists, it is assumed that it is not operating.
Mode 4 Rate (Controlled Policy Rate) – This emission rate reflects a state of the art configuration of combustion controls. If a post combustion NOx control such as a SCR or a SNCR exists, it is assumed that it is operating.

For more details on the development of these rates please refer to http://www.epa.gov/airmarkets/epa-ipm/section3powsysop.pdf

Existing Unit Additions

Exhibit C2.10: Additional Units included in NEEDS in VISTAS Phase II

Plant Name	Unique ID	Plant Name	Unique ID
Premcor	52193_G_MECCU1	AMF Energy Systems	70011_G_IC1
Premcor	52193_G_MECCU2	AMF Energy Systems	70011_G_IC2
NRG Energy Center Dover	10030_B_COGEN1	AMF Energy Systems	70011_G_IC3
NRG Energy Center Dover	10030_G_2	Burlington Energy Inc.	70012_G_IC1
NRG Energy Center Dover	10030_G_3	Burlington Energy Inc.	70012_G_IC2
Brunot Island	3096_G_2A	Venice	913_C_03
Brunot Island	3096_G_2B	Venice	913_C_04
Hunterstown	55976_G_1	Venice	913_C_05
Hunterstown	55976_G_2	Mankato Energy Center	56104_C_1
Hunterstown	55976_G_3	Mankato Energy Center	56104_C_2
PPL/Lower Mt Bethel	55667_C_1	WESTON	4078_B_4
PPL/Lower Mt Bethel	55667_C_2	Sheboygan Falls	56186_C_1
PPL/Lower Mt Bethel	55667_C_3	Sheboygan Falls	56186_C_2
Shenango -- Neville Island Coke Works	54532_G_2WH	Lagoon Creek	7845_G_GT9
Shenango -- Neville Island Coke Works	54532_G_3GE	Lagoon Creek	7845_G_GT10
United States Steel -- Mon Valley Works	50732_G_GEN2	Lagoon Creek	7845_G_GT11
United States Steel -- Mon Valley Works	50732_G_GEN1	Lagoon Creek	7845_G_GT12
United States Steel -- Mon Valley Works	50732_G_GEN3	Perryville	55620_G_U2-1
United States Steel -- Clairton Works	50729_G_GEN3	Perryville	55620_G_U1-1
United States Steel -- Clairton Works	50729_G_GEN1	Perryville	55620_G_U 1-2
Allegheny Energy -- Springdale Station	3182_G_8	Skeets 4	7388_G_4
Allegheny Energy -- Springdale Station	3182_G_7	Wheelabrator Concord Facility	50873_G_GEN2
PPG Industries -- PPG Place	54359_G_EG-2	Riverton	1239_C_21
PPG Industries -- PPG Place	54359_G_EG-1		
PPG Industries -- PPG Place	54359_G_EG-3		

Exhibit C2.10(continued): Additional Units included in NEEDS in VISTAS Phase II

Plant Name	Unique ID	Plant Name	Unique ID
Buchanan	1754_G_3	Dayville Pond	70004_G_1
Buchanan	1754_G_4	Glan Falls	70005_G_1
Buchanan	1754_G_5	Mechanicsville	70006_G_1
Buchanan	1754_G_6	Putnam	70007_G_1
Buchanan	1754_G_7	Rocky Glen	70008_G_1
Buchanan	1754_G_8	Toutant	70009_G_1
Buchanan	1754_G_9	Plymouth State College Cogeneration	54803_G_GEN2
Buchanan	1754_G_10	Plymouth State College Cogeneration	54803_G_1
TACONITE HARBOR	10075_B_1	Plymouth State College Cogeneration	54803_G_2
TACONITE HARBOR	10075_B_2	Plymouth State College Cogeneration	54803_G_3
TACONITE HARBOR	10075_B_3	Dunbarton Energy PartnersL P	50347_G_2
RIVERSIDE	1927_G_101	Foss Hampton Facility	10108_G_GEN1
RIVERSIDE	1927_G_103	Foss Hampton Facility	10108_G_GEN2
RIVERSIDE	1927_G_102	Foss Hampton Facility	10108_G_GEN3
RIVERSIDE	1927_G_104	Foss Hampton Facility	10108_G_GEN4
Pleasant Valley	7843_G_13	Foss Hampton Facility	10108_G_GEN5
HIGH BRIDGE	1912_G_101	Foss Hampton Facility	10108_G_GEN6
HIGH BRIDGE	1912_G_103	Foss Hampton Facility	10108_G_GEN7
HIGH BRIDGE	1912_G_102	SCHILLER	2367_C_5
HIGH BRIDGE	1912_G_104	Groveton Paper board	56140_G_GEN1
faribault energy park	56164_C_6	Groveton Paper board	56140_G_GEN2
faribault energy park	56164_C_1	Concord Steam	70010_G_1
Blue Lake	8027_G_7	Concord Steam	70010_G_3
Blue Lake	8027_G_8	Concord Steam	70010_G_5
St Bonifacius	6824_G_2	Concord Steam	70010_G_6
Robert P Mone Plant	7872_G_1	ANP Blackstone Energy Company	55212_G_1
Robert P Mone Plant	7872_G_2	ANP Blackstone Energy Company	55212_G_2
Robert P Mone Plant	7872_G_3	South Boston Combustion Turbines	10176_G_1
Burlington	2399_G_12	South Boston Combustion Turbines	10176_G_2
CHALK POINT	1571_B_3	Deer Island Treatment	10823_G_G101
Burlington GT	3754_G_GT2	Deer Island Treatment	10823_G_G201
Milford Power	55126_G_CTG1	Lowell Cogen	10802_G_GEN1
Milford Power	55126_G_STG1	Lowell Cogen	10802_G_GEN2
Waterside Power LLC	56189_G_2	Hay Road	7153_G_5
Waterside Power LLC	56189_G_1	Hay Road	7153_G_6
Lake Road	55149_G_U3	Hay Road	7153_G_7
Milford Power	55126_G_CTG2	Invista	10793_B_BLR1
Milford Power	55126_G_STG2	Invista	10793_B_BLR2
Waterside Power LLC	56189_G_3	Invista	10793_B_BLR3
Greenville Dam	70001_G_1	Premcor	52193_B_BLR1
Willimantic	70002_G_1	Premcor	52193_B_BLR2
Willimantic	70002_G_2	Premcor	52193_B_BLR3
Wyre Wynd	70003_G_1	Premcor	52193_B_BLR4

Exhibit C2.10(continued): Additional Units included in NEEDS in VISTAS Phase II

Plant Name	Unique ID2	Plant Name	Unique ID
Mabelvale	171_G_1	Clay Center	1270_G_8
Mabelvale	171_G_2	Larned	1299_G_5
Mabelvale	171_G_4	Larned	1299_G_6
THOMAS B FITZHUGH	201_B_06	Larned	1299_G_7
Anita	1123_G_6	Larned	1299_G_8
Coggon	1132_G_IC5	Larned	1299_G_9
Graettinger	1142_G_6	Mulvane	1308_G_7
Independence	1149_G_1A	Mulvane	1308_G_8
Indianola	1150_G_8	St John	1322_G_2
Manning	1160_G_1	Sterling	1326_G_5
Manning	1160_G_2	Sterling	1326_G_6
Manning	1160_G_4	Sterling	1326_G_7
Maquoketa 1	1162_G_2A	GARDEN CITY	1336_B_GC3
Maquoketa 1	1162_G_1A	Hugoton 2	7011_G_13
Mt Pleasant	1166_G_1	Strotherfield Substation	56022_G_1
Mt Pleasant	1166_G_10	NEOSHO	1243_B_7
Mt Pleasant	1166_G_11	Erie	1276_G_2
Mt Pleasant	1166_G_12	Horton	1288_G_1
Mt Pleasant	1166_G_2	Horton	1288_G_2
Mt Pleasant	1166_G_3	Horton	1288_G_3
Mt Pleasant	1166_G_4A	Horton	1288_G_4
Mt Pleasant	1166_G_5A	Pratt	1317_G_IC2
Mt Pleasant	1166_G_6	Wellington Municipal	1330_G_7
Mt Pleasant	1166_G_7	Wellington Municipal	1330_G_8
Mt Pleasant	1166_G_8	Westar Energy	22500_G_J1
Mt Pleasant	1166_G_9	Westar Energy	22500_G_J2
Story City	1188_G_4A	Sharpe	7973_G_1
Earl F Wisdom	1217_G_2	Mulvane 2	7976_G_9
Greenfield	7856_G_1	Mulvane 2	7976_G_10
Greenfield	7856_G_2	Mulvane 2	7976_G_11
Maquoketa 2	7921_G_13	Baldwin 2	8020_G_1
Maquoketa 2	7921_G_14	Baldwin 2	8020_G_2
Brooklyn	1128_G_6	MONROE	1448_B_10
South Strawberry	7926_G_1A	NRG Sterlington Power LLC	55099_G_10
South Strawberry	7926_G_2A	DOW Plaquemine	55419_C_501
Emery Station	8031_C_11	DOW Plaquemine	55419_C_601
Emery Station	8031_C_12	DOW Plaquemine	55419_C_701
Exira Station	56013_G_1	DOW Plaquemine	55419_C_801
Exira Station	56013_G_2	Southwest	6195_G_GT2
Attica	1260_G_4A	Sand Hill	7900_C_SH5
Baldwin	1262_G_1	PORT WASHINGTON POWER PLANT	4040_G_1
Burlington	1266_G_1A	PORT WASHINGTON POWER PLANT	4040_G_2
Burlington	1266_G_4A	Buchanan	1754_G_2

Existing Unit Online changes

Exhibit C2.11: Online Year Revisions by Unit in Vistas Phase II

Plant Name	Unique ID	Online Year from Phase I	Online Year for Phase II
Indianola	1150_G_3	1953	1954
Indianola	1150_G_4	1961	1960
Indianola	1150_G_7	1977	1976
PELLA	1175_B_8	1964	1974
PELLA	1175_B_6	1964	1974
COFFEYVILLE	1271_B_5	1956	1997
Colby	1272_G_5	1958	1952
Colby	1272_G_8	1971	1964
Osage City	1313_G_10	2001	1990
Osage City	1313_G_8	2001	1990
Osage City	1313_G_9	2001	1990
Stafford	1325_G_1	1960	1973
Stafford	1325_G_2	1953	1973
Wellington City	7339_G_6	1989	1986
Erie	1276_G_4	1964	1992
Erie	1276_G_1	1953	2004
Erie	1276_G_3	1958	2004
Perryville	A328_G_A328	2002	2001
HAWTHORN	2079_B_5	1969	2001
Elkhart	986_G_1	1913	1921
Elkhart	986_G_2	1921	1913
Elkhart	986_G_3	1921	1913
Twin Branch	989_G_H2W	1989	1992
Twin Branch	989_G_H3W	1989	1992
Twin Branch	989_G_H4W	1989	1992
Twin Branch	989_G_H5W	1989	1992
Constantine	1760_G_3	1929	1923
Black Dog	A461_G_A461	2007	2002
South Oak Creek	4041_G_9	1968	1969
Rainbow	559_G_1	1925	1980
Rainbow	559_G_2	1925	1980
Devon	544_G_11	1988	1996
Clement Dam Hydroelectric LLC	10276_G_49	1984	1985
Pinetree Power Tamworth Inc	50739_G_GEN1	1987	1988
Amoskeag	2354_G_1	1924	1922
Dunbarton Energy PartnersL P	50347_G_MA15	1988	1996
Gregg Falls	50384_G_1	1985	1986
Hillsborough Hosiery	10036_G_GEN1	1989	1988
Briar Hydro Associates Rolfe Canal Facil	50351_G_1	1987	1988

Exhibit C2.11 (continued): Online Year Revisions by Unit in Vistas Phase II

Plant Name	Unique ID	Online Year from Phase I	Online Year for Phase II
Eastman Falls	2356_G_1	1937	1912
EHC West Hopkinton	54384_G_GEN1	1985	1982
Franklin Industrial Complex	10109_G_1	1985	1978
Franklin Industrial Complex	10109_G_2	1982	1978
Merrimack	2364_G_GT1	1968	1969
Merrimack	2364_G_GT2	1969	1968
Pembroke Hydro	50312_G_1	1985	1986
Milton Hydro	10519_G_1	1914	1929
Milton Hydro	10519_G_2	1914	1929
Rollinsford	54418_G_GEN1	1986	1980
Somersworth Lower Great Dam	50704_G_GEN1	1985	1984
Hunterstown_1960	3110_G_1	1971	1960
Hunterstown_1960	3110_G_2	1971	1960
Hunterstown_1960	3110_G_3	1971	1960
Hunterstown_2002	A248_G_A248	2003	2002
Reusens	3779_G_1	1903	1931
Reusens	3779_G_2	1903	1931
Reusens	3779_G_3	1903	1931
Reusens	3779_G_4	1903	1931
Reusens	3779_G_5	1903	1931
Mid Connecticut Facility	54945_G_NO 5	1988	1987
Mid Connecticut Facility	54945_G_NO 6	1988	1987

Exhibit C2.12: Particulate Matter (PM) Control) Changes by Unit in Vistas Phase II

Plant Name	UniqueID	PM Control in Phase I	PM Control in Phase II
DUBUQUE	1046_B_6	Hot-side ESP	Cold-side ESP
DUBUQUE	1046_B_5	Hot-side ESP	Cold-side ESP
DUBUQUE	1046_B_1	Hot-side ESP	Cold-side ESP
SIXTH STREET	1058_B_2	Hot-side ESP	Cold-side ESP
SIXTH STREET	1058_B_3	Hot-side ESP	Cold-side ESP
SIXTH STREET	1058_B_4	Hot-side ESP	Cold-side ESP
SIXTH STREET	1058_B_5	Hot-side ESP	Cold-side ESP
PRAIRIE CREEK	1073_B_1	Hot-side ESP	Cold-side ESP
PRAIRIE CREEK	1073_B_2	Hot-side ESP	Cold-side ESP
PRAIRIE CREEK	1073_B_3	Hot-side ESP	Cold-side ESP
PRAIRIE CREEK	1073_B_4	Hot-side ESP	Cold-side ESP
FAIR STATION	1218_B_1	none	Cold-side ESP
FAIR STATION	1218_B_2	Hot-side ESP	Cold-side ESP
R S NELSON	1393_B_4	none	Cold-side ESP
CHAMOIS	2169_B_1	none	Cold-side ESP
WHELAN ENERGY CENTER	60_B_1	Hot-side ESP	Cold-side ESP
GERALD GENTLEMAN	6077_B_2	Hot-side ESP	Fabric Filter
PRESQUE ISLE	1769_B_1	Cyclone	Fabric Filter
PRESQUE ISLE	1769_B_5	Cold-side ESP	Cold-side ESP + Fabric Filter
PRESQUE ISLE	1769_B_6	Cold-side ESP	Cold-side ESP + Fabric Filter
WESTON	4078_B_3	Fabric Filter	Fabric Filter
CONNERS CREEK	1726_B_15	Cold-side ESP	none
CONNERS CREEK	1726_B_16	Cold-side ESP	none
SHERBURNE COUNTY	6090_B_1	Hot-side ESP	Cold-side ESP
SHERBURNE COUNTY	6090_B_2	Hot-side ESP	Cold-side ESP
Bridgeport Resco	50883_G_GEN1	none	Fabric Filter
Exeter Energy Project	50736_G_GEN1	none	Fabric Filter
Riley Energy Sys of Lisbon Wheelabrator	54758_G_GEN1	none	Fabric Filter
Wallingford Resource Recovery Facility	50664_G_GEN1	none	Fabric Filter
American Ref Fuel Company Of SE CT	10646_G_GEN1	none	Fabric Filter
Bristol Resource Recovery Facility	50648_G_GEN1	none	Fabric Filter
Mid Connecticut Facility	54945_G_NO 5	none	Fabric Filter
Mid Connecticut Facility	54945_G_NO 6	none	Fabric Filter
Pinetree Power Tamworth Inc	50739_G_GEN1	none	Cold-side ESP + Cyclone
Whitefield Power and Light Co	10839_G_GEN1	none	Cold-side ESP + Cyclone
Bridgewater Power Company LP	10290_G_GEN1	none	Fabric Filter
Pinetree Power Incoporated Bethlehem	50208_G_GEN1	none	Cold-side ESP + Cyclone
Bio Energy Corporation	52041_G_GEN1	none	Fabric Filter
Wheelabrator Concord Facility	50873_G_GEN1	none	Fabric Filter
Wheelabrator Claremont Facility	50872_G_GEN1	none	Fabric Filter
Hemphill Power and Light Company	10838_G_GEN1	none	Cold-side ESP + Cyclone
WILLMAR	2022_B_1	none	Cyclone
ELK RIVER	2039_B_1	none	Fabric Filter
ELK RIVER	2039_B_2	none	Fabric Filter
ELK RIVER	2039_B_3	none	Fabric Filter

Control Technology Changes

Exhibit C2.13: NOx Post Combustion Control Changes by Unit in Vistas Phase II

Plant Name	Unique ID	Post Combustion Control in Phase I	Post Combustion Control in Phase II
CEDAR BAYOU	3460_B_CBY1	None	SCR
Sweeny Cogeneration Facility	55015_G_GEN1	None	SCR
Sweeny Cogeneration Facility	55015_G_GEN2	None	SCR
SIOUX	2107_B_1	None	SNCR
SIOUX	2107_B_2	None	SNCR
DUCK CREEK	6016_B_1	None	SCR
Riley Energy Sys of Lisbon Wheelabrator	54758_G_GEN1	none	SNCR
American Ref Fuel Company Of SE CT	10646_G_GEN1	none	SNCR
Bristol Resource Recovery Facility	50648_G_GEN1	none	SNCR
Mid Connecticut Facility	54945_G_NO 5	none	SNCR
Mid Connecticut Facility	54945_G_NO 6	none	SNCR
Bridgeport Energy	55042_G_GEN3	None	SCR
Whitefield Power and Light Co	10839_G_GEN1	none	SCR
Plymouth State College Cogeneration	54803_G_A	None	SCR
Wheelabrator Concord Facility	50873_G_GEN1	none	SNCR
Ocean State Power	51030_G_GEN3	none	SCR
Calpine Tiverton Power	55048_G_UNT2	None	SCR
Block Island	6567_G_23	None	SCR
Linden Cogen Plant	50006_G_STG1	None	SCR
Bridgeport Resco	50883_G_GEN1	none	SNCR
FORT MARTIN	3943_B_1	None	SNCR
Noblesville	A313_G_A313	SCR	none

xisting Unit Change – Retirement Year

Exhibit C2.14: Retirement Year Changes by Unit in Vistas Phase II

Plant Name	Unique ID	Retirement Year from Phase I	Retirement Year for Phase II
Corning	1134_G_4	-	2006
Corning	1134_G_1	-	2006
Corning	1134_G_2	-	2006
Corning	1134_G_3	-	2006
MUSCATINE	1167_B_7	-	2010
MUSCATINE	1167_B_8	-	2019
MUSCATINE	1167_B_9	-	2033
HOLLY STREET	3549_B_1	-	2004
HOLLY STREET	3549_B_2	-	2004
HOLLY STREET	3549_B_3	-	2007
HOLLY STREET	3549_B_4	-	2007
VENICE	913_B_3	-	2002
VENICE	913_B_4	-	2002
VENICE	913_B_5	-	2002
VENICE	913_B_6	-	2002
VENICE	913_B_7	-	2002
VENICE	913_B_8	-	2002
Fourth Street	1025_G_1	-	2000
RIVERSIDE	1927_B_6	-	2009
RIVERSIDE	1927_B_7	-	2009
RIVERSIDE	1927_B_8	-	2009
HOOT LAKE	1943_B_1	-	2005
COLLINS	6025_B_2	-	2004
COLLINS	6025_B_3	-	2004
COLLINS	6025_B_4	-	2004
COLLINS	6025_B_5	-	2004
Bloom	865_G_333	-	2004
Bloom	865_G_334	-	2004
Bloom	865_G_341	-	2004
Bloom	865_G_342	-	2004
Bloom	865_G_344	-	2004
Calumet	866_G_311	-	2004
Calumet	866_G_312	-	2004
Calumet	866_G_313	-	2004
Calumet	866_G_314	-	2004
Calumet	866_G_331	-	2004
Calumet	866_G_332	-	2004
Calumet	866_G_333	-	2004
Calumet	866_G_341	-	2004
Calumet	866_G_342	-	2004
Calumet	866_G_343	-	2004
Calumet	866_G_344	-	2004
Electric Junction	870_G_311	-	2004

Exhibit C2.14 (continued): Retirement Year Changes by Unit in Vistas Phase II

Plant Name	Unique ID	Retirement Year from Phase I	Retirement Year for Phase II
Electric Junction	870_G_312	-	2004
Electric Junction	870_G_313	-	2004
Electric Junction	870_G_314	-	2004
Electric Junction	870_G_321	-	2004
Electric Junction	870_G_322	-	2004
Electric Junction	870_G_323	-	2004
Electric Junction	870_G_324	-	2004
Electric Junction	870_G_331	-	2004
Electric Junction	870_G_332	-	2004
Electric Junction	870_G_333	-	2004
Electric Junction	870_G_334	-	2004
Lombard	877_G_311	-	2004
Lombard	877_G_321	-	2004
Lombard	877_G_322	-	2004
Lombard	877_G_331	-	2004
Sabrooke	882_G_311	-	2004
Sabrooke	882_G_312	-	2004
Sabrooke	882_G_321	-	2004
Sabrooke	882_G_322	-	2004
Sabrooke	882_G_331	-	2004
Sabrooke	882_G_332	-	2004
Sabrooke	882_G_341	-	2004
South Norwalk	6598_G_1	-	2002
South Norwalk	6598_G_2	-	2002
South Norwalk	6598_G_3	-	2002
South Norwalk	6598_G_4	-	2002
South Norwalk	6598_G_5	-	2002
South Norwalk	6598_G_6	-	2002
SCHILLER	2367_B_5	-	2006
Harrisburg Facility	10118_G_GEN1	-	2003
Johnston Willis Facility	54777_G_GEN1	-	2005
Johnston Willis Facility	54777_G_GEN2	-	2005
Johnston Willis Facility	54777_G_GEN3	-	2005
Byrd Press Cogeneration Facility	54776_G_GEN1	-	2005
Byrd Press Cogeneration Facility	54776_G_GEN2	-	2005
Byrd Press Cogeneration Facility	54776_G_GEN3	-	2005
Handcraft Facility	54601_G_VII1	-	2005
Handcraft Facility	54601_G_VII2	-	2005
Handcraft Facility	54601_G_VII3	-	2005
Scott Wood	50863_C_ST2	-	2005
Scott Wood	50863_C_ST3	-	2005
Chesterfield County LFG	ZZ175_C_1	-	2005
Va Beach Mt Trashmore II LFG	ZZ173_C_1	-	2005

Exhibit C2.14 (continued): Retirement Year Changes by Unit in Vistas Phase II

Plant Name	Unique ID	Retirement Year from Phase I	Retirement Year for Phase II
CRIST	641_B_1	-	2002
Camden Cogen L P	10751_G_GEN2	-	2002
Howard Down	2434_G_6	-	1999
Kinsleys Landfill Inc.	10045_G_11	-	1998
Kearny	2404_G_12	-	2002
Gilbert	2393_G_8	-	2000
NRG Generating Parlin Cogeneration Inc	50799_G_GEN3	-	1999
NRG Generating Parlin Cogeneration Inc	50799_G_GEN4	-	1999
Lakewood Cogeneration L P	54640_G_GEN3	-	2000
PRESQUE ISLE	1769_B_1	-	2013
PRESQUE ISLE	1769_B_2	-	2013
PRESQUE ISLE	1769_B_3	-	2013
PRESQUE ISLE	1769_B_4	-	2013
GREEN RIVER	1357_B_1	-	2004
GREEN RIVER	1357_B_2	-	2004
GREEN RIVER	1357_B_3	-	2004
PINEVILLE	1360_B_3	-	2003

Exhibit C2.15: Units Removed in Vistas Phase II

Plant Name	Unique ID	Plant Name	Unique ID
Blytheville	8109_G_1	T H Wharton	3469_G_3
Blytheville	8109_G_2	T H Wharton	3469_G_4
Blytheville	8109_G_3	Va Beach Mt Trashmore II LFG	ZZ173_C_1
Maquoketa	1067_G_1	Fourth Street	1025_G_1
Maquoketa	1067_G_2	Fourth Street	1025_G_1
Algona	1120_G_3	Maple Lake	2042_G_5A
Algona	1120_G_4	GOULD STREET	1553_B_3
Algona	1120_G_5	L Street	1587_G_GT1
Anita	1123_G_1	NEW BOSTON	1589_B_2
Coon Rapids	1133_G_4	Kendall Square	1595_G_GT2
Coon Rapids	1133_G_6	Somerset	1613_G_J1
Coon Rapids	1133_G_7	Mystic Generating Station	A309_G_A309
Maquoketa	1162_G_2	Mystic Generating Station	A310_G_A310
Maquoketa	1162_G_1	Madison Street	596_G_1
Primghar	1177_G_2	Hay Road	A7153_G_A435
Nimeca Diesels	7694_G_DSL	NA1	A7962_G_A424
Wichita Diesel	1245_G_5	Cogentrix of Pennsylvania Incorporated	10383_G_GEN1
Burlington	1266_G_1	Cogentrix of Pennsylvania Incorporated	10383_G_GEN2
Burlington	1266_G_4	Cogentrix of Pennsylvania Incorporated	10383_G_GEN3
Burlington	1266_G_3	Cogentrix of Pennsylvania Incorporated	10383_G_GEN4
Chanute 1	1267_G_5	General Electric Erie PA Power Station	50358_G_STM4
Clay Center	1270_G_4	General Electric Erie PA Power Station	50358_G_DSL3
Clay Center	1270_G_5	General Electric Erie PA Power Station	50358_G_STM3
Erie	1276_G_1	General Electric Erie PA Power Station	50358_G_STM2
Erie	1276_G_3	General Electric Erie PA Power Station	50358_G_DSL1
Erie	1276_G_4	Allegheny Energy Units 3 4 & 5	A388_G_A388
Erie	1276_G_5	Tupperware	50177_G_GEN1
City Light Plant	1284_G_1	Tupperware	50177_G_GEN2
Hugoton 1	1289_G_1	Tupperware	50177_G_GEN3
Hugoton 1	1289_G_5	Tupperware	50177_G_GEN4
La Crosse	1297_G_3	A365_G_A365	A365_G_A365
Ottawa	1316_G_GT1	South Norwalk	6598_G_1
Wellington Municipal	1330_G_5	South Norwalk	6598_G_2
Hugoton 2	7011_G_9	South Norwalk	6598_G_3
R S NELSON	1393_B_1A	South Norwalk	6598_G_4
R S NELSON	1393_B_2A	NENG_CT_Combined Cycle	050_C_050
State Line Combined Cycle (1)	7296_B_HRSG21	South Norwalk	6598_G_5
State Line Combined Cycle (2)	7296_B_HRSG22	South Norwalk	6598_G_6
Scott Wood	50863_C_ST3	Bridgeport Energy	55042_G_GEN1
Scott Wood	50863_C_ST2	Chesterfield County LFG	ZZ175_C_1
Perryville	A328_G_A328	Decker Creek <Delete this Unit>	3548_G_PV3

Existing Units Scrubber Controls

Exhibit C2.16: Scrubber Control Changes by Unit in Vistas Phase II

Plant Name	Unique ID	Scrubber from Phase I	Scrubber for Phase II
Nelson Industrial Steam Company	50030_G_GEN1	-	Dry Scrubber
Nelson Industrial Steam Company	50030_G_GEN2	-	Dry Scrubber
PLEASANT PRAIRIE	6170_B_2	-	Wet Scrubber
Bridgeport Resco	50883_G_GEN1	-	Dry Scrubber
Exeter Energy Project	50736_G_GEN1	-	Wet Scrubber
Riley Energy Sys of Lisbon Wheelabrator	54758_G_GEN1	-	Dry Scrubber
Wallingford Resource Recovery Facility	50664_G_GEN1	-	Dry Scrubber
American Ref Fuel Company Of SE CT	10646_G_GEN1	-	Dry Scrubber
Bristol Resource Recovery Facility	50648_G_GEN1	-	Dry Scrubber
Mid Connecticut Facility	54945_G_NO 5	-	Dry Scrubber
Mid Connecticut Facility	54945_G_NO 6	-	Dry Scrubber
Wheelabrator Concord Facility	50873_G_GEN1	-	Dry Scrubber
CARDINAL	2828_B_2	-	Wet Scrubber
ELK RIVER	2039_B_1	-	Dry Scrubber
ELK RIVER	2039_B_2	-	Dry Scrubber
ELK RIVER	2039_B_3	-	Dry Scrubber

Exhibit C2.17: Scrubber Efficiency Changes by Unit in Vistas Phase II

Plant Name	Unique ID	Scrubber efficiency % from Phase I	Scrubber efficiency % from Phase II
WESTON	4078_B_4	-	92
DOLET HILLS	51_B_1	92.4	76
GRDA	165_B_2	75.9	74
LIMESTONE	298_B_LIM1	95.1	81
LIMESTONE	298_B_LIM2	95.1	81
W A PARISH	3470_B_WAP8	73	81
PLEASANT PRAIRIE	6170_B_1	88	95
Bridgeport Resco	50883_G_GEN1	-	75
Riley Energy Sys of Lisbon Wheelabrator	54758_G_GEN1	-	75
Wallingford Resource Recovery Facility	50664_G_GEN1	-	75
HARRISON	3944_B_1	98	95
HARRISON	3944_B_2	98	95
HARRISON	3944_B_3	98	95
PLEASANTS	6004_B_1	90	95
PLEASANTS	6004_B_2	90	95
ELK RIVER	2039_B_1	-	91
ELK RIVER	2039_B_2	-	91
ELK RIVER	2039_B_3	-	91
PLEASANT PRAIRIE	6170_B_2	-	95

Exhibit C2.17: Sulfur Dioxide Rate Limit Changes by Unit in Vistas Phase II

Plant Name	Unique ID	SO2 Rate from Phase I (lbs/MMBtu)	SO2 Rate for Phase II (lbs/MMBtu)
WHITE BLUFF	6009_B_1	9999.00	0.82
WHITE BLUFF	6009_B_2	9999.00	0.82
FLINT CREEK	6138_B_1	9999.00	1.20
INDEPENDENCE	6641_B_1	9999.00	0.40
INDEPENDENCE	6641_B_2	9999.00	0.40
DUBUQUE	1046_B_6	2.50	0.79
DUBUQUE	1046_B_5	6.00	0.73
DUBUQUE	1046_B_1	6.00	0.77
LANSING	1047_B_1	5.00	0.01
LANSING	1047_B_2	5.00	0.01
LANSING	1047_B_3	5.00	0.81
LANSING	1047_B_4	1.32	0.61
MILTON L KAPP	1048_B_2	6.00	0.65
SIXTH STREET	1058_B_2	6.00	0.39
SIXTH STREET	1058_B_3	6.00	0.40
SIXTH STREET	1058_B_4	6.00	0.62
SIXTH STREET	1058_B_5	6.00	0.64
PRAIRIE CREEK	1073_B_3	6.00	0.66
PRAIRIE CREEK	1073_B_4	6.00	0.70
SUTHERLAND	1077_B_1	5.00	0.57
SUTHERLAND	1077_B_2	5.00	0.57
SUTHERLAND	1077_B_3	5.00	0.56
RIVERSIDE	1081_B_6	6.00	0.81
RIVERSIDE	1081_B_7	6.00	0.81
RIVERSIDE	1081_B_8	6.00	0.81
RIVERSIDE	1081_B_9	6.00	0.81
COUNCIL BLUFFS	1082_B_1	5.00	0.53
COUNCIL BLUFFS	1082_B_2	5.00	0.54
COUNCIL BLUFFS	1082_B_3	1.32	0.52
GEORGE NEAL NORTH	1091_B_1	5.00	0.73
GEORGE NEAL NORTH	1091_B_2	1.32	0.71
GEORGE NEAL NORTH	1091_B_3	1.32	0.71
BURLINGTON	1104_B_1	6.00	0.73
MUSCATINE	1167_B_7	6.00	1.22
MUSCATINE	1167_B_8	6.00	0.80
MUSCATINE	1167_B_9	0.14	0.45
PELLA	1175_B_7	5.00	0.70
PELLA	1175_B_8	2.50	0.10
PELLA	1175_B_6	5.00	0.70
EARL F WISDOM	1217_B_1	5.00	2.70
FAIR STATION	1218_B_1	6.00	5.16
FAIR STATION	1218_B_2	6.00	5.16
OTTUMWA	6254_B_1	1.32	0.67
LOUISA	6664_B_101	1.32	0.65

Exhibit C2.17 (continued): Sulfur Dioxide Rate Limit Changes by Unit in Vistas Phase II

Plant Name	Unique ID	SO2 Rate from Phase I (lbs/MMBtu)	SO2 Rate from Phase II (lbs/MMBtu)
GEORGE NEAL SOUTH	7343_B_4	1.32	0.63
CIMARRON RIVER	1230_B_1	9999.00	3.00
LA CYGNE	1241_B_2	3.00	1.20
MURRAY GILL	1242_B_1	9999.00	3.00
HUTCHINSON	1248_B_1	9999.00	3.00
HUTCHINSON	1248_B_2	9999.00	3.00
HUTCHINSON	1248_B_3	9999.00	3.00
COFFEYVILLE	1271_B_4	9999.00	3.00
COFFEYVILLE	1271_B_5	9999.00	3.00
KAW	1294_B_1	9999.00	3.00
KAW	1294_B_3	9999.00	3.00
WELLINGTON	1330_B_4	9999.00	3.00
JEFFREY ENERGY CENTE	6068_B_1	0.25	1.20
JEFFREY ENERGY CENTE	6068_B_2	0.25	1.20
JEFFREY ENERGY CENTE	6068_B_3	0.25	1.20
TECHE	1400_B_1	0.80	0.00
TECHE	1400_B_2	0.80	0.00
TECHE	1400_B_3	0.80	0.70
ARSENAL HILL	1416_B_5A	0.80	0.09
LIEBERMAN	1417_B_1	0.80	0.78
LIEBERMAN	1417_B_2	0.80	0.78
LIEBERMAN	1417_B_3	0.80	0.78
LIEBERMAN	1417_B_4	0.80	0.79
ASBURY	2076_B_1	12.00	1.16
MONTROSE	2080_B_1	1.30	0.85
MONTROSE	2080_B_2	1.30	0.88
MONTROSE	2080_B_3	1.30	0.88
MERAMEC	2104_B_1	6.11	2.30
MERAMEC	2104_B_2	6.11	2.30
JAMES RIVER	2161_B_1	9.20	1.50
JAMES RIVER	2161_B_2	9.20	1.50
JAMES RIVER	2161_B_3	9.20	1.50
JAMES RIVER	2161_B_4	9.20	1.50
JAMES RIVER	2161_B_5	9.20	2.00
IATAN	6065_B_1	8.00	0.70
PLATTE	59_B_1	2.50	1.20
WHELAN ENERGY CENTER	60_B_1	2.50	1.20
LON WRIGHT	2240_B_8	2.50	1.20
GERALD GENTLEMAN	6077_B_2	2.50	1.20
NEBRASKA CITY	6096_B_1	2.50	1.20
GRDA	165_B_2	1.21	0.60
NORTHEASTERN	2963_B_3302	0.74	0.40
NORTHEASTERN	2963_B_3313	0.80	1.20
TULSA	2965_B_1402	0.74	0.50

Existing Unit changes – Sulfur Dioxide

Exhibit C2.17 (continued): Sulfur Dioxide Rate Limit Changes by Unit in Vistas Phase II

Plant Name	Unique ID	SO2 Rate from Phase I (lbs/MMBtu)	SO2 Rate for Phase II (lbs/MMBtu)
TULSA	2965_B_1403	0.74	0.50
TULSA	2965_B_1404	0.74	0.50
RIVERSIDE	4940_B_1501	0.80	0.50
RIVERSIDE	4940_B_1502	0.80	0.50
KNOX LEE	3476_B_2	3.00	0.70
KNOX LEE	3476_B_3	3.00	0.70
KNOX LEE	3476_B_4	3.00	0.70
KNOX LEE	3476_B_5	3.00	0.70
LONE STAR	3477_B_1	3.00	0.31
LAKE PAULINE	3521_B_1	3.00	0.70
LAKE PAULINE	3521_B_2	3.00	0.70
LAKE PAULINE	3521_B_3	3.00	0.70
LAKE PAULINE	3521_B_4	3.00	0.70
OAK CREEK	3523_B_1	3.00	0.70
PAINT CREEK	3524_B_1	3.00	0.70
PAINT CREEK	3524_B_2	3.00	0.70
PAINT CREEK	3524_B_3	3.00	0.70
PAINT CREEK	3524_B_4	3.00	0.70
RIO PECOS	3526_B_6	3.00	0.70
FORT PHANTOM	4938_B_1	3.00	0.70
FORT PHANTOM	4938_B_2	3.00	0.70
WELSH	6139_B_1	3.00	1.20
WELSH	6139_B_2	3.00	1.10
WELSH	6139_B_3	3.00	1.12
SAM SEYMOUR	6179_B_1	3.00	0.69
SAM SEYMOUR	6179_B_2	3.00	0.70
MERAMEC	2104_B_3	2.30	0.89
SIOUX	2107_B_1	4.80	1.30
SIOUX	2107_B_2	4.80	1.33
PULLIAM	4072_B_3	0.50	1.20
PULLIAM	4072_B_4	0.50	1.20
PULLIAM	4072_B_5	0.50	1.20
PULLIAM	4072_B_6	0.50	1.20
PULLIAM	4072_B_7	0.50	1.20
PULLIAM	4072_B_8	0.50	1.20
ALMA	4140_B_B1	5.50	1.43
ALMA	4140_B_B2	5.50	1.43
ALMA	4140_B_B3	5.50	1.43
ALMA	4140_B_B4	3.20	1.43
ALMA	4140_B_B5	3.20	1.43
J P MADGETT	4271_B_B1	3.20	1.20
COLUMBIA	8023_B_1	3.20	1.20
COLUMBIA	8023_B_2	3.20	1.20
NELSON DEWEY	4054_B_1	3.20	2.15

Exhibit C2.17 (continued): Sulfur Dioxide Rate Limit Changes by Unit in Vistas Phase II

Plant Name	Unique ID	SO2 Rate from Phase I (lbs/MMBtu)	SO2 Rate for Phase II (lbs/MMBtu)
NELSON DEWEY	4054_B_2	3.20	2.17
WESTON	4078_B_1	3.20	1.20
WESTON	4078_B_2	3.20	1.20
WESTON	4078_B_3	3.20	1.20
VALLEY	4042_B_1	3.28	1.20
VALLEY	4042_B_2	3.28	1.20
VALLEY	4042_B_3	3.28	1.20
VALLEY	4042_B_4	3.28	1.20
EDGEWATER	4050_B_3	3.20	1.20
EDGEWATER	4050_B_4	3.20	1.20
EDGEWATER	4050_B_5	3.20	1.20
GENOA	4143_B_1	3.20	1.20
COFFEEN	861_B_01	7.29	1.41
COFFEEN	861_B_02	7.29	1.39
E D EDWARDS	856_B_1	4.71	3.60
E D EDWARDS	856_B_2	4.71	0.86
E D EDWARDS	856_B_3	4.71	2.15
MEREDOSIA	864_B_01	6.80	5.52
MEREDOSIA	864_B_02	6.80	5.27
MEREDOSIA	864_B_03	6.80	5.40
MEREDOSIA	864_B_04	6.80	5.40
MEREDOSIA	864_B_05	2.42	0.41
NEWTON	6017_B_2	1.20	0.48
LABADIE	2103_B_1	4.80	0.75
LABADIE	2103_B_2	4.80	0.75
LABADIE	2103_B_3	4.80	0.74
LABADIE	2103_B_4	4.80	0.73
MERAMEC	2104_B_4	2.30	0.88
RUSH ISLAND	6155_B_1	2.30	0.68
RUSH ISLAND	6155_B_2	2.30	0.67
MONROE	1733_B_1	1.67	1.60
MONROE	1733_B_2	1.67	1.60
MONROE	1733_B_3	1.67	1.60
MONROE	1733_B_4	1.67	1.60
BELLE RIVER	6034_B_1	1.67	1.20
BELLE RIVER	6034_B_2	1.67	1.20
GREENWOOD	6035_B_1	1.67	0.80
CONNERS CREEK	1726_B_15	2.50	0.00
CONNERS CREEK	1726_B_16	2.50	0.00
ROCKPORT	6166_B_MB1	6.00	1.20
ROCKPORT	6166_B_MB2	6.00	1.20
CONESVILLE	2840_B_5	0.63	1.20
CONESVILLE	2840_B_6	0.63	1.20
GEN J M GAVIN	8102_B_1	0.17	7.42

Exhibit C2.17 (continued): Sulfur Dioxide Rate Limit Changes by Unit in Vistas Phase II

Plant Name	Unique ID	SO2 Rate from Phase II (lbs/MMBtu)	SO2 Rate for Phase II (lbs/MMBtu)
GEN J M GAVIN	8102_B_2	0.10	7.42
CARDINAL	2828_B_3	1.80	2.00
WILMARTH	1934_B_1	9999.00	0.08
WILMARTH	1934_B_2	9999.00	0.08
NEW ULM	2001_B_1	9999.00	0.05
NEW ULM	2001_B_2	9999.00	0.05
NEW ULM	2001_B_4	9999.00	4.00
Springfield	2012_G_4	9999.00	4.00
MINNESOTA VALLEY	1918_B_4	4.00	1.19
BLACK DOG	1904_B_3	3.00	1.30
BLACK DOG	1904_B_4	3.00	1.30
RED WING	1926_B_1	9999.00	0.08
RED WING	1926_B_2	9999.00	0.08
HOOT LAKE	1943_B_1	4.00	0.56
HOOT LAKE	1943_B_2	4.00	0.56
HOOT LAKE	1943_B_3	4.00	0.60
HIGH BRIDGE	1912_B_5	3.00	1.95
HIGH BRIDGE	1912_B_6	3.00	1.95
SHERBURNE COUNTY	6090_B_1	0.59	0.96
SHERBURNE COUNTY	6090_B_2	0.59	0.96
SHERBURNE COUNTY	6090_B_3	0.57	0.60
M L HIBBARD	1897_B_3	9999.00	1.20
M L HIBBARD	1897_B_4	9999.00	1.20
SYL LASKIN	1891_B_1	4.00	4.00
SYL LASKIN	1891_B_2	4.00	4.00
ALLEN S KING (Existing Configuration)	1915_B_1	0.44	1.60
PLEASANT PRAIRIE	6170_B_2	3.20	1.00
DEVON	544_B_7	0.55	0.30
DEVON	544_B_8	0.55	0.30
NORWALK HARBOR	548_B_1	0.55	0.30
NORWALK HARBOR	548_B_2	0.55	0.30
MIDDLETOWN	562_B_2	0.55	0.30
MONTVILLE	546_B_5	0.55	0.30
MONTVILLE	546_B_6	0.55	0.30
MIDDLETOWN	562_B_4	0.55	0.30
MIDDLETOWN	562_B_3	0.55	0.30
BRIDGEPORT HARBOR	568_B_BHB2	0.55	0.33
BRIDGEPORT HARBOR	568_B_BHB3	1.10	0.33
Exeter Energy Project	50736_G_GEN1	0.00	0.11
NEW HAVEN HARBOR	6156_B_NHB1	0.55	0.33
MERRIMACK	2364_B_1	4.00	2.40
MERRIMACK	2364_B_2	4.00	2.40
SCHILLER	2367_B_4	4.00	2.40
SCHILLER	2367_B_5	4.00	2.40

Exhibit C2.17 (continued): Sulfur Dioxide Rate Limit Changes by Unit in Vistas Phase II

Plant Name	Unique ID	SO2 Rate from Phase I (lbs/MMBtu)	SO2 Rate for Phase II (lbs/MMBtu)
SCHILLER	2367_B_6	4.00	2.40
EDGE MOOR	593_B_3	1.53	1.13
EDGE MOOR	593_B_4	1.53	0.81
EDGE MOOR	593_B_5	1.05	1.07
INDIAN RIVER	594_B_1	0.79	1.20
INDIAN RIVER	594_B_2	0.79	1.20
INDIAN RIVER	594_B_3	0.79	1.20
INDIAN RIVER	594_B_4	0.79	1.20
BOWEN	703_B_2BLR	1.20	1.67
BOWEN	703_B_3BLR	1.20	1.67
BOWEN	703_B_4BLR	1.20	1.67
YATES	728_B_Y6BR	1.20	1.67
YATES	728_B_Y7BR	1.20	1.67
MCINTOSH	6124_B_1	1.20	1.27
WANSLEY	6052_B_1	1.20	1.67
WANSLEY	6052_B_2	1.20	1.67
RIVERSIDE	1927_B_6	3.00	0.90
RIVERSIDE	1927_B_7	3.00	0.90
RIVERSIDE	1927_B_8	3.00	2.50
HUTSONVILLE	863_B_05	4.48	3.21
HUTSONVILLE	863_B_06	4.37	3.11
ELK RIVER	2039_B_1	9999.00	0.02
ELK RIVER	2039_B_2	9999.00	0.02
ELK RIVER	2039_B_3	9999.00	0.02
BAY FRONT	3982_B_1	3.00	2.00
BAY FRONT	3982_B_2	3.00	2.00
BAY FRONT	3982_B_5	3.20	2.00
BLOUNT STREET	3992_B_7	4.25	2.00
BLOUNT STREET	3992_B_8	4.25	2.00
BLOUNT STREET	3992_B_9	4.25	2.00
BLOUNT STREET	3992_B_1	3.00	0.00
BLOUNT STREET	3992_B_11	1.16	0.00
BLOUNT STREET	3992_B_2	3.00	0.00
BLOUNT STREET	3992_B_3	1.16	0.00
BLOUNT STREET	3992_B_5	1.16	0.00
BLOUNT STREET	3992_B_6	1.16	0.00
MANITOWOC	4125_B_5	5.50	2.00
MANITOWOC	4125_B_6	3.20	2.00
MANITOWOC	4125_B_7	3.20	2.00
MANITOWOC	4125_B_8	1.04	2.00
BLACKHAWK	4048_B_3	3.00	0.00
BLACKHAWK	4048_B_4	3.00	0.00
ROCK RIVER	4057_B_1	0.00	2.00
ROCK RIVER	4057_B_2	0.00	2.00

Unit ID Changes

Exhibit C2.18: Unit ID Changes in Vistas Phase II

Plant Name	Unique ID	Unit ID from Phase I	UNIT ID for Phase II
AES Granite Ridge Energy	A093_G_A093	093	Units 1 & 2
Newington Power Facility	A311_G_A311	311	Units 1 & 2
Claremont Facility	50872_G_GEN1	GEN1	GEN1 & GEN2
Northeastern	2963_B_3301A	3301A	3301A&3301B
West Gardner	A429_G_A429	429	A429
Russell Energy Cntr	A374_G_A374	374	A374
Bayou Cove Peaking Power	A55433_G_A112	112	CTG-1
Big Cajun 1 Peakers	55958_G_1	1	CTG1
Big Cajun 1 Peakers	55958_G_2	2	CTG2
HAWTHORN	2079_B_5	5	5A
Sweeny Cogeneration Facility	55015_G_GEN1	GEN1	1
Sweeny Cogeneration Facility	55015_G_GEN2	GEN2	2
Sweeny Cogeneration Facility	55015_G_GEN3	GEN3	3
Sweeny Cogeneration Facility	55015_G_GEN4	GEN4	4
Berrien Springs	1753_G_1A	1A	1
Berrien Springs	1753_G_2A	2A	2
Berrien Springs	1753_G_3A	3A	3
Berrien Springs	1753_G_4A	4A	4
Plymouth State College Cogeneration	54803_G_A	A	GEN1
Dunbarton Energy PartnersL P	50347_G_MA15	MA15	1
St Bonifacius	6824_G_1	1	2
State Line Combined Cycle	7296_G_2	2	2-2

Summary Of Changes Made By Ladco / Illinois Epa

The following tables reflect changes made by LADCO/ Illinois EPA regarding fuel assignments for Illinois plants, mercury cost controls, unit characteristics and ESP changes.

Fuel Assignment

Table 3.1
Fuel Assignment Changes for Illinois Plants

Plant Name	Unique ID	Original Modeled Fuel	Illinois EPA Corrected Fuel
VERMILION	897_B_1	Bituminous	Bituminous
VERMILION	897_B_2	Bituminous	Bituminous
WOOD RIVER	898_B_4	Bituminous, Subbituminous	Subbituminous, Bituminous
HAVANA	891_B_9	Bituminous	Bituminous
DALLMAN	963_B_31	Bituminous	Bituminous
BALDWIN	889_B_3	Bituminous, Subbituminous	Subbituminous
DALLMAN	963_B_33	Bituminous	Bituminous
LAKESIDE	964_B_7	Bituminous	Bituminous
LAKESIDE	964_B_8	Bituminous	Bituminous
MARION	976_B_1	Bituminous, Subbituminous	Bituminous
MARION	976_B_2	Bituminous, Subbituminous	Bituminous
MARION	976_B_3	Bituminous, Subbituminous	Bituminous
WOOD RIVER	898_B_5	Bituminous, Subbituminous	Subbituminous, Bituminous
JOPPA STEAM	887_B_2	Bituminous, Subbituminous	Subbituminous
MARION	976_B_4	Bituminous, Subbituminous	Bituminous
WILL COUNTY	884_B_1	Bituminous, Subbituminous	Subbituminous
WILL COUNTY	884_B_2	Bituminous, Subbituminous	Subbituminous
WILL COUNTY	884_B_3	Bituminous, Subbituminous	Subbituminous
WILL COUNTY	884_B_4	Bituminous, Subbituminous	Subbituminous
HENNEPIN	892_B_1	Bituminous, Subbituminous	Subbituminous
JOPPA STEAM	887_B_1	Bituminous, Subbituminous	Subbituminous
WAUKEGAN	883_B_7	Bituminous, Subbituminous	Subbituminous
JOPPA STEAM	887_B_3	Bituminous, Subbituminous	Subbituminous
JOPPA STEAM	887_B_4	Bituminous, Subbituminous	Subbituminous
JOPPA STEAM	887_B_5	Bituminous, Subbituminous	Subbituminous
JOPPA STEAM	887_B_6	Bituminous, Subbituminous	Subbituminous
BALDWIN	889_B_1	Bituminous, Subbituminous	Subbituminous
BALDWIN	889_B_2	Bituminous, Subbituminous	Subbituminous
FISK	886_B_19	Bituminous, Subbituminous	Subbituminous

Table 3.1: Fuel Assignment Changes for Illinois Plants (Continued)

Plant Name	Unique ID	IPM Modeled Fuel	Illinois EPA Corrected Fuel
HUTSONVILLE	863_B_05	Bituminous	Bituminous
POWERTON	879_B_62	Bituminous, Subbituminous	Subbituminous
POWERTON	879_B_61	Bituminous, Subbituminous	Subbituminous
POWERTON	879_B_52	Bituminous, Subbituminous	Subbituminous
POWERTON	879_B_51	Bituminous, Subbituminous	Subbituminous
KINCAID	876_B_2	Bituminous, Subbituminous	Subbituminous
KINCAID	876_B_1	Bituminous, Subbituminous	Subbituminous
JOLIET 9	874_B_5	Subbituminous	Subbituminous
CRAWFORD	867_B_8	Bituminous, Subbituminous	Subbituminous
CRAWFORD	867_B_7	Bituminous, Subbituminous	Subbituminous
MEREDOSIA	864_B_05	Bituminous, Subbituminous	Subbituminous, Bituminous
MEREDOSIA	864_B_04	Bituminous, Subbituminous	Bituminous
MEREDOSIA	864_B_03	Bituminous, Subbituminous	Bituminous
MEREDOSIA	864_B_02	Bituminous, Subbituminous	Bituminous
MANO_IL_Coal Steam	041_C_041	Bituminous	Bituminous
PEARL STATION	6238_B_1A	Bituminous	Bituminous
JOLIET 29	384_B_71	Subbituminous	Subbituminous
JOLIET 29	384_B_72	Subbituminous	Subbituminous
JOLIET 29	384_B_81	Subbituminous	Subbituminous
JOLIET 29	384_B_82	Subbituminous	Subbituminous
DUCK CREEK	6016_B_1	Bituminous	Bituminous
MEREDOSIA	864_B_01	Bituminous, Subbituminous	Bituminous
NEWTON	6017_B_2	Bituminous, Subbituminous	Subbituminous
HUTSONVILLE	863_B_06	Bituminous	Bituminous
E D EDWARDS	856_B_1	Bituminous, Subbituminous	Bituminous
E D EDWARDS	856_B_2	Bituminous, Subbituminous	Bituminous
E D EDWARDS	856_B_3	Bituminous, Subbituminous	Bituminous
COFFEEN	861_B_01	Bituminous, Subbituminous	Bituminous, Subbituminous
COFFEEN	861_B_02	Bituminous, Subbituminous	Bituminous, Subbituminous
WAUKEGAN	883_B_8	Bituminous, Subbituminous	Subbituminous
NEWTON	6017_B_1	Bituminous, Subbituminous	Subbituminous
DALLMAN	963_B_32	Bituminous	Bituminous
WAUKEGAN	883_B_17	Bituminous, Subbituminous	Subbituminous
HENNEPIN	892_B_2	Bituminous, Subbituminous	Subbituminous

Changes in Mercury Control Costs

Table 3.2
Changes in Mercury Control Costs

#	Coal Type	Existing Pollution Control Technology	Sulfur Grade: H - High, L - Low	Sorbent Feed 90%	Capital Cost Components	O&M Cost Components
1A	Bituminous	ESP	L	2	(2)+(3)+(4)	1a+2b+2c+2e+2g+1b
2A	Bituminous	ESP/O	L	2	(2)+(3)+(4)	1a+2b+2c+2e+2g+1b
3A	Bituminous	ESP+FF	L	2	(2)+(3)	1a+2b+2c+2e+2f
4A	Bituminous	ESP+FGD	H	1	(2)+(3)+(4)	1a+2b+2c+2e+2g+1b
5A	Bituminous	ESP+FGD+SCR	H	none	none	none
6A	Bituminous	ESP+SCR	L	2	(2)+(3)+(4)	1a+2b+2c+2e+2g+1b
7A	Bituminous	FF	L	0.5	(2)+(3)	1a+2b+2c+2e+2f
10A	Bituminous	HESP	L	2	(2)+(3)+(4)	1a+2b+2c+2e+2g+1b
11A	Bituminous	HESP+FGD	H	2	(2)+(3)+(4)	1a+2b+2c+2e+2g+1b
12A	Bituminous	HESP+SCR	L	2	(2)+(3)+(4)	1a+2b+2c+2e+2g+1b
13A	Bituminous	PMSCRUB+FGD	H	1	(2)+(3)+(4)	1a+2b+2c+2e+2g+1b
14A	Bituminous	PMSCRUB+FGD+SCR	H	none	none	none
1B	Bituminous	ESP	H	2	(2)+(3)+(4)	1a+2b+2c+2e+2g+1b
2B	Bituminous	ESP/O	H	2	(2)+(3)+(4)	1a+2b+2c+2e+2g+1b
3B	Bituminous	ESP+FF	H	2	(2)+(3)	1a+2b+2c+2e+2f
4B	Bituminous	ESP+FGD	L	1	(2)+(3)+(4)	1a+2b+2c+2e+2g+1b
5B	Bituminous	ESP+FGD+SCR	L	none	none	none
6B	Bituminous	ESP+SCR	H	2	(2)+(3)+(4)	1a+2b+2c+2e+2g+1b
7B	Bituminous	FF	H	0.5	(2)+(3)	1a+2b+2c+2e+2f
10B	Bituminous	HESP	H	2	(2)+(3)+(4)	1a+2b+2c+2e+2g+1b
11B	Bituminous	HESP+FGD	L	2	(2)+(3)+(4)	1a+2b+2c+2e+2g+1b
12B	Bituminous	HESP+SCR	H	2	(2)+(3)+(4)	1a+2b+2c+2e+2g+1b
13B	Bituminous	PMSCRUB+FGD	L	1	(2)+(3)+(4)	1a+2b+2c+2e+2g+1b
14B	Bituminous	PMSCRUB+FGD+SCR	L	none	none	none
15	Lignite	ESP	L	3	(2)+(3)	1a+2b+2c+2e+2f
16	Lignite	ESP+FF	L	1	(2)+(3)	1a+2b+2c+2e+2f
17	Lignite	ESP+FGD	L	3	(2)+(3)	1a+2b+2c+2e+2f
18	Lignite	FF+DS	L	1	(2)+(3)	1a+2b+2c+2e+2f
19	Lignite	FF+FGD	L	3	(2)+(3)	1a+2b+2c+2e+2f
20	Subbituminous	ESP	L	3	(2)+(3)	1a+2b+2c+2e+2f
21	Subbituminous	ESP+DS	L	3	(2)+(3)	1a+2b+2c+2e+2f
22	Subbituminous	ESP+FGD	L	3	(2)+(3)	1a+2b+2c+2e+2f
23	Subbituminous	ESP+SCR	L	3	(2)+(3)	1a+2b+2c+2e+2f
24	Subbituminous	FF	L	3	(2)+(3)	1a+2b+2c+2e+2f
25	Subbituminous	FF+DS	L	3	(2)+(3)	1a+2b+2c+2e+2f
26	Subbituminous	FF+FGD	L	3	(2)+(3)	1a+2b+2c+2e+2f
27	Subbituminous	HESP	L	1	(2)+(3)+(4)	1a+2b+2c+2e+2g+1b
28	Subbituminous	HESP+FGD	L	1	(2)+(3)+(4)	1a+2b+2c+2e+2g+1b
29	Subbituminous	HESP+SCR	L	1	(2)+(3)+(4)	1a+2b+2c+2e+2g+1b
30	Subbituminous	PMSCRUB	L	3	(2)+(3)	1a+2b+2c+2e+2f
31	Subbituminous	PMSCRUB+FGD+SCR	L	3	(2)+(3)	1a+2b+2c+2e+2f

See EPA documentation for 2.1.9 definition of cost components. Illiinois EPA Assumptions Changes reflected differing combinations of these Than EPA. Source Illinois EPA.

Existing Unit Specific Plant Changes

Table 3.3
Changes for Marion Plant

Plant Name	Unique ID	
MARION	976_B_1	
	Original	**Revised**
Unit ID	1	123
Capacity (MW)	34	120
Particulate Matter Type	Hot-side ESP	Fabric Filter
Post Combustion Control	None	SNCR
Online Year	1963	2001
Heat Rate (Btu/KWh)	14455	11965
Uncontrolled NOX Base Rate (lbs/MMBtu)	0.72	0.76
Controlled NOX Base Rate (lbs/MMBtu)	0.72	0.76
Note: Boiler #2 and #3 were retired at this facility. Thus capacity for boiler #1 changed from 34MW to 123 MW.		

Table 3.4
Particulate Matter Type Changes for Select Plants

Plant Name	Unique ID	Original Particulate Matter Type	Revised Particulate Matter Type
WOOD RIVER	898_B_4	Hot-side ESP	Cold-side ESP
DALLMAN	963_B_31	Hot-side ESP	Cold-side ESP
LAKESIDE	964_B_7	Hot-side ESP	Cold-side ESP
LAKESIDE	964_B_8	Hot-side ESP	Cold-side ESP